Effect of Seismic Loads on Water-Retaining Structures in Areas of Moderate Seismicity

by

Johanna Aletta Fourie

Thesis presented in partial fulfilment of the requirements for the degree

Master of Science at the University of Stellenbosch

Supervisor:

Professor J.A. Wium

Stellenbosch December 2009

DECLARATION

By submitting this dissertation electronically, I declare that the entirety of the work contained therein is my own, original work, that I am the owner of the copyright thereof (unless to the extent explicitly otherwise stated) and that I have not previously in its entirety or in part submitted it for obtaining any qualification.

Signature: 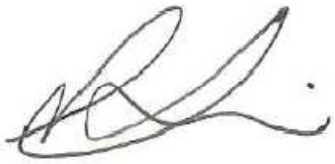

December 2009

SYNOPSIS

Water-retaining structures are commonly used in South Africa for the storage of potable water and waste water. However, a South African code pertaining to the design of concrete water-retaining structures do not currently exist and therefore use is made of the British Standard BS 8007 (1987). For the design of concrete water-retaining structures in South Africa, only the hydrostatic loads are considered while forces due to seismic activity are often neglected even though seismic excitations of moderate magnitude occur within some regions of the country. Hence, the primary aim of this study was to determine whether seismic activity, as it occurs in South Africa, has a significant influence on water-retaining structures and whether it should be considered as a critical load case.

In order to assess the influence of seismic activity on the design of water-retaining structures the internal forces in the wall and the required area of reinforcement were compared. Comparisons were made between the seismic analyses and static analyses for both the ultimate and serviceability limit states. In order to obtain the internal forces in the wall use was made of an appropriate Finite element model. Three Finite element models were investigated in this study and the accuracy of each model was assessed based on the fundamental frequency, base shear force and overturning moment. These values were compared to the values obtained with the numerical method presented by Veletsos (1997) which was verified with Eurocode 8: Part 4 (2006).

The results obtained indicated that seismic excitations of moderate magnitude do have a significant influence on the reinforcement required in concrete water-retaining structures. For both the ultimate limit state and serviceability limit state the required reinforcement increased significantly when seismic loads were considered in the design. As in the case for static design of water-retaining structures, the serviceability limit state also dominated the design of these structures under seismic loading.

SINOPSIS

Beton waterhoudende strukture in Suid-Afrika word op ‘n gereelde basis gebruik vir die stoor van drink- sowel as afvalwater. ‘n Suid-Afrikaanse kode vir die ontwerp van hierdie strukture bestaan egter nie en dus word die Britse kode BS 8007 (1987) hiervoor gebruik. Vir ontwerp doeleindes word soms slegs die hidrostatiese kragte beskou terwyl kragte as gevolg van seismiese aktiwiteite nie noodwendig in berekening gebring word nie. Seismiese aktiwiteite van gematigde grootte kom egter wel voor in sekere dele van Suid-Afrika. Die hoofdoel van hierdie studie was dus om die invloed van seismiese aktiwiteite, soos voorgeskryf vir Suid-Afrikaanse toestande, op beton waterhoudende strukture te evalueer asook om te bepaal of dit ‘n kritiese lasgevalle sal wees.

Vir hierdie doel is die interne kragte asook die area staal bewapening vir elk van die statiese en dinamiese lasgevalle vergelyk. Vergelykings is getref tussen die dinamiese en statiese resultate vir beide die swigtoestand en die diensbaarheidstoestand. Vir die bepaling van die interne kragte is gebruik gemaak van eindige element modelle. Tydens hierdie studie was drie eindige element modelle ondersoek en die akkuraatheid van elk geëvalueer op grond van die fundamentele frekwensie, die fondasie skuifkrag en die omkeermoment. Hierdie waardes was ondermeer bereken met twee numeriese metodes soos uiteengesit in Veletsos (1997) en Eurocode 8: Part 4 (2006).

Die resultate dui daarop dat die invloed van seismiese aktiwiteite op beton waterhoudende strukture in Suid-Afrika nie weglaatbaar klein is nie en wel in berekening gebring behoort te word tydens die ontwerp. Die interne kragte vir beide die swigtoestand en diensbaarheidstoestand is aansienlik hoër vir die seismiese lasgeval as vir die statiese geval. Die diensbaarheidstoestand het deurentyd die ontwerp van beton waterhoudende strukture vir seismiese toestande oorheers.

ACKNOWLEDGEMENTS

I would like to acknowledge the contribution and support of a few people in making this thesis possible.

- I would like to acknowledge Professor J.A. Wium for the time and effort that he has put into making countless drawings and explaining everything in the hope of a decent project.
- My fellow MSc students namely Johann, Estee, Christo, Arthur and Ife. Thank you for all of the brainstorming sessions, the laughs and all of the coffee breaks.
- The secretaries of the structural department namely Natalie and Amanda. Thank you for all of the good memories and your willingness to help in every situation.
- Lastly I would like to acknowledge the support of my family and friends throughout the duration of this project. Your support has meant everything.

TABLE OF CONTENTS

LIST OF FIGURES

LIST OF TABLES

NOTATION

General:

a_g	Peak ground acceleration [g]
A_{c1}	Pseudoacceleration experienced by the convective component [g]
A_s	Area of steel reinforcement [m^2]
c_{min}	Minimum concrete cover [m]
d	Diameter of the tank [m]
d_{max}	Height of the sloshing wave [m]
E	Modulus of elasticity of wall material [N/m^2]
E_s	Modulus of elasticity of reinforcement [N/m^2]
f_{el}	Elastic strength [N/m^2]
f_{i1}	Fundamental frequency of the tank-liquid system [Hz]
f_y	Tensile yield strength of reinforcement [N/m^2]
$f_{y,d}$	Design yield strength [N/m^2]
g	Gravitational acceleration [m/s^2]
h_c	Height at which convective mass is situated to produce M_c [m]
h_i	Height at which impulsive mass is situated to produce M_i [m]
h_i'	Height at which impulsive mass is situated to produce M_i' [m]
H	Height measured from base of the tank wall to the free surface of contained liquid [m]
I	Second moment of inertia of section [m^4]
k	Bending stiffness of the tank wall [N/m]
K_c	Spring stiffness of convective component [N/m]
m	Axial wave number
m	Mass of contained liquid [kg]
m_c	Liquid mass associated with convective component [kg]
m_i	Liquid mass associated with impulsive component [kg]
m_w	Mass of tank wall [kg]
M	Bending moment in wall [N.m/m]
M_c	Overturning moment of wall ring, associated with convective component [N.m]
M_i	Overturning moment of wall ring, associated with impulsive component [N.m]
M_i'	Overturning moment with inclusion of foundation due to impulsive

	component [N.m]
M_s	Serviceability bending moment [N.m]
M_u	Ultimate bending moment [N.m]
$M_{x\text{-}x}$	Bending moment about a vertical axis [N.m/m]
$M_{y\text{-}y}$	Bending moment about a horizontal axis [N.m/m]
n	Circumferential wave number
p_c	Pressure exerted by the convective component [N/m^2]
p_i	Pressure exerted by the impulsive component [N/m^2]
p_w	Pressure due to inertia of the tank wall [N/m^2]
P	Vertical force acting on wall [N/m]
q	Behaviour factor
q_{max}	Maximum pressure exerted on tank wall [N/m^2]
Q_c	Base shear force associated with convective component [N]
Q_i	Base shear force associated with impulsive component [N]
R	Radius of the tank [m]
$(S_A)_c$	Pseudoacceleration experienced by the convective component [g]
T	Period of vibration of the structure [seconds]
T	Tensile force [N]
T_{imp}	Fundamental frequency of the tank-liquid system [seconds]
V	Shear force in wall [N/m]
X	Depth of neutral axis [m]
x_{el}	Yield displacement
x_y	Displacement at design yield strength
z	Height measured from base of tank to specific point on tank wall [m]
z	Lever arm [m]
α_3	Participation factor
Δh	Height increment between the nodes on the tank wall [m]
ε_2	Strain due to tension stiffening of concrete
ε_m	Average tensile strain in reinforcement, ε_s-ε_2
ε_s	Tensile strain in reinforcement
λ	First derivative of the Bessel function of the first kind and first order
ν	Poisson ratio of tank wall material
ν	Reduction factor

ω_c	Frequency of convective component [radians/second]
ρ	Density of contained liquid [kg/m^3]
ρ_w	Density of tank wall [kg/m^3]
σ_h	Hoop stress [N/m^2]
σ_s	Tensile stress in reinforcement [N/m^2]
θ	Circumferential angle measured counter clockwise from direction of excitation [degrees]

Notations specific to BS 8007 (1987):

a_{cr}	Distance measured from position of maximum tensile strain to surface of closest reinforcement bar [m]
b_t	Thickness of the tank wall [m]
h	Overall depth of the member [m]
w	Crack width [m]

Notations specific to Eurocode 8: Part 4 (2006):

A_{f1}	Pseudoacceleration experienced by the structure [g]
C_i	Dimensionless parameter used to calculate period of vibration of tank-liquid system
d_1	Dimensionless parameter used to determine p_f
h_f	Height at which “flexibility” mass is placed to produce M_f [m]
I_1	Modified Bessel function of the first order
I_1'	First derivative of the modified Bessel function of the first order
J_1	Bessel function of the first order
m_f	Mass associated with “flexibility” of the tank wall [kg]
M_f	Overturning moment of wall ring, associated with “flexibility” component [N.m]
n	Modal number of vibration
p_f	Pressure due to “flexibility” of the tank wall [N/m^2]
Q_f	Base shear force associated with “flexibility” component [N]
r	Distance measured along the radius of the tank [m]
s	Thickness of tank wall [m]
γ	H/R ratio

v_1	Dimensionless parameter used to determine p_f
Ψ	Dimensionless parameter used to determine p_f
Ψ_1	Dimensionless parameter used to determine p_c
ς	z/H ratio
ξ	r/R

Notations specific to Ghali (1979):

h	Thickness of tank wall [m]
l_1	Height of bottom cylinder for tall tanks
L	Height measured from base of the tank wall to the free surface of the contained liquid [m]
M_ϕ	Restraining bending moment in wall [N.m/m]
N	Hoop force [N/m]
q	Pressure exerted on tank wall [N/m^2]
q_{l1}	Pressure measured at height l_1 along tank wall [N/m^2]
$\bar{q}$	Reaction force [N/m^2]
r	Radius of the tank [m]
w	Displacement of tank wall [m]
η	dimensionless parameter equal to $L^2/(2rh)$

Notations specific to Veletsos (1997):

c_{ij}	Dimensionless parameter used for impulsive component with consideration of the j-th mode of vibration
E_w	Modulus of elasticity of wall material [N/m^2]
j	Modal number of vibration
m_{ij}	Mass associated with impulsive component for the j-th mode of vibration [kg]
t_w	Wall thickness of the tank [m]
$\ddot{x}_g$	Peak ground acceleration [g]
η	z/H ratio

ACRONYMS

BS	British Standard
DL_{wall}	Self-weight of the tank wall [N]
DL_{water}	Self-weight of the contained liquid [N]
eq	Equation
EQ	Earthquake load [N]
FE	Finite Element
GPa	GigaPascal
LC	Load Combination
max	Maximum
MPa	MegaPascal
PGA	Peak Ground Acceleration
SLS	Serviceability limit state
ULS	Ultimate limit state

1. INTRODUCTION

The focus of this study was to determine the influence of moderate seismic activity on water-retaining structures in South Africa. This chapter provides information on the significance of water-retaining structures and their design for South African conditions. The aims of this project as well as the methodology followed in order to reach these goals are outlined along with the scope and limitations of this research project. Finally a brief overview of the various chapters and their contents is presented.

1.1. BACKGROUND INFORMATION

Liquid-storage tanks are widely used in practice for the storage of nuclear waste, oil, fuel as well as various other chemical fluids. Water-retaining structures specifically are of great importance not only for the storage of potable water for everyday use, but also in the event of a natural disasters, both for the provision of clean drinkable water and subsequent avoidance of diseases, as well as water for fire-fighting. The need for potable water has increased immensely due to the rapid growth of the human population which entailed an increase in capacity and therefore size of these structures. Due to the increase in size and subsequent increase in risk of failure, numerous studies have been completed to aid in the prediction of tank behaviour, analysis and design for static and dynamic conditions.

The static analysis and design of these structures are relatively well-known but only in the last two decades have there been significant progress in the dynamic evaluation and design of water-retaining structures. Dynamic conditions include seismic activity which is of great importance for South Africa, especially in the Western Cape since moderate seismic activity occurs within this region. Figure 1.1 indicates the various zones of seismic activity in South Africa including natural and mining induced earthquakes.

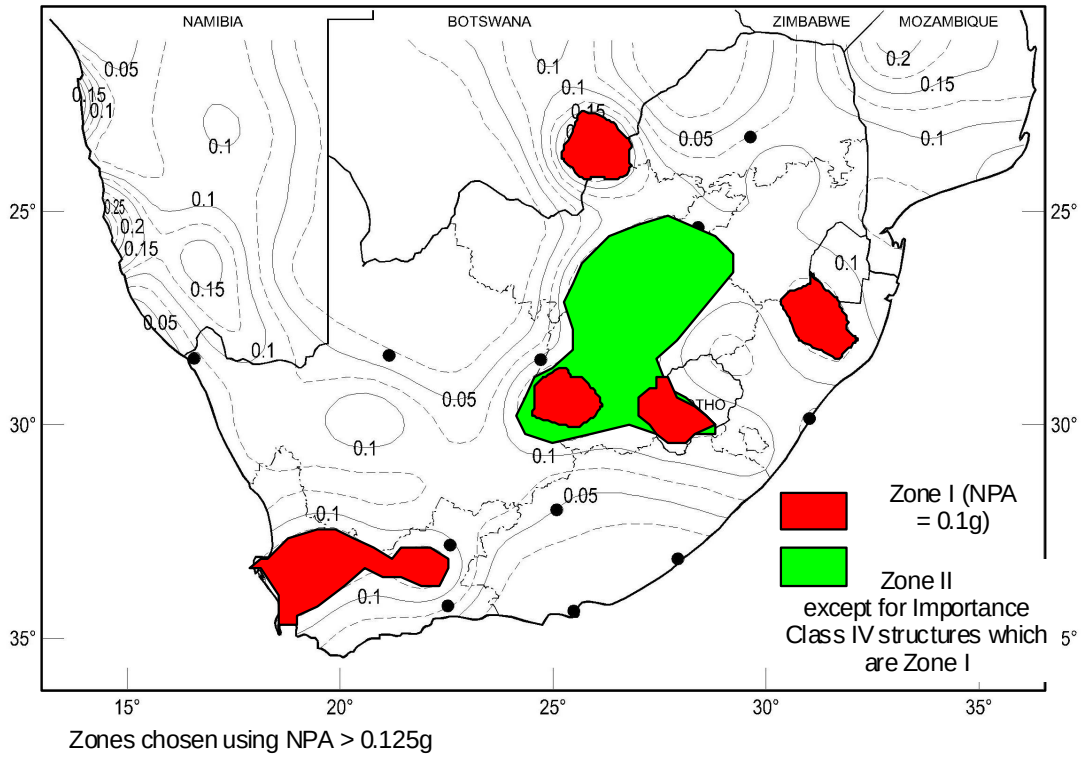

Figure 1.1: Seismic zones in South Africa (SANS 10160, 2009)

It is well known that these excitations have a significant influence on houses, multi-storey buildings, stadiums etc. The question arises of whether seismic loads should be regarded as a critical load case in the design of water-retaining structures in South Africa due to the moderate magnitude of these excitations. The answer is unknown since there is currently no existing South African code for the design of water-retaining structures for seismic loading. Various codes exist for the design of water-retaining structures such as the Eurocode 8: Part 4 (2006) and BS 8007 (1987) which contains not only information on the design of water-retaining structures for static conditions, but also for dynamic conditions. However, these codes were not specifically compiled for South Africa and for this reason the Water Research Commission established a project with the aim of compiling a design code with regard to design, construction, quality control and maintenance of water-retaining structures in South Africa. Information obtained through the completion of this thesis contributes to the aim of the Water Research Commission, since it provides information on the analysis and design of water-retaining structures for South African conditions.

1.2. AIM OF STUDY

Currently there is no existing South African code for the design of water-retaining structures for seismic loads. The option of introducing the Eurocodes in South Africa for design purposes is being investigated but some uncertainties remain with regard to the application of the Eurocodes for South African conditions. The first aim of the study is to determine whether seismic loading is indeed a determinate loading condition for concrete water-retaining structures in seismic zones in South Africa. A peak ground acceleration of 0.15g can be expected in the Western Cape, which is considered to be of moderate magnitude.

In the case of static design of water-retaining structures, the serviceability load case is usually dominant due to restrictions on maximum allowable crack width. If this study indicates that seismic loading is a dominant load case for the design of water-retaining structures in South Africa, another question arises. This would be to determine whether the serviceability load case would still be dominant in the design of these structures or whether the ultimate limit state would become the governing factor for design.

The design process of water-retaining structures for seismic loads according to the Eurocodes can be a complicated and cumbersome process. The third aim of this study is to give an indication of the accuracy and practicality of simplified numerical methods as proposed by various authors in terms of the design of these structures for seismic loads.

Uncertainties surrounding the dynamic FE modelling of these structures also exist. The fourth aim of this study is to evaluate the accuracy of different simplified FE models with regard to numerical solutions.

1.3. METHODOLOGY OF STUDY

The methodology followed during this project is summarized in Figure 1.2.

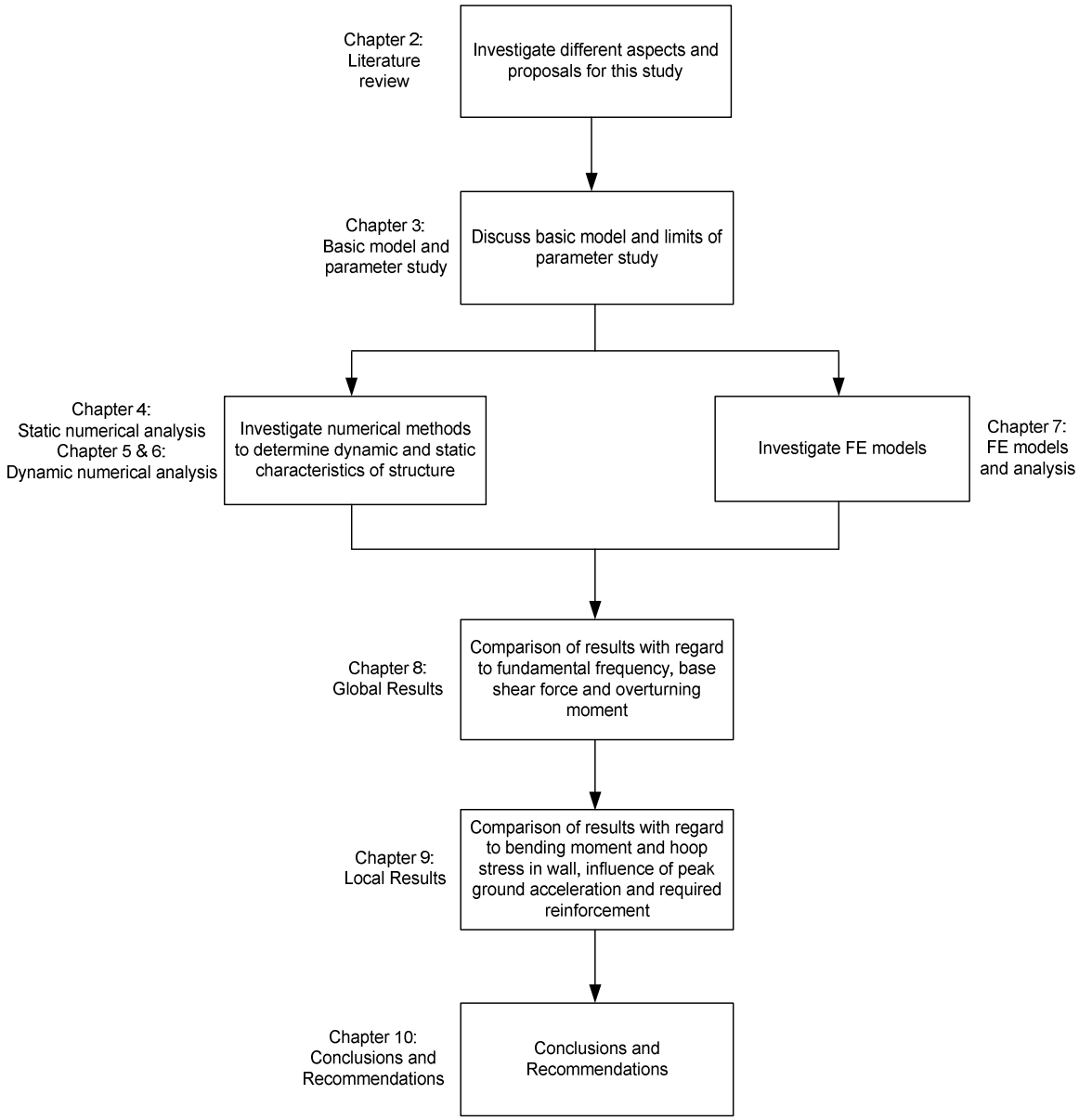

Figure 1.2: Methodology of study

1.4. SCOPE AND LIMITATIONS

The structures investigated in this study were limited to the following:

- Circular-cylindrical tanks above ground. Therefore no rectangular, buried or elevated tanks were considered.
- Tanks with uniform walls were considered, therefore the behaviour of tanks with varying wall thickness were not investigated.
- Only reinforced concrete tanks were analysed, pre-stressed concrete tanks were not investigated.
- The foundation was considered as rigid and therefore no rocking or tilting motion of the foundation was considered.
- The parametric study consisted of a variance in H/R ratio between 0.3 and 1.5 and a wall thickness ratio t_w/R between 0.006 and 0.03, as discussed in the following chapters.
- The peak ground acceleration in the parametric study was varied between values of 0.15g and 0.35g.

Calculations regarding water-retaining structures were restricted to the following:

- Crack width calculations were restricted to the use of BS 8007 (1987). Cracking due to bending of the wall and cracking resulting from the hoop stress were considered separately.
- Only water and earthquake loads were considered. Wind loading was neglected as well as temperature effects and shrinkage since this study investigates the influence of seismic loading on the design of water-retaining structures.
- Static calculations were restricted to the use of tables and figures by Ghali (1979).
- Dynamic calculations were restricted to the use of Veletsos (1997) and Eurocode 8: Part 4 (2006).
- The finite element analyses of structures were restricted to the use of a FE package called STRAND7 (2005) with three models as proposed by Nachtigall (2003) and Virella (2006).
- Only the horizontal motion due to earthquake excitation was considered while the vertical motion was neglected. This is justified by the magnitude of events considered.

1.5. OVERVIEW OF DOCUMENT

A brief overview of the document is provided in the following paragraphs. Chapter 2 provides background information to this project. Important concepts and terms used during this investigation are defined in this chapter. This chapter also gives a brief review of different methods of analysis of water-retaining structures for both static and dynamic loads.

The basic model used for all numerical and FE analyses is presented in detail in Chapter 3 along with the scope of the parametric study and reasons for limitations. The static analysis of a structure is presented in Chapter 4 with the dynamic analyses discussed in Chapters 5 and 6 with the methods presented in Eurocode 8: Part 4 (2006) and Veletsos (1997) respectively. Both the ultimate and serviceability limit states are discussed in detail in these three chapters.

Different FE models were considered for the purposes of this project and more information is provided in Chapter 7. This study investigated ways in which the water can be taken into account in a finite element model and more information with regard to the elements, types of analyses, mode of vibration and mode shapes of a water-retaining structure subjected to horizontal seismic excitation is provided in this chapter.

Global results are presented in Chapter 8 with regard to the classification of water-retaining structures subjected to seismic loading, the fundamental frequency and corresponding mode shape and the base shear force and overturning moment. Local results are presented In Chapter 9 pertaining to the bending moment and hoop stress in a wall, the influence of the peak ground acceleration on both entities, the governance of either the serviceability or limit state with regard to the reinforcement required. The use of a modified response spectrum and corresponding influence on the internal forces and area of reinforcement required is also presented in this chapter. All of these entities were use to determine and evaluate the respective FE models with regard to the numerical method proposed by Veletsos (1997).

Chapter 10 provides a summary of results obtained and draws conclusions from these results in terms of (1) the importance of seismic design of water-retaining structures in

South Africa, (2) consideration of ultimate and serviceability limit state for analysis and design purposes, (3) use of numerical methods for practical purposes, (4) use of FE models with consideration of the contained liquid.

In the following chapter all literature pertaining to this study is presented and important concepts used for the evaluation and design of water-retaining structures are discussed.

2. LITERATURE REVIEW

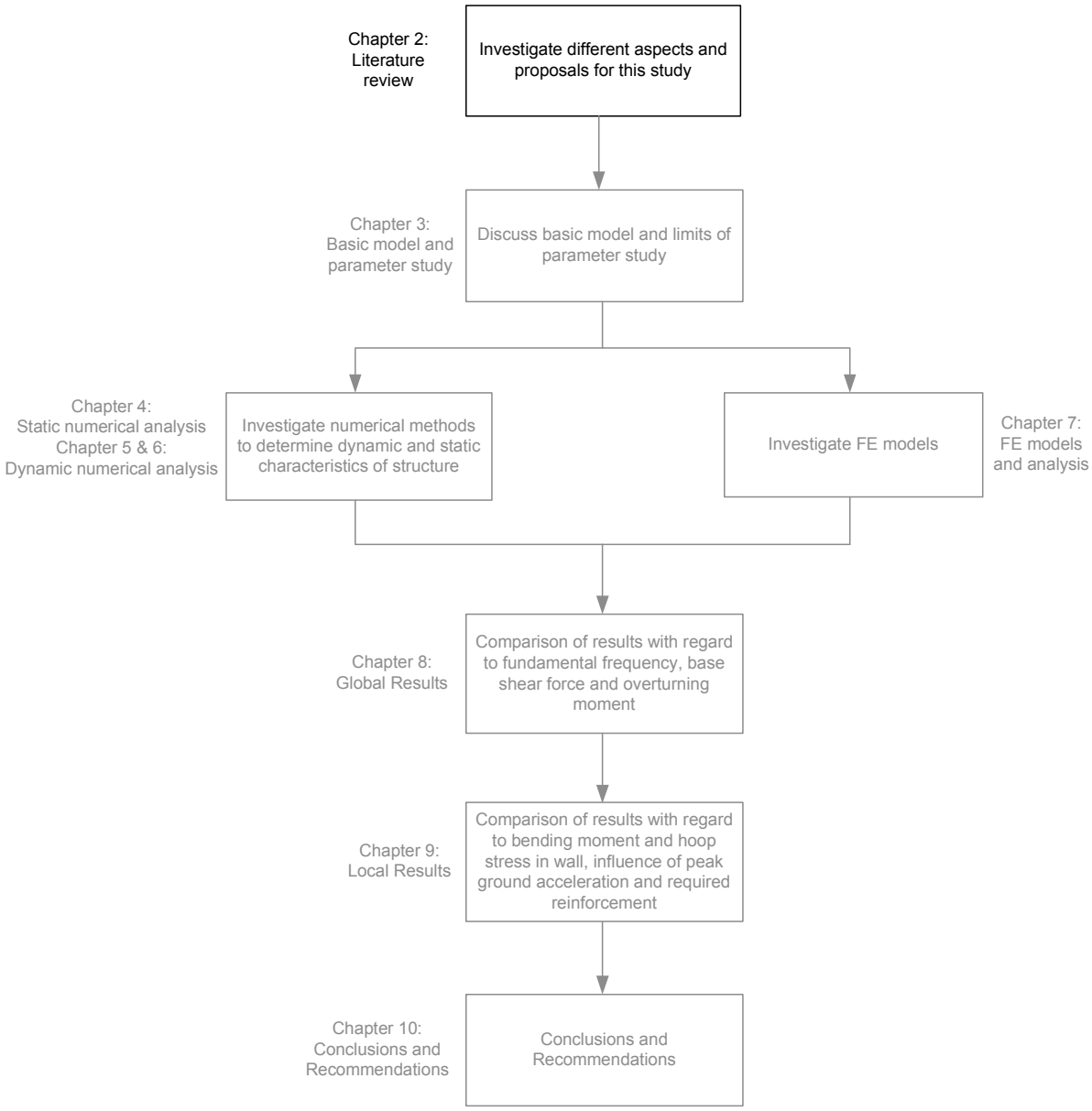

Figure 2.1: Methodology of study

In order to better understand the behaviour of a tank during an earthquake as well as the various design methods and consequent results, it is necessary to explain some of the most important concepts. A brief summary of the most significant research completed in the last two decades pertaining to water-retaining structures is presented. For the evaluation and design of a water-retaining structure, two limit states are considered namely the ultimate

and the serviceability limit state. Both of these limit states are discussed since they differ from that of building structures.

The behaviour of a tank during seismic excitation is influenced by a number of external parameters. These include the influence of the contained liquid, which consists of a number of components, as well as the flexibility of the wall and soil conditions. All of the above mentioned factors have a significant influence on the behaviour of a tank during horizontal seismic excitation and therefore further information on the influence of each of these factors on the behaviour of a tank during horizontal excitation is provided.

Practical information on material properties and dimensions of circular tanks used by South African designers was gathered and these along with a summary on the static analysis of circular tanks are provided. Several numerical methods exist to aid in the evaluation of a water-retaining structure for dynamic and static loading conditions and some of these are addressed in this chapter. The static design as presented by Ghali (1979) is discussed in detail in this chapter as well as the two methods used for the dynamic evaluation as proposed by Eurocode 8: Part 4 (2006) and Veletsos (1997). These methods are discussed with regard to the various assumptions made by the authors, the coordinate system used by each as well as the various design steps.

During horizontal excitation the structure deforms in a particular manner due to water and seismic loads. The FE package STRAND7 (2005) was used to analyse the structures and obtain results in terms of fundamental mode of vibration, mode shape as well as resulting forces and stresses. For this reason more information is provided on the modes of vibration as discussed by various authors and the most important definitions used in STRAND7 (2005).

In the last section of this literature overview, a brief summary is presented on the most significant proposals for FE models used in the prediction and evaluation of seismic behaviour of circular cylindrical tanks. Two of these models were used extensively during this project.

2.1. DEVELOPMENT OF METHODS

Numerous papers have been published on the seismic analysis of water-retaining structures with the most important of these summarized in Virella (2006). This summary is provided again in this paper and serves as background information to this project. The respective papers are as follows:

- Housner (1963) investigated rigid cylindrical tanks fixed to the base and concluded that the liquid composes of two separate components, (1) impulsive component which moves with the tank and (2) convective component which causes the sloshing motion during horizontal seismic activity. Housner (1963) also derived formulae for calculating the liquid mass associated with each component, their effective height above the tank base as well as the impulsive frequency based on beam-like behaviour of the structure.
- Veletsos and Yang (1977) as well as Haroun and Housner (1981) found that the pressure distribution due to the liquid was similar for rigid and flexible tanks fixed to their base. The flexibility of the wall only influenced the magnitude of pressure applied to the wall.
- The impulsive frequency is calculated based on the assumption that the structure exhibits beam-like behaviour during horizontal excitation and this assumption is widely accepted in Housner (1963), Haroun and Housner (1981) and Veletsos (1997).
- The wall flexibility can be included in the various response equations. The peak ground acceleration is substituted with the pseudoacceleration of the tank-liquid system in the case of flexible tanks as stated in Veletsos (1997).
- Malhotra and Veletsos (1994) found that the impulsive and convective components can be uncoupled due to the large differences in natural frequency. The flexibility of the tank wall only influences the impulsive component and the convective component remains the same as for the case of rigid tanks.
- An alternative method for the calculation of the tank-liquid system frequency is proposed by Nachtigall (2003) which is not based on the beam-like behaviour of the tank wall during horizontal seismic excitation. Nachtigall (2003) proposed the use of the shell modal forms during the evaluation of circular tanks for seismic loading conditions. The shell modal forms can be modelled with a

circumferential wavy pattern of cos (nθ) with 5<n<25 with these modes not corresponding with the fundamental mode of a cantilever beam.

- Experimental papers (Mazuch, 1996) have also been published with regard to the fundamental frequency and modes shapes of circular cylindrical tanks. The results from the experimental studies were not successful in determining the fundamental mode of vibration of a tank-liquid system when subjected to horizontal excitation.
- Barton and Parker (1987) used finite elements to study the seismic response of tanks. Shell elements were used to model the tank while liquid finite elements and added masses were used to accurately model the liquid. Barton and Parker (1987) found that modes involving the form cos (nθ) with n greater than 1, are not important in predicting the response of tank-liquid systems with H/R [Height/Radius] ratios greater than 0.5. It was found that the higher modes of vibration had very small participation masses and may be neglected. The cantilever beam mode with n equal to 1 is fairly accurate in predicting the response of a tank-liquid system to horizontal excitation. Findings by Barton and Parker (1987) therefore contradict the findings by Nachtigall (2003).

As indicated the fundamental frequency and mode shape of a water-retaining structure subjected to horizontal seismic excitation are of great interest. Some uncertainty still remains in the determination of the fundamental frequency and mode shape. The FE method proposed by Barton and Parker (1987) used specialized finite elements not readily available in standard FE packages. The determination of the fundamental frequency and mode shape with the use of a standard FE package was further investigated in this study. The FE results could then be verified with the use of the numerical methods as outlined above.

2.2. PHILOSOPHY OF DESIGN

2.2.1. ULTIMATE AND SERVICEABILITY LIMIT STATE

Both the ultimate and serviceability limit states are considered in the design of water-retaining structures for seismic excitation. These terms are defined in Eurocode 8: Part 4 (2006) as:

- The ultimate limit state usually corresponds to complete structural failure of a system. If failure of the tank is associated with severe consequences, the ultimate limit state excludes brittle failure and allows for the controlled release of the contents. For the ultimate limit state the structure is permitted to deform in the non-linear region resulting in local plastic deformations. In order to avoid explicit inelastic analysis, use is made of the behaviour factor which is considered to be equal to 1.5.
- In the case of the serviceability limit state, the structure should remain fully functional and leak proof or optionally it must be possible to repair the tank to restore functionality to a pre-defined level of service.
- A reduction factor is prescribed for use in the serviceability limit state in order to reduce the forces associated with this particular limit state. A reduction of the serviceability forces is permitted since the reference return period is 95 years for serviceability whilst being 475 years for the ultimate limit state. The seismic demand on a structure in the serviceability limit state will therefore occur more frequently than for the ultimate limit state.
- The maximum allowable crack width for water-retaining structures in South Africa is prescribed in the British codes BS 8007(1987). Considering the reduced forces acting on the structure and the restrictions on the allowable crack width, the structure will remain fully elastic.

2.2.2. BEHAVIOUR FACTOR

The term “behaviour factor” is used throughout this study to describe the behaviour of the contained liquid during seismic ground motion and is defined in more detail in this section.

A structure is normally designed to remain fully elastic when subjected to externally applied loads. The seismic loads usually govern the design and the design of a structure to remain elastic during seismic excitation becomes unfeasible due to the magnitude of the seismic load exerted on the structure. The occurrence of seismic activity in South Africa is considered to be of moderate magnitude. In order to make the seismic design of a structure more practical use is made of a behaviour

factor q, which reduces the seismic force for which a structure is analysed. With the use of a behaviour factor, the yield force of the structure is lowered while still aiming for the deflection as obtained with a fully elastic structure. With the lowered yield force and same amount of deflection an amount of plastic deformation is required in the structure when subjected to seismic loads. The amount of plastic deformation in the structure is dependent on the magnitude of the behaviour factor, with increasing plastic deformation allowed in the structure with increasing values of the behaviour factor. Figure 2.2 graphically illustrates the use of a behaviour factor.

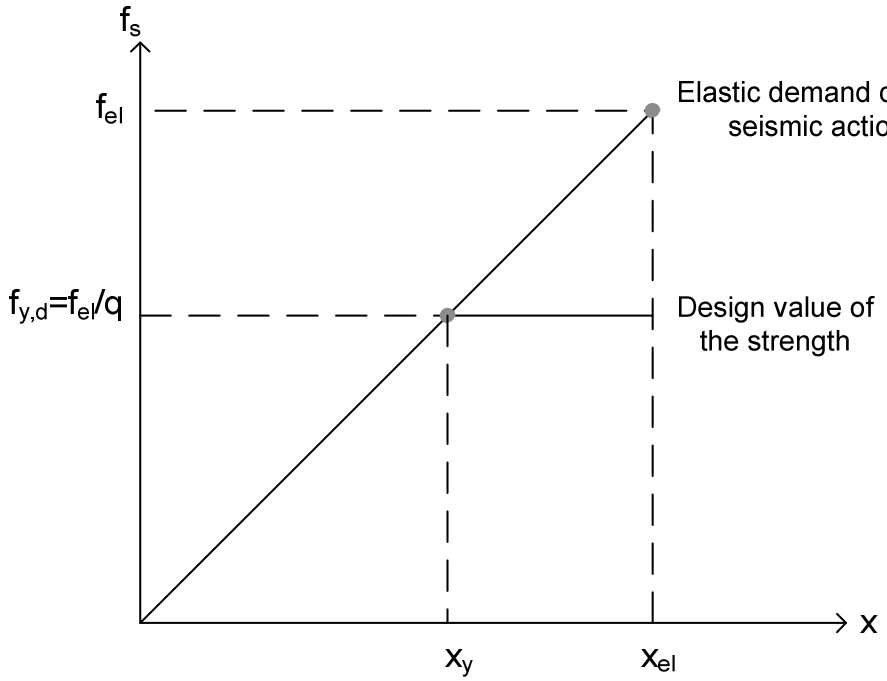

Figure 2.2: Definition of behaviour factor (Dazio, 2009)

A behaviour factor of 1.0 therefore implies the structure has a yield strength equal to the elastic strength and will undergo no plastic deformation while a behaviour factor greater than 1.0 implies the structure is designed for a lower yield strength and plastic deformation needs to occur when the structure is subjected to seismic loads.

2.2.3. COORDINATE SYSTEM AND ASSUMPTIONS OF NUMERICAL METHODS

The coordinate system defined in Veletsos (1997) and Eurocode 8: Part 4 (2006) was adopted in this project and is shown in Figure 2.3. The coordinate system and symbols are defined as:

- The tank has a radius R, a height H and a wall thickness denoted by t_w.
- Points on the tank wall can be defined with coordinate z with z measured upwards from the base.
- The circumferential angle θ, is measured counter-clockwise from the direction of excitation.

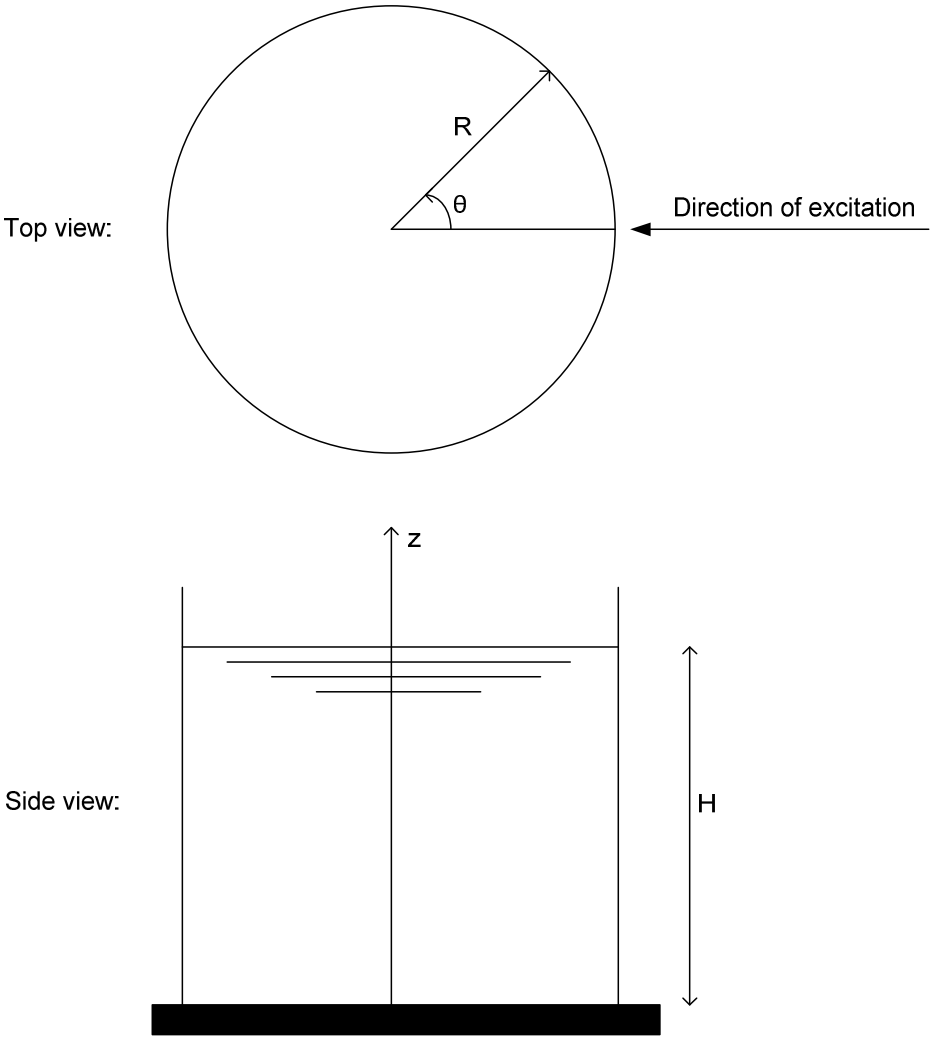

Figure 2.3: Coordinate system of circular tank (Veletsos, 1997)

The fundamental mode of vibration of a tank is considered by various authors (Veletsos, 1997), (Haroun, 1980) to be similar to the fundamental mode of a

cantilever beam. Simplification of the water-retaining model along with various assumptions is required to aid in the evaluation of a structure with numerical methods. These include (Veletsos, 1997):

- The tank is supported by a circular foundation that can be either rigid or flexible. Flexible foundations can undergo a rocking or tilting motion during horizontal excitation and are discussed further in section 2.4.
- Perfect bonding exists between the foundation and supporting soil.
- The tank is considered to have a constant radius R and a constant wall thickness of t_w.
- It is assumed that the tank wall is fully clamped or fixed to the foundation to prevent uplift or sliding of the wall with respect to the foundation.
- The tank is filled up to a height H with a homogeneous, incompressible and non-viscous liquid.

Two numerical methods were used during the course of this project, the first method is presented by Veletsos (1997) and the second method is prescribed in Eurocode 8: Part 4 (2006). The design philosophy of both methods is based upon two assumptions regarding the tank-liquid behaviour during horizontal excitation. It is assumed that the oscillation of the tank relative to the foundation exhibits the same behaviour as a vertical cantilever beam. With the use of the cos θ term in the determination of the hydrodynamic pressure, it is also assumed that the initial cross-section of the tank will remain circular during excitation and cannot deform in an oval shape.

2.2.4. LIQUID SURFACE CONDITIONS

The liquid surface conditions have a major influence on the behaviour of the liquid during horizontal excitation which subsequently influences the behaviour of the tank. The liquid surface can be defined as either a capped or a free surface as defined in Veletsos (1997). A capped surface refers to tanks that are filled up to roof-level with a liquid, while a free surface refers to tanks in which the liquid level is below the roof-level and sufficient freeboard was provided for the sloshing motion of the liquid.

In the case of capped surfaces the liquid cannot experience any vertical motion or sloshing and therefore the entire mass of the liquid moves in combination with the tank. In contrast, the movement of the liquid is described with the use of two components in the case of free surfaces. These liquid components are the impulsive and the convective component respectively with more information provided in the following section.

The magnitude and influence of the impulsive and convective components on tank behaviour is highly dependent on the H/R ratio of the tank. The contribution of the impulsive component to the global response of the tank becomes more pronounced with an increase in H/R ratio, while the contribution of the convective component decreases. The convective component has a significant influence on the hydrodynamic pressure down to the bottom for broad tanks, but is restricted to the liquid surface in the case of tall tanks with H/R greater than 1.0. The sloshing frequency becomes independent of the H/R ratio for tall tanks due to the superficial influence of the convective component as illustrated in Figure 2.4 with the first mode of vibration of the sloshing component indicated as 1 and the second mode of vibration indicated with 2.

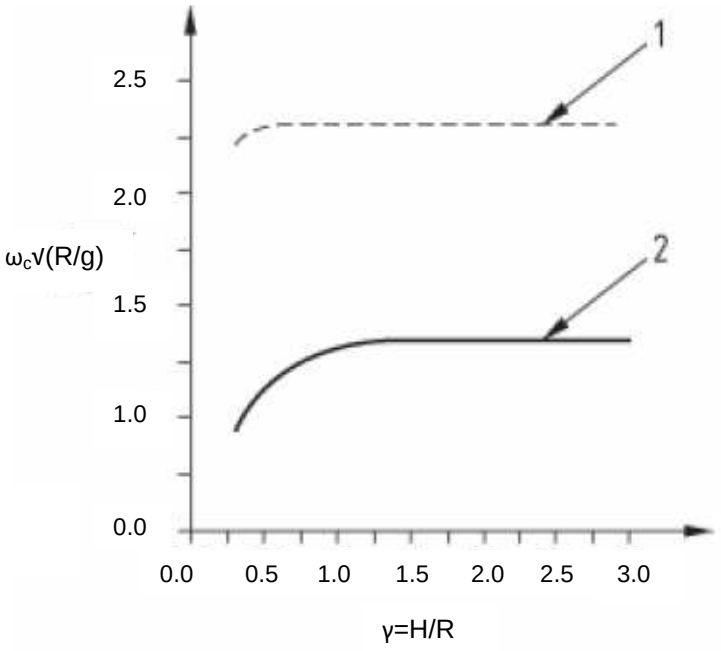

Figure 2.4: Variation of sloshing frequency with H/R ratio (Eurocode 8: Part 4, 2006)

2.2.5. LIQUID BEHAVIOUR

During the course of this project it was assumed that all surfaces are considered as free. For this reason, the behaviour of the liquid is discussed. Housner (1963) concluded that the behaviour of the tank liquid can be accurately represented with the use of two components known respectively as the impulsive and convective component in the case of free surface. The impulsive component satisfies the boundary conditions at the walls and bottom of the tank but does not include the effect of the sloshing motion of the liquid. Sloshing of the liquid results in a non-zero pressure at the original surface of the liquid and the convective component satisfies this condition without altering the boundaries of the impulsive component.

The fundamental frequency of the impulsive and convective components differ greatly which results in a weak coupling between these two components. For this reason they may be evaluated separately, with the convective pressure evaluated with the use of a rigid tank, whilst the impulsive pressure can be evaluated by analyzing the tank-liquid system while neglecting the sloshing component as proposed in Haroun and Housner (1981).

The convective component is considered as an elastic response with no hysteretic energy dissipation during an earthquake. For the convective component a behaviour factor of 1.0 is used in conjunction with the horizontal elastic response spectrum as prescribed in Eurocode 8: Part 1 (2004) according to Eurocode 8: Part 4 (2006).

The tank-liquid system comprises of the impulsive component and tank wall since the impulsive component is rigidly attached to the wall. It is assumed the tank-liquid system dissipates hysteretic energy during their response to an earthquake. The overstrength, dissipation of energy by the tank-liquid system and the local plastic deformations which may occur during the ultimate limit state are all considered with the use of a behaviour factor. The tank-liquid system is designed for the ultimate and serviceability limit states respectively. Local plastic deformation may occur during the ultimate limit state and a behaviour factor of 1.5

is used in conjunction with the design response spectrum for elastic analysis in Eurocode 8: Part 1 (2004). The structure remains elastic under serviceability loads and a behaviour factor of 1.0 is prescribed with the elastic response spectrum in Eurocode 8: Part 1 (2004).

The impulsive and convective components have a combined influence on the behaviour of the tank during seismic activity. Various methods have been proposed to combine these components, Eurocode8: Part 4 (2006) suggests the use of the "upper bound" rule in which the absolute maximum values are added. The "square root of sums" rule may be unconservative due to the wide separation between the frequency of the ground motion and sloshing motion.

2.3. RIGID OR FLEXIBLE STRUCTURE

No information is provided in any literature consulted for this study on the classification of a structure as either rigid or flexible. Steel structures are classified as flexible since the wall thickness of these structures is very small in comparison to the overall dimensions of the tank. Concrete structure may be classified as either rigid or flexible but the assumption that all concrete tanks are rigid and therefore the wall inertia may be neglected, are highly unconservative (Eurocode 8: Part 4, 2006).

In the case of rigid tanks, the tank experiences the same motion as the ground. The tank-liquid system is subjected to the peak ground acceleration while the convective component moves independently of the wall and ground.

For flexible tanks, the movement of the tank is different from the motion of the ground and the tank experiences an acceleration known as the pseudoacceleration of the system. The flexibility of the tank wall only influences the impulsive component of the liquid and is included in the calculations of the impulsive component as proposed by Veletsos (1997). The inclusion of the flexibility of the wall in the impulsive component can be attributed to two different aspects, (1) the convective component has a long period of vibration which is significantly larger than the period of the tank-liquid system or the ground motion and remains unchanged, and (2) it is assumed that the impulsive

component is rigidly attached to the tank wall and therefore experiences the same motion as the wall.

Eurocode 8: Part 4 (2006) follows a different approach from Veletsos (1997) in assuming that the impulsive and convective components remain unchanged by the flexibility of the wall and is included in the design process with the use of a “flexible” component. The “flexible” component is considered separately from the impulsive and convective components since large differences in frequency for the ground motion, sloshing motion and tank wall are obtained and the dynamic coupling between these components is relatively weak.

The major difference between Veletsos (1997) and Eurocode 8: Part 4 (2006), with regard to including the effect of wall flexibility, is the consideration of the impulsive component and flexibility of the wall as a unit by Veletsos (1997) and therefore both are subjected to the pseudoacceleration of the system instead of the peak ground acceleration. Eurocode 8: Part 4 (2006) proposes that the impulsive component remains unchanged and is subjected to the peak ground acceleration while the flexible tank wall is subjected to the pseudoacceleration.

Veletsos (1997) assumed the impulsive component and tank wall are both subjected to the pseudoacceleration of the system which may fall within the highly amplified region of the response spectrum. The method of Veletsos (1997) will therefore provide more conservative results than Eurocode 8: Part 4 (2006) which assumes only the structure experiences pseudoacceleration while the impulsive component is subjected to the peak ground acceleration which may be significantly smaller than the pseudoacceleration. With the influence of the impulsive component increasing with wall height it is recommended by Eurocode 8: Part 4 (2006) that Veletsos (1997) only be used for broad tanks with a H/R ratio smaller than 1.0 since it will provide highly conservative results for taller tanks in which the impulsive component governs the design.

Veletsos (1997) illustrated that in the case of broad tanks there are no significant difference between the results obtained for flexible and rigid tanks with regard to the impulsive component. The influence of the higher modes of vibration is also negligible for broad tanks. Significant differences in the impulsive component between flexible and

rigid structure were obtained for taller tanks and the second mode of vibration could not be neglected as illustrated in Figure 2.5. The dimensionless parameter c_{ij} is used to calculate the mass participating in the j-th mode of vibration which is plotted as a function of η, which is equal to z/H and indicates the height of a point along the tank wall.

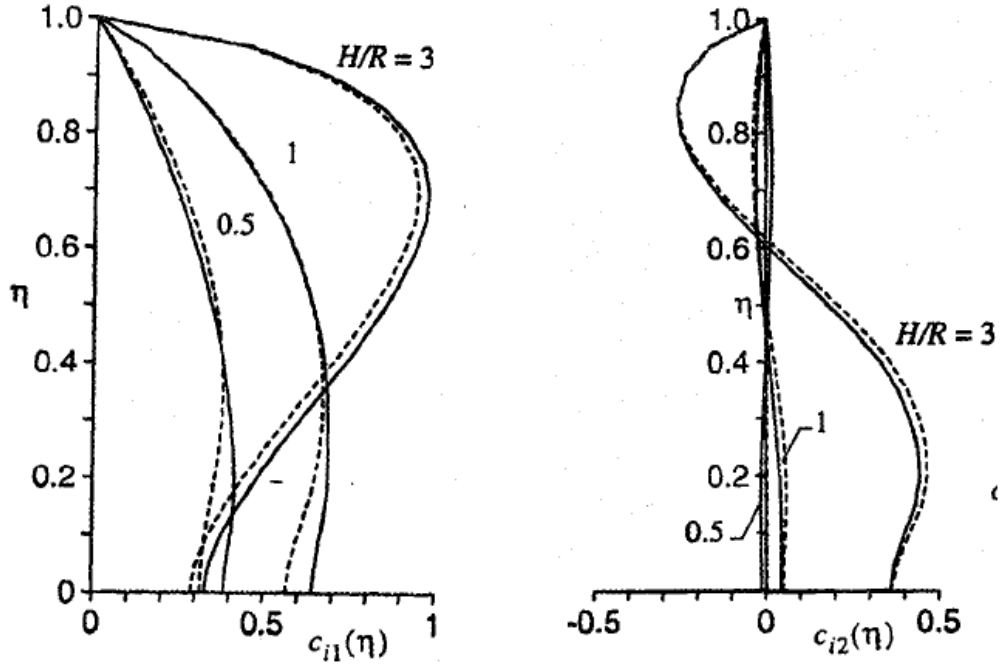

Figure 2.5: Influence of higher modes of vibration for impulsive component (Veletsos, 1997)

It should be noted, the inclusion of the influence of wall inertia differs between rigid and flexible tanks. In the case of rigid tanks the effect of the wall inertia must be considered separately from the impulsive and convective components. These inertia forces act parallel to the direction of excitation and results in a pressure normal the surface of the tank shells which may be added to the pressure resulting from the impulsive component (Eurocode 8: Part 4, 2006). The inertia effect of the tank wall is not considered separately for flexible tanks and assumed to be included with the impulsive calculations (Veletsos 1997).

No conclusive information on the classification of a circular cylindrical tank as either rigid or flexible could be found. This was further investigated in this study and all structures evaluated in the course of this project were considered as flexible with reasons provided in Chapter 8.

2.4. SOIL CONDITION

All structures analyzed in this project were considered to be rigidly supported. Flexibility of the soil may be considered but presents new challenges in terms of FE modelling. Since flexibility of the soil was not considered in this study, the influence on the behaviour of the liquid is presented briefly.

Flexibility of the soil only influences the impulsive component (Veletsos, 1997) and affects the tank-liquid system in two ways, (1) flexibility decreases the fundamental natural frequency of the system and (2) the damping of the system is increased. The rocking motion of the foundation may therefore not have a significant effect in broad tanks but may be prominent for tall tanks.

A tank is assumed to be rigidly supported if no rocking or tilting motion of foundation can occur. If rocking or tilting around an axis perpendicular to the direction of excitation is permitted, the support is viewed as flexible.

2.5. INCLUSION OF THE ROOF

In most practical cases a roof is provided over a water-retaining structure to minimize evaporation of the liquid and to prevent foreign objects from falling into the tank. During this project the influence and the weight of the roof has been neglected since experimental work completed by Haroun (1980) has indicated that the roof only restrains the top of the tank against cos (nθ) deformation with n≥2. Only the first mode of vibration with n=1, which coincides with a cantilever model, is considered in this study.

A more practical consideration is the provision of a joint between the roof and tank wall as stated by Haroun (1980). This connection is considered to be weak in order to fail in the event of overflow of the tank and the roof provides minimal restraint against horizontal motion of the tank wall. Even in dynamic behaviour, the section of wall perpendicular to the direction of excitation acts as a shear wall, supporting the roof weight and the roof does not contribute to the mass associated with bending. The negligence of the tank roof is therefore considered a safe assumption.

2.6. MODES OF VIBRATION OF FLEXIBLE TANKS

Haroun and Housner (1981) as well as Veletsos (1997) have based their philosophy of design on the assumption that the first mode of vibration of a flexible tank, in response to an earthquake, is the same as the fundamental mode of vibration of a vertical cantilever beam. Nachtigall (2003) views this cantilever model as obsolete and rather proposes the use of the shell modal forms in the design of water-retaining structures for seismic loading. The modes of vibration considered in Nachtigall (2003) and Haroun (1980) are presented to aid in the understanding of the behaviour of a circular cylindrical tank subjected to horizontal seismic excitation.

According to Nachtigall (2003) a flexible circular cylindrical tank with normal loads acting on the structure tend to vibrate in two directions namely in the axial (wave number m) and circumferential (wave number n) directions. The direction of vibration is dependent on the frequency of the seismic excitation and can be graphically represented as shown in Figure 2.6. The height/radius ratio and wall thickness ratio for the structure depicted in Figure 2.6 are unknown, but the parametric study of Nachtigall (2003) consisted of a height/radius ratio varied between 2 and 100 with the wall thickness ratio varied between 20 and 500. The modes of vibration shown in Figure 2.6 were determined specifically for steel tanks. For design purposes the circumferential wave numbers between 5 and 25 should be considered since recent tank failures have occurred due to resonance effects.

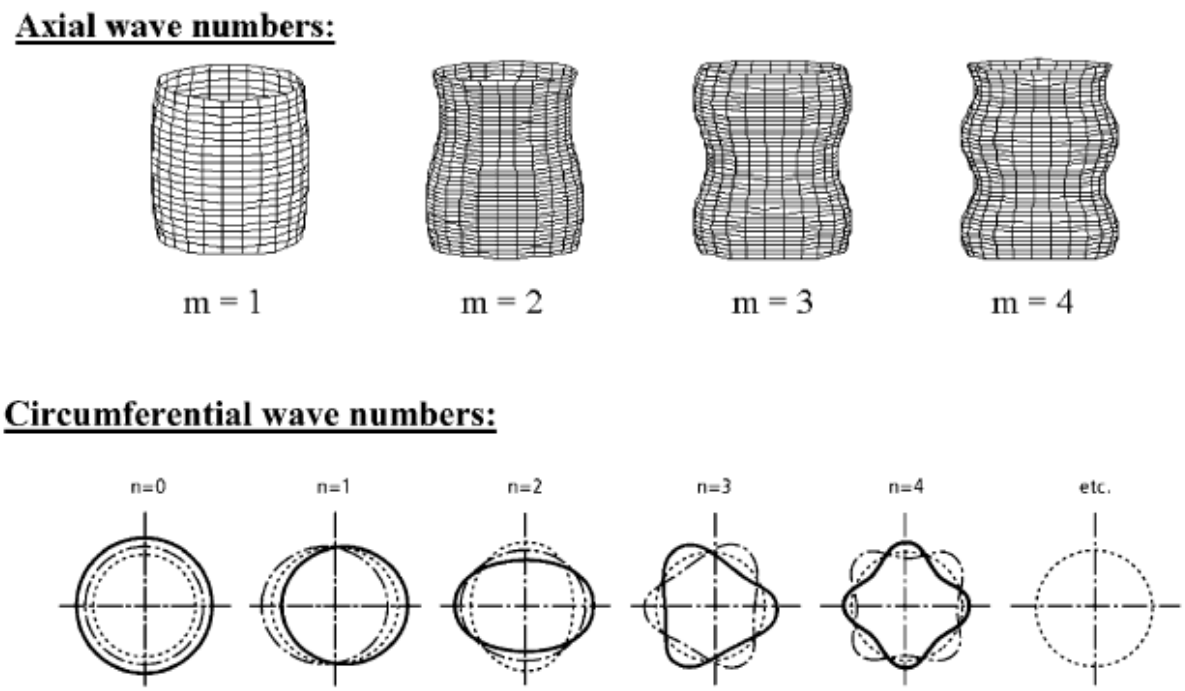

Figure 2.6: Modes of vibration according to Nachtigall (2003)

The vertical cantilever model is adopted by Veletsos (1997), Haroun (1980) and Eurocode 8: Part 4 (2006). The tank-liquid system is considered to be a single degree of freedom system and assumed to have the same fundamental mode of frequency as that of a vertical cantilever beam. Figure 2.7 illustrates both the axial and circumferential modes of vibration as assumed by the above mentioned authors. Fischer (1999) supports the use of a vertical cantilever model. However, the shape of deformation differs between broad and tall tanks, with broad tanks exhibiting a typical "concave" deformation shape while the deformation of tall tanks becomes more or less linear in displacement along the height of the wall.

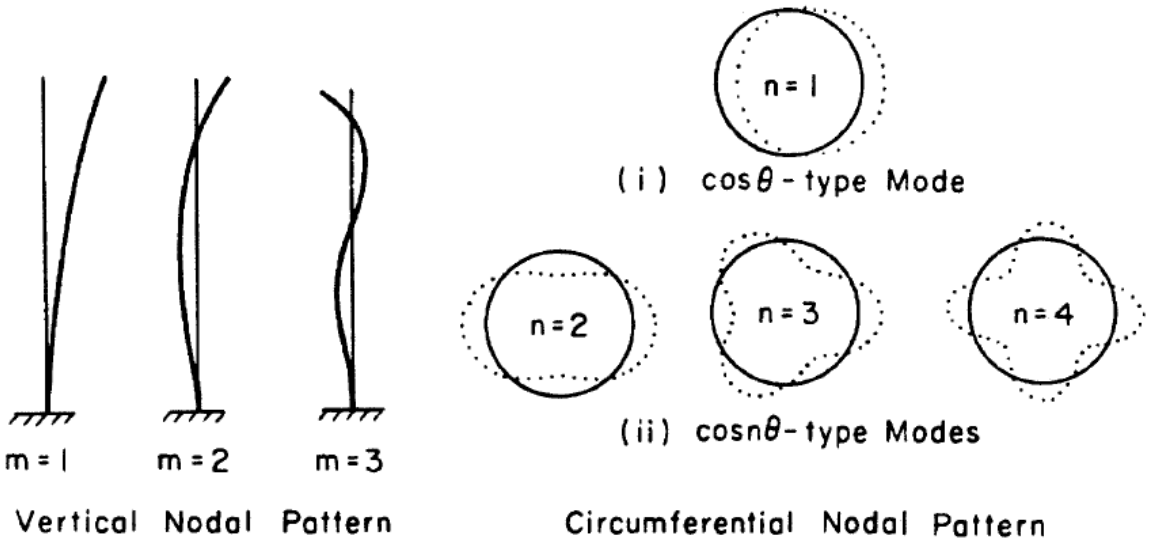

Figure 2.7: Modes of vibration according to Haroun (1980)

Barton and Parker (1987) made use of FE models consisting of shell elements and liquid elements to predict the seismic behaviour of a tank filled with water. They concluded that for tanks with a H/R ratio greater than 0.5, the behaviour can be accurately predicted with the use of only the first mode of vibration if the deformation form cos (nθ) is used. The higher modes have very small participation factors and are not important in predicting the behaviour of a tank under horizontal seismic excitation.

Practical experiments completed by Haroun (1980) have indicated the buckling of tanks are mostly dependent on the n=1 response which coincides with the cantilever model. The higher modes of vibration with n≥2 have a secondary influence on the response of tanks during dynamic loading and may be neglected.

2.7. PRACTICAL MATERIAL PROPERTIES AND DIMENSIONS

Some practical information with regard to tank dimensions and material properties used by South African designers (Van Dalsen, 2009) was gathered. These can be summarized as follows:

- Circular cylindrical tanks are used for tanks with a storage capacity of 15-20 megaliter. For smaller capacity tanks a rectangular shape is used.
- South Africans designers generally use a H/R ratio of 0.5 with the wall thickness varying between 250-300 millimetres.

- For water-retaining structures a concrete cover of 40 millimetres is sufficient.
- The minimum concrete cube strength required for water-retaining structures is 35 MPa and reinforcement yield strength of 450 MPa.

2.8. STATIC ANALYSIS ACCORDING TO GHALI (1979)

In order to determine whether the seismic design of water-retaining structures in South Africa is a dominant loading condition, the dynamic results in terms of hoop stress and bending moment were compared with results obtained for the static analyses. The area of reinforcement required for dynamic and static design was also compared and therefore a brief summary of the static design of water-retaining structures is presented in the following section.

Ghali (1979) provides information on the analysis of liquid-retaining structures for static conditions. In order to compile a method for the evaluation of the structure, simplifications of the numerical model were made as well as some assumptions. The contained liquid exerts a radial pressure on the wall. The intensity of the pressure varies linearly along the height of the wall but remains constant along the circumference of the cylindrical wall. The pressure acts perpendicular to the tank shells and remains normal to the surface even during bending and consequent deformation of the shell. During the static design of a water-retaining structure it is assumed the tank material behaves in a linear elastic manner since the wall thickness is small in comparison to the overall dimensions of the structure.

An analytical method is presented by Ghali (1979) for the evaluation of circular cylindrical tanks subjected to hydrostatic pressure. The hydrostatic pressure results in an outward deflection of the wall, producing a hoop force which varies along the height of the wall. Depending on the fixity of the wall edges, radial shear forces and bending moments are produced along the height of the wall.

For analytical purposes it is sufficient to consider an element strip of one meter along the circumference of the wall. The elemental strip behaves as a beam on an elastic foundation subjected to reaction forces produced by the hoop force and is proportional to the deflection of the wall at a specific point. A differential equation relating the

deflection of the wall to the applied forces can be derived. The reactions at the wall edges and internal forces in the wall can be obtained from the equation for deflection. The method followed by Ghali (1979) in the derivation of the relevant equations as mentioned, is summarized below. For the derivation of equations specific to various boundary conditions, refer to the book published by Ghali (1979). The general equation for the deflection of the wall is summarized below with the use of a number of steps.

Step 1: A strip of unit width is considered along the circumference of the tank wall. The strip is loaded with a force per unit area with intensity q. The force applied to the strip is representative of the contained liquid otherwise known as the hydrostatic pressure and assumed to vary linearly along the height of the wall but not along the circumference of the tank. The notations used for the various tank dimensions and the hydrostatic load are illustrated in Figure 2.8.

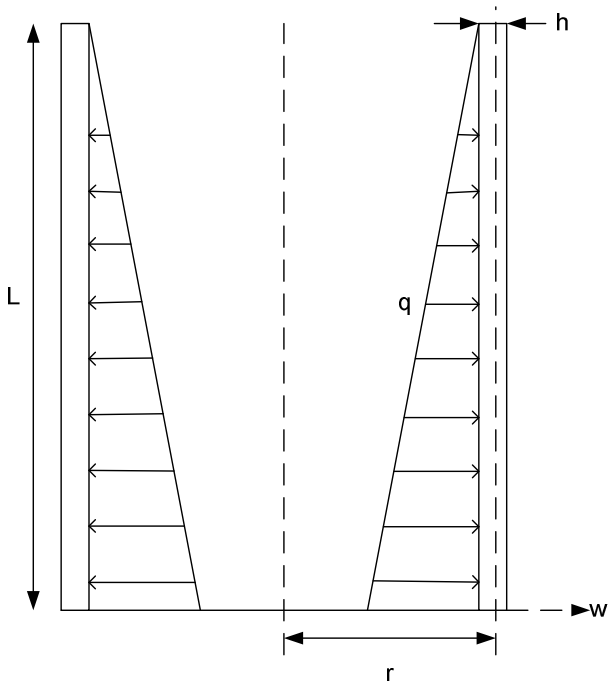

Figure 2.8: Notation of symbols defined in Ghali (1979)

The hydrostatic pressure results in an outward deflection w, resulting in a hoop force N and an increase in the tank radius r. The strip is considered as a beam on an elastic foundation and due to the hoop force a resulting force $\bar{q}$ is applied to the strip which is proportional to the deflection at any point along the wall.

The hoop force and reaction force are illustrated in Figure 2.9 and may be written in mathematical terms as:

Hoop force: $N = \frac{Eh}{r}w$ eq 2.1

Reaction force: $\bar{q} = -\frac{N}{r} = -\frac{Eh}{r^2}w$ eq 2.2

With N = hoop force

E = modulus of elasticity of wall material

h = thickness of wall

w = outward deflection of wall

r = radius of tank

$\bar{q}$ = resulting force

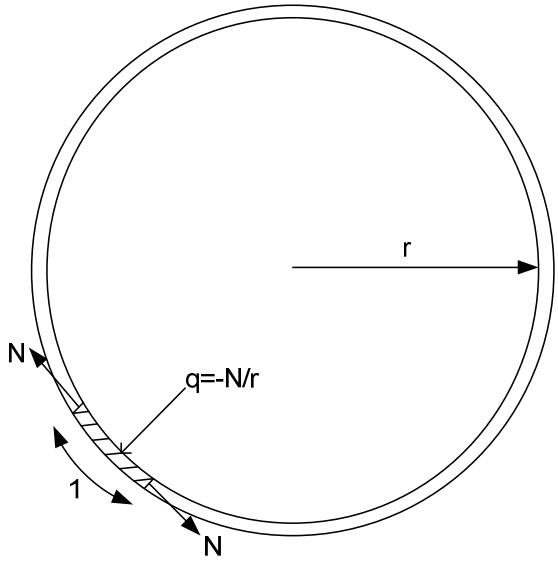

Figure 2.9: Plan view of circular tank used in Ghali (1979)

Step 2: Bending stiffness of the beam

A positive bending moment M, around the global horizontal axis is produced at the base of the wall due to the hydrostatic pressure applied along the height of the wall. Due to bending of the elemental strip, tensile stresses are produced along the inner face of the wall with compressive stresses on the outer face of the wall. The outer edges of the elemental strip tend to rotate out of the

original radial plane due to the Poisson effect. The rotation of the strip edges is, however, restricted due to the symmetry of the wall and lateral extension of the strip is prevented.

An elemental strip is considered for the numerical method and a restraining bending moment M_ϕ around the global vertical axis is applied in consideration of the symmetry of the structure. The restraining moment M_ϕ, is equal to νM and is equivalent to an increase in the modulus of elasticity by the ratio $1/(1-\nu^2)$, with ν equal to the Poisson ratio of the tank material. The resulting moment applied to the elemental strip is therefore smaller than the moment produced by the hydrostatic pressure and smaller deflections will be obtained for the resulting moment than the bending moment from pressure. The reduced deflection of the elemental strip is considered with the use of a higher modulus of elasticity and the flexural stiffness may be written as:

$$EI = \frac{Eh^3}{12(1-\nu^2)} \qquad \text{eq 2.3}$$

Step 3: Derivation of equation for deflection

The elemental strip is considered to be an Euler-Bernoulli beam for which is it assumed that the plane cross-section of the beam remains plane during bending. The bending moment and beam deflection are related with:

$$M = -EI\frac{d^2w}{dx^2} \qquad \text{eq 2.4}$$

The shear force, bending moment and resultant transverse load are related with:

$$V = \frac{dM}{dx} = -\frac{d}{dx}\left(EI\frac{d^2w}{dx^2}\right) \qquad \text{eq 2.5}$$

$$\frac{dV}{dx} = \frac{d^2M}{dx^2} = \frac{d^2}{dx^2}\left(EI\frac{d^2w}{dx^2}\right) \qquad \text{eq 2.6}$$

$$\frac{dV}{dx} = -(q+\bar{q}) \qquad \text{eq 2.7}$$

$$\frac{d^2}{dx^2}\left(EI\frac{d^2w}{dx^2}\right) = -\left(q - \frac{Eh}{r^2}w\right) \quad \text{eq 2.8}$$

$$\frac{d^2}{dx^2}\left(EI\frac{d^2w}{dx^2}\right) + \frac{Eh}{r^2}w = q \quad \text{eq 2.9}$$

For beams with a constant flexural stiffness, the equation for the elastic line can be written as:

$$EI\frac{d^4w}{dx^4} + \frac{Eh}{r^2}w = q \quad \text{eq 2.10}$$

Based on the general differential equation for deflection of the beam due to an applied load, design tables were compiled for elemental strips with various edge conditions. These edge conditions may be considered to be either free, hinged or fixed supports. For the purposes of this research project the design tables provided in Ghali (1979) were used and therefore some information is provided on the use of these tables.

The design tables compiled by Ghali (1979) are usable for circular tanks with walls of either constant or varying thickness. The tables were compiled for concrete with a Poisson ratio equal to 1/6. A Poisson ratio of 1/5 has a negligible effect on the values presented in these design tables. All tabulated values are dimensionless and can be used for systems with any units.

The loading patterns considered for the compilation of the tables were uniformly distributed loads and linearly varying loads along the height of the wall. The hoop force, bending moments and shear forces at intervals of 1/10 of the wall height can be calculated with the use of the design tables.

Both short and long cylinders, otherwise known as broad and tall tanks, can be analysed with the tables presented in Ghali (1979). However, the tables only provide information for a dimensionless parameter η, between 0.4 and 24, with $\eta = \frac{L^2}{2r.h}$, refer to Figure 2.10 for a definition of the symbols.

In most practical cases the value of η ranges between 4 and 24 but for tall tanks this value may be greater than 24. The values of η for this study ranged between a value of

1.5 and 187.4 for the tall structures with very thin walls. It can be shown that for η values greater than 7.3, forces applied at one edge of the wall have a negligible effect on the other end of the wall since these forces die out along the height of the wall. For tall tanks with η greater than 24, the structure may be regarded as consisting of 2 cylinders with the bottom cylinder having a height of $l_1 = \sqrt{24.2r.h}$ with a corresponding hydrostatic pressure applied over the length l_1 as illustrated in Figure 2.10. The values provided in the design tables of Ghali (1979) may still be used with η equal to 24 for tall tanks.

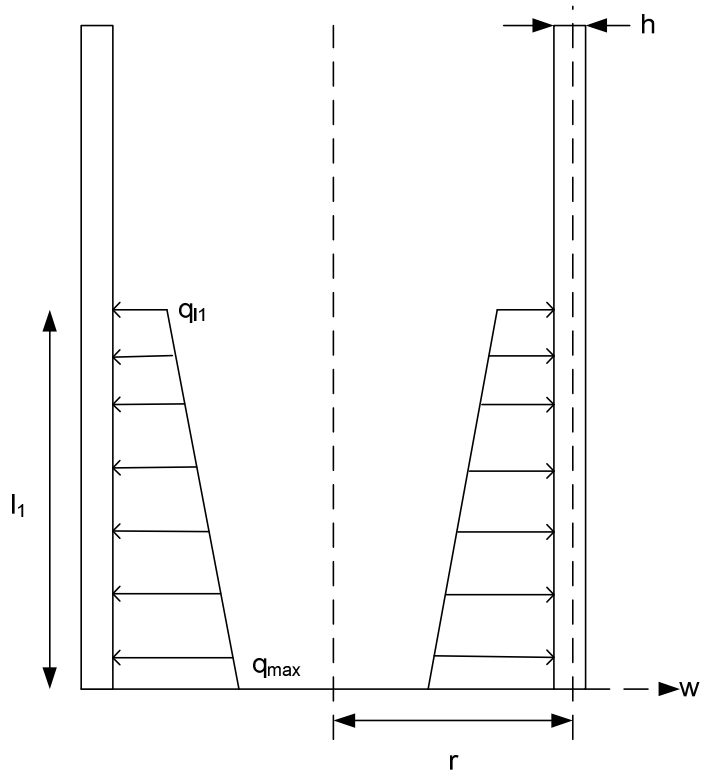

Figure 2.10: Pressure distribution for tall tanks (Ghali, 1979)

2.9. DYNAMIC ANALYSIS WITH EUROCODE 8: PART 4 (2006)

Currently water-retaining structures in South Africa are only designed for static loading and in order to determine the influence of seismic loading on these structures, the results from the static analyses were compared with the results obtained for the seismic analyses in terms of the hoop stress and bending moment in the tank wall. Two numerical methods were used for the seismic analysis of a structure, namely Eurocode

8: Part 4 (2006) and Veletsos (1997). This section provides more information on the seismic analysis of a structure with the use of Eurocode 8: Part 4 (2006).

A series of steps is defined in Eurocode 8: Part 4 (2006) to determinate the hydrodynamic loads and resulting forces acting on a water-retaining structure due to seismic excitation. This section provides information on the individual steps with step 1 to 7 applicable to the ultimate limit state and step 8 to the serviceability limit state. The steps include:

Step 1: Tank dimensions and material properties

The tables provided in Eurocode 8: Part 4 (2006) were compiled for tanks with H/R ratio's ranging between 0.3 and 3. Restrictions on the H/R ratio's of tanks are therefore provided. In this study the height/radius ratio was varied between 0.3 and 1.5.

Step 2: Sloshing and wall frequency

The frequency of the sloshing motion is required to determine the pseudoacceleration experienced by this component during seismic excitation. The convective component is considered to be elastic and the elastic response spectrum in Eurocode 8: Part 1 (2004) is applicable which is dependent on the peak ground acceleration. For the serviceability limit state the reduction factor must also be considered, depending on the importance class of the structure as defined in Eurocode 8: Part 4 (2006).

The frequency of the tank-liquid system is different from that of the ground motion in the case of flexible tanks. The frequency of the tank-liquid system is required to determine the pseudoacceleration experienced by the structure either from the design response spectrum for the ultimate limit state or the elastic response spectrum for the serviceability limit state as provided in Eurocode 8: Part 1 (2004). Even though local plastic deformations may occur during the ultimate limit state, the overall response of the tank-liquid system may be considered to be elastic and therefore the response spectrum is used for the ultimate limit state in conjunction with a behaviour factor equal to 1.5. The structure remains elastic under serviceability loads due to restrictions on

the allowable crack width and the elastic response spectrum is used with a behaviour factor equal to 1.0 and consideration of the reduction factor appropriate for the importance class assigned to the structure.

Step 3: Effects of impulsive component

The impulsive component is subjected to the peak ground acceleration and moves rigidly with the tank wall. The mass associated with this component is determined along with the height at which this mass is situated to produce the correct base shear force and overturning moment. Due to the acceleration of the impulsive mass, a horizontal shear force Q_i, at the base of the tank wall is produced along with an overturning moment Mi about the global horizontal axis, resulting from the eccentricity of the impulsive mass with respect to an axis perpendicular to the direction of excitation. Eurocode 8: Part 4 (2006) and Veletsos (1997) provides information on the calculation of two overturning moments. M_i refers to the rotation of the tank alone about an axis perpendicular to the direction of excitation while M_i' refers to the overturning of the structure including the foundation, both resulting from the hydrodynamic pressure on the wall. A height h_i' is used to calculate this overturning moment M_i'. Both of these concepts are illustrated in Figure 2.11 and Figure 2.12.

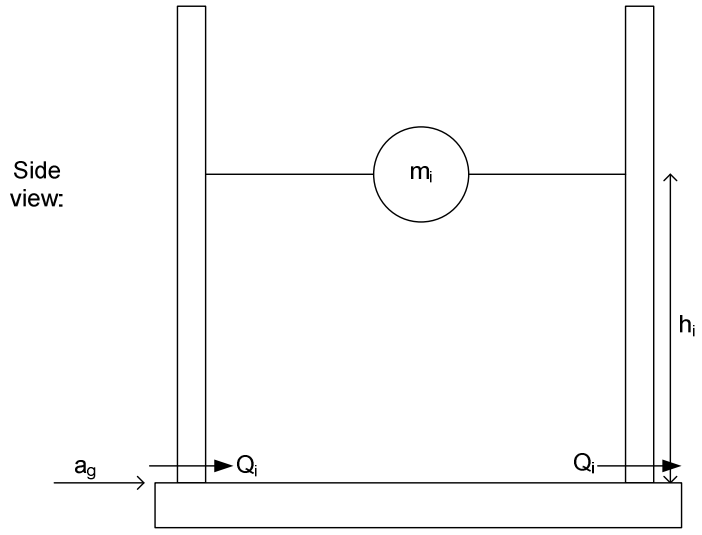

Figure 2.11: Base shear force associated with impulsive component

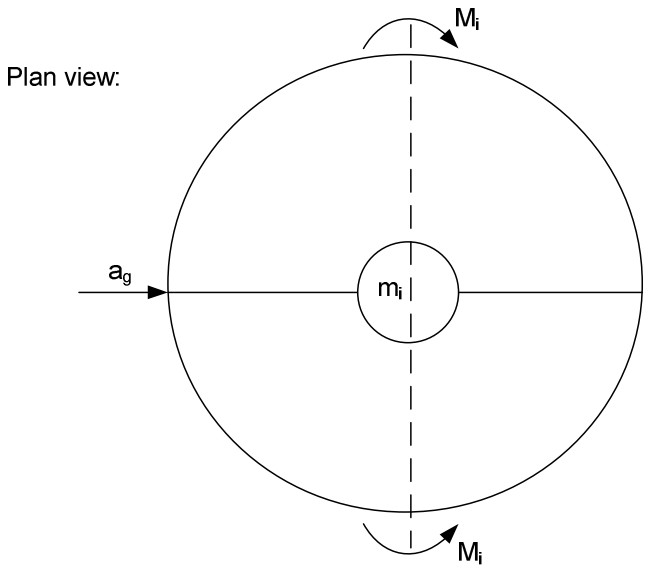

Figure 2.12: Overturning moment associated with impulsive component

The ratio of the impulsive mass to total liquid mass increases as the H/R ratio increases, reaching nearly total liquid mass for tall tanks. This can be attributed to the restriction of the convective component to the liquid surface in tall tanks. The height h_i, at which the impulsive mass is placed to produce an overturning moment above base remains relatively constant with an increase in the H/R ratio and is a little less than midheight of the tank wall. Figure 2.13 illustrates the increase of the impulsive mass as well as impulsive height with H/R ratio with the solid line referring to h_i and the dashed line to h_i'. The impulsive mass is denoted by m_i and the total contained liquid mass by m.

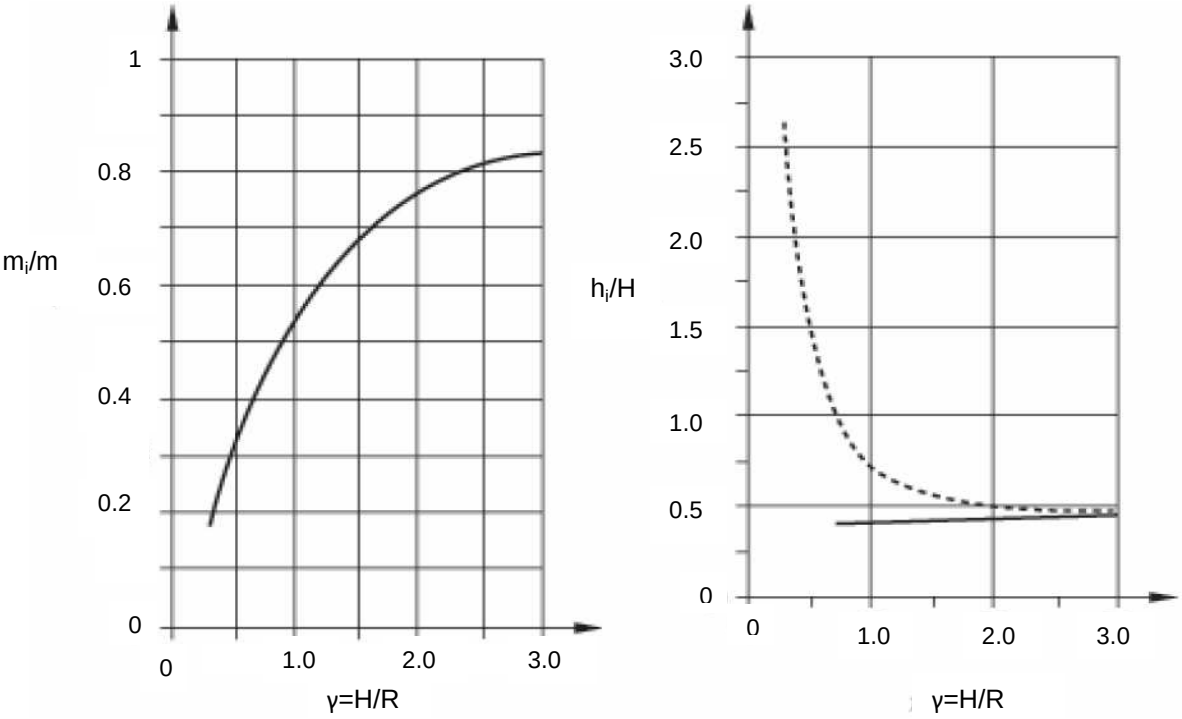

Figure 2.13: Variance of m_i and h_i with H/R ratio (Eurocode 8: Part 4, 2006)

Step 4: Effects of convective component

The respective frequencies of the sloshing component are calculated with the use of the corresponding roots λ, defined as the first derivative of the Bessel function of the first kind and first order. For design purposes it is only necessary to consider the first mode of vibration and therefore λ_1=1.841 (Eurocode 8: Part 4, 2006).

The convective component has a significant influence, in broad tanks, on the hydrodynamic loads down to the tank bottom, while it is mostly restricted to the liquid surface for tall tanks. The mass associated with the convective component decreases with increased H/R ratios which correspond to an increase in the impulsive mass. This is consistent with step 3. The variance of the convective mass as well as the height, at which the convective mass is placed, is presented in Figure 2.14. The solid line in Figure 2.14 is used for parameters associated with the first mode of vibration while the dashed line is associated with the second mode of vibration.

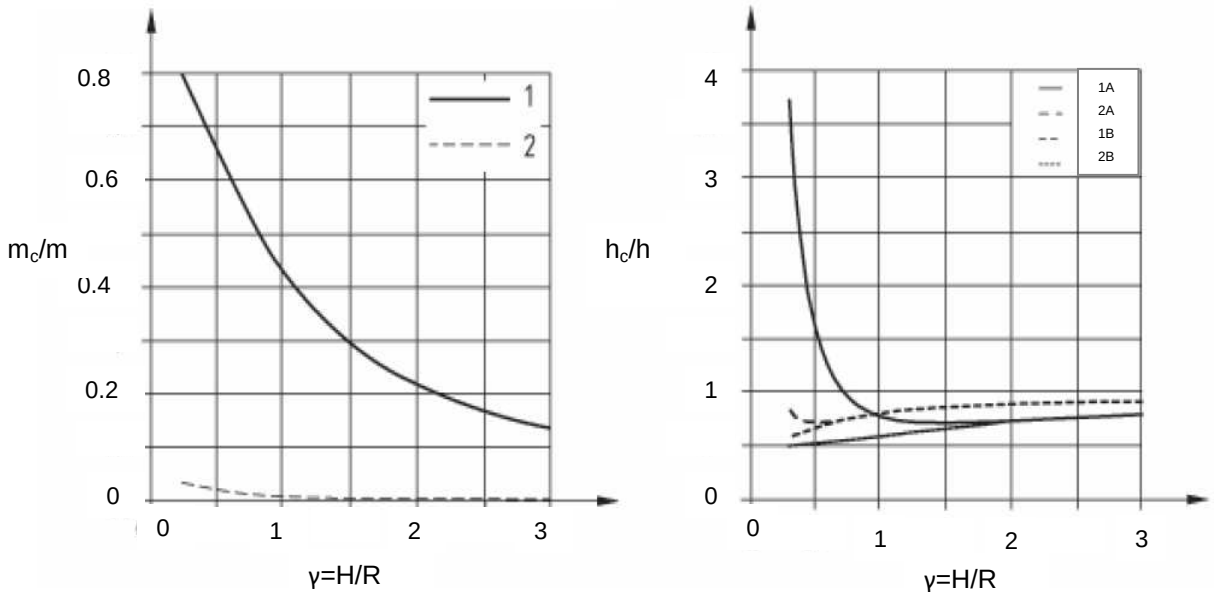

Figure 2.14: Variance of m_c and h_c with H/R ratio (Veletsos, 1997)

The convective mass is not rigidly attached to the tank wall, since this component is by no means influenced by the flexibility of the wall and the frequency differs from that of the tank-liquid system or ground motion. In a finite element model, the convective component may be attached to the wall with the use of springs with a prescribed stiffness which corresponds with the frequency of the sloshing motion. This is illustrated in Figure 2.15 and Figure 2.16.

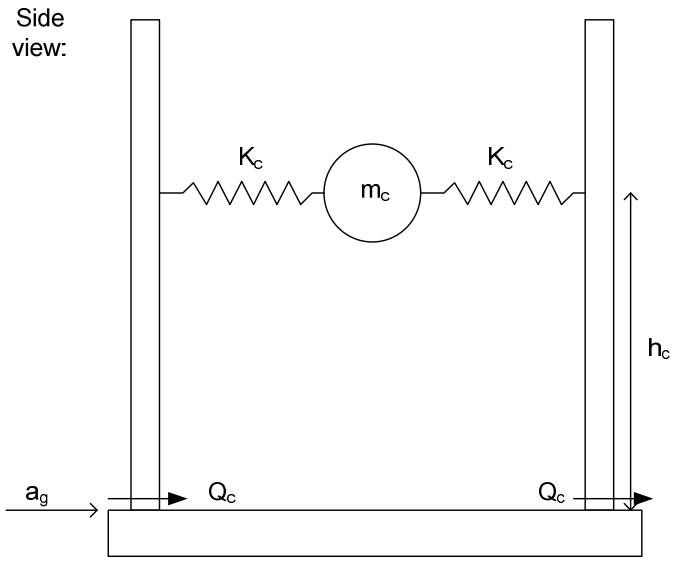

Figure 2.15: Base shear force associated with convective component

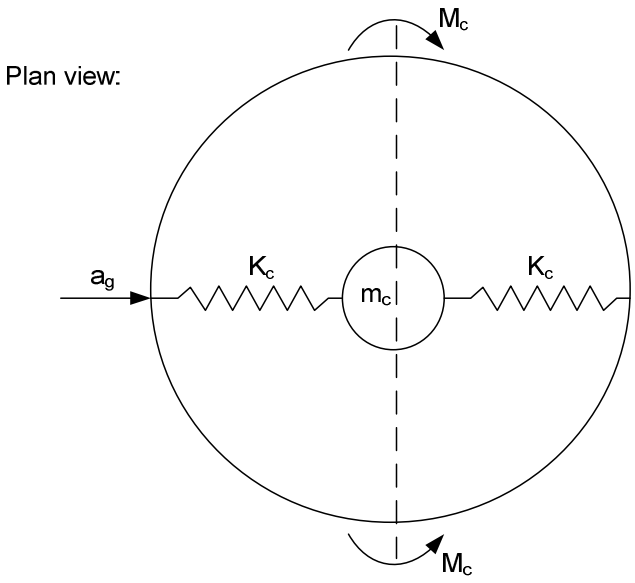

Figure 2.16: Overturning moment associated with convective component

Step 5: Effects of flexibility of the wall

In the case of rigid structures, step 5 is ignored since only the impulsive and convective components exists and needs to be considered for design purposes.

For design purposes it is sufficient to only consider the fundamental or first mode of vibration in the case of flexible walls (Eurocode 8: Part 4, 2006). The tank is subjected to horizontal excitation from the earthquake but due to the flexibility of the wall, the tank wall does not experience the same acceleration as the ground but is rather subjected to its relevant pseudoacceleration, which may be highly amplified with respect to the peak ground acceleration. Due to the increased value of the pseudoacceleration with respect to the ground peak acceleration, the contribution of the "flexibility" may be the governing contribution to the hydrodynamic pressure exerted on a wall during horizontal seismic excitation.

Pressure resulting from the flexibility of the wall produces a base shear force Q_f, as well as an overturning moment M_f, above the base. The flexibility mass m_f and height of placement h_f can be calculated and the layout is similar to that of the impulsive component as shown in Figures 2.11 and 2.12.

Step 6: Effect of wall inertia

The inertia effects of the tank wall are small in comparison to the hydrodynamic forces and may be neglected in the case of steel tanks. However, for concrete tanks the loads resulting from wall inertia may be significant and needs to be considered for design purposes.

Pressure resulting from the wall inertia is added to that of the impulsive component. In a similar way the base shear force and overturning moment resulting from the inertia effect of the tank wall is added to that of the impulsive component.

Step 7: Combination of the respective components

Eurocode 8: Part 4 (2006) suggests when combining the action effects of the various components, affecting the hydrodynamic pressure, the absolute values should be added to provide an upper bound estimate. The "square root of sums" rule may be unconservative due to the wide separation in frequency between the different components.

Step 8: Height of the convective wave

It is important to provide adequate freeboard when considering the serviceability limit state, in order to avoid damage to the roof or spillage of the liquid in the absence of a roof. The freeboard height is determined by the height of sloshing wave and only first mode of vibration needs to be considered (Eurocode 8: Part 4, 2006).

2.10. DYNAMIC ANALYSIS WITH VELETSOS (1997)

The method proposed by Veletsos (1997) differs slightly from that of Eurocode 8: Part 4 (2006) with the inclusion of the flexibility of the tank wall. For this reason the method presented by Veletsos (1997) is presented in much detail in the following section. Both methods were used for the numerical calculations and subsequent comparison of forces and other parameters. The design steps by Veletsos (1997) include the following:

Step 1: Define tank dimensions and material parameters

Research material presented by Veletsos (1997) contains information for tanks with a H/R ratio ranging between 0.3 and 3. Both steel and concrete tanks are discussed in his work and a concrete reference tank with a t_w/R ratio of 0.01 and Poisson's ratio of 0.17 is used. An equation is provided to correlate the information for the reference tank to that of the actual structure being analyzed. In order to achieve accurate results, a tank with parameters close to the reference model used by Veletsos (1997) is preferable.

Step 2: Determine natural frequency of tank-liquid system

The natural frequency of both the tank-liquid system, in the case of flexible tanks, as well as the sloshing frequency is determined in order to obtain the pseudoacceleration that each component is subjected to. It should be noted that the effect of wall inertia is neglected when calculating the tank-liquid system frequency. These pseudoaccelerations are determined with the use of the relevant response spectrums as presented in Eurocode 8: Part 1 (2004). The reduction factor is applicable to the serviceability limit state and lowers the pseudoacceleration to which the various components are subjected during seismic activity.

Step 3: Contribution of impulsive component

In the case of rigid tanks the tank-liquid system is subjected to the peak ground acceleration and the influence of wall flexibility is not considered. For flexible tanks the flexibility of the wall has a significant influence on the magnitude of the hydrodynamic pressure acting on the tank wall and should be included in the design process.

The flexibility of the tank wall is not considered separately as in the case of Eurocode 8: Part 4 (2006) but is rather included in the computation of the impulsive component with the use of the pseudoacceleration instead of the peak ground acceleration. Hydrodynamic wall pressure in flexible tanks is usually greater than in rigid tanks since the natural period of most tanks falls within the highly amplified region of the response spectrum. It is therefore unconservative to regard concrete structures as rigid structures.

The impulsive mass m_i, is relatively easy to obtain for rigid tanks and refers only to the liquid mass moving in combination with the wall. The mass of the wall is considered separately in terms of wall inertia. This is not the case with flexible tanks since the impulsive mass m_{ij}, refers to the sum of the wall mass and impulsive mass which participates in vibration mode j. Wall inertia is not considered as a separate component during the design of flexible structures. The variation of the impulsive mass m_{ij} for flexible tanks is shown in Figure 2.17 with j indicating the mode of vibration. The total contained liquid mass is denoted by m, the height up to the free liquid surface H and the tank radius by R.

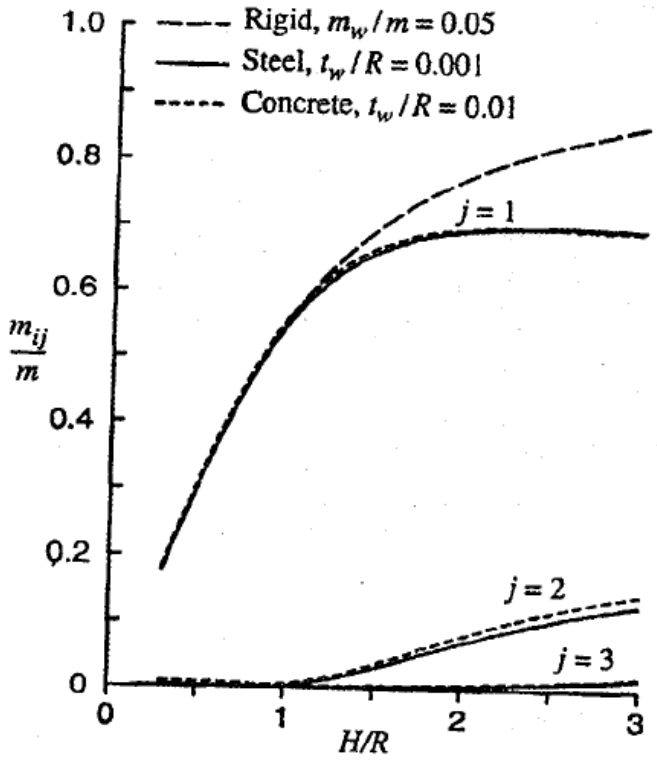

Figure 2.17: Variation of flexible impulsive mass with H/R ratio (Veletsos, 1997)

Due to the acceleration experienced by the impulsive mass a shear force Q_i, is produced at the base of the wall along with an overturning moment M_i, around an axis perpendicular to the direction of excitation. Veletsos (1997) suggests the inclusion of the second mode of vibration for tanks with a H/R ratio equal to one or greater as illustrated in Figure 2.5, since the dimensionless parameter c_{ij} increases with increasing H/R ratios.

Step 4: Contribution of convective component

The influence of the convective component on the hydrodynamic wall pressure and resulting forces is calculated in the same way as that proposed by Eurocode 8: Part 4 (2006).The decrease in convective mass with increasing H/R ratio is illustrated in Figure 2.18 and can be attributed to the superficial influence of the convective component in tall tanks. The total contained liquid is denoted by m, the impulsive mass by m_i, the convective mass for the first mode of vibration by m_{c1} and for the second mode by m_{c2}. The height up to the free liquid surface is denoted by H and the tank radius by R.

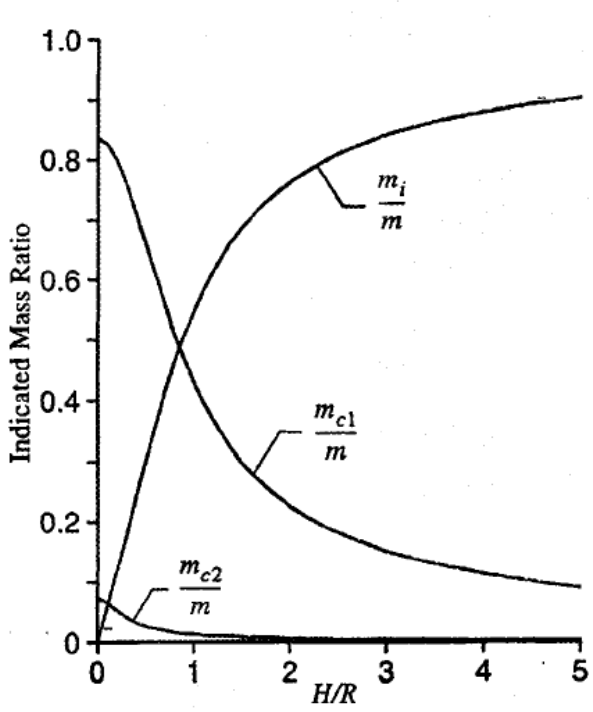

Figure 2.18: Variance of impulsive and convective mass with H/R ratio (Veletsos, 1997)

Step 6: Effect of wall inertia

The influence of wall inertia on the pressure applied to a wall is considered separately in the case of rigid tanks and may not be neglected. For flexible tanks the inertia effect of the wall is included in the computation of the impulsive component. However, as stated in Eurocode 8: Part 4 (2006) the method of analysis presented by Veletsos (1997) provides an upper bound estimation of the hydrodynamic pressure and resulting forces and are overly conservative. The method of Veletsos (1997) is especially over-conservative in the case of tall

tanks since the impulsive component governs the behaviour of the structure and therefore wall inertia should be neglected.

Step 7: Combination of the respective components

The upper bound rule of adding the absolute values of the impulsive and convective component is used as in the case of Eurocode 8: Part 4 (2006).

Step 8: Height of the convective wave

Consideration and provision of adequate freeboard is of great importance for the serviceability limit state. All modes of vibration of the convective component needs to be considered for the calculation of the freeboard, however, as shown previously the higher sloshing modes may be neglected for tall tanks due to the superficial influence of the sloshing component.

2.11. DYNAMIC FE MODELLING

The accurate prediction of the fundamental frequency of the water-retaining structure under horizontal seismic loading is of critical importance. One of the aims of this study is to investigate and propose a suitable FE model which is reliable and accurate with the prediction of the fundamental frequency. Various models have been proposed, with the most significant of these being the model used by Nachtigall (2003) and a model proposed by Virella (2006).

The first model proposed by Nachtigall (2003) explores the possibility of applying the inertia force, generated by the liquid during horizontal excitation, as a separate external force acting perpendicular to the shell elements in a structure. This model is complex since the inertia forces generated by the liquid differs with every mode shape of the structure. The second model proposed by Nachtigall (2003) seems more feasible since the impulsive mass of the liquid is uniformly added to the tank wall, implying that the effective density of the wall is increased. With the increased effective density of the wall, the fundamental frequency of the tank can be determined in the same manner as that of empty tanks.

Virella (2006) proposes a more complex FE model which is further discussed in the following section.

2.12. FE MODELLING – VIRELLA (2006)

An article published by Virella (2006) on the FE modelling of water-retaining structures subjected to seismic excitation was primarily used during this project. The aim of their research was to investigate the various modes of vibration, mode shapes as well as the response of the tank to dynamic loading. However, the structures investigated by Virella (2006) were steel tanks and therefore some uncertainty existed regarding the use and accuracy of these models for concrete structures. A brief summary is presented here of the assumptions, FE package and conclusions drawn by Virella (2006) on FE modelling of steel tank for seismic loading.

An accurate representation of the seismic behaviour of a tank is critical, since a study completed by Nachtigall (2003) has indicated that most tank failures subjected to seismic excitation due to resonance effects. The FE modelling for the determination of the natural frequency of the tank-liquid system is therefore essential.

Three models were considered in Virella's (2006) work in terms of their respective H/R ratios namely, (1) H/R equal to 0.8, (2) H/R equal to 1.26 and (3) H/R ratio equal to 1.9. In all instances the FE package ABAQUS (2002) was used to complete the analyses of all three models. Simplifications of the FE model include:

- Consideration of only the impulsive component since Housner (1963) suggested the separation of the impulsive and convective components and separate evaluation of the components with fairly accurate results.
- Only anchored tanks were considered by Virella (2006) which indicates that no uplifting or rotation of the foundation was permitted. For this reason the base plate of the tank was not modelled.
- Hydrostatic pressure and self-weight of the structure are considered.

In order to obtain a model for the analysis of a tank subjected to seismic loading, a number of steps were followed. These steps include:

Step 1: Determine hydrodynamic pressure

Only the impulsive hydrodynamic pressure exerted on the tank wall was used during this study. The method presented by Veletsos (1997) in determining the impulsive pressure for rigid tanks was used which has a cosine distribution along the height of the wall as well as along the circumferential direction as illustrated in Figure 2.19.

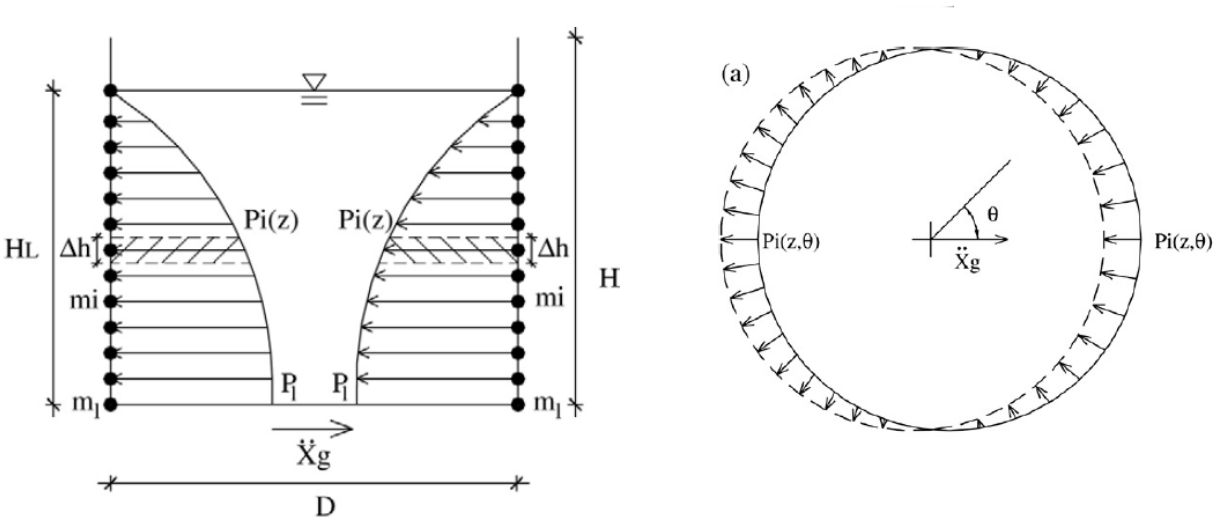

Figure 2.19: Distribution of the impulsive pressure (Virella, 2006)

Step 2: Determination of the impulsive mass

The natural frequency of vibration can be calculated as $\omega = \sqrt{k/m}$ with m equal to the mass participating in the fundamental mode of vibration. The pressure applied to a structure cannot be directly considered in the determination of the natural frequency of a structure even though it may have a significant influence. For this reason it is important to calculate the impulsive mass participating in the fundamental mode of vibration.

A series of nodes is located along the height of the wall with the edge nodes located at the top and bottom of the wall and the internal nodes located between the two edge nodes. The impulsive mass moving rigidly with the wall can be calculated for each node with $m_i = \frac{P_i \Delta h}{a_g}$ for internal nodes and $m_i = \frac{P_i \Delta h}{2a_g}$ for edge nodes. The maximum impulsive mass is determined from the maximum impulsive pressure which acts in the direction of excitation and the

distribution of the impulsive mass along the height of the wall will be similar to that of the impulsive pressure.

The impulsive pressure varies along the circumference of the wall but the impulsive lumped masses are not distributed in the same way along the circumference but rather remain constant. This presents two problems, firstly the impulsive mass is representative of the pressure which always acts perpendicular and only has an inertia effect normal to the surface of the shell element. The impulsive mass should therefore always remain perpendicular to the shell element even after deformation. Secondly, the contribution of the impulsive mass to the mode of vibration varies with the circumferential angle. If the variance of the lumped masses are neglected with only the maximum impulsive mass attached to all nodes, it implies that twice the actual mass of the liquid participates in the mode of vibration.

The solution is the use of rigid pinned links between the lumped impulsive mass and the shell node, with movement of the lumped mass restricted to the radial direction and rotation of the mass. The lumped masses are supported in the vertical and tangential direction. With the proposed model, the total mass participating in the mode of vibration is half the mass attached to the structure. The lumped masses in the direction of excitation contribute primarily to the frequency of vibration while the masses perpendicular to the direction of excitation have no contribution. The contribution of the masses therefore decreases with an increase in circumferential angle. The layout of the tank with pinned rigid links, impulsive lumped masses and supports is schematically shown in Figure 2.20.

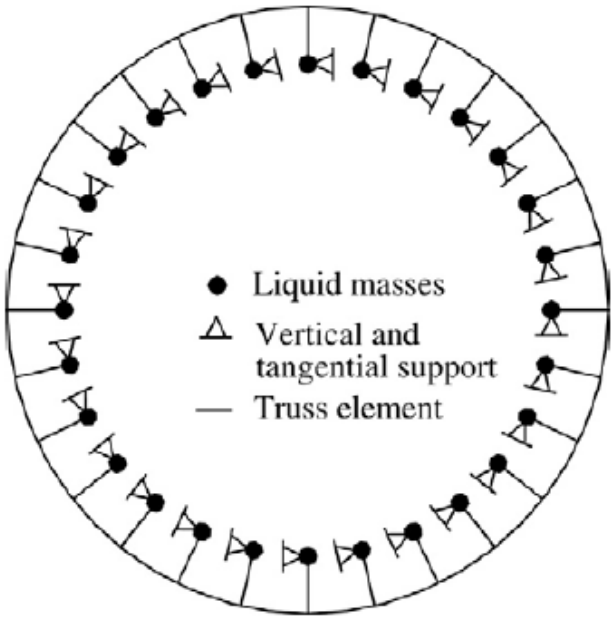

Figure 2.20: FE model proposed by Virella (2006)

Step 3: Fundamental mode of vibration

In order to determine the amount and different modes of vibration of a structure, the number of modes was increased until the total mass participating in vibration was larger than 70% of the impulsive mass. The vibration mode with the highest participation factor in the direction of translation was identified as the fundamental mode of vibration. Table 2.1 provides information on the first three modes with the highest participation factors α_3, for each for the three mentioned models.

Modes of the tank-liquid systems relevant for the response to horizontal ground motion												
	Model A				Model B				Model C			
Mode	**T(s)**	**α_3**	**n**	**m**	**T(s)**	**α_3**	**n**	**m**	**T(s)**	**α_3**	**n**	**m**
1	0.2116	0.64	1[a]	1	0.2395	0.79	1[a]	1	0.3001	0.77	1[a]	1
2	0.2021	0.02	1	5	0.2362	0.01	28	7	0.296	0.01	20	6
3	0.1957	0.02	1	4	0.2046	0.01	1	7	0.2998	0.01	25	6
[a] Fundamental mode												

Table 2.1: Participation factor for n-modes (Virella, 2006)

The variables in Table 2.1 are as follows:

T(s) = Period of vibration with the highest participation factor

α_3 = participation factor

n = circumferential wave number

m = axial half-wave number

As indicated the first mode of vibration for each mode has a participation factor much higher than those of the second or third mode of vibration. It is therefore sufficient to consider only the fundamental mode of vibration for practical purposes, with the higher modes of vibration having a negligible effect on the structure during horizontal seismic excitation.

Step 4: Mode of vibration

The radial displacements along the tank wall were considered in determining the various mode shapes, with the maximum displacements corresponding with the fundamental mode of vibration. The fundamental mode of each model is shown in Figure 2.21 and it is observed that the highest displacement does not occur at the top of the structure as expected for a cantilever beam. In relatively broad tanks a bulge is formed mid-way indicating the fundamental mode is a bending mode (n=1) with an axial half-wave (m), while the taller model exhibits beam-like behaviour similar to the first mode of a cantilever beam with maximum displacement near the top of the structure.

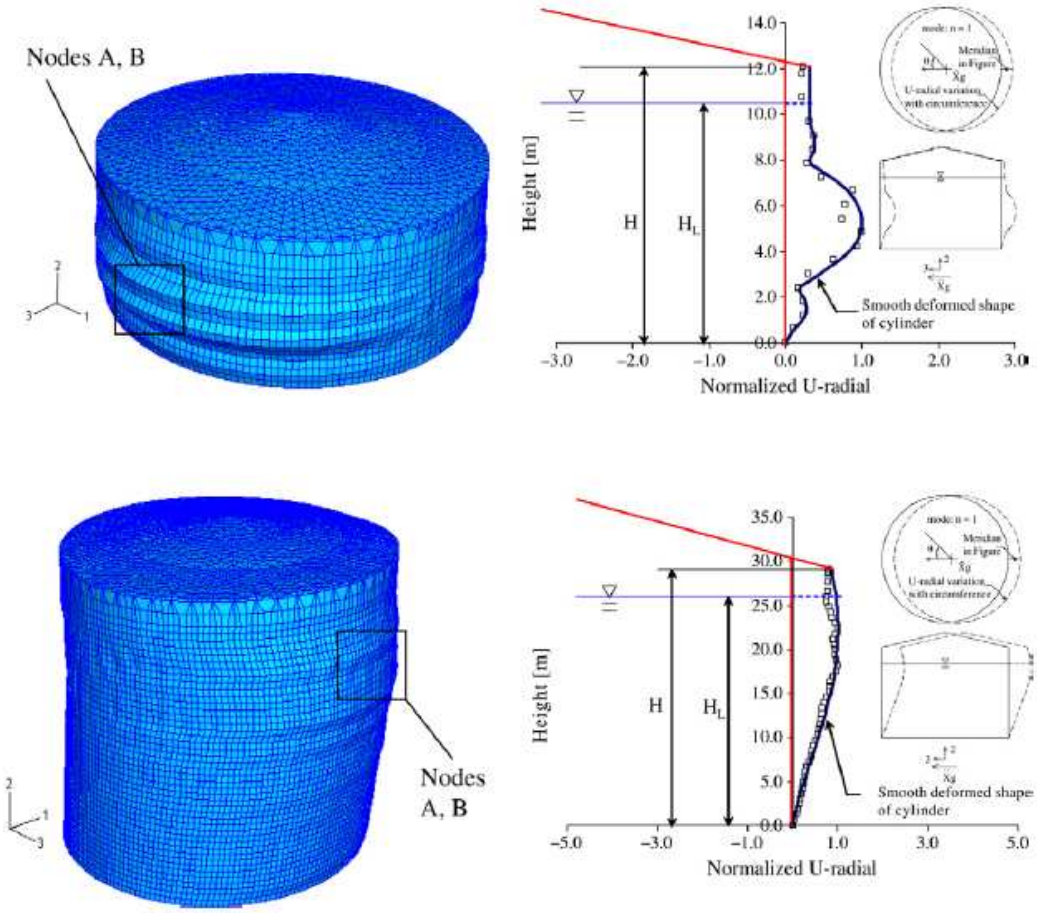

Figure 2.21: Fundamental mode shape (Virella, 2006)

It can therefore be concluded that regardless of the H/R ratio, the response of a system to horizontal base motion is dominated by the fundamental mode of vibration which is a bending mode with n equal to 1. As the height of the structure increases, the fundamental mode shape tends to that of a vertical cantilever beam.

2.13. STRAND7 (2005) DEFINITIONS

The FE package STRAND7 (2005) was used extensively during this study in order to evaluate the accuracy and extent of the various proposed FE models. For clarity purposes some of the most important terms used in STRAND7 (2005) are defined along with the methods of analysis. The FE models used in the course of this study are described in more detail in Chapter 7. In this section information is provided on the properties of various elements used to construct an FE model and the solvers used in STRAND7 (2005) to obtain the fundamental frequency of a model.

2.13.1. PROPERTIES OF PLATES AND SHELLS

Shells were used in all FE models since they are a combination of membrane and bending elements. The pressure applied normal the element in a structure will result in both bending of the plate as well as tensile forces due to hoop stress. Shells can undergo both in-plane deformation as well as out-of-plane bending and are sufficient for use in this project.

Shell or plate elements in STRAND7 (2005) are classified as either thick or thin elements depending on the thickness of the element with respect to the overall dimension of the structure. A plate in a circular model is considered thin if the thickness of the element is less than one-tenth of the radius of the model. The major difference between thick and thin shells being that only bending contributes to the out-of-plane deformation in thin shells while both bending and shear contributes to the out-of-plane deformation of thick shells. All shells used in the models analyzed during the course of this project are considered as thin shells and therefore it is only the bending moment that contributes to the out-of-plane deformation of a shell element.

Sufficient results are obtained with the use of 3- and 4-node shells elements in the case of thin shells, but additional bending moments may be generated by the approximation of a curved shell with a flat surface. These additional moments vanish with the refinement of the mesh. Only 4-node shell elements were used in this project with a sufficiently fine model mesh.

The local axis of a 4-node element is shown in Figure 2.22 with the local x- and y-axis in the plane of the plate.

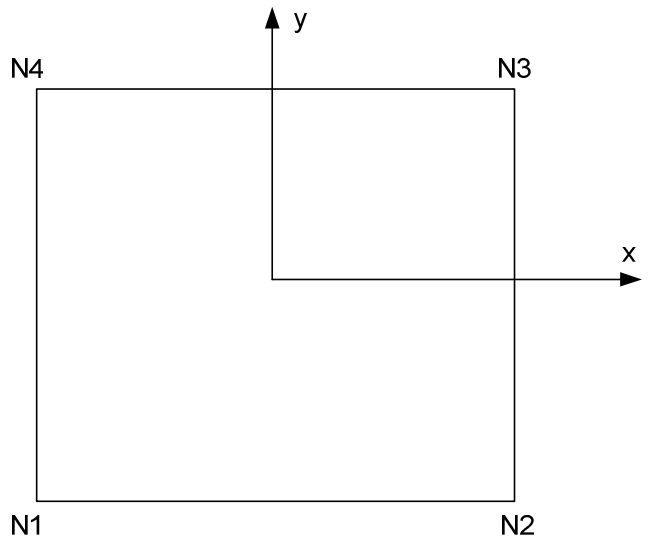

Figure 2.22: Local coordinate system of STRAND7 (2005) plate

2.13.2. PROPERTIES OF LINKS

Models based on the FE models proposed by Virella (2006) made use of links to prescribe the movement of the impulsive mass relative to the tank during horizontal seismic excitation. Pinned links were used during this project and can be defined as beam elements of infinite stiffness linking two nodes. The distance between these two nodes will always remain constant and no restraint is placed on the rotation of the nodes, they can therefore rotate independently of the each other.

2.13.3. NON-STRUCTURAL MASS ATTRIBUTES

The impulsive mass was attached to the structure with the use of non-structural mass elements. These elements are load case specific and may have different partial factors than the structure. The influence of gravity on non-structural mass can also be defined separate from that of the structure. Inertia forces generated by the non-structural mass can be either included in the analysis or neglected. Lumped masses were attached to all FE models analyzed during this project to consider the influence of the impulsive mass on the behaviour of the structure during seismic loading. The addition of the impulsive mass to the structure was achieved with the use of nodal non-structural masses.

In dynamic analysis the non-structural mass is used to simulate the pressure exerted on the tank wall in order to determine the natural frequency of the system. The dynamic factor of a non-structural mass is associated with a default value of one which indicates that the effective mass considered in the dynamic behaviour of the structure is equal to the non-structural mass attached. The spectral response solver determines the amount of the effective mass that contributes to a specific mode of vibration, this amount is known as the participation mass (STRAND7, 2005).

2.13.4. NATURAL FREQUENCY OVERVIEW

The natural frequency problem is based on the following equation:

$$[K]\{u\} = \omega^2[M]\{u\} \qquad \text{eq 2.11}$$

With [K] = global stiffness matrix
[M] = global mass matrix
{u} = vibration mode vector
Ω = natural frequency

In order to determine the modes of vibration, the following steps are followed:
Step 1: Assembly of the element stiffness and mass matrices to form the global matrices.
Step 2: Solve the eigenvalue problem to obtain frequency of vibration.

2.13.5. MODE SUPERPOSITION METHOD

The mode superposition method is convenient to use in dynamic analyses since it reduces the problem size and dynamic equilibrium equations are decoupled.

The equation for dynamic loading is:

$$[M]\{a\} + [C]\{v\} + [K]\{u\} = \{F(t)\} \qquad \text{eq 2.12}$$

With [M] = Mass matrix

[C] = Damping matrix

[K] = Stiffness matrix

{a} = Nodal acceleration vector

{v} = Nodal velocity vector

{u} = Nodal displacement vector

{F(t)} = Dynamic load vector

The modal mass, damping and stiffness matrices are diagonal and therefore the equilibrium equations are decoupled and may be solved separately. It is important to include only the natural frequencies that have converged during the natural frequency analysis, since non-converged frequencies may lead to a participation mass factor greater than 100%. The criteria for non-converged frequencies are discussed in detail in the Chapter 7. In order to include all modes of vibration that may have an influence on the structure, a participation mass factor sum equal to 90% is required for analytical purposes (STRAND7, 2005).

The mass participation factor for each mode is the factor of the total mass of the model that participates in the particular mode of vibration and is calculated as:

$$P.F. = \frac{(\{\varphi_i\}^T[M]\{E\})^2}{\{E\}^T[M]\{E\}} \qquad \text{eq 2.13}$$

With [M} = Global mass matrix

{E} = Global displacement vector

{ϕ$_i$} = i-th mode shape vector

The contribution of each mode is added by a chosen method to obtain the total structural response.

2.13.6. SPECTRAL RESPONSE

The spectral response analysis is a special application of the mode superposition method and is used to determine the response of a structure subjected to a non-harmonic dynamic loading as in the case of seismic base excitation. A response

spectrum which represents the response of a single-degree-of-freedom system to a base excitation (typically an earthquake) is used in the analysis.

The method followed in the spectral response analysis is:
Step 1: Assemblage of the element mass matrix
Step 2: Calculation of the modal excitation factors for each vibration mode as well as the mass participation factors.
Step 3: Determination of the spectral value associated with each mode of vibration from the response spectrum provided.
Step 4: Calculation of modal displacement magnitudes
Step 5: Calculation of maximum response with either the CQC or SRSS method.

In the following chapter information is provided on the example water-retaining structure used during this research project and the design of this structure for static loads. The design method is discussed in greater detail pertaining to the assumptions and simplification of this method during the course of this project. The ultimate and serviceability limit states are discussed with the partial load factors used for each. The computation of the resulting forces and stresses is discussed along with the determination of the crack width. The calculation of the area reinforcement required for each of these entities is provided.

3. EXAMPLE MODEL & PARAMETRIC STUDY

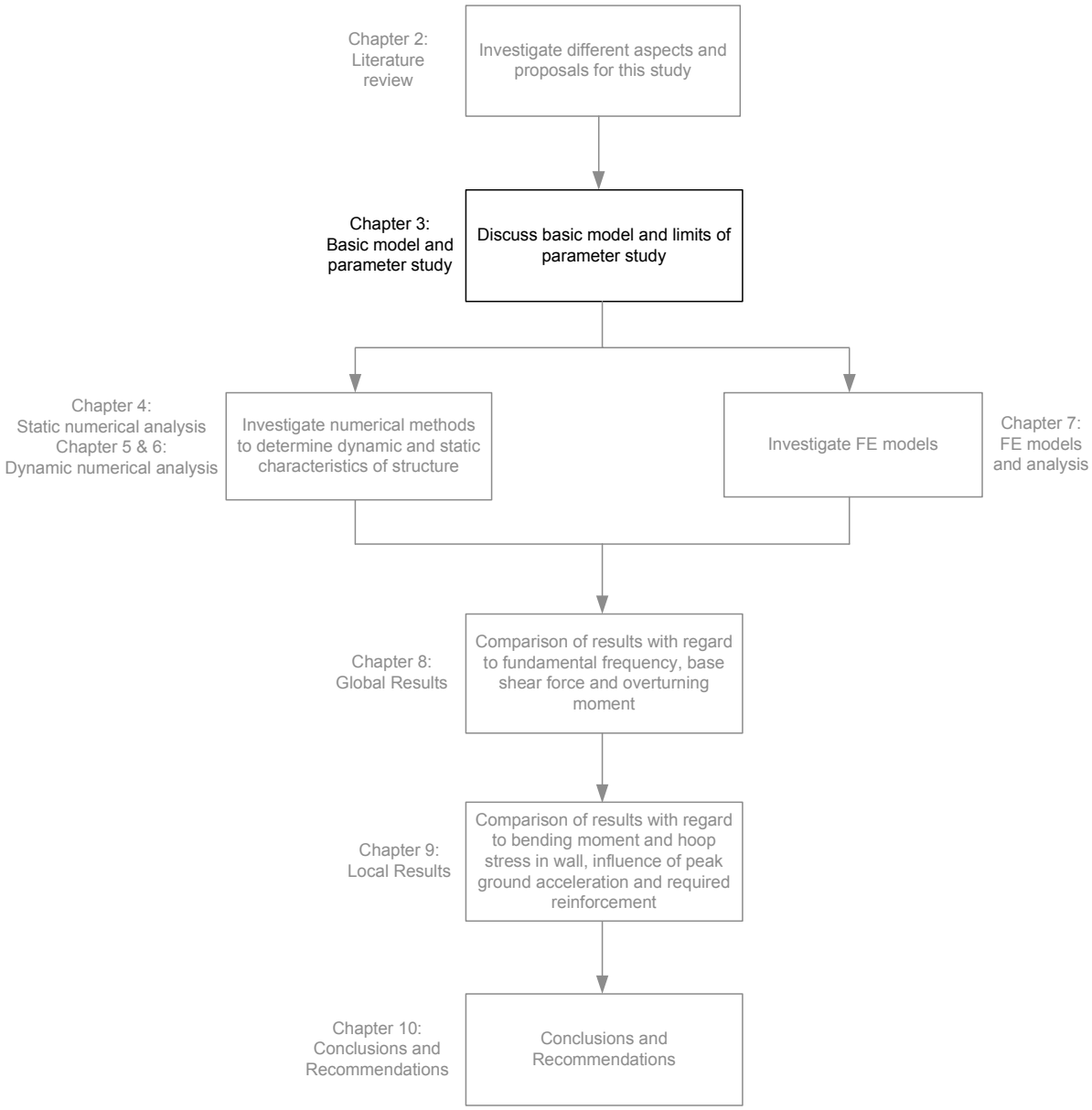

Figure 3.1: Methodology of study

Information was gathered on the static and seismic analyses of a structure and important concepts pertaining to each are provided in Chapter 2 in the literature review. With these in mind, the following step in this project was the definition of the example model and material properties as indicated in Figure 3.1. This example model was used to perform a parametric study for achieving the various aims of this project as stated in Chapter 1. These include the assessment of seismic loading as a critical load case and the governance of

either the ultimate or serviceability limit state in the design process. The proposal of a simplified and accurate numerical method and finite element model was also considered. The scope of the parametric study was determined in this step and information with regard to the example model and parametric study is provided in this section.

In order to define the geometry of the example model and material properties, practical information as provided by the South African design fraternity was considered. For the scope of the parametric study the practical information and the information provided in the numerical methods of Veletsos (1997) and Eurocode 8: Part 4 (2006) was considered.

South African designers prefer to use a circular cylindrical structure for tanks with a storage capacity of 15 to 20 megaliter while structures with a capacity smaller than 300 kiloliter are designed as rectangular or square tanks (Van Dalsen, 2009). In this study, only circular cylindrical tanks were considered since the influence of an earthquake on these structures would be more pronounced due to their higher storage capacity. In practise the connection between the tank wall and foundation is considered as a combination between a fixed support and pinned support. The reinforcement required at the base of the wall is calculated with consideration of the wall as fully fixed and only half of the required reinforcement calculated is provided. Since only half of the required reinforcement is provided, some rotation at the base of the wall can occur. For simplification purposes, the connection between the tank wall and foundation was considered to be fully fixed in this study and the foundation considered to be rigidly supported with no rocking or tilting of the foundation allowed during horizontal excitation.

Information provided by the South African industry indicated that a H/R [Height/Radius] ratio of 0.5 is preferred when designing circular cylindrical tanks (Van Dalsen, 2009). The material presented by both Veletsos (1997) and Eurocode 8: Part 4 (2006) contained information for tanks with a H/R ratio ranging between 0.3 and 3.0. However, a value of 3.0 for the H/R ratio is extremely high, with the structure exhibiting membrane behaviour with correspondingly more complex analyses (Veletsos, 1997). With consideration of the practical information provided by the South African industry and the research material by Veletsos (1997) it was decided to limit the H/R ratio in this study to a maximum value of 1.5 which is still practical. With the various H/R ratios in mind a radius of 10 meters was chosen. Figure 3.2 graphically presents the example model as used in this study.

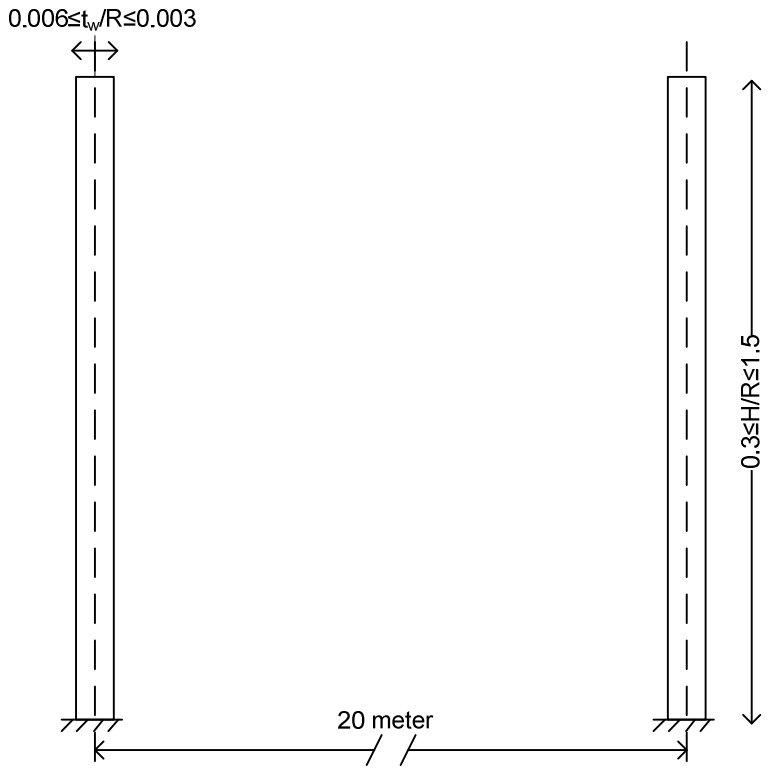

Figure 3.2: Tank layout

All water-retaining structures investigated in this study were considered as reinforced concrete structures. The concrete was assumed to have a cube strength of 40 MPa with a modulus of elasticity of 34.3 GPa, Poisson ratio of 0.2 and density of 2500 kg/m^3. It was assumed that the structure is filled up to a height H with water which has a density of 1000 kg/m^3.

With the geometry of the structure and material properties known, the structure could be classified as having either a rigid or flexible wall. The criteria for the classification of a water-retaining structure as either rigid or flexible were unknown at this point and were further investigated. Since the radius of the structure is known as well as the scope of variance of the wall height, the only other variable pertaining to the geometry of the structure is the thickness of the wall. In literature published by Veletsos (1997), a t_w/R [wall thickness/Radius] ratio of 0.009 was used as a reference tank for the analysis of a flexible structure. However, practical information provided by the engineering industry (Van Dalsen, 2009) indicated that a t_w/R ratio between 0.025 and 0.03 is preferred. For these reasons the t_w/R ratio in this study was varied between 0.006 and 0.03.

Static and seismic analyses were completed for each structure. The method as prescribed in Ghali (1979) was used for the static analysis while two numerical methods were used for the seismic analysis of a structure. These were the methods proposed by Veletsos (1997) and that of the Eurocode 8: Part 4 (2006). A value of 0.15g was used for the peak ground acceleration in the seismic analysis of water-retaining structures. In order to determine whether South African designers indeed need to consider earthquakes as a critical load case in the design of water-retaining structures, the peak ground acceleration was varied between 0.15g and 0.35g.

In summary, the parametric study consisted of:

- Variance of the H/R ratio between 0.3 and 1.5 with increments of 0.3
- Variance of the t_w/R ratio between 0.006 and 0.03 with increments of 0.003
- Variance of peak ground acceleration between 0.15g and 0.35g with increments of 0.1g

In the following chapter the static analysis of a water-retaining structure is discussed. The method presented by Ghali (1979) was used to obtain the hoop force and bending moment in each of the structures when subjected to hydrostatic liquid pressure. The corresponding load combinations for the ultimate and serviceability limit states are also presented along with the calculation of the reinforcement required for each of the limit states.

4. STATIC NUMERICAL ANALYSIS

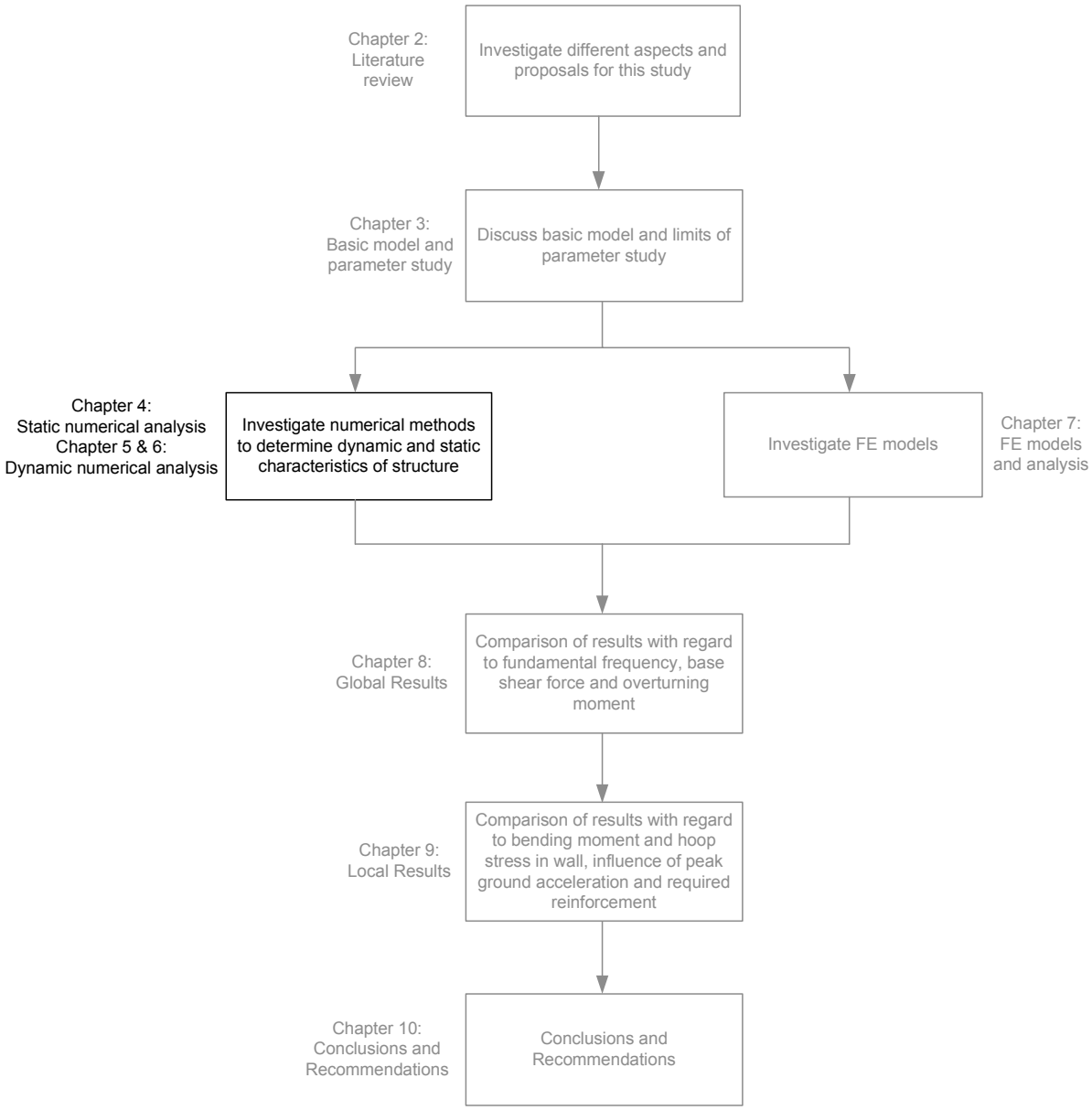

Figure 4.1: Methodology of study

With the example model and scope of the parametric study defined in the previous chapter, the following step in the methodology of this study was the numerical analysis of each structure as indicated in Figure 4.1. The first of the numerical methods to be discussed is the static analysis of a water-retaining structure since all structures in South Africa are currently only designed for static loading conditions. The seismic loads on a structure are often disregarded and in order to assess the influence of seismic loading on water-retaining

structures, the dynamic results were compared to the static results. Comparisons were made with regard to the base shear force, overturning moment, hoop stress and bending moment in the wall as well as the area of reinforcement required for the respective internal forces.

In this chapter the various loads acting on the structure are provided pertaining to the static conditions with their partial load factors. The method of analysis proposed by Ghali (1979) is discussed with regard to the various steps in the method including the assumptions and simplifications made during this study. The resulting ultimate limit state forces and stresses are determined along with the area of reinforcement. The crack width calculations according to BS 8007 (1987) are presented in detail which determined the area of reinforcement required for the serviceability limit state. The area of reinforcement required for the static loads were compared to that obtained for the seismic loads in order to assess whether seismic design is a critical loading condition in South Africa. The reinforcement required for the ultimate limit state was subsequently compared to that of the serviceability limit state to assess which limit state governs the design of the structure in the case of seismic analysis.

4.1. LOADS AND PARTIAL LOAD FACTORS

The loads considered to act on all structures were the gravitational load and the hydrostatic load resulting from the contained liquid. Additional loads due to temperature and shrinkage were neglected for the purposes of this study, since the aim of this project is to determine the effect of seismic activity on water-retaining structures.

4.1.1. GRAVITATIONAL LOADS

The tank wall is considered to be fully fixed to the base and cannot lift up while the foundation is considered to be rigidly supported with no tilting of the foundation. Subsequently the modelling of the foundation and the forces acting on the foundation were not considered, which includes the weight of the water. The roof was also neglected since it was assumed the weight of the roof does not contribute to the bending moment about a horizontal axis or hoop stress in the wall. Only the self-weight of the tank wall was considered as a gravitational load resulting in a

vertical axial force in the tank wall. Refer to Figure 4.2 which schematically shows all applied static forces considered acting on a water-retaining structure.

4.1.2. HYDROSTATIC LOADS

A horizontal pressure is exerted on the tank wall by the contained liquid which is known as the hydrostatic pressure. The hydrostatic pressure is considered to be constant along the circumference of the wall but varies linearly along the height of the wall. Figure 4.2 illustrates the static forces acting on a water-retaining structure as considered in this project.

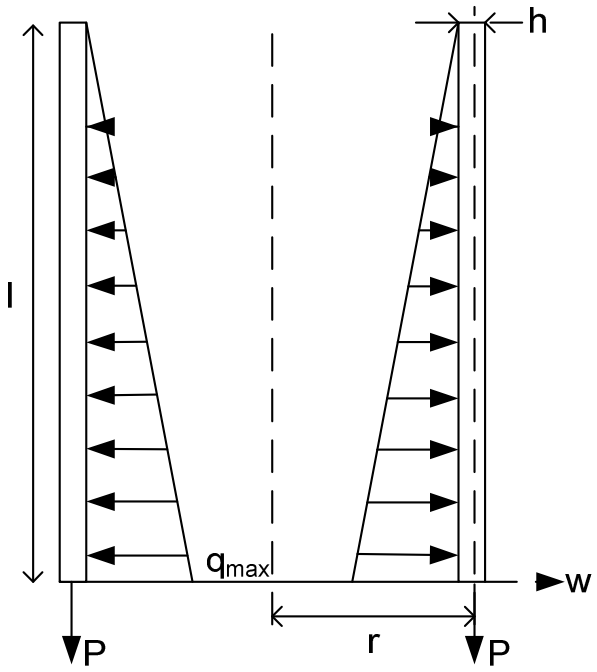

Figure 4.2: External forces acting on the tank wall

The horizontal pressure acting on the wall results in an outward displacement of the wall. However, the displacement is restricted due to symmetry of the structure, resulting in a hoop stress and bending moment at the bottom nodes since they were considered as fixed. Bending of the wall around a vertical axis was not considered since no torsional effects are induced by the application of the hydrostatic pressure. The reaction forces are illustrated in Figure 4.3.

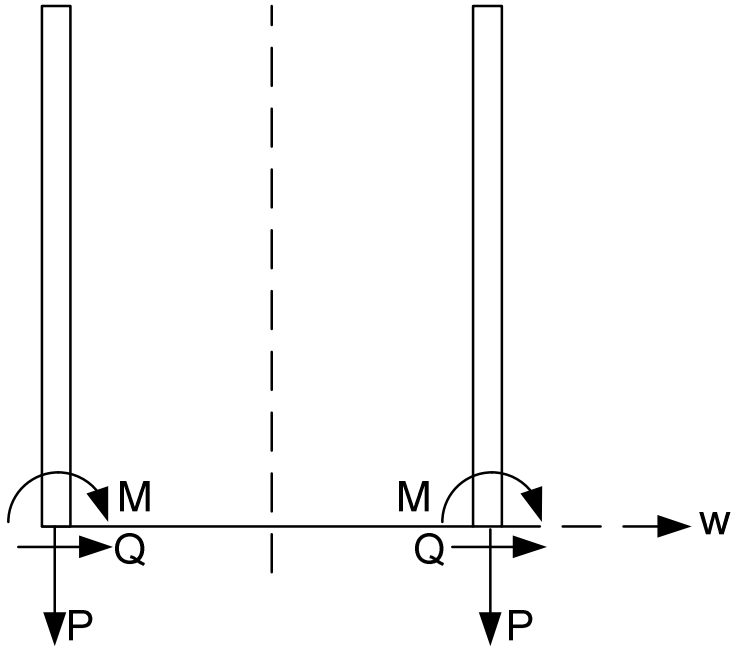

Figure 4.3: Internal forces in structure

The methodology to determine the hoop force and bending moment according to Ghali (1979) was provided in detail in Chapter 2 section 2.8. A brief summary is provided again for clarity purposes:

- The dimensionless parameter η of the structure is calculated as $l^2/(dh)$ with l the height of the wall, d the diameter of the tank and h the wall thickness.
- With consideration of the wall edge conditions, the appropriate design tables are determined as provided in Ghali (1979).
- The design factors for the hoop stress and bending moment respectively are determined from the appropriate design table as obtained in the previous step.
- The values of the hoop force and bending moment are calculated with the use of the design factors.

For the determination of the hoop stress, the hoop force was divided by the thickness of the tank wall only and considered to act per meter height of the tank wall.

4.1.3. PARTIAL LOAD FACTORS

The hoop force and bending moment in the wall as determined with the use of Ghali (1979) were characteristic loads. The appropriate load combinations were used as prescribed for design purposes in the South African loading code (SANS 10160, 2009) and EN 1991-4 (2006).

The self-weight of the structure and the hydrostatic pressure were considered in combination for all structures. The ultimate limit state combinations are expressed in equation 4.1 and 4.2 with the first load combination applicable to the axial load resulting from the own weight of the wall. The second load combination is applicable to the computation of the bending moment and hoop stress resulting from the horizontal pressure exerted on the wall by the contained liquid.

$$LC1 = 1.35DL_{wall} \quad \text{eq 4.1}$$

$$LC2 = 1.2DL_{water} \quad \text{eq 4.2}$$

The serviceability limit state combinations are provided below with load combination 3 corresponding with the axial force and load combination 4 applicable to the determination of the bending moment and hoop stress resulting from the water load.

$$LC3 = 1.1DL_{wall} \quad \text{eq 4.3}$$

$$LC4 = 1.1DL_{water} \quad \text{eq 4.4}$$

4.2. AREA OF REINFORCEMENT

A hoop stress and bending moment are obtained in the wall due to the hydrostatic pressure exerted on the wall. With the use of the design values obtained for the ultimate and serviceability limit state respectively, the area of reinforcement required was determined. The area of reinforcement required for both the static and seismic analyses of a structure was of interest to assess whether seismic loads are a dominant load case. The area of reinforcement required for the ultimate and serviceability limit states were also needed to assess which of the limit states govern the design of a water-retaining structure.

4.2.1. ULTIMATE LIMIT STATE

For the purposes of this study it was assumed the concrete provides no resistance to tensile forces. The hoop stress in a section results in a tensile force per meter height of the wall with resistance only provided by the horizontal reinforcement in the wall.

The area of reinforcement required to resist the tensile force per meter height of the tank wall was calculated based on the tensile capacity of reinforcement at yield point:

$$T = 0.87 f_y A_s \qquad \text{eq 4.5}$$

With T = tensile force per meter height of the wall

f_y = yield strength of reinforcement steel

A_s = area of reinforcement required per meter height to resist tensile force

Bending about a horizontal axis also exists and the reinforcement required to resist the ultimate limit state bending moment was calculated with equation 4.6 as prescribed by the design codes.

$$A_{s,req} = \frac{M_u}{0.87 f_y z} \qquad \text{eq 4.6}$$

With M_u = ultimate limit state bending moment

f_y = yield stress of reinforcement

z = lever arm as calculated using SABS 0100-1 (2000)

The reinforcement required for the ultimate limit state is governed by the yield stress of reinforcement while that of the serviceability limit state is governed by the allowable crack width as presented in the following section.

4.2.2. SERVICEABILITY LIMIT STATE

The serviceability limit state is governed by the limitations placed on the maximum allowable crack width in a structure and is prescribed in South Africa as 0.2 millimetres. The BS 8007 (1987) code is currently used in South Africa to determine the area of reinforcement required to limit the crack width to the specified value.

Due to the hydrostatic pressure exerted on the wall, a hoop stress is produced. It was assumed the concrete provides no resistance to the tensile forces and therefore the hoop stress had to be converted to the appropriate stress in the reinforcement. The tensile strain in the reinforcement was calculated with the use of the normal elastic theory as presented in equation 4.7.

$$\sigma_s = E_s \varepsilon_s \qquad \text{eq 4.7}$$

With σ_s = stress in reinforcement
E_s = modulus of elasticity of reinforcement
ε_s = tensile strain in reinforcement

The stiffening effect of the concrete between the cracks was considered and deducted from that of the tensile strain in the reinforcement to obtain the actual strain in the reinforcement. Equation 4.8 was used for the calculation of the stiffening effect of the concrete (BS 8007, 1987).

$$\epsilon_2 = \frac{2 b_t h}{3 E_s A_s} \qquad \text{eq 4.8}$$

With ε_2 = strain from stiffening effect of concrete
b_t = width of the tank wall
h = overall depth of member, considered as 1 meter
E_s = modulus of elasticity of reinforcement
A_s = area of reinforcement provided to resist the tensile force

A vertical spacing of 200 millimetres was chosen for the horizontal reinforcement with the maximum tensile strain in the concrete obtained mid-way between the

reinforcement bars. Cracks will therefore develop first at a point mid-way between the horizontal reinforcement bars. Equation 4.9 is used to calculate the crack width for a pre-determined area of reinforcement. The area of reinforcement required to limit the crack width to 0.2 millimetres was determined with the use of equation 4.9.

$$w = 3a_{cr}\varepsilon_m \qquad \text{eq 4.9}$$

With w = crack width

a_{cr} = distance measured from position of maximum tensile strain to surface of closest reinforcement bar

ε_m = tension stiffening, equal to ε_s-ε_2

Horizontal cracks may also develop in the wall resulting from the bending moment around a horizontal axis. The reinforcement required to limit the crack width to 0.2 millimetre in the case of bending was calculated with the use of equation 4.10.

$$w = \frac{3a_{cr}\varepsilon_m}{(1+2(\frac{a_{cr}-c_{min}}{h-x})} \qquad \text{eq 4.10}$$

With a_{cr} = distance measured from position of maximum tensile strain to surface of closest reinforcement bar

ε_m = tension stiffening, equal to ε_s-ε_2

c_{min} = minimum cover to reinforcement

h = wall thickness

x = depth of neutral axis

All parameters regarding the static analysis of water-retaining structures have been discussed in this chapter with regard to the hoop stress, bending moment and required reinforcement for both the ultimate and serviceability limit states.

The following chapter provides information regarding the dynamic analysis of water-retaining structures for seismic excitation as proposed in Eurocode 8: Part 4 (2006). Both the static and dynamic design methods are discussed in detail with the comparison of the

respective results presented in Chapters 8 and 9. It should be kept in mind that one of the aims of this project was to determine whether the seismic design of water-retaining structures in South Africa is a critical load case with either the ultimate or serviceability limit state governing the design. This could only be concluded through the comparison of the seismic and static results with consideration of the ultimate and serviceability limit states respectively.

The determination of the fundamental frequency of the structure and corresponding mode shape is discussed in the following chapter. The method for determining the various components of the hydrodynamic pressure exerted on the wall by the fluid during horizontal movement is presented. The load combinations and partial factors with consideration of the seismic loads are provided from which the base shear force and overturning moment were calculated. The freeboard requirements for the serviceability limit state are also discussed.

5. DYNAMIC NUMERICAL ANALYSIS - EUROCODE

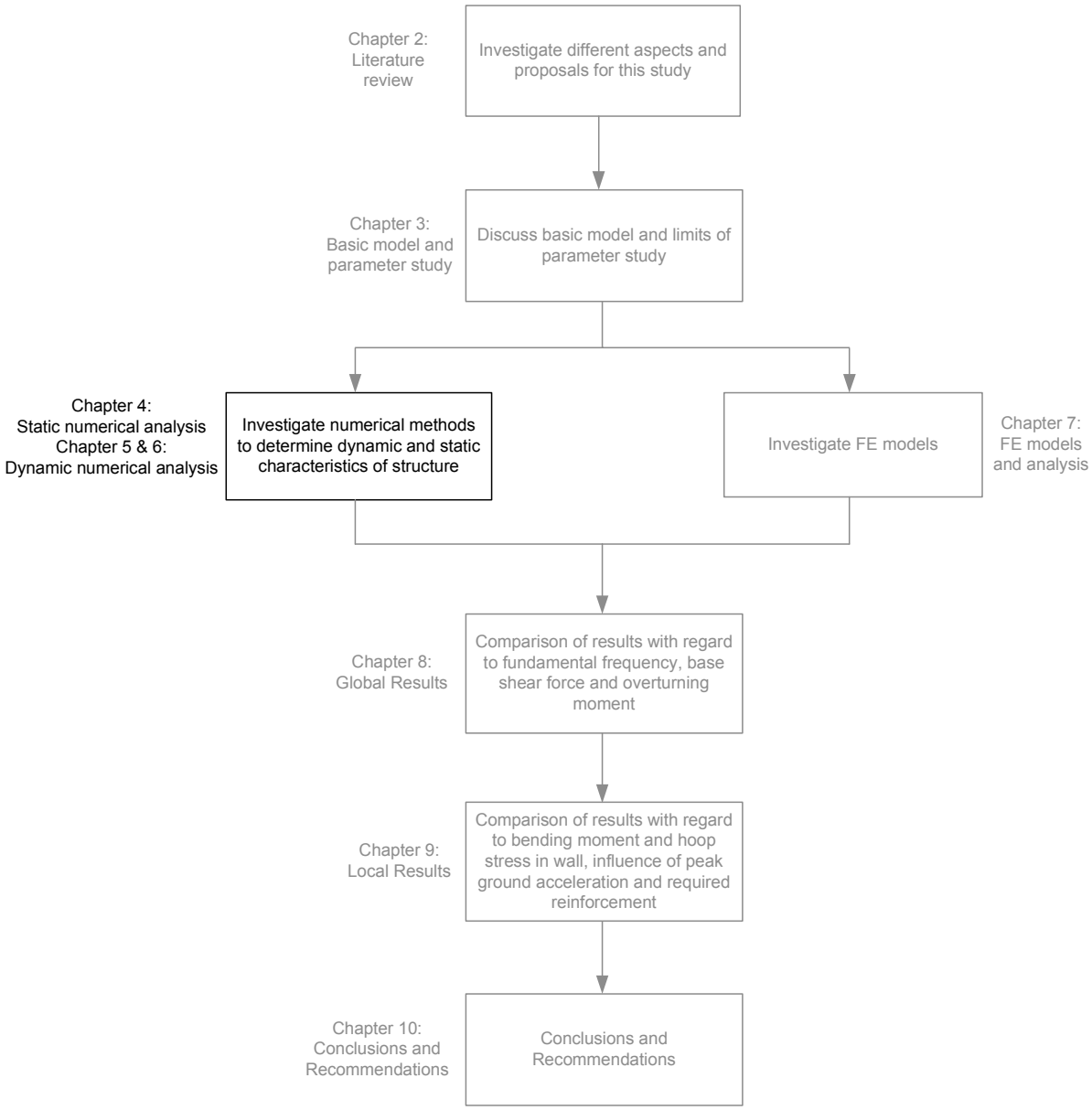

Figure 5.1: Methodology of study

The numerical analyses of structures subjected to seismic excitation were performed with the use of two different methods and with reference to Figure 5.1 both of these methods are discussed in this chapter and the following chapter. The first method as presented in Eurocode 8: Part 4 (2006) is discussed in this chapter with regard to the determination of the fundamental frequency and corresponding pseudoacceleration. The determination of the various components of the hydrodynamic pressure is discussed and the load

combinations for the ultimate and serviceability limit states are provided. The determination of the base shear force and overturning moment is also discussed along with the freeboard requirements for the serviceability limit state. An example of the relevant calculations for a structure with a H/R ratio of 0.9 and t_w/R ratio of 0.024 is provided in Appendix B. It should be noted all equations provided in this section were obtained from Eurocode 8: Part 4 (2006) unless otherwise stated.

5.1. FUNDAMENTAL FREQUENCY

The determination of the fundamental frequency of a water-retaining structure subjected to horizontal seismic excitation is of critical importance since the majority of tank failures under seismic conditions occur due to resonance effects (Nachtigall, 2003). Determining the natural frequency of a structure is complex and a number of different aspects need to be considered. These include the flexibility of the tank wall, the influence of the contained liquid on the behaviour of the tank, the fixity of the wall to the base and soil conditions.

In Eurocode 8: Part 4 (2006) it is assumed that the fundamental mode shape of a water-retaining structure is similar to the fundamental mode shape of a vertical cantilever beam. The adoption of the cantilever mode shape implies that the cross-section of the wall remains circular during oscillation and no deformation of the cross-section is considered. This is a critical point, since the higher modes of vibration associated with deformation of the cross-section are neglected. For the purposes of this study, only the first mode of vibration of the system was considered.

The first step in determining the fundamental frequency of a water-retaining structure was the consideration of the tank wall to be either rigid or flexible. The choice of flexibility influences a number of different aspects since a rigid wall implies the structure experiences the same motion as the soil during seismic activity. In the case of flexible walls, the movement of the tank wall is different from that of the soil producing additional pressure on the wall. Assuming the wall to be rigid may be unconservative, since the structure is subjected to the peak ground acceleration and not the pseudoacceleration as obtained for flexible structures. No literature could be obtained which gave any clarity on the criteria used to classify a structure as either rigid or

flexible. This matter was further investigated in this study and results pertaining to the classification of a structure are provided in Chapter 8. All water-retaining structures investigated in this study were assumed to have flexible walls.

During horizontal excitation of a structure, the liquid consists of two components known as the impulsive and convective components respectively. The impulsive component of the liquid is considered to move rigidly with the tank wall. In the case of rigid structures the motion of the tank-liquid system is the same as the ground motion. In contrast, the tank wall and impulsive component experiences a different motion than the ground in structures with a flexible wall. The frequency of the tank-liquid system for flexible structures was calculated with equation 5.1.

$$T_{imp} = C_i \frac{\sqrt{\rho} H}{\sqrt{s/R}\sqrt{E}} \qquad \text{eq 5.1}$$

With T_{imp} = fundamental period of the tank-liquid system

C_i = dimensionless parameter from Eurocode 8: Part 4 (2006)

ρ = density of the contained liquid

H = height from the base to the surface of the liquid

s = width of the tank wall

R = radius of the tank

E = modulus of elasticity of tank material

The second component is representative of the sloshing motion of the liquid and has a different fundamental frequency than the ground motion and the tank-liquid system. A wide separation exists between these frequencies and the convective component is not influenced by the flexibility of the wall. The convective component was therefore considered separately with the use of a rigid tank and the sloshing frequency was calculated with equation 5.2. Only the first mode of vibration of the sloshing component was considered in this study.

$$\omega_{c1} = \sqrt{g \frac{\lambda_1}{R} \tanh(\lambda_1 \gamma)} \qquad \text{eq 5.2}$$

With ω_{c1} = first mode of vibration of sloshing component

g = gravitational acceleration equal to 9.81 m/s^2

λ_1 = dimensionless parameter equal to 1.841

R = radius of the tank

γ = Height/Radius ratio

With the fundamental frequency of each component known, the pseudoacceleration corresponding to each of the frequencies could be determined with the use of the response spectrum as provided in Eurocode 8: Part 1 (2004). The pseudoacceleration is required for the calculation of the hydrodynamic pressure and resulting forces exerted on the structure subjected to seismic excitation.

5.2. PSEUDOACCELERATION

In the case of rigid tanks, the tank-liquid system is subjected to the peak ground acceleration and the pseudoacceleration of the system is not required. This is not the case for flexible tanks, since the motion of the tank-liquid system is different from that of the ground and is subjected to the pseudoacceleration instead of the peak ground acceleration.

With the fundamental frequency of the tank-liquid system known, the pseudoacceleration of the system was determined with the use of Eurocode 8: Part 1 (2004). The pseudoacceleration of the system for the ultimate limit state differs from that of the serviceability limit state since different values of the behaviour factor are prescribed for each limit state. A reduction factor is also prescribed for the serviceability limit state.

All structures in this study were assumed to be Class IV structures. This refers to structures of which the failure poses exceptional risk to life and would have large economic and social consequences. The reduction factor of a Class IV structure is prescribed as 0.4 with an importance factor of 1.6 for water-retaining structures as outlined in Eurocode 8: Part 4 (2006). For both the ultimate and serviceability limit states a damping ratio of 5% was used (Eurocode 8: Part 4, 2006).

Only ground type A was investigated during this project which is associated with rock or rock-like geological formations, including a maximum of 5 meter of weaker material at the surface which is typical ground conditions in the Western Cape of South Africa.

For the ultimate limit state it is assumed that local plastic deformation may occur in the structure during horizontal seismic activity. However, to avoid the explicit use of a non-linear analysis, a behaviour factor of 1.5 is prescribed for the ultimate limit state and used in conjunction with the response spectrum for elastic analysis from Eurocode 8: Part 1 (2004). A behaviour factor of 1.0 is prescribed for the serviceability limit state since the structure remains fully elastic under serviceability loads. The elastic response spectrum in Eurocode 8: Part 1 (2004) is used for the serviceability limit state in conjunction with the reduction factor. The pseudoacceleration for the ultimate and serviceability limit states was determined separately, depending on the fundamental frequency of the structure.

The pseudoacceleration experienced the convective component is calculated with the use of the elastic response spectrum in Eurocode 8: Part 1 (2004). The fundamental period of the sloshing component was in all instances greater than four seconds and a limiting value for the pseudoacceleration was assumed to be 0.03g for the ultimate limit state and 0.014g for the serviceability limit state. Both values correspond to a period of vibration of 4 seconds in the elastic response spectrum.

5.3. GRAVITATIONAL LOADS

Only the self-weight of the tank wall was considered during this project while neglecting the own weight of the contained liquid. The weight of the contained liquid acts perpendicular to the base of the tank, resulting in reaction forces acting on the foundation of the structure. The vertical forces acting on the foundation of the structure are of no interest in this project and the weight of the water was therefore neglected. The weight of the roof was also neglected since it does not contribute to the bending moment or hoop stress in the wall which was of significant interest in this study.

5.4. HYDRODYNAMIC LOADS:

The hydrodynamic loads consist of the impulsive pressure, the convective pressure and in the case of flexible tanks, the flexible pressure exerted on the wall by the contained liquid. The hydrodynamic pressure varies along the height of the tank wall and along the circumference of the wall, with maximum pressure obtained in the direction of excitation while zero hydrodynamic pressure is obtained perpendicular to the direction of excitation. The inertia effect of the wall during horizontal motion is also considered and the computation of each component is discussed in the following paragraphs with reference to Eurocode 8: Part 4 (2006).

It should be noted that only the horizontal component of seismic excitation was considered and the influence of the vertical component on the structure was neglected.

5.4.1. IMPULSIVE COMPONENT

The impulsive component of the liquid is rigidly attached to the tank wall and subjected to the peak ground acceleration, regardless of whether the structure is considered to be rigid or flexible. The pressure exerted on the tank wall by the impulsive component was calculated with equation 5.3 (Eurocode 8: Part 4, 2006).

$$p_i(\xi, \varsigma, \theta, t) = C_i(\xi, \varsigma)\rho H cos\theta A_g(t) \qquad \text{eq 5.3}$$

With ξ = r/R, considered equal to 1, since the pressure acting on the wall is being determined

ς = z/H, with z measures upwards from the bottom of the wall

ρ = density of the contained liquid

H = height from the base to the free surface of the liquid

θ = circumferential angle, taken as 0 degrees to obtain maximum pressure

$A_g(t) = a_g$, peak ground acceleration

The distribution of the impulsive component over the height of the tank wall is illustrated in Figure 5.2 (Veletsos, 1997) with γ=H/R ratio.

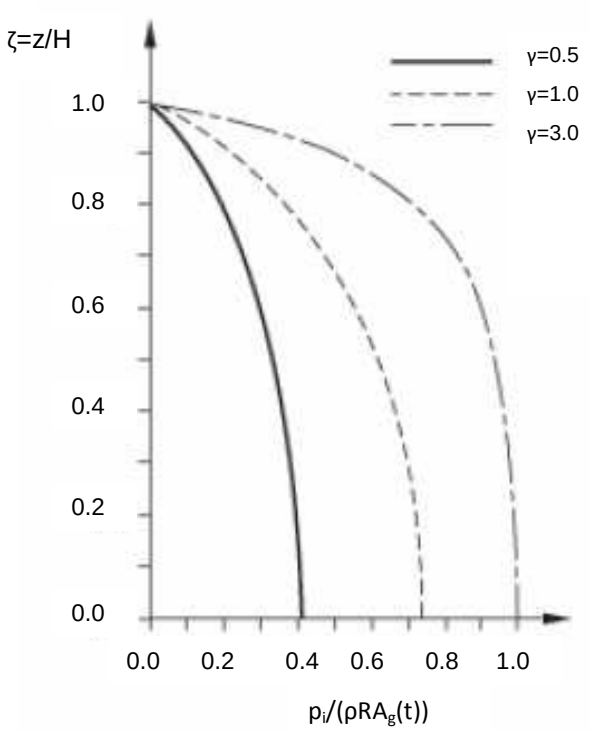

Figure 5.2: Impulsive pressure distribution (Veletsos, 1997)

5.4.2. CONVECTIVE COMPONENT

The convective component is representative of the sloshing motion of the liquid and is independent of the wall flexibility due to the wide separation in fundamental frequency of the sloshing component and tank-liquid system. The convective component is therefore determined with the use of a rigid tank and is subjected to pseudoacceleration instead of the peak ground acceleration. For the determination of the pseudoacceleration experienced by the convective component, use is made of the elastic response spectrum and a behaviour factor equal to 1.0.

The pressure exerted on the tank wall by the convective component was calculated with equation 5.4, with consideration of only the first mode of vibration (Eurocode 8: Part 4, 2006).

$$p_c(\xi, \varsigma, \theta, t) = \rho\psi_1 \cosh(\lambda_1\gamma\varsigma)\, J_1(\lambda_1\xi) cos\theta A_{c1}(t) \qquad \text{eq 5.4}$$

With ρ = density of the contained liquid

ψ_1 = dimensionless parameter determined from Eurocode 8: Part 4 (2006)

λ_1 = dimensionless parameter equal to 1.841

γ = Height/Radius ratio

ς = z/H, with z measured from bottom of tank

J_1 = Bessel function of the first order

ξ = r/R, equal to 1.0 since pressure acting on wall is measured

$A_{c1}(t)$ = pseudoacceleration corresponding to the first mode of vibration

The distribution of the convective pressure, with consideration of the first and second mode of vibration, along the height of the tank wall is illustrated in Figure 5.3 (Veletsos, 1997) with γ=H/R ratio.

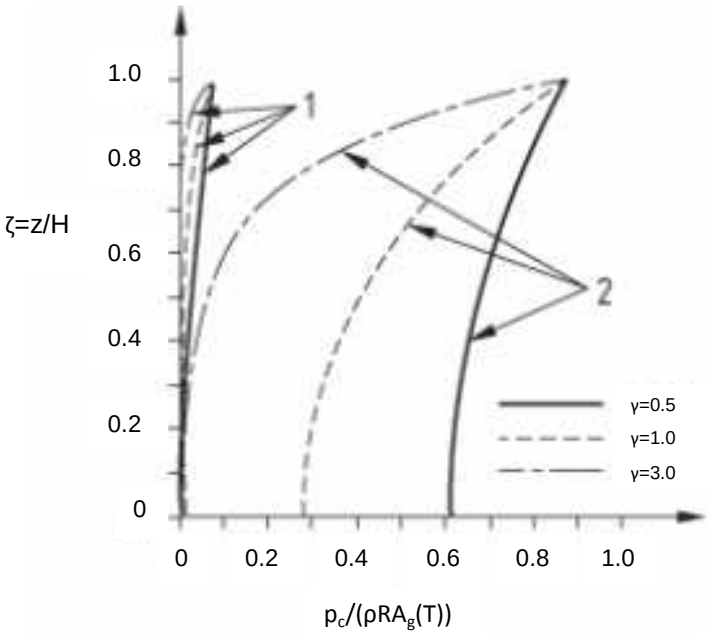

Figure 5.3: Distribution of convective pressure (Veletsos, 1997)

5.4.3. FLEXIBLE COMPONENT

In the case of flexible structures, the flexibility of the wall produces an additional pressure on the tank wall while the impulsive and convective components remain unchanged. The tank is subjected to pseudoacceleration instead of the peak ground acceleration since the motion of the structure is different than the ground motion.

The determination of the flexibility pressure is significantly more complex than that of the impulsive and convective components. A number of assumptions were made during this study for the determination the flexibility pressure.

The first of these assumptions was the determination of a function f(ς). Eurocode 8: Part 4 (2006) defines this function as a function describing the fundamental mode shape of a tank which is proportional to the parameter ς, with ς equal to z/H. It was assumed f(ς) is a function which describes the deflection of specific point along the height of the wall for the first mode of vibration.

The maximum hydrodynamic pressure is obtained in the direction of excitation with the circumferential angle ϑ, equal to 0 degrees. A line along the height of the tank wall in the direction of excitation was considered and from the analysis performed in STRAND7 (2005) the deflection of each node on this line could be obtained. A third order differential equation was obtained to describe the deformation of the tank for the fundamental frequency and was considered to be f(ς). Several tanks were analyzed in STRAND7 (2005) during this study and it was assumed a third order differential equation is adequate to describe the shape of a line undergoing maximum deflection with only the constants in equation 5.5 that differs.

$$f(\varsigma) = a\varsigma^3 + b\varsigma^2 + c\varsigma + d \qquad \text{eq 5.5}$$

With ς = point on a line along the height of the wall

a, b, c, d = constants depending on the first mode shape

For a tank with H/R ratio equal to 0.3 and a t_w/R ratio equal to 0.024 the first mode shape had a distribution illustrated in Figure 5.4 with the third order function provided on the figure.

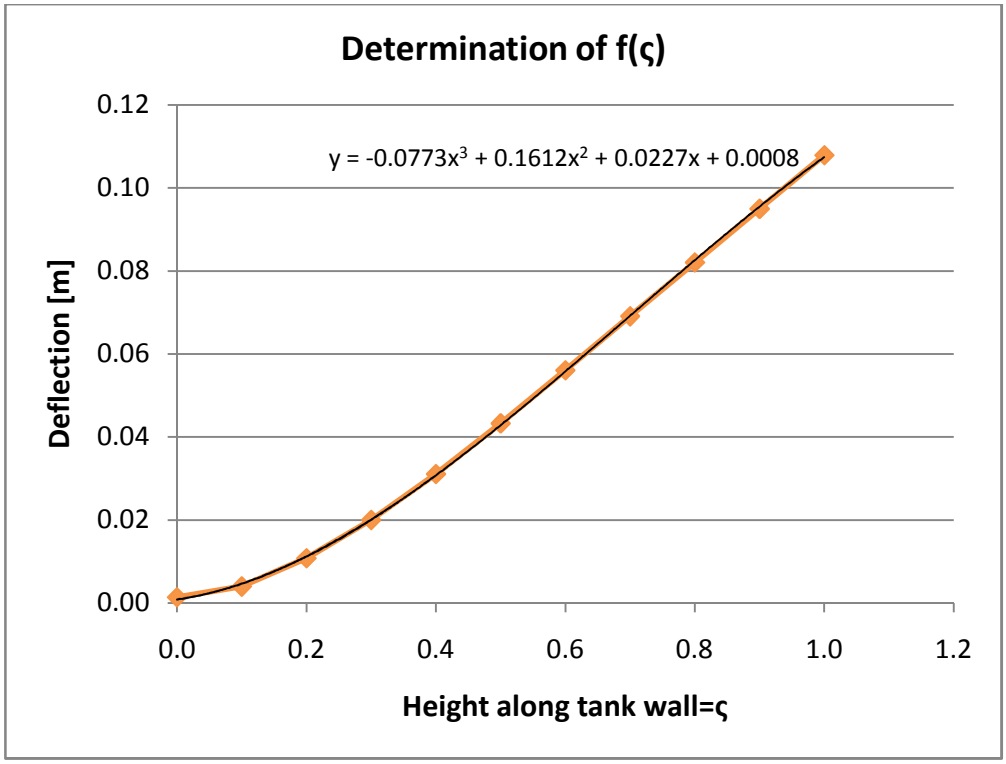

Figure 5.4: First mode shape

The pressure due to flexibility of the wall was determined from equation 5.6 with consideration of only the fundamental frequency (Eurocode 8: Part 4, 2006).

$$p_f(\varsigma, \theta, t) = \rho H \psi cos\theta d_1 \cos(v_1 \varsigma) A_{f1}(t) \qquad \text{eq 5.6}$$

With ρ = density of the contained liquid

H = height from the base to the free surface of the liquid

ψ = dimensionless parameter not equal to that of the convective component, obtained from Eurocode 8: Part 4 (2006)

θ = circumferential angle equal to 0 degrees for maximum pressure distribution

d_1 = dimensionless parameter obtained from Eurocode 8: Part 4 (2006)

v_1 = dimensionless parameter obtained from Eurocode 8: Part 4 (2006)

ς = z/H, with z measured from bottom of wall

$A_{f1}(t)$ = pseudoacceleration experienced by the tank

The flexible pressure may be the governing factor for design since the pseudoacceleration of the structure may be within the highly amplified region of the response spectrum, depending on the frequency of the structure.

5.4.4. INERTIA EFFECT OF THE WALLS

The inertia effect of the walls during horizontal excitation may be neglected for a steel structure due to the thinness of the wall, but cannot be neglected for concrete tanks that have a considerable wall thickness compared to steel tanks. The inertia forces are generated parallel to the direction of excitation and are applied normal to the surface of the tank wall. The inertia pressure on the wall varies with the circumferential angle with the maximum pressure obtained in the direction of the excitation and a minimum perpendicular to the direction.

The inertia pressure was calculated with consideration of the peak ground acceleration and added to that of the impulsive component.

5.4.5. COMBINATION OF LOADS

The upper bound rule is prescribed in Eurocode 8: Part 4 (2006) when combining the various hydrodynamic loads and therefore the absolute maximum value of each component was added. The “square root of sums” rule may be unconservative due to the wide separation between the frequencies of the different components.

5.5. LOAD FACTORS

It should be kept in the mind that the hydrodynamic pressure is additional pressure exerted on the structure and does not replace the hydrostatic pressure exerted on the tank wall by the contained liquid. The sum of the hydrostatic and hydrodynamic pressure was calculated to obtain the total pressure acting on the tank wall. Both the ultimate and serviceability limit states were investigated for the seismic analysis of a structure and the load combinations obtained accordingly.

The load combinations provided in equations 5.7 to 5.10 were obtained from SANS 10160, 2009. Equations 5.7 and 5.8 are applicable to the ultimate limit state with

equation 5.7 pertaining to the axial load acting on a wall while equation 5.8 was used to calculate the bending moment and hoop stress in a wall.

$$LC1 = 1.35DL_{wall} \quad \text{eq 5.7}$$

$$LC2 = 1.0DL_{water} + 1.0EQ \quad \text{eq 5.8}$$

With DL_{wall} = self weight of the tank wall

DL_{water} = self weight of the contained liquid (hydrostatic)

EQ = force induced by the earthquake (hydrodynamic)

The load combinations for the serviceability limit state are presented in equation 5.9 and 5.10 with the reduction factor *v*, equal to 0.4 for Class IV structures (Eurocode 8: Part 4, 2006).

$$LC3 = 1.1DL_{wall} \quad \text{eq 5.9}$$

$$LC4 = 1.1DL_{water} + vEQ \quad \text{eq 5.10}$$

5.6. OVERTURNING MOMENT AND BASE SHEAR FORCE

The acceleration of the liquid mass during horizontal excitation produces a shear force at the base of the structure as well as an overturning moment of the structure about an axis perpendicular to the direction of excitation. These values, which are calculated immediately above the foundation, are used for the design of the tank wall and not the foundation itself.

The contained liquid is divided into several components when subjected to horizontal excitation. These are known as the impulsive, convective and in the case of flexible tanks, the flexible component. Each of these components are associated with a fraction of the contained liquid mass and in this section the computation of each mass is discussed along with the influence of each of these masses on the behaviour of the structure and contribution to the reaction forces.

5.6.1. IMPULSIVE MASS

The impulsive mass is associated with the impulsive pressure and is subjected to the peak ground acceleration and not the pseudoacceleration of the structure. The impulsive mass is rigidly attached to the tank wall and may have a significant influence on the behaviour of the wall during seismic excitation.

The impulsive mass may be expressed as a fraction of the total liquid mass and this fraction varies with the H/R ratio of the tank. For broad tanks the impulsive mass is about half of the total liquid mass but an increase in H/R ratio correspond to an increase in the fraction of impulsive mass. The influence of the impulsive component becomes more pronounced in taller structures.

The impulsive mass was calculated with equation 5.11, while the base shear force and overturning moment resulting from the horizontal acceleration of this mass was calculated with the use of equations 5.12 and 5.13. Only the first mode of vibration was considered in all instances (Eurocode 8: Part 4, 2006).

$$m_i = m2\gamma \frac{I_1(\frac{\nu_1}{\gamma})}{\nu_1^3 I_1'(\frac{\nu_1}{\gamma})} \qquad \text{eq 5.11}$$

With m = total contained liquid mass

γ = Height/Radius ratio of tank

I_1 = Modified Bessel function of order 1

I_1' = First derivation of the modified Bessel function of order 1

ν_1 = dimensionless parameter defined in Eurocode 8: Part 4 (2006)

The base shear force was calculated as (Eurocode 8: Part 4, 2006):

$$Q_i(t) = m_i A_g(t) \qquad \text{eq 5.12}$$

With m_i = impulsive mass determined from equation 5.11

$A_g(t)$ = peak ground acceleration

The overturning moment was calculated as (Eurocode 8: Part 4, 2006):

$$M_i(t) = m_i h_i A_g(t) \qquad \text{eq 5.13}$$

With m_i = impulsive mass

h_i = height of the impulsive mass calculated with Eurocode 8: Part 4 (2006)

$A_g(t)$ = peak ground acceleration

5.6.2. CONVECTIVE MASS

The convective mass is associated with the sloshing motion of the liquid. The sloshing component moves independently of the tank wall at its fundamental frequency and is subjected to a corresponding pseudoacceleration. The convective mass may be significant for broad tanks but decreases with an increase in H/R ratio until the influence of the sloshing motion becomes negligible for tall tanks.

The convective mass was calculated with equation 5.14 with consideration of only the first mode of vibration (Eurocode 8: Part 4, 2006).

$$m_{c1} = m \frac{2\tanh(\lambda_1 \gamma)}{\gamma \lambda_1 (\lambda_1^2 - 1)} \qquad \text{eq 5.14}$$

With m = total contained liquid mass

λ_1 = dimensionless parameter equal 1.841

γ = Height/Radius ratio of tank

The base shear force resulting from the convective component was calculated with equation 5.15 (Eurocode 8: Part 4, 2006).

$$Q_{c1}(t) = m_{c1} A_{c1}(t) \qquad \text{eq 5.15}$$

With m_{c1} = convective mass

$A_{c1}(t)$ = pseudoacceleration of first mode of vibration

The overturning moment was calculated with equation 5.16 (Eurocode 8: Part 4, 2006).

$$M_{c1} = m_{c1} A_{c1}(t) h_{c1} \qquad \text{eq 5.16}$$

With m_{c1} = convective mass associated with first mode of vibration
$A_{c1}(t)$ = pseudoacceleration of first mode of vibration
h_{c1} = height of convective mass

5.6.3. FLEXIBILITY COMPONENT

The mass associated with the flexibility of the tank wall is only considered for flexible tanks and is neglected for rigid tanks. The flexibility mass was computed from equation 5.17 (Eurocode 8: Part 4, 2006).

$$m_f = m\psi\gamma \frac{(-1)d_1}{\nu_1} \qquad \text{eq 5.17}$$

With m = total contained liquid mass
ψ, d_1, ν_1 = dimensionless parameters from Eurocode 8: Part 4 (2006)
γ = Height/Radius ratio

The base shear force resulting from the flexibility of the wall was determined from equation 5.18 (Eurocode 8: Part 4, 2006).

$$Q_f(t) = m_f A_f(t) \qquad \text{eq 5.18}$$

With m_f = flexibility mass
$A_f(t)$ = pseudoacceleration of structure

The overturning moment resulting from the flexibility of the wall was calculated with equation 5.19 (Eurocode 8: Part 4, 2006).

$$M_f(t) = m_f h_f A_f(t) \qquad \text{eq 5.19}$$

With m_f = flexibility mass

h_f = height of flexibility mass

$A_f(t)$ = pseudoacceleration of structure

5.6.4. INERTIA MASS

The base shear force resulting from the inertia effect of the wall is equal to the total weight of the tank wall multiplied by the peak ground acceleration while the overturning moment is calculated as the weight of the wall multiplied by the peak ground acceleration multiplied by half the height of the tank wall.

5.6.5. COMBINATION OF FORCES

The total base shear force and overturning moment was calculated with the upper bound rule in which the absolute maximum of each component force was added to one another.

5.7. FREEBOARD REQUIREMENTS

The amount of the freeboard required for the serviceability limit state was calculated with equation 5.20 with consideration of only the first mode of vibration of the sloshing component (Eurocode 8: Part 4, 2006).

$$d_{max} = \frac{0.84RA_{c1}(t)}{g} \qquad \text{eq 5.20}$$

With R = radius of tank

$A_{c1}(t)$ = pseudoacceleration of first mode of vibration

g = gravitational acceleration equal to 9.81 m/s^2

5.8. AREA REINFORCEMENT REQUIRED

The method presented in Eurocode 8: Part 4 (2006) was only used to verify some of the results obtained with the numerical method by Veletsos (1997). The area of reinforcement required to resist the bending moment and tensile force were thus not

determined for the forces computed with the method presented in Eurocode 8: Part 4 (2006).

This chapter contained information on the method presented in Eurocode 8: Part 4 (2006) for the determination of the hydrodynamic pressure, associated liquid mass and reaction forces. In the following chapter the method presented by Veletsos (1997) is discussed with regard to the determination of the hydrodynamic pressure, the mass associated with each liquid component and resulting forces. The amount of reinforcement required for the ultimate and serviceability limit states respectively is also discussed.

6. DYNAMIC NUMERICAL ANALYSIS – VELETSOS

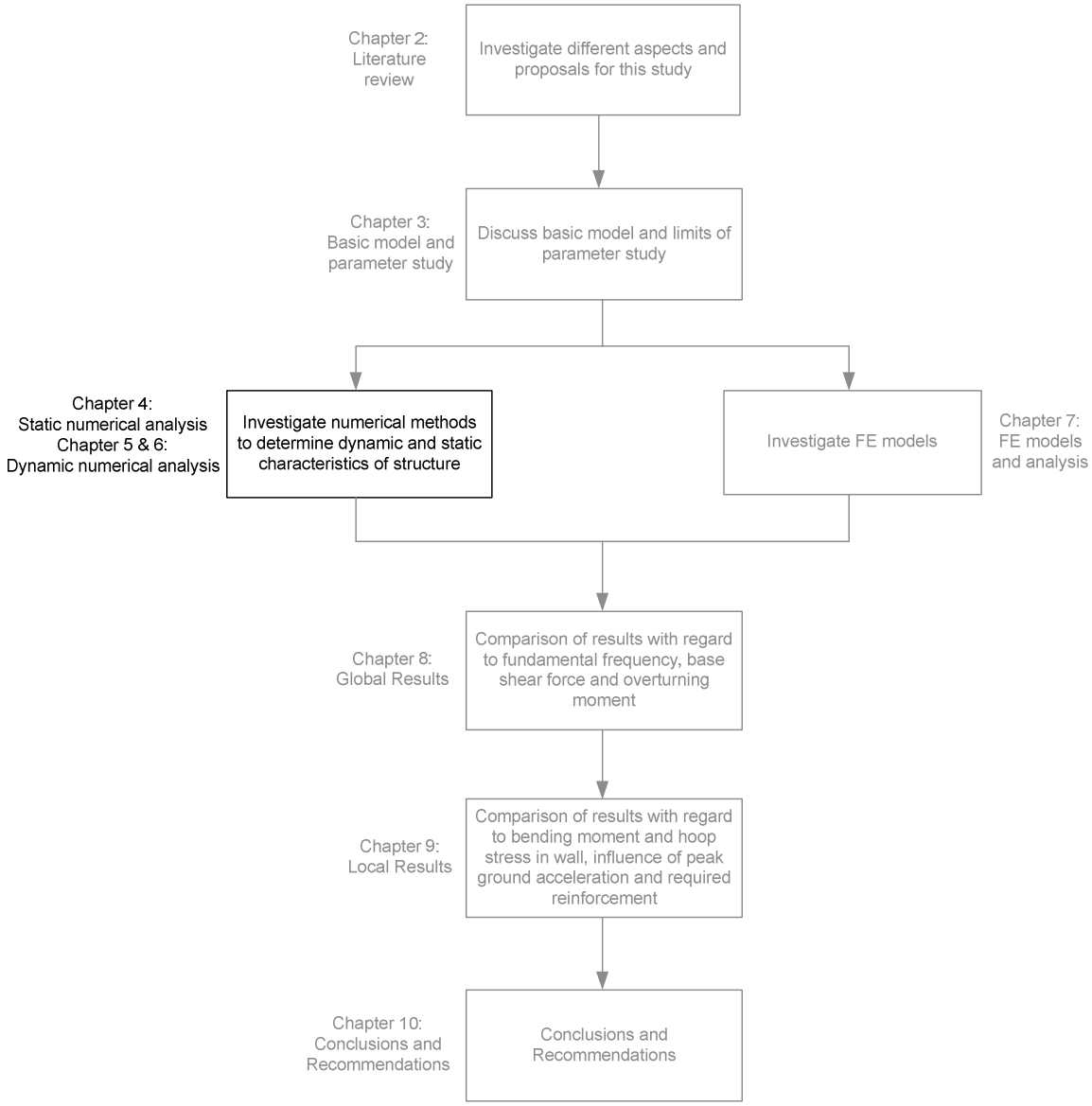

Figure 6.1: Methodology of study

With reference to Figure 6.1, three numerical methods were used throughout this study for the analysis of each water-retaining structure. In this chapter the method presented in Veletsos (1997) for the determination of the dynamic effects resulting from seismic excitation is discussed. The method presented by Veletsos (1997) is less cumbersome then the method presented by Eurocode 8: Part 4 (2006). For this reason the method presented by Veletsos (1997) was used for the numerical analyses of all structures in this study. In this chapter the method presented by Veletsos (1997) for the determination of

the fundamental frequency, hydrodynamic pressure and resulting forces is presented along with the determination of the reinforcement required for the ultimate and serviceability limit state respectively. In Appendix A an example of the calculations for a structure with a H/R ratio of 0.6 and t_w/R ratio of 0.024 is provided. All of the equations presented in this chapter were obtained from Veletsos (1997) unless otherwise stated.

6.1. FUNDAMENTAL FREQUENCY OF MODEL

A water-retaining structure is classified based upon the flexibility of the wall and may be regarded as either rigid or flexible. In this study it was assumed all structures have flexible walls as discussed in Chapter 8. The fundamental mode shape of a flexible structure was assumed to be similar to the fundamental mode shape of a cantilever beam (Veletsos, 1997). The fundamental frequency of the tank-liquid system was calculated with the use of equation 6.1 (Veletsos, 1997).

$$f_{i1} = \frac{1}{2\pi}\frac{C_{i1}}{H}\sqrt{\frac{E_w}{\rho_w}} \qquad \text{eq 6.1}$$

With C_{i1} = dimensionless parameter in Veletsos (1997)
H = height up to free surface of liquid
E_w = modulus of elasticity of wall material
ρ_w = density of tank material

The motion of the convective component is different from the motion of the flexible wall structure and the ground motion. The fundamental frequency of the sloshing component was determined with equation 6.2 (Veletsos, 1997).

$$f_{c1} = \frac{1}{2\pi}\sqrt{\lambda_1 \frac{g}{R}\tanh\left[\lambda_1\left(\frac{H}{R}\right)\right]} \qquad \text{eq 6.2}$$

With λ_1 = dimensionless parameter equal to 1.841
g = gravitational acceleration equal to 9.81 m/s^2
R = radius of the tank
H = height measured from the base to the free liquid surface

6.2. PSEUDOACCELERATION

The pseudoacceleration experienced by a flexible structure is determined from the fundamental impulsive period in conjunction with the spectral response for elastic analysis, in the case of the ultimate limit state, and the elastic response spectrum, for the serviceability limit state.

The pseudoacceleration of the sloshing component is determined with the use of the elastic response spectrum since the sloshing motion is considered to be elastic. The second mode of vibration may be neglected unless the pseudoacceleration of the second and higher modes of vibration is significantly larger than the first mode of vibration. If the pseudoacceleration of the higher modes of vibration is larger than the fundamental mode of vibration, the magnitude of pressure corresponding with the higher modes of vibration is larger than pressure obtained for the first mode and higher reaction forces and hoop stress are obtained. The pseudoacceleration corresponding to the fundamental frequency of the convective component is usually significantly smaller than the peak ground acceleration. The contribution of the sloshing motion to the hydrodynamic pressure may therefore be neglected for tanks of large radii (Veletsos, 1997). For this reason, only the pressure exerted on the tank wall by the impulsive component was considered during this study.

6.3. GRAVITATIONAL LOAD

Only the self-weight of the tank walls were considered in this study. The self-weight of the contained liquid exerts a pressure on the foundation and was neglected. The pressure acting on the base is considered in the design of the foundation which is not within the scope of this study. The self-weight of the roof was also neglected since the bending moment and hoop stress in the tank wall was of interest in this project. It was assumed the weight of the roof does not contribute to the mass participating in bending of the tank wall.

6.4. HYDRODYNAMIC LOADS

With the fundamental frequency of the tank-liquid system and corresponding pseudoacceleration known, the hydrodynamic pressure exerted on the tank wall could

be determined. Both the determination of the impulsive and convective components is discussed in this chapter for rigid and flexible tanks. However, in this study all structures were considered to be flexible as discussed in Chapter 8.

6.4.1. IMPULSIVE PRESSURE

In the case of flexible tanks, the impulsive component of the liquid mass experiences the same motion as the wall and is subjected to the pseudoacceleration of the tank-liquid system. It should be noted the method presented in Veletsos (1997) differs from that of Eurocode 8: Part 4 (2006) with the inclusion of the flexibility of the tank wall. The flexibility of the tank wall is not considered as a separate entity in Veletsos (1997) but rather included in the determination of the impulsive component with the use of the parameter c_i. In Eurocode 8: Part 4 (2006) the flexibility of the wall is considered separately with the use of the flexible component. The impulsive pressure for flexible tanks was determined with the use of equation 6.3 (Veletsos, 1997).

$$p_i(\eta, \theta, t) = c_i(\eta)\rho R \mathrm{A_{i1}}(t) cos\theta \qquad \text{eq 6.3}$$

With η = z/H, with z measured from the bottom of the tank wall

c_i = dimensionless parameter in Veletsos (1997)

ρ = density of the contained liquid

R = radius of the tank

θ = circumferential angle, considered equal to 0 degrees to obtain maximum impulsive pressure

A_{i1} = pseudoacceleration of fundamental frequency

In the case of rigid tanks, both the impulsive component and the structure experience the same motion as the soil during horizontal seismic excitation. The impulsive pressure for rigid tanks is calculated by substitution of the pseudoacceleration in equation 6.3 with the peak ground acceleration.

6.4.2. CONVECTIVE COMPONENT

The fundamental frequency of the convective component differs significantly from the ground motion and the frequency of the tank-liquid system in the case of flexible tanks. The convective component is therefore independent of the wall flexibility and may be determined with the use of rigid tanks which are less complex than flexible structures. The pressure exerted on the tank wall by the convective component was calculated with equation 6.4. It was assumed the higher modes of vibration are negligible and only the first mode of vibration was considered for all structures (Veletsos, 1997).

$$p_c(\eta, \theta, t) = c_{c1}(\eta) A_{c1}(t) \rho R cos\theta \qquad \text{eq 6.4}$$

With η = z/H, with z measured upward from the bottom of the wall

θ = circumferential angle, equal to 0 degrees for maximum pressure

c_{c1} = dimensionless parameter from Veletsos (1997)

$A_{c1}(t)$ = pseudoacceleration corresponding to first mode of vibration

ρ = density of the contained liquid

R = radius of the tank

6.4.3. INERTIA OF THE TANK WALL

All structures in this study were considered to be flexible and the inertia effect of the tank wall is included in the computation of the impulsive component. However, if the tank wall is assumed to be rigid, the horizontal pressure resulting from the inertia effect of the wall is considered separately and calculated from equation 6.5.

$$p_w = \rho_w t_w \ddot{x}_g cos\theta \qquad \text{eq 6.5}$$

With ρ_w = density of the wall material

t_w = thickness of tank wall

$\ddot{x}_g$ = peak ground acceleration

θ = circumferential angle, equal to 0 degrees for maximum pressure

6.5. LOAD FACTORS

The load factors for the combination of the hydrostatic and hydrodynamic loads are the same as described in Chapter 5 for Eurocode 8: Part 4 (2006). All of the load combinations were obtained from SANS 10160 (2009) and are presented here in equations 6.6 and 6.7 for the ultimate limit state. Equation 6.6 is applicable to the vertical axial force in the tank wall while equation 6.7 was used for the calculation of the bending moment and for the hoop stress in the tank wall.

$$LC1 = 1.35DL_{wall} \quad \text{eq 6.6}$$

$$LC2 = 1.0DL_{water} + 1.0EQ \quad \text{eq 6.7}$$

With DL_{wall} = self weight of the tank wall

DL_{water} = self weight of the contained liquid (hydrostatic)

EQ = force induced by the earthquake (hydrodynamic)

Equations 6.8 and 6.9 are applicable to the serviceability limit state. The reduction factor v, is equal to 0.4 for Class IV structures (Eurocode 8: Part 4, 2006).

$$LC3 = 1.1DL_{wall} \quad \text{eq 6.8}$$

$$LC4 = 1.1DL_{water} + vEQ \quad \text{eq 6.9}$$

6.6. OVERTURNING MOMENT AND BASE SHEAR

The horizontal acceleration of the liquid mass results in a shear force at the base of the structure and an overturning moment around an axis perpendicular to the direction of excitation. The total liquid mass consists of the mass associated with the impulsive and convective components. These masses are considered separately since they experience different accelerations.

6.6.1. CONVECTIVE COMPONENT

The motion of the sloshing (convective) component of the liquid is independent of the flexibility of the tank wall. The mass corresponding with the sloshing motion of

the liquid was calculated with equation 6.10 with consideration of only the first mode of vibration (Veletsos, 1997).

$$m_{c1} = \left\{ \frac{2}{\lambda_1(\lambda_1^2-1)\left(\frac{H}{R}\right)} \tanh\left[\lambda_1\left(\frac{H}{R}\right)\right] \right\} m \qquad \text{eq 6.10}$$

With λ_1 = dimensionless parameter equal to 1.841

H = height up to free liquid surface

R = radius of the tank

m = total mass of contained liquid

The vibration of the convective mass introduces a shear force at the base of the structure, calculated with equation 6.11 and an overturning moment determined with equation 6.12 (Veletsos, 1997).

$$Q_{c1} = m_{c1} A_{c1}(t) \qquad \text{eq 6.11}$$

$$M_{c1} = m_{c1} h_{c1} A_{c1}(t) \qquad \text{eq 6.12}$$

With m_{c1} = convective mass for fundamental frequency

A_{c1} = pseudoacceleration associated with fundamental frequency

h_c1 = height from base to convective mass determined from Veletsos (1997)

6.6.2. IMPULSIVE COMPONENT

The computation of the impulsive mass differs from the convective mass since the impulsive mass is influenced by the flexibility of the wall. In the case of rigid tank walls, the impulsive mass moves rigidly with the wall and is subjected to the peak ground acceleration. The impulsive mass was calculated with the use of equation 6.13 and it should be noted the impulsive mass calculated does not include the mass of the wall and therefore the inertia mass was considered separately (Veletsos, 1997).

$$m_i + m_{c1} = m \qquad \text{eq 6.13}$$

With m = total mass of contained liquid

m_{c1} = convective mass for fundamental frequency

However, all structures in this study were considered to be flexible. The impulsive mass for the flexible tanks was calculated with equation 6.14 which includes the inertia effect of the tank wall (Veletsos, 1997).

$$m_{i1} = m_i + m_w \qquad \text{eq 6.14}$$

With m_{i1} = impulsive mass participating in the first mode of vibration of structure, determined from Veletsos (1997)

m_i = total impulsive mass

m_w = mass of tank wall

The base shear force and overturning moment resulting from the horizontal acceleration of the impulsive mass were calculated with equation 6.15 and 6.16 for the case of a flexible tank wall (Veletsos, 1997).

$$Q_i(t) = m_{i1}\mathrm{A_{i1}(t)} \qquad \text{eq 6.15}$$

$$M_i(t) = m_{i1}h_{i1}\mathrm{A_{i1}}(t) \qquad \text{eq 6.16}$$

With m_{i1} = impulsive mass participating in the first mode of vibration of the structure

A_{i1} = pseudoacceleration of tank-liquid system

h_{i1} = height from base to impulsive mass

For the determination of the base shear force and overturning moment in rigid tanks, the pseudoacceleration of the tank-liquid system is substituted with the peak ground acceleration.

6.6.3. INERTIA OF TANK WALL

The base shear force and overturning moment resulting from the inertia of the tank wall was not determined in this study. All structures were considered to be flexible

and the inertia effect of the wall is included in the computations of the impulsive component.

However, in the case of rigid tanks the inertia effect of the tank wall is considered separately. The base shear force and overturning moment resulting from the inertia of the tank wall were calculated with equations 6.19 and 6.20 (Veletsos, 1997).

$$Q_w = m_w \ddot{x}_g \qquad \text{eq 6.19}$$

$$M_w = m_w \left(\frac{H}{2}\right) \ddot{x}_g \qquad \text{eq 6.20}$$

With m_w = mass of the tank wall

$\ddot{x}_g$ = peak ground acceleration

H = height up to free liquid surface

6.6.4. COMBINATION OF FORCES

The upper bound rule was used to combine the influence of the impulsive and convective component in terms of pressure, base shear force and overturning moment as prescribed in Veletsos (1997). The absolute maximum of each component is therefore added to obtain the total forces.

In all instances, only the first mode of vibration was considered for the impulsive and convective components. Since the radius of the example tank is large, the influence of the sloshing motion of the liquid was neglected and only the contribution of the impulsive component to the base shear force and overturning moment was considered (Veletsos, 1997).

6.7. FREEBOARD REQUIREMENTS

The freeboard was calculated with the use of equation 6.21. Veletsos (1997) considers the contribution all the modes of vibration of the sloshing component with the use of the “square-root-of-sums” rule for the combination of the all the modes.

$$d_s = R\sqrt{(0.837\frac{(S_A)_{c1}}{g})^2 + (0.073\frac{(S_A)_{c2}}{g})^2 + (0.028\frac{(S_A)_{c3}}{g})^2 + \cdots} \qquad \text{eq 6.21}$$

With R = radius of the tank

$(S_A)_{cn}$ = pseudoacceleration of n-th mode

g = gravitational acceleration equal to 9.81 m/s^2

With consideration of the first mode of vibration of the sloshing component only, equation 6.21 reduces to equation 6.22 which is similar to the equation presented in Eurocode 8: Part 4 (2006).

$$d_s = 0.837R\frac{(S_A)_{c1}}{g}) \qquad \text{eq 6.20}$$

The method of calculation of the required freeboard has been provided for both of the numerical methods. However, the required freeboard was not of interest in this study and therefore no results are presented in this document.

6.8. AREA OF REINFORCEMENT

The area of reinforcement required for the static design of water-retaining structures has already been discussed in Chapter 4. In this section the area of reinforcement required for the seismic design of water-retaining structures is discussed. One of the aims of this study was to determine whether seismic loads are a critical load case in South Africa and which of the limit states govern the design of water-retaining structures for seismic design. Subsequently, the area of reinforcement required for the static analysis was compared with the reinforcement required for the seismic analysis of a water-retaining structure. The area of reinforcement required for the ultimate and serviceability limit states were also compared. Both limit states are discussed in this section.

6.8.1. ULTIMATE LIMIT STATE

The total hoop stress in the wall was considered as the sum of the hoop stress resulting from the hydrostatic pressure, and the hoop stress resulting from the hydrodynamic pressure. The same method for computing the area of

reinforcement required was used as presented for the static analysis. Refer to section 4.2.1 for a layout of the method followed.

It should be noted the minimum area of reinforcement required for sections subjected to a tensile force as prescribed by the design codes was not considered in this study. Comparisons between different structural geometries and peak ground accelerations were made to assess the influence of seismic excitation on a water-retaining structure. Hence the actual value of the required reinforcement was used.

6.8.2. SERVICEABILITY LIMIT STATE

The serviceability limit state is governed by the maximum allowable crack width resulting from the bending moment and hoop stress in the wall. The same method as presented for static analysis was followed in computing the area of reinforcement required for both the bending moment and hoop stress. Refer to section 4.2.2 for a layout of the method used for the calculation of the required reinforcement.

This chapter provides information on the primary numerical method used during this study. The computation of the hydrodynamic effects due to seismic excitation of a water-retaining structure as well as the determination of reinforcement for both the ultimate and serviceability limit state were discussed in this chapter. The numerical method for the static analysis and both the numerical methods for the seismic analysis of a structure have been discussed in the three preceding chapters.

In the following chapter the finite element analyses of water-retaining structures considered in this project are presented with regard to the basic layout of a model and the various methods of distributing the impulsive mass to obtain accurate results for the frequency, reaction and internal forces. Both the static and seismic analyses of a structure are discussed as well as the incorporation of the relevant response spectrum. The finite element package STRAND7 (2005) was used throughout this study for the analysis of a structure. The analysis of a structure in STRAND7 (2005) for the ultimate and serviceability limit states are also presented and results are presented in the following chapters.

7. FINITE ELEMENT MODELS AND ANALYSIS

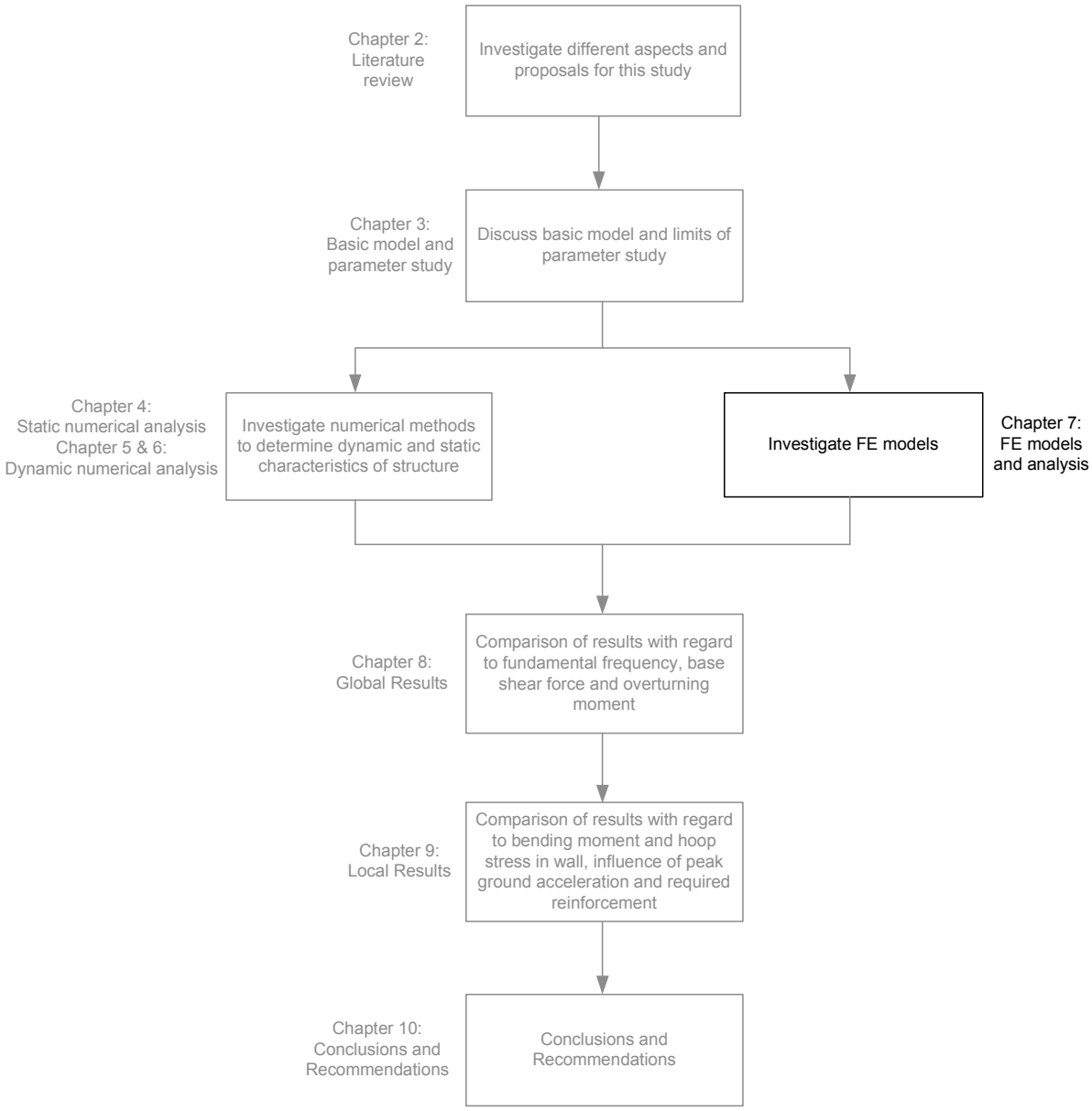

Figure 7.1: Methodology of study

All structures in the parametric study were analysed with the use of the three numerical models as outlined in the preceding chapters. With reference to Figure 7.1 the following step in the methodology of this study was the analysis of each structure with the use of a finite element program. In the course of this project the FE package STRAND7 (2005) was used to investigate various FE models as discussed in this chapter. The results obtained from the FE analysis of a structure was subsequently compared with the results obtained from

the numerical method as presented in Veletsos (1997) in order to assess the accuracy of the FE model.

The FE analysis of a water-retaining structure can be very complex with consideration of the interaction between the water and structure at the water-structure boundary. However, in the engineering practice in South Africa sophisticated FE models are rarely used and simplified models which provide accurate results are preferred. For the purposes of this study simplified FE models were investigated as proposed by two authors, namely Nachtigall (2003) and Virella (2006). The first model as proposed by Nachtigall (2003) suggests the uniform distribution of the impulsive mass among the nodes in a model, with the lumped masses attached directly to the wall element nodes. The second model as proposed by Virella (2006) suggests the distribution of the impulsive mass in the same manner as the hydrodynamic pressure along the wall, with the impulsive lumped masses attached to the wall nodes with the use of pinned links. A third model was investigated in this project with the distribution of the impulsive mass similar to the hydrodynamic pressure along the height of the wall with the attachment of the lumped masses directly to the wall element nodes.

In this chapter the basic FE model is discussed in terms of the elements used for the modelling of the structure, the properties of the wall material and the fixity of the nodes. The model used for the static analysis of a structure is presented with addition of the hydrostatic pressure to the basic model. Information is provided on the seismic analysis of a structure with regard to the distribution of the impulsive mass, the use of the response spectrum in the program and analyses for the ultimate and serviceability limit state respectively. It should be noted that the convective mass was neglected in all models since the effect of the convective component becomes negligible for large radii tanks (Veletsos, 1997).

7.1. BASIC FE MODEL

The basic FE model consisted only of the tank wall with no additional water pressure or liquid mass. The tank roof was not modelled since it provides no restraint against the cos(nθ) type of deformation (Housner, 1963). The foundation was also not modelled since the foundation is considered to be rigidly supported with no rocking or tilting of

the foundation and the forces acting on the foundation were not investigated in this study.

A cylindrical coordinate system was used with coordinates *R* and *z* as the radius and vertical distance respectively. All FE models had a radius of 10 meters and nodes were placed at a circumferential angle increment of 3 degrees. The height increment was varied between 0.6 meter and 0.45 meter depending on the H/R ratio of the model. For the broad tanks with H/R ratio of 0.3 meter and 0.6 a nodal height increment of 0.6 meter was used which corresponds to an element aspect ratio of 1.14. For tanks with a H/R ratio of 0.9, 1.2 and 1.5 a height increment of 0.45 meter was used with an element aspect ratio of 0.86. The aspect ratio of an element is considered acceptable if the aspect ratio is less than 2.0 (Cook, 2002).

The wall elements were chosen with consideration of the hydrostatic and hydrodynamic pressure. The contained liquid exerts a horizontal pressure on the tank wall resulting in out-of-plane deformation of the wall elements. The horizontal outward pressure produces an internal hoop stress resulting in in-plane deformation. With both out-of-plane and in-plane deformation expected, use was made of plate/shell elements. Various FE packages exists, but the STRAND7 (2005) program was used throughout this study for the finite element analyses of all structures within the scope of this project. STRAND7 (2005) suggests the use of 8-node shell elements for curved shells since additional moments are generated at the edge between adjoining elements if 4-node "flat" shell elements are used. Only 4-node shell elements were used for the FE models in this project which was considered to provide sufficiently accurate results as discussed in Chapter 9. For all FE models a relatively fine mesh were used with the additional bending moments at the adjoining edges becoming negligible (STRAND7, 2005).

The prediction of the behaviour of the tank wall during seismic excitation was the primary consideration in this study. The influence of seismic excitation on the foundation of the structure was not considered since it was assumed the foundation is rigidly supported with no tilting or rocking of the foundation. Since the behaviour and design of the foundation were not of importance in this project it was subsequently not modelled in STRAND7 (2005).

The wall was considered to be fixed at the base and therefore all the bottom nodes in the model were restrained against both translation and rotation. Seismic excitation was considered to be in the direction of the global x-axis and nodes situated on this line of excitation can therefore only move in the direction of the x-axis. A number of these nodes are situated along the height of the wall and these nodes were all restricted from translation in the direction of the y-axis which is perpendicular to the direction of excitation. Refer to Figure 7.2 for a layout of the basic model with nodes indicated in yellow, shell elements in blue and restraints in pink.

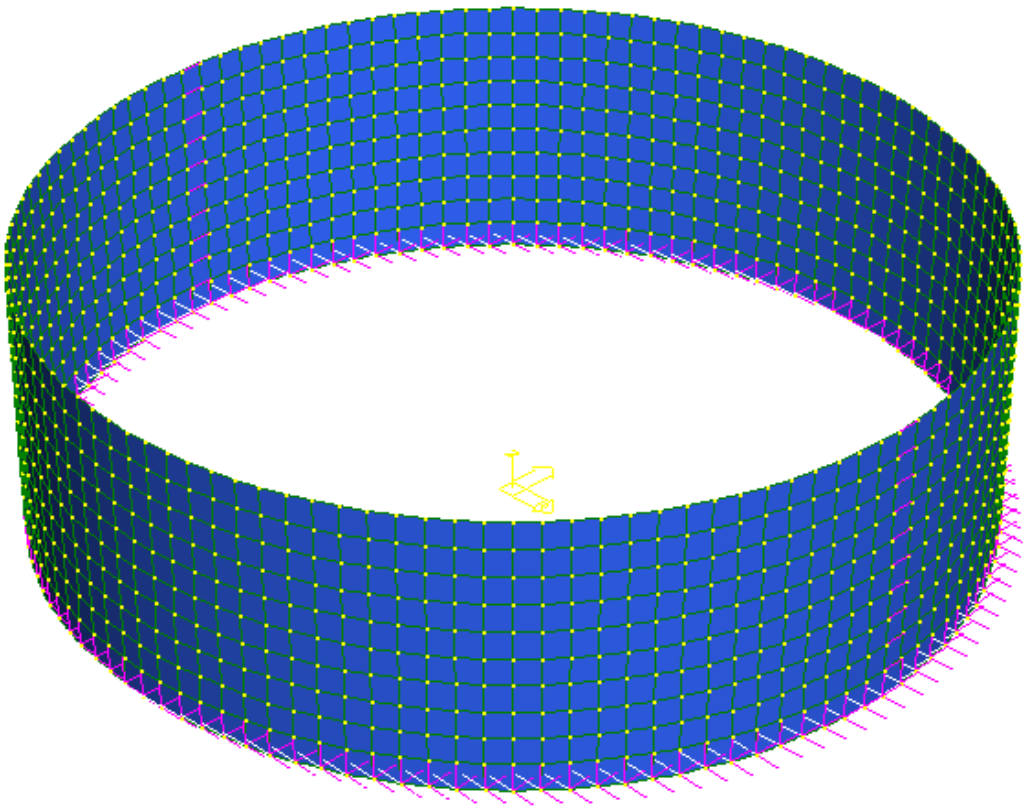

Figure 7.2: Layout of basic FE model

With the global geometry and restraints known, the properties of the elements could be specified. As outlined in the parametric study in Chapter 3, the t_w/R ratio of each model was varied between 0.006 and 0.03 and all shell elements were considered to be thin since the thickness of the element was less than one-tenth the radius of the structure. The classification of a shell element as either a thin or thick shell is important with only

bending action contributing to out-of-plane deformation in the case of thin shells and no deformation resulting from shear action (STRAND7, 2005).

The wall material was expected to remain elastic when subjected to hydrostatic and hydrodynamic loads and no non-linear material behaviour was specified in STRAND7 (2005). The material was prescribed as 40 MPa concrete with a modulus of elasticity equal to 34.3 GPa, Poisson's ratio of 0.2 and density of 2500 kg/m^3.

The static and dynamic analyses of each structure were completed in STRAND7 (2005) with the application of either the hydrostatic pressure or addition of the impulsive mass to the basic model. The static analysis of a model is discussed further in the next section followed by the FE models with different impulsive mass distributions used for the seismic analysis of a structure.

7.2. STATIC ANALYSIS

The static numerical analysis of a structure was completed with the use of design tables provided in Ghali (1979) from which the hoop force and bending moment in a wall could be determined. The results obtained with the use of Ghali (1979) were used to verify the static results obtained with the finite element models. Results obtained in STRAND7 (2005) were compared with the method of Ghali (1979) for both the hoop stress and bending moment in the wall and the comparative graphs are provided in Chapter 9 and Appendix C.

The hydrostatic pressure exerted on the tank wall by the contained liquid was applied to the basic model in STRAND7 (2005). The hydrostatic pressure has a linear variation along the height of the wall, but due to modelling restrictions in STRAND7 (2005) the average pressure acting on a shell element was uniformly applied perpendicular to the element area. A linear static analysis was completed with the use of the FE model and the hoop stress and bending moment in the wall could be obtained. A FE model with applied hydrostatic pressure is presented in Figure 7.3.

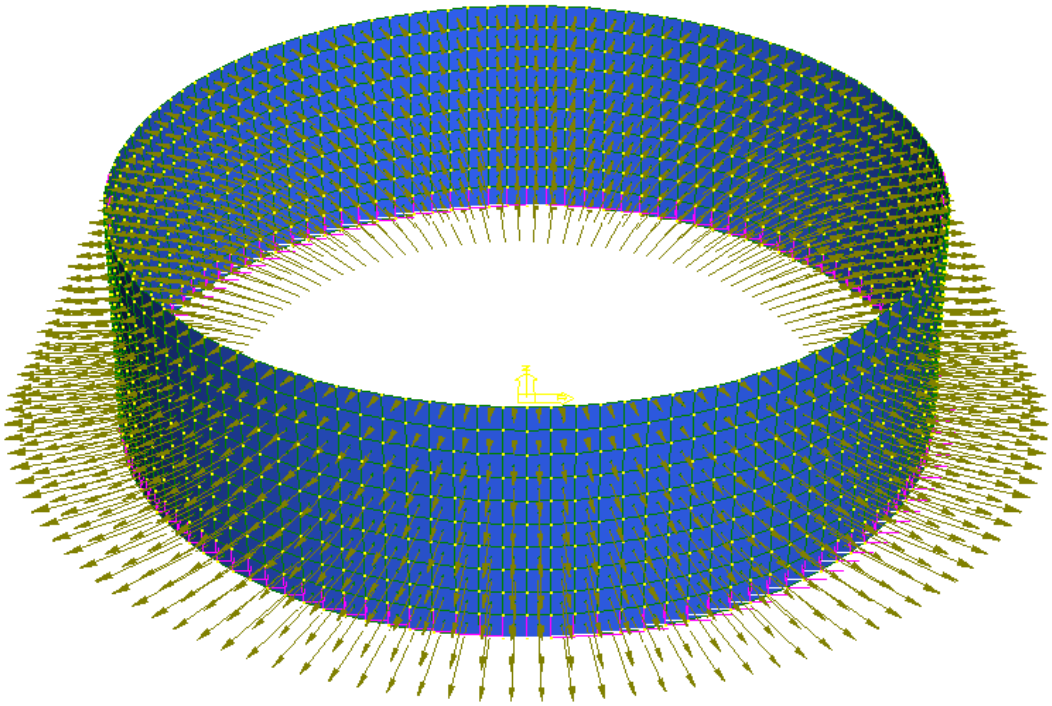

Figure 7.3: FE model with hydrostatic pressure

7.3. IMPULSIVE MASS DISTRIBUTION

For the seismic analysis, three different FE models were investigated for the distribution of the impulsive mass. The purpose of the investigation was to assess the accuracy of each model in the prediction of the fundamental frequency of vibration and associated mode shape. The correct values of the reaction and internal forces were also important since one of the aims of this project was to propose a model suitable for practical use. The three FE models are discussed in this section, ranging from the simpler model to the most complex one. The different FE models are summarized below for clarity purposes.

- Uniformly distributed mass (ED-m_i) model as proposed by Nachtigall (2003)
- Pressure distributed mass (PD-m_i) model, a model proposed by the supervisor and author of this study
- Virella model as proposed by Virella (2006)

7.3.1. UNIFORMLY DISTRIBUTED IMPULSIVE MASS

The first model investigated was proposed by Nachtigall (2003) in which the impulsive mass is uniformly distributed among the nodes located on the tank wall

and fixed directly to the element nodes on the wall. With the consideration of all structures as flexible, the maximum impulsive mass participating in the first mode of vibration was calculated with the method presented in Veletsos (1997) and circumferential angle equal to 0 degrees. Refer to Figure 7.4 for the STRAND7 (2005) model as proposed in Nachtigall (2003).

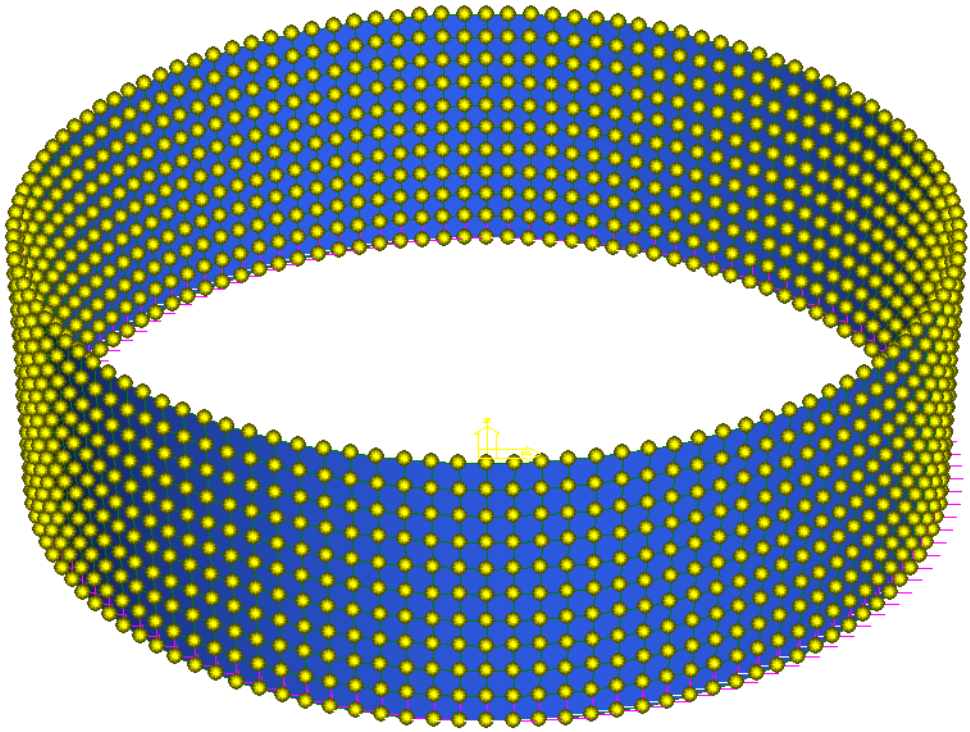

Figure 7.4: Uniformly distributed mass model

The FE model proposed by Nachtigall (2003) is not entirely correct since the impulsive mass is representative of the hydrodynamic pressure which varies along the height and circumference of the tank wall while the impulsive mass is distributed here uniformly in both directions. With the use of the maximum impulsive pressure and constant distribution along the circumference of the wall it implies that double the numerically calculated impulsive mass participates in the vibration of the structure which is incorrect.

7.3.2. PRESSURE DISTRIBUTED IMPULSIVE MASS

The second model addresses the issue of variance in the lumped impulsive mass along the height of the tank wall. This model was proposed by the supervisor and

author of this study. In all instances the tank was assumed to be flexible and the impulsive mass participating in the fundamental frequency and corresponding with the maximum hydrodynamic pressure was calculated with the method presented in Veletsos (1997). The impulsive mass in this model was distributed along the height of the wall in the same manner as the hydrodynamic pressure but was not varied along the circumference of the wall. The computation of the lumped masses with the correct distribution along the height and circumference of the wall is a cumbersome process and not suitable for practical use in the engineering industry. One of the aims of this project was to propose a FE model suitable for practical use and therefore a simplified model in which the lumped masses are not varied along the circumference of the wall was investigated.

With the non-variance of the lumped masses along the circumference of the wall the problem remains with the contribution of the lumped masses to the behaviour of the tank during horizontal excitation. This model again implies double the numerically computed impulsive mass contributes to the horizontal motion of the wall. The appropriate STRAND7 (2005) model is provided in Figure 7.5.

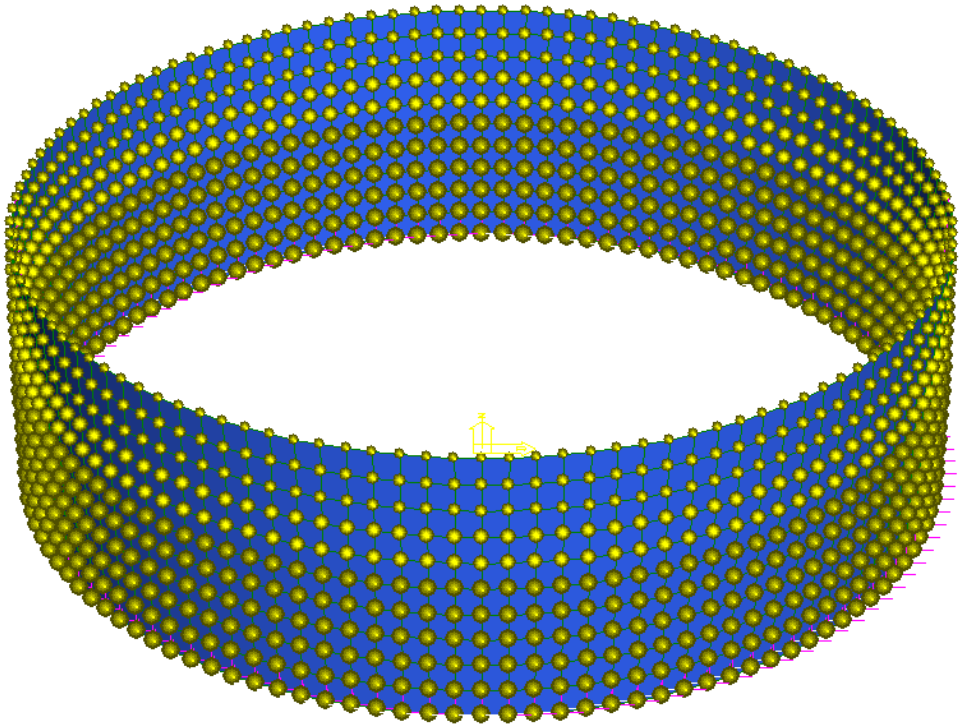

Figure 7.5: Pressure distributed mass model

7.3.3. VIRELLA MODEL (2006)

The model proposed by Virella (2006) is significantly more complex than the previous two models and differ in a number of ways from the first two models. The first difference is the consideration of the tank wall to be rigid by Virella (2006) while it was assumed in the previous two models that the tank wall is flexible. The impulsive pressure for rigid tanks is obtained with the method presented in Veletsos (1997). With the use of the maximum hydrodynamic pressure, the lumped impulsive masses are determined and varied along the height of the wall in the same manner as the pressure. However, the lumped impulsive masses are not varied along the circumference of the tank wall. This solves the problem with the variance in the hydrodynamic pressure along the height of the wall but not the variance along the circumference of the wall.

The second difference between Virella (2006) and the first two FE models is the way in which the lumped impulsive masses are attached to the tank wall. In the previous models the lumped impulsive masses were fixed to the element nodes on the tank wall. However, Virella (2006) proposes the use of pinned links to avoid the direct attachment of the lumped masses to the nodes on the tank wall. With the use of pinned links the movement of the lumped masses and structure can be prescribed separately in the various directions while the impulsive mass is still allowed to move in combination with the wall since the length of a pinned link always remains constant.

An important aspect to be kept in mind is that the impulsive mass is representative of the impulsive pressure. The pressure always acts perpendicular to the surface of the shell element and therefore the lumped impulsive mass must remain normal the shell surface even during deformation. The lumped masses were restrained in a tangential and vertical direction with only radial movement permitted, ensuring the movement of the lumped mass remains perpendicular to the shell surface at all times. Restriction of the tangential and vertical motion of the lumped mass also ensures that the lumped masses on the line of excitation (x-axis) undergoes maximum radial deformation, representing maximum hydrodynamic pressure while the lumped masses on a line perpendicular to the direction of excitation (y-

axis) will have zero displacement which represent zero hydrodynamic pressure. Refer to Figure 7.6 for a schematical layout of the model proposed by Virella (2006).

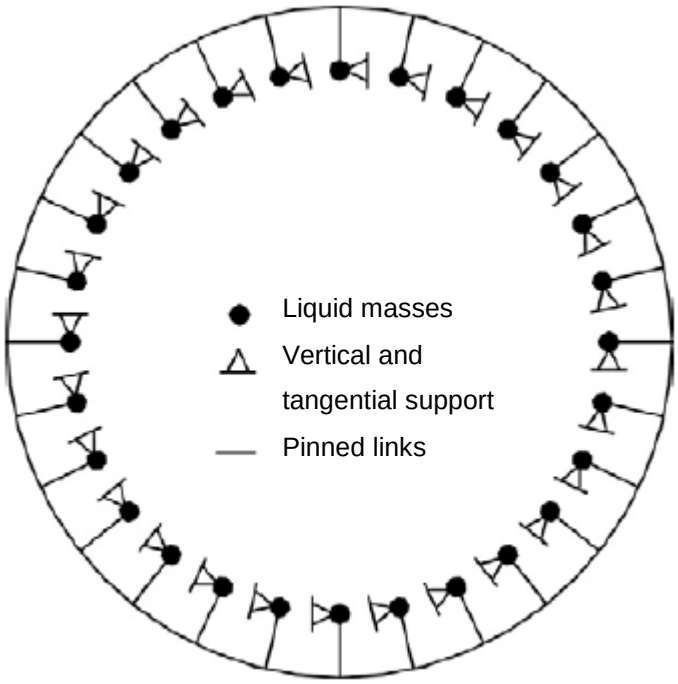

Figure 7.6: Schematical layout of Virella (2006)

With the use of only the maximum impulsive pressure and no variance around the circumference of the wall, double the actual impulsive mass is added to the structure. However, the contribution of the lumped masses to the behaviour of the structure decreases with an increase in circumferential angle due to the transverse restraints of movement. With maximum contribution of the lumped masses in the direction of excitation and zero contribution of the masses perpendicular to the direction, only half of the total masses added to the structure contribute to the behaviour of the structure during seismic excitation. This is equal to the mass calculated from the equation for rigid tanks as presented by Veletsos (1997). The STRAND7 (2005) model proposed by Virella (2006) is presented in Figure 7.7.

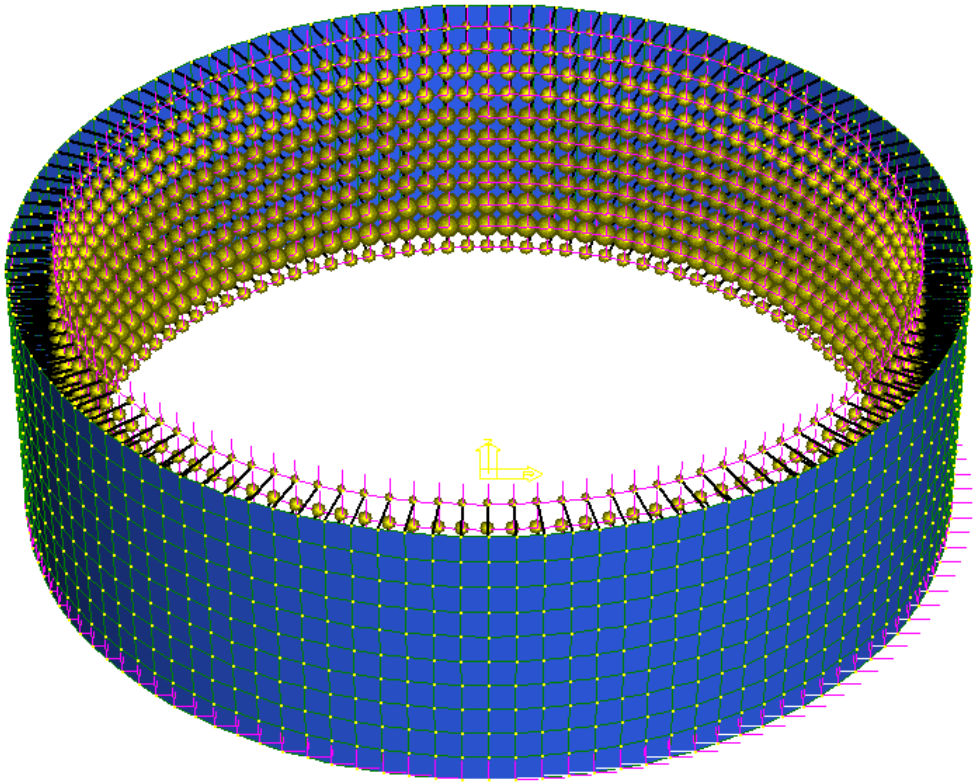

Figure 7.7: FE model proposed by Virella (2006)

7.4. LOAD COMBINATIONS

The hydrostatic pressure and impulsive mass applied to a basic FE model were characteristic loads and did not include the partial design factors. For clarity purposes the load combinations as obtained from SANS 10160 (2009) are presented here again. The load combinations for static loading conditions are presented in equation 7.1 and 7.2 for the ultimate and serviceability limit states respectively.

$$LC1 = 1.2DL_{water} \quad \text{eq 7.1}$$

$$LC2 = 1.1DL_{water} \quad \text{eq 7.2}$$

With DL_{water} = self-weight of the contained liquid

The ultimate limit state load combinations for the seismic analysis of a structure are presented below. The load combinations for the ultimate limit state are presented in

equation 7.3 and 7.4 for the vertical force and bending moment about a horizontal axis respectively.

$$LC3 = 1.35DL_{wall} \quad \text{eq 7.3}$$

$$LC4 = 1.0DL_{water} + 1.0EQ \quad \text{eq 7.4}$$

With DL_{wall} = self weight of the tank wall

DL_{water} = self weight of the contained liquid (hydrostatic)

EQ = force induced by the earthquake (hydrodynamic)

Equations 7.5 and 7.6 are applicable to the serviceability limit state with load combination 5 applicable to the vertical force and load combination 6 applicable to the bending moment about a horizontal axis and hoop stress in the wall.

$$LC5 = 1.1DL_{wall} \quad \text{eq 7.5}$$

$$LC6 = 1.1DL_{water} + 1.0EQ \quad \text{eq 7.6}$$

7.5. RESPONSE SPECTRUM GRAPH

Only the contribution of the impulsive component to the structural behaviour during seismic activity was considered for all FE models. The contribution from the convective component was not considered since the influence of the convective component becomes negligible in tanks with large radii (Veletsos, 1997). For the consideration of the ultimate limit state of the structure a behaviour factor of 1.5 is prescribed in Eurocode 8: Part 4 (2006) along with the response spectrum for elastic analysis. The response spectrum for elastic analysis as shown in Figure 7.8 was entered in STRAND7 (2005). The results obtained for the ultimate limit state were scaled appropriately to obtain the serviceability limit state forces as discussed in the following sections. The peak ground acceleration was varied between 0.15g and 0.35g with steps of 0.1g and the appropriate response spectrum for elastic analysis was determined for the respective peak ground acceleration. Figure 7.8 is an example of the response spectrum representative of horizontal excitation and entered in STRAND7 (2005). A peak ground acceleration of 0.15g was used and a behaviour factor of 1.5. The damping ratio of 5% was used and soil

type A was assumed to be representative of the soil conditions in the Western Cape region of South Africa.

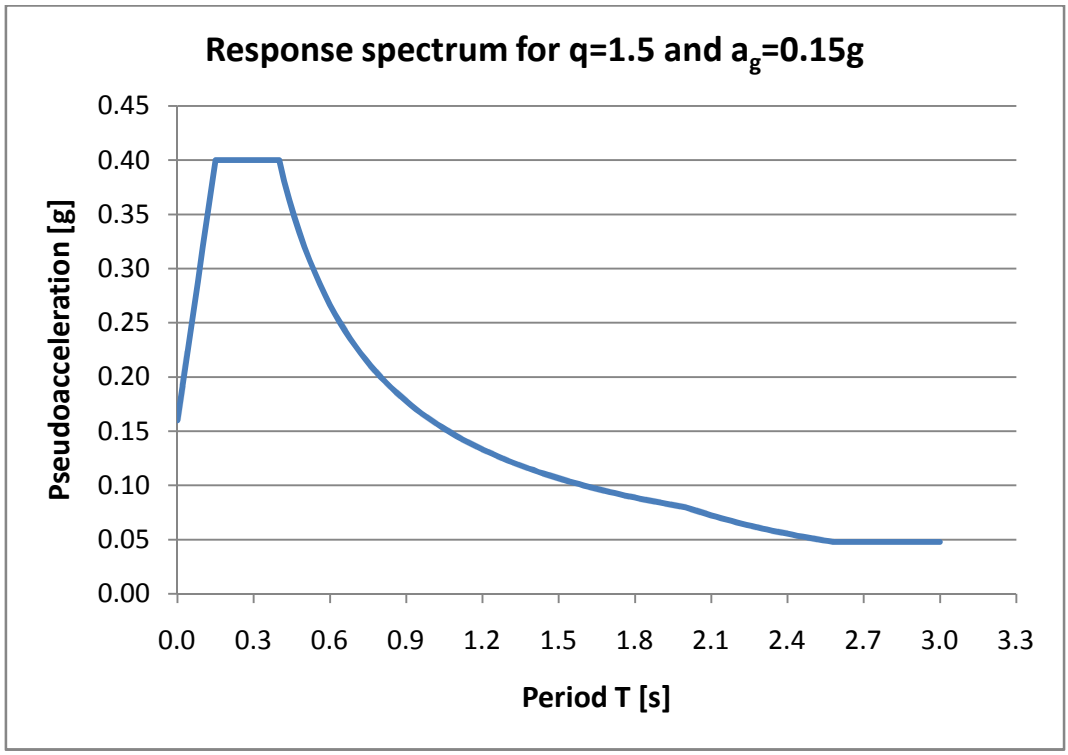

Figure 7.8: Response spectrum in STRAND7 (2005)

7.6. TYPES OF ANALYSIS

With the use of the natural frequency and response spectrum solvers in STRAND7 (2005) the fundamental frequency of vibration, mode shape, reaction and internal forces were determined for each FE model. The results of the FE analyses were compared with the results of the numerical analysis obtained with the method in Veletsos (1997) to assess the accuracy of the three proposed FE models.

In STRAND7 (2005) a two step procedure is required to determine the fundamental frequency and corresponding mode shape of a structure subjected to horizontal seismic excitation. The various modes of vibration of a structure are determined with the natural frequency solver. The participation factor of each mode of vibration is obtained from the spectral response solver. It is recommended a total participation factor of 90% is required to ensure all modes of vibration contributing to the behaviour of the structure are considered (Fardis, 2005).

For the determination of the participation factor, only the natural frequencies that converged in the natural frequency solver were used in the spectral response solver. The criterion for the convergence of a frequency is based on the iteration tolerance which has a default value of $1x10^{-5}$ in STRAND7 (2005) with a maximum number of iterations equal to 20. The eigenvalue of the frequency corresponding to mode x is considered to be converged if the value in equation 7.5 is smaller than the iteration tolerance.

$$ABS(\frac{f_i - f_{i-1}}{f_i}) \qquad \text{eq 7.5}$$

With f_i = frequency in iteration i

f_{i-1} = frequency in iteration i-1

In this study it was assumed the frequency with the highest participation factor is the fundamental frequency. This does not necessarily correspond with the first mode of vibration as obtained in the natural frequency solver.

7.7. SERVICEABILITY LIMIT STATE

Only the response spectrum applicable to the ultimate limit state was entered into STRAND7 (2005) for the seismic analysis of a structure. The analysis of a structure for the serviceability limit state was not performed in STRAND7 (2005) since the difference between the response spectrum for the ultimate limit state and serviceability limit state is only a factor. This scaling factor is dependent on the behaviour factor for each limit state and the reduction factor used for the serviceability limit state.

The aim of this study was to determine whether the seismic load case is a dominant factor in the design of water-retaining structures and whether the ultimate or serviceability limit state governs the design. For this reason the hoop stress and bending moment in the wall was required for each of the limit states. The area of reinforcement required for both the ultimate and serviceability limit states was also determined and consequently compared to determine which of the limit states govern the seismic design of a water-retaining structure.

The values of the hoop stress and bending moment in the wall obtained for the ultimate limit were scaled with the use of the behaviour factor and reduction factor to obtain the appropriate values for the serviceability limit state. In general the serviceability moment is calculated with the use of Equation 7.6 while the ultimate limit state moment is calculated with equation 7.7. The factor indicated in both equations is dependent on the relative response spectrum used and on the period of vibration of the structure.

Serviceability moment: $M_s = \nu S_A mh$

$$M_s = \frac{\nu}{q_s}.factor.m.h \qquad \text{eq 7.6}$$

Ultimate moment: $M_u = S_A mh$

$$M_u = \frac{1}{q_u}.factor.m.h \qquad \text{eq 7.7}$$

With M_s = serviceability limit state bending moment

M_u = ultimate limit state bending moment

ν = reduction factor (Eurocode 8: Part 4, 2006)

S_A = pseudoacceleration of structure

m = mass of contained liquid

h = height measured from base to liquid mass

q_s = behaviour factor for serviceability limit state (Eurocode 8: Part 4, 2006)

q_u = behaviour factor for ultimate limit state (Eurocode 8: Part 4, 2006)

factor = obtained from the relevant response spectrum (Eurocode 8: Part 1, 2004)

The serviceability limit state moment can be written in terms of the ultimate limit state moment as indicated in equation 7.8.

$$m.h = \frac{M_u q_u}{factor}$$

$$M_s = \frac{\nu}{q_s} factor.\frac{M_u q_u}{factor}$$

$$M_s = \frac{\nu}{q_s} q_u M_u \qquad \text{eq 7.8}$$

With M_s = bending moment for serviceability limit state

ν = reduction factor (Eurocode 8: Part 4, 2006)

q_s = behaviour factor for serviceability limit state (Eurocode 8: Part 4, 2006)

q_u = behaviour factor for ultimate limit state (Eurocode 8: Part 4, 2006)

M_u = bending moment for ultimate limit state

All aspects pertaining to the numerical analyses as well as the FE analyses of all the models considered in this study were discussed in detail in the previous four chapters. The results obtained for each model in terms of the fundamental frequency, mode shape, base shear force and overturning moment are presented in the following chapter. The classification of a structure as either rigid or flexible is also discussed.

8. GLOBAL RESULTS

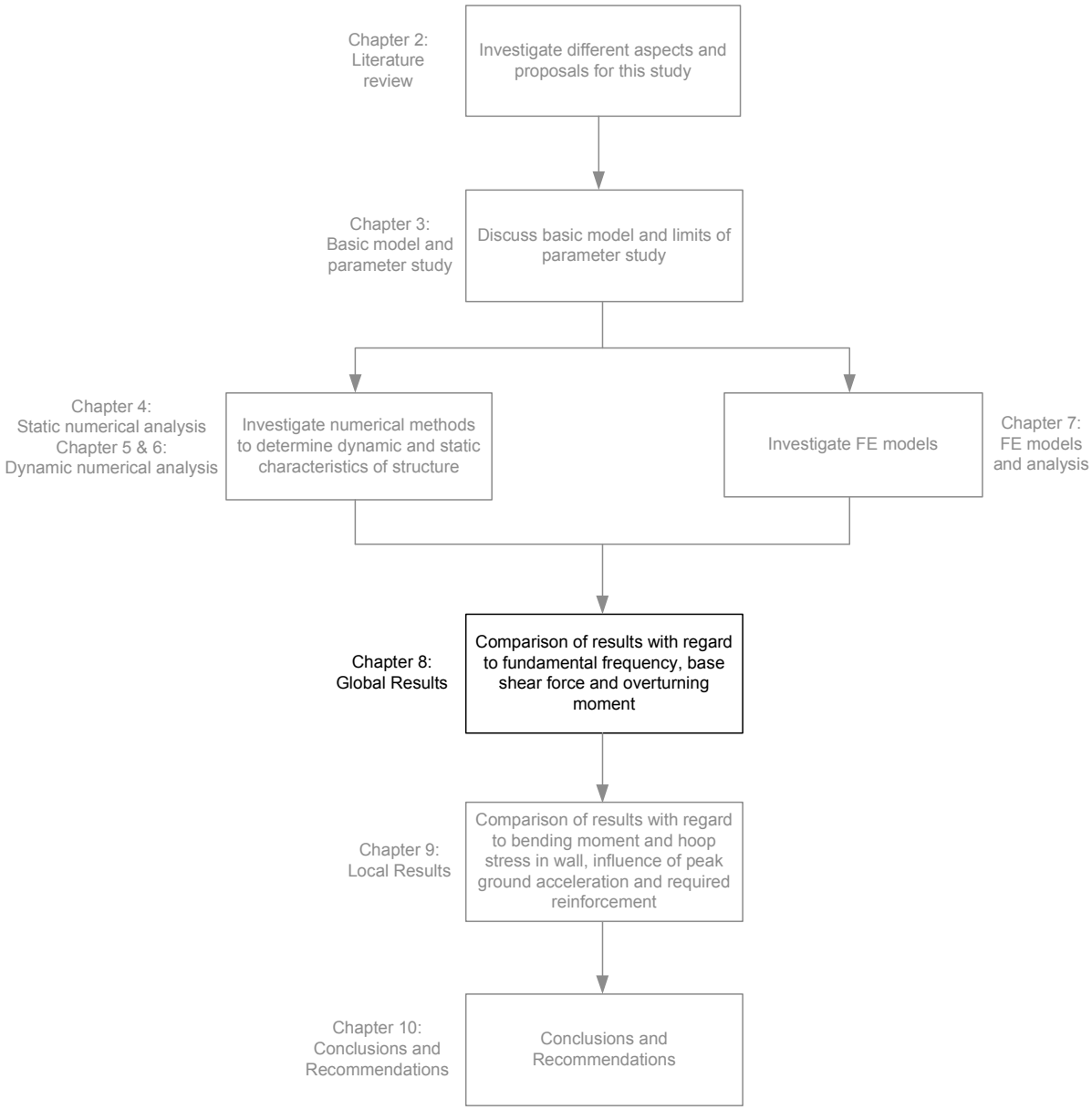

Figure 8.1: Methodology of study

All structures in the parametric study were analysed for both static and seismic loading conditions. With the static and seismic analyses of each model completed, the next step in the methodology of this study was the comparison of results as indicated in Figure 8.1.

For clarification purposes the respective methods of analysis and the scope of the parametric study are presented first in this chapter. The criteria required for the

classification of a tank wall as either rigid or flexible were investigated in this study. The results obtained for the classification of a structure are presented secondly in this chapter.

One of the aims of this study was the proposal of a simplified finite element model for the analysis of a water-retaining structure subjected to horizontal seismic excitation. For this purpose the fundamental frequency, base shear force and overturning moment as obtained with a numerical method and an FE model are compared in this chapter. Comparisons are made between the numerical methods of Veletsos (1997) and Eurocode 8: Part 4 (2006) in terms of the fundamental frequency. The fundamental frequency results obtained with the respective FE models are compared with the numerical method of Veletsos (1997) and discussed in this chapter. The mode shape of the fundamental frequency is discussed in detail after the presentation of the fundamental frequency results. The base shear force and overturning moment were calculated for each model and the correlation between the numerical methods and FE models are discussed.

8.1. METHODS OF ANALYSIS AND PARAMETRIC STUDY

In this section a brief summary is presented of the scope of the parametric study used in this study. The two numerical methods are also presented along with the respective finite element models. General information is provided on the definition of the fundamental frequency and other parameters.

A basic model was defined in Chapter 3. The basic model had a radius of 10 meters with the height of the tank wall and thickness of the wall varied within the scope of the parametric study. Reinforced concrete with a cube strength of 40 MPa, density of 2500 kg/m^3 and Poisson ratio of 0.2 was used for the tank wall. An importance class IV was assigned to the structures investigated in this study with consideration of only the horizontal component of an earthquake. The parametric study used in this study can be summarized as follows:

- Variance of the H/R [Height/Radius] ratio between 0.3 and 1.5 in steps of 0.3.
- Variance of the t_w/R [wall thickness/Radius] ratio between 0.006 and 0.03 in steps of 0.003.
- Variance of the peak ground acceleration between 0.15g and 0.35g in steps of 0.1g.

Each structure in the parametric study was analysed for both static and seismic loading conditions. Three different numerical methods were used for the analysis of a structure. The methods included the following:

- The method presented by Ghali (1979) was used for the static analysis of each structure.
- The method presented by Veletsos (1997) was the primary method used in this study for the seismic analysis of each structure investigated in this project.
- The method presented by Eurocode 8: Part 4 (2006) was used only to verify some of the results obtained with the method by Veletsos (1997). This method was not used for the seismic analysis of each structure in the parametric study.

In addition to the numerical methods of analysis, a finite element model was also constructed of each structure in the parametric study. Three different FE models were investigated in this study to assess the accuracy of each model in terms of the seismic analysis of a structure. The three different FE models investigated can be summarized as follows:

- The first model was proposed by Nachtigall (2003). In this model the impulsive liquid mass was uniformly distributed between the nodes on the tank wall. Each lumped mass was directly fixed to the respective node on the tank wall. This model is known as the uniformly-distributed mass model or ED-m_i model in this study.
- The second model was proposed by the supervisor and author of this thesis. In this model the impulsive liquid mass was distributed along the height of the tank wall in the same way as the impulsive pressure. The lumped impulsive masses were not varied along the circumference of the tank wall, but kept constant. Each lumped mass was directly fixed to the respective node on the tank wall. In this study the name pressure-distributed mass model or PD-m_i was used for this model.
- The third model was proposed by Virella (2006). The impulsive liquid mass was distributed along the height of the tank wall in the same manner as the impulsive pressure. The lumped impulsive masses were not varied along the circumference of the tank wall, but kept constant. The lumped masses were not fixed directly to the respective nodes on the tank wall, but rather attached to the node on the wall with a link. Pinned links were used to attach the lumped

masses to their respective nodes on the wall. The lumped masses were constrained against vertical and tangential translation, with translation only possible in the radial direction. This model is known as the Virella (2006) model in this report.

It should be kept in mind only the influence of the impulsive mass on the behaviour of a structure when subjected to seismic excitation was considered in this study. The convective component of the liquid was neglected in all instances since the influence of the convective component becomes negligible for tanks of large radii (Veletsos, 1997). It should be noted that all results and conclusions presented in this chapter are specifically for flexible tanks with a rigid foundation.

In all instances, the fundamental frequency of a structure was determined with the method by Veletsos (1997) and an FE model in STRAND7 (2005). However, the fundamental frequency obtained in STRAND7 (2005) is the frequency with the highest participation mass. This does not necessarily coincide with the first frequency obtained in STRAND7 (2005). The higher mode of vibration term refers to frequencies obtained in STRAND7 (2005) that have significant participation masses but excludes the dominant frequency which has the highest participation mass. However, the higher mode of vibration is not necessarily the second frequency obtained in STRAND7 (2005).

In order to keep this chapter brief, only the results obtained for a peak ground acceleration equal to 0.15g are presented. Results obtained for different values of the peak ground accelerations can be found in Appendix D. The results presented in this chapter were obtained with the use of the response spectrum as provided in Eurocode 8: Part 1 (2004) with a damping ratio of 5% for both the ultimate and serviceability limit state. The influence of a modified response spectrum on the design of water-retaining structures for seismic loading is discussed in Chapter 9.

8.2. CLASSIFICATION OF A STRUCTURE

In the numerical methods presented by Veletsos (1997) and Eurocode 8: Part 4 (2006) the wall of a water-retaining structure is classified as either rigid or flexible. However, no information was provided on the criteria required for the classification of a structure as

rigid or flexible and was further investigated in this study. The classification of a structure as either rigid or flexible is of critical importance since it influences the acceleration experienced by the structure during horizontal seismic excitation which in turn influences the hydrodynamic pressure and resulting forces.

The hydrodynamic pressure and resulting forces were determined with consideration of only the impulsive component. With reference to Veletsos (1997), it is the impulsive component that is influenced by the flexibility of the tank wall. The convective component remains unchanged since a large difference in frequency exists between the sloshing motion and ground motion. For these reasons, only the impulsive pressure as obtained for rigid and flexible tanks was compared. The method presented by Veletsos (1997) was used to obtain the impulsive pressure at the liquid surface and the bottom of the tank wall. Only the maximum impulsive pressure was investigated which correspond to a circumferential angle of zero degrees. A peak ground acceleration of 0.15g was used as prescribed in SANS 10160 (2009).

Figure 8.2 shows the influence of the wall thickness ratio and wall height ratio on the maximum impulsive pressure obtained for both rigid and flexible tanks for the ultimate limit state. It should be noted that the impulsive pressure obtained at the liquid surface of a rigid structure is independent of the wall thickness ratio [t_w/R] since the structure experiences the same motion as the ground during seismic excitation.

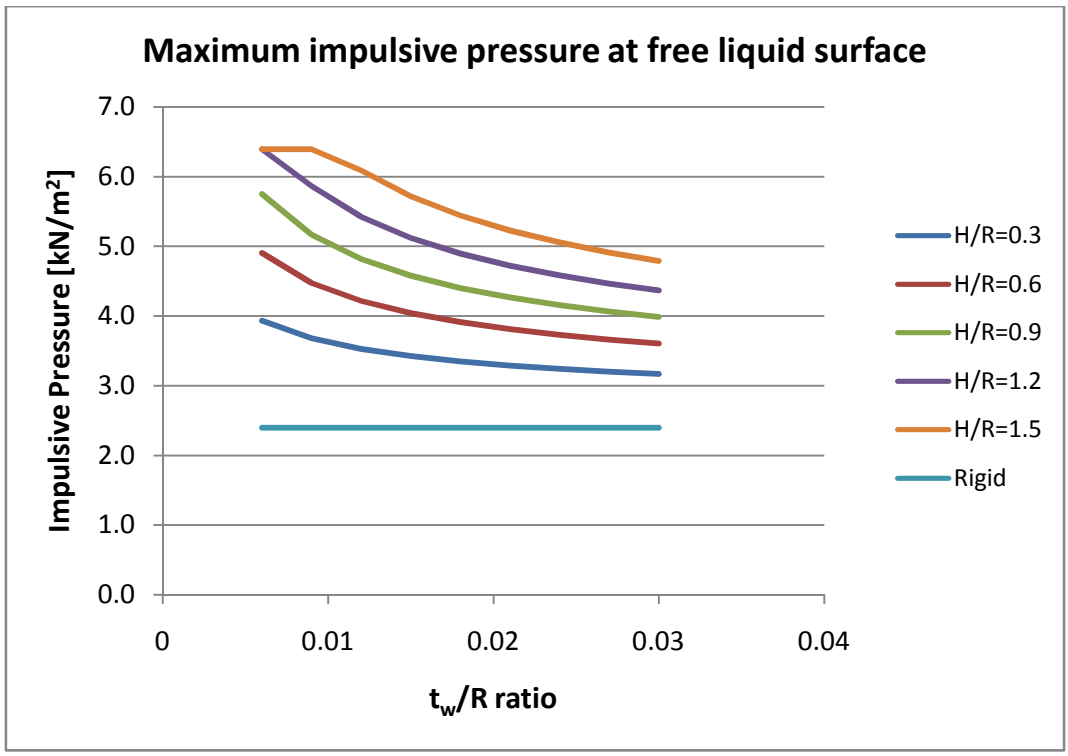

Figure 8.2: Variance of impulsive frequency with t_w/R and H/R ratio for ULS (PGA=0.15g)

As shown in Figure 8.2 the impulsive pressure at the free liquid surface remains constant for rigid tanks and is independent of the t_w/R and H/R ratio. In the case of flexible tanks, the impulsive pressure increases with an increase in the wall height. The impulsive pressure also increases with a decrease in wall thickness.

The impulsive pressure in flexible tanks is dependent on the pseudoacceleration experienced by the structure which in turn depends on the fundamental period of the vibration. Water-retaining structures with a fundamental period between 0.15 and 0.4 seconds are subjected to the maximum pseudoacceleration as can be seen from Figure 8.3. With the exception of three models having a H/R ratio of 1.2 and 1.5 with t_w/R ratio equal to 0.006 and 0.009, all models had a fundamental period in the first part of the response spectrum (T<0.15s). This implies an increase in the fundamental period of a structure will correspond to an increase in the pseudoacceleration experienced by the structure. The fundamental period is increased with either a decrease in the wall thickness or an increase in the wall height. This is consistent with results depicted in Figure 8.2.

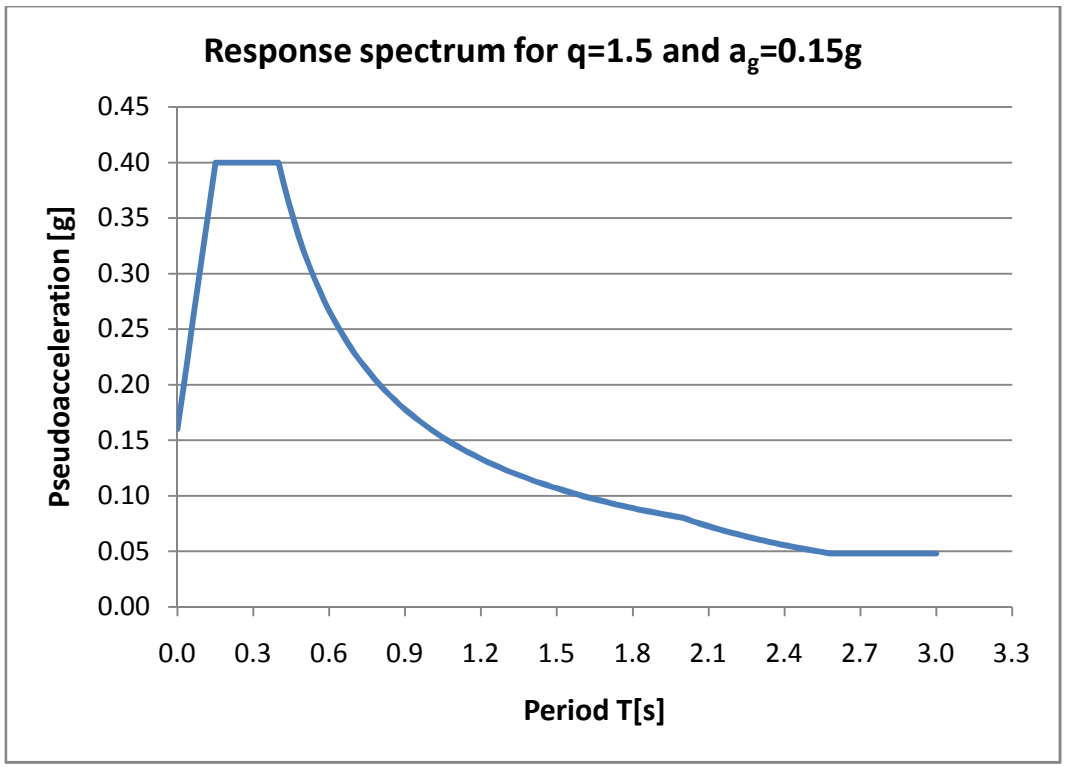

Figure 8.3: Response spectrum for the ultimate limit state

The percentage difference obtained between the maximum impulsive pressure calculated for flexible and rigid tanks respectively, is presented in Figure 8.4 for the ultimate limit state. See Appendix D for results obtained for the serviceability limit state as well as the maximum impulsive pressure measured at the bottom of the wall.

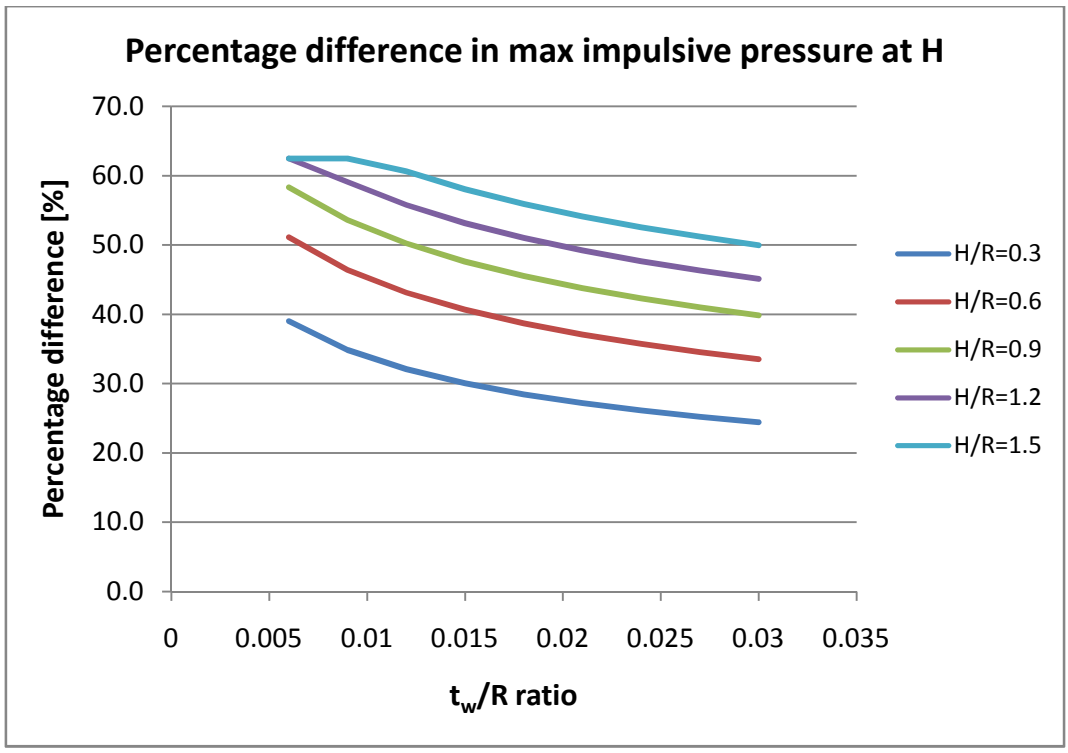

Figure 8.4: Percentage difference between flexible and rigid structures for ULS (PGA=0.15g)

With reference to Figure 8.4 the percentage difference between rigid and flexible structures, with consideration of the maximum impulsive pressure, is consistently greater than 20%. Considering the tank wall to be rigid is therefore unconservative and for this reason all structures in this study were considered as flexible structures for both the ultimate and serviceability limit state.

8.3. FUNDAMENTAL FREQUENCY

The fundamental frequency of a water-retaining structure is of great interest since the main cause of structural failure during seismic activity is resonance effects (Nachtigall, 2003). The wall of each structure in the parametric study was considered to be flexible. The impulsive mass of the liquid is rigidly attached to the tank wall which creates a tank-liquid system. The movement of the tank-liquid system is different from the ground movement during horizontal excitation and therefore the frequency of the tank-liquid system had to be determined. The fundamental frequency of each structure in the parametric study was determined with the numerical method by Veletsos (1997) and some were verified with the method presented in Eurocode 8: Part 4 (2006). Three FE models were also investigated for the determination of the fundamental frequency of

the tank-liquid system. These three FE models were discussed in Chapter 7, but information is provided here for clarity purposes. The three FE models were:

- The equally distributed impulsive mass model (ED-m_i) proposed by Nachtigall (2003), section 7.3.1.
- The pressure distributed impulsive mass model (PD-m_i), section 7.3.2.
- The model proposed by Virella (2006), section 7.3.3.

It should be noted that only the first mode of vibration (n=1) was calculated using the numerical methods. The primary numerical method used for all structures in the parametric study was the method presented by Veletsos (1997). Some of the results obtained using Veletsos (1997) were verified with the method presented in Eurocode 8: Part 4 (2006). The values obtained with the methods by Veletsos (1997) and Eurocode 8: Part 4 (2006) are presented in Figure 8.5. These values were obtained for a structure with a t_w/R ratio of 0.024 with consideration of the ultimate limit state.

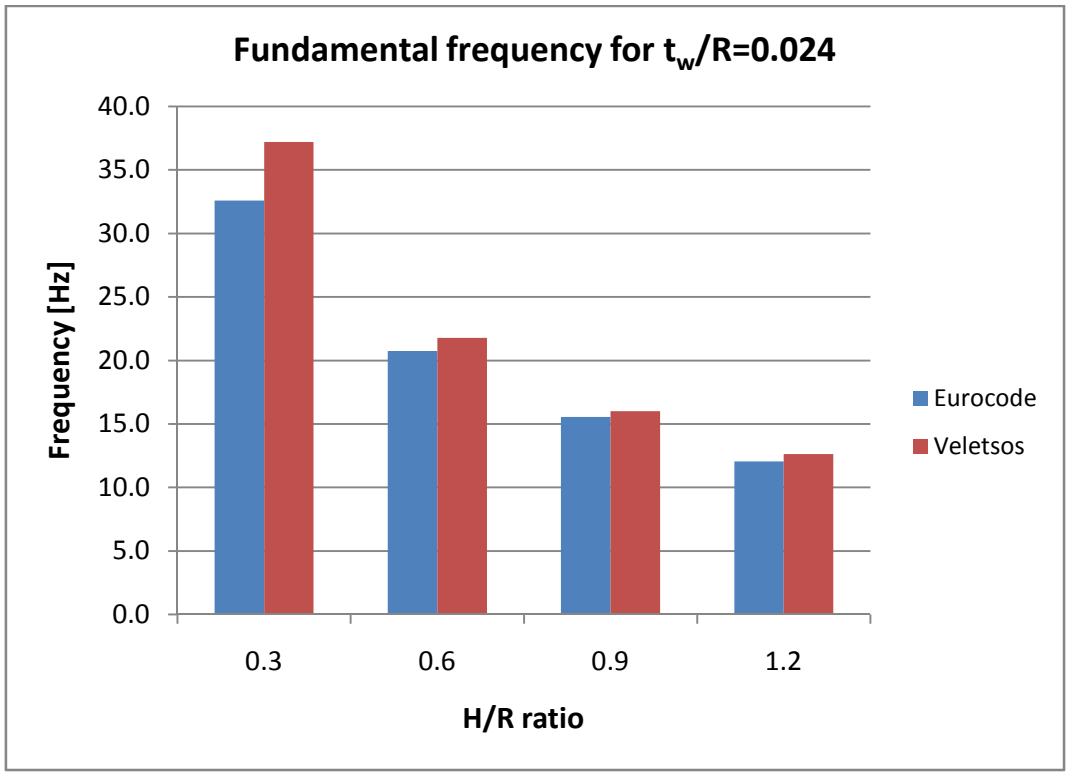

Figure 8.5: Fundamental frequency obtained with numerical methods

As shown in Figure 8.5 the fundamental frequency of a water-retaining structure, as determined with the method by Veletsos (1997), is consistently higher than the results

obtained with the method by Eurocode 8: Part 4 (2006). However, the difference in fundamental frequency decreases as the H/R ratio of the structure increases.

The fundamental frequency of a structure as determined from Veletsos (1997) was also compared to the dominant frequency obtained for the three different FE models. Figure 8.6 presents the actual values obtained for the fundamental frequency using the formulae by Veletsos (1997). The dominant frequency obtained from STRAND7 (2005) using the Virella (2006) model is presented on the same graph. Only the t_w/R ratios of 0.024, 0.027 and 0.03 are provided on Figure 8.6 for clarity purposes. The graphs for the comparison between Veletsos (1997) and the other two FE models, namely the equally distributed (ED-m_i) and pressure distributed impulsive mass (PD-m_i) models, as well as results obtained for other the t_w/R ratios can be found in Appendix D.

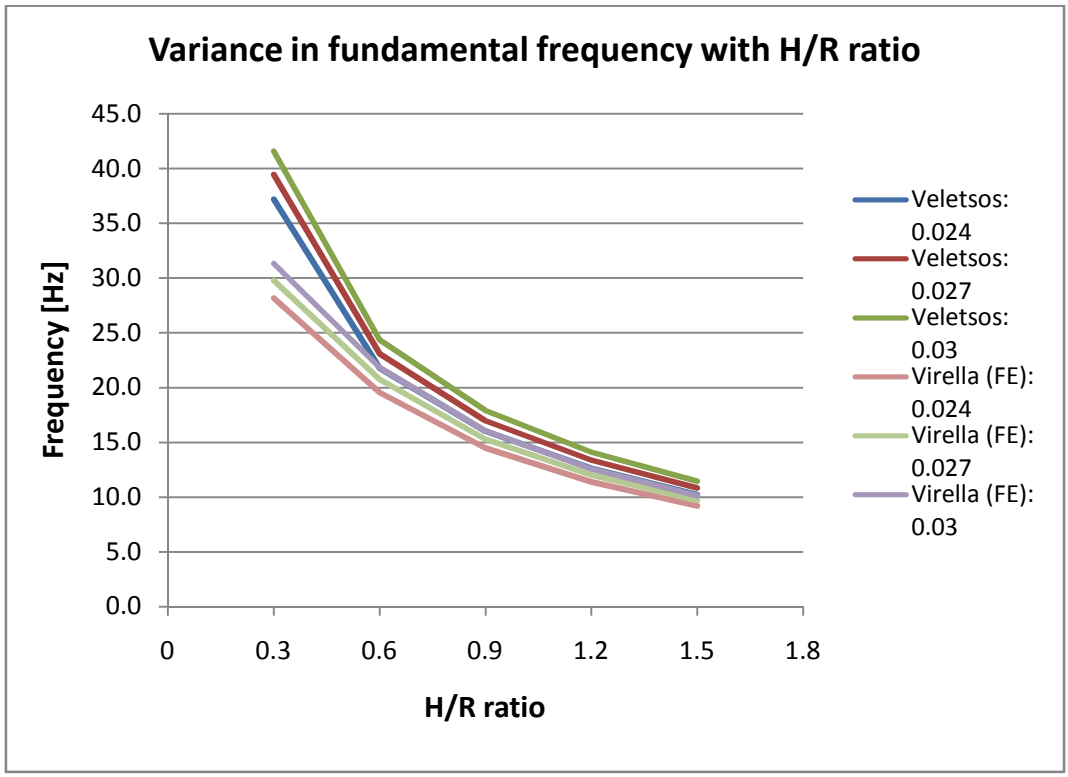

Figure 8.6: Fundamental frequency obtained with Veletsos (1997) and Virella (2006)

With reference to figure 8.6, the fundamental frequencies obtained using the FE model proposed by Virella (2006) are consistently lower than the results obtained using the numerical method by Veletsos (1997). The difference between the numerical method and FE model becomes less pronounced as the H/R ratio increases from 0.3 to 1.5.

However, a significant difference in results is obtained between a value of 0.3 and 0.6 for the H/R ratio. Water-retaining structures in South Africa are typically designed within this region with a value of 0.5 commonly used. Figure 8.7 presents the percentage difference obtained between the numerical method of Veletsos (1997) and the FE model of Virella (2006).

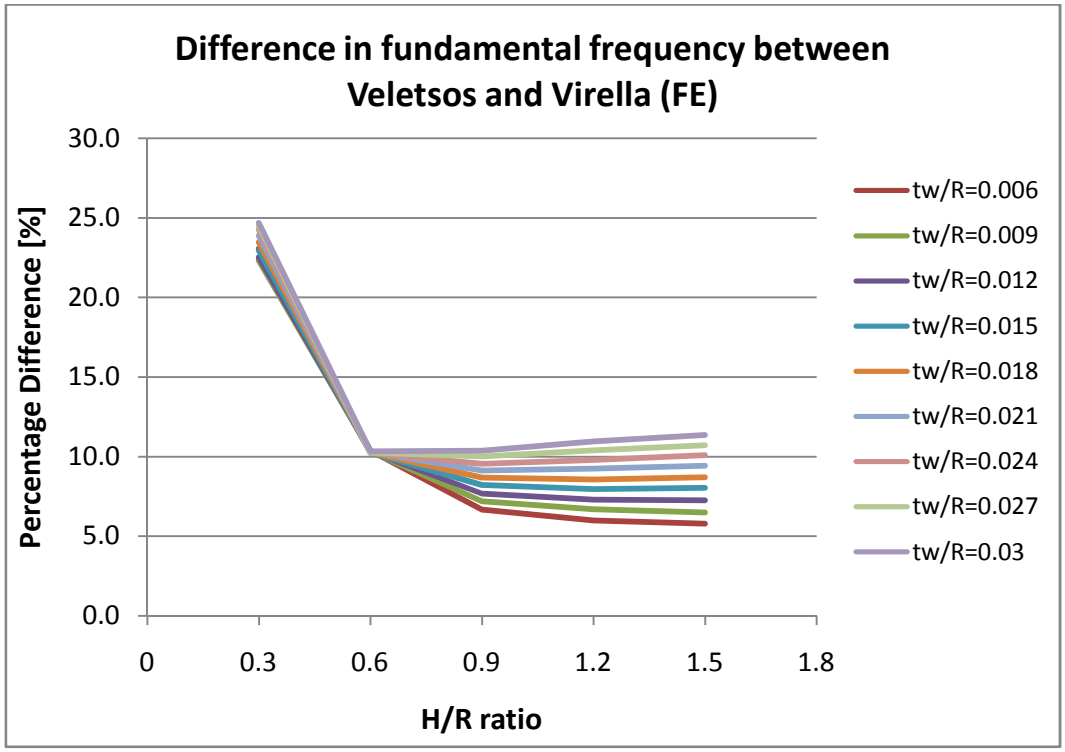

Figure 8.7: Percentage difference in fundamental frequency between Veletsos (1997) and Virella (2006)

Figure 8.7 shows a significant decrease in the percentage difference obtained between the numerical method by Veletsos (1997) and the FE model by Virella (2006) for H/R values between 0.3 and 0.6. The percentage difference remains relatively constant between the H/R values of 0.6 and 1.5. A possible reason for the high percentage difference obtained for broad tanks (H/R≤0.6) is the adoption of a cantilever beam model by Veletsos (1997) for the computation of the fundamental frequency of a water-retaining structure. The cantilever beam model is not suitable for the computation of the fundamental frequency for broad tanks with a H/R≤0.6 since the mode shape does not coincide with that of a cantilever beam. Refer to section 8.4 in which the fundamental mode shapes are presented as obtained in STRAND7 (2005).

The percentage difference obtained between the equally-distributed (ED-m_i) mass model and the numerical method by Veletsos (1997) is presented in Figure 8.8.

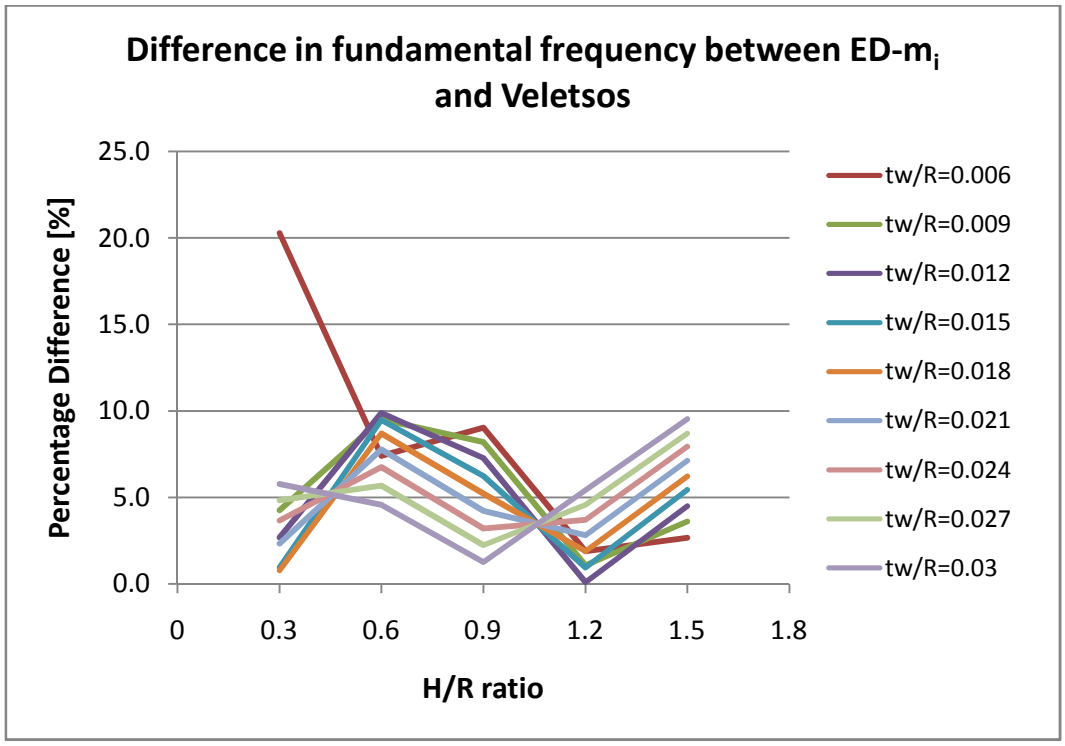

Figure 8.8: Percentage difference in fundamental frequency between ED-m_i and Veletsos (1997)

The difference in fundamental frequency between the equally distributed (ED-m_i) mass model and numerical method by Veletsos (1997) is consistently smaller than 10% except for a structure with H/R ratio of 0.3 and t_w/R ratio of 0.006. The results obtained with this model are similar to the results obtained with the method by Veletsos (1997) in which the fundamental mode shape was assumed to be that of a cantilever beam.

Figure 8.9 illustrates the percentage difference in fundamental frequency between the pressure-distributed (PD-m_i) mass model and method by Veletsos (1997). The fundamental frequency obtained with the PD-m_i model was consistently higher than the values obtained with the method by Veletsos (1997).

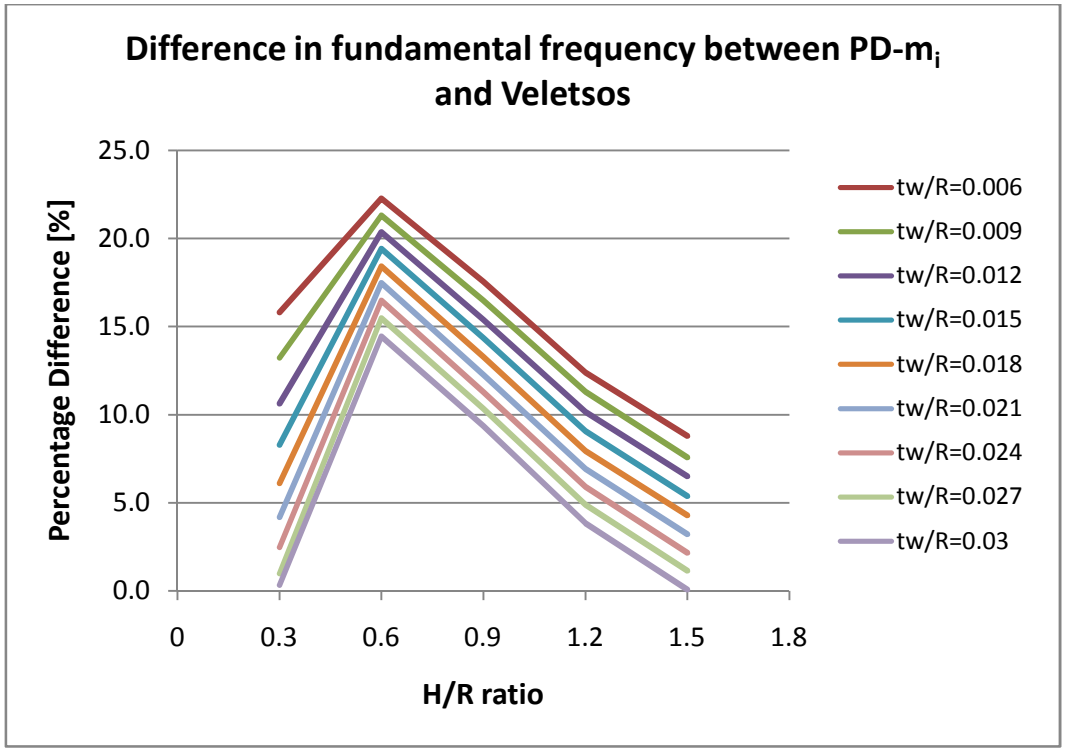

Figure 8.9: Percentage difference between frequency of PD-m_i and Veletsos (1997)

Figure 8.9 indicates an increase in percentage difference with a decrease in wall thickness. The percentage difference also decreases with an increase in wall height from a H/R ratio of 0.6. This model correlates well with the method by Veletsos (1997) for structures with higher H/R ratios or t_w/R ratios.

In Figure 8.10 the frequency results as obtained with the method by Veletsos (1997) and the three FE models are presented for a t_w/R ratio of 0.024. Figure 8.10 is representative of the general trend of results obtained for the fundamental frequency with the use of Veletsos (1997) and the three FE models.

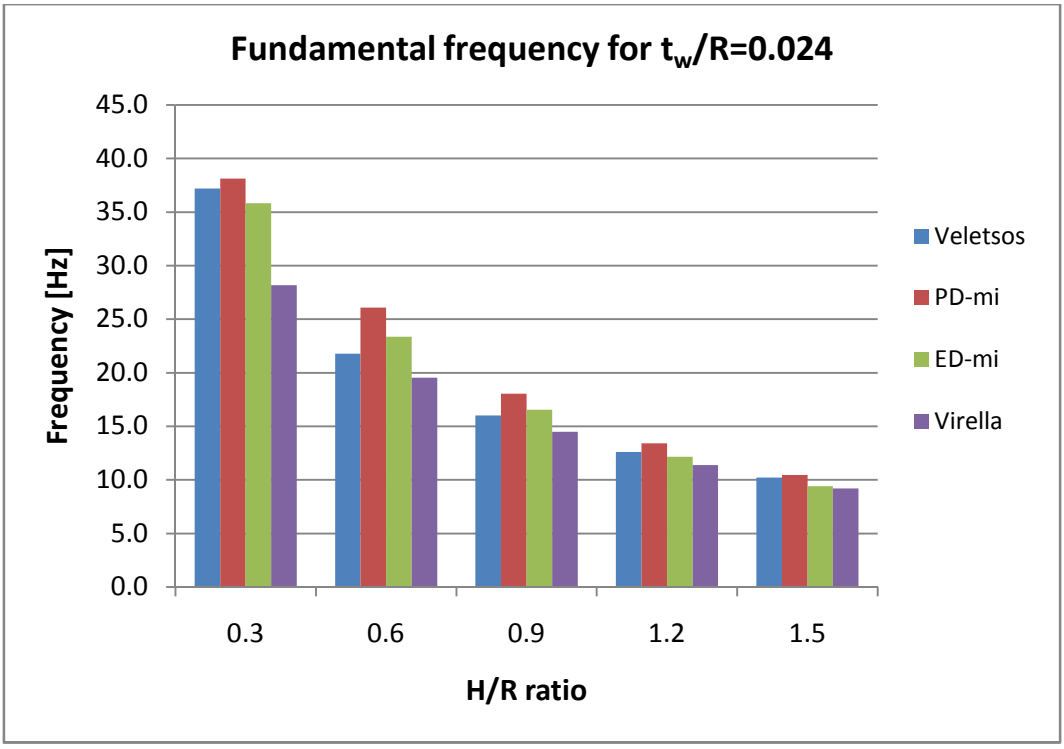

Figure 8.10: Summary of the fundamental frequency results

Figure 8.10 shows that the fundamental frequency obtained with the method by Veletsos (1997) is continuously underestimated by the Virella (2006) FE model. The pressure-distributed (PD-m_i) mass model continuously overestimates the fundamental frequencies while the results obtained with the equally-distributed (ED-m_i) mass model are similar to that of Veletsos (1997).

A summary of the results presented in this section is provided below. A difference of 10 percent or less between the FE model and the numerical method by Veletsos (1997) was considered to be adequate. With this in mind, the results obtained for the fundamental frequency are:

- The FE model of Virella (2006) correlates well with the numerical method for models with a H/R ratio of 0.6 and larger.
- The FE model with equally-distributed (ED-m_i) impulsive mass is consistent with the numerical method by Veletsos (1997) except for a very broad tank with a very thin wall.
- The pressure-distributed (PD-m_i) mass model provides inaccurate results for thin-walled structures with a t_w/R ratio smaller than 0.012. In South Africa water-retaining structures are designed with a t_w/R ratio between 0.025 and

0.03. Corresponding to this range of wall thickness, the model is inaccurate for H/R ratios between 0.35 and 1.03. A H/R ratio of 0.5 is commonly used in South Africa which lies within the region of 0.35 and 1.03. This model should therefore not be used in the South African practice since it provides inaccurate results.

8.4. MODE SHAPE

The mode shape of a water-retaining structure subjected to horizontal seismic excitation has been a point of great discussion. Nachtigall (2003) suggests the use of modes with a cos(nθ)-form of deformation with $5 \leq n \leq 25$ while considering the cantilever beam model as obsolete. Consideration of the fundamental mode shape of a water-retaining structure as similar to that of a vertical cantilever beam has been suggested by Haroun (1980), Veletsos (1997) and Eurocode 8: Part 4 (2006).

The FE analysis of each structure in this study was completed with the use of the STRAND7 (2005) package. The mode shape corresponding to the fundamental frequency was determined and is presented in this section. It should be kept in mind that the fundamental frequency was assumed as the frequency with the highest participation mass in STRAND7 (2005), therefore the dominant frequency. This frequency does not necessarily correspond to the first mode of vibration as obtained in STRAND7 (2005).

The participation factor for each of the dominant frequencies is provided in Table 8.1. These results were obtained for water-retaining structures with consideration of only the impulsive component of the liquid while the convective component was neglected. Only the results of structures with a t_w/R ratio between 0.024 and 0.03 are provided for clarity purposes.

		Participation factor (%)		
H/R:	**t_w/R:**	**ED-m_i:**	**PD-m_i:**	**Virella:**
0.3	0.024	37.1	37.4	56.0
	0.027	37.4	37.4	54.8
	0.03	37.7	37.5	53.6
0.6	0.024	50.6	64.8	77.9
	0.027	51.4	64.1	77.0
	0.03	52.0	63.3	76.1
0.9	0.024	72.2	74.4	81.2
	0.027	72.0	74.1	80.5
	0.03	71.8	73.8	79.9
1.2	0.024	76.5	76.5	83.4
	0.027	76.4	76.4	82.8
	0.03	76.3	76.3	82.3
1.5	0.024	76.8	77.7	83.2
	0.027	76.7	77.5	82.8
	0.03	76.6	77.3	82.4

Table 8.1: Participation factor of fundamental frequency

Table 8.1 shows an increase in the participation factor as the wall thickness and wall height increases. The highest participation factors were obtained for the Virella (2006) model.

The side-view of the dominant mode shape obtained for the Virella (2006) model with a H/R ratio equal to 0.6 and t_w/R ratio equal to 0.024 is presented in Figure 8.11. The mode shape of the dominant frequency obtained with a Virella (2006) model with a H/R ratio equal to 1.5 and t_w/R ratio of 0.024 is presented in Figure 8.12.

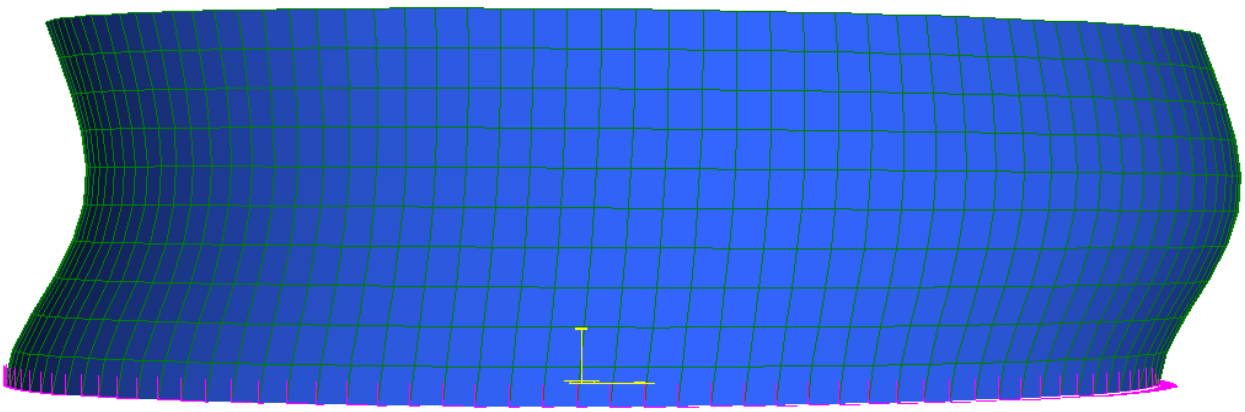

Figure 8.11: Fundamental mode shape for H/R ratio equal to 0.6

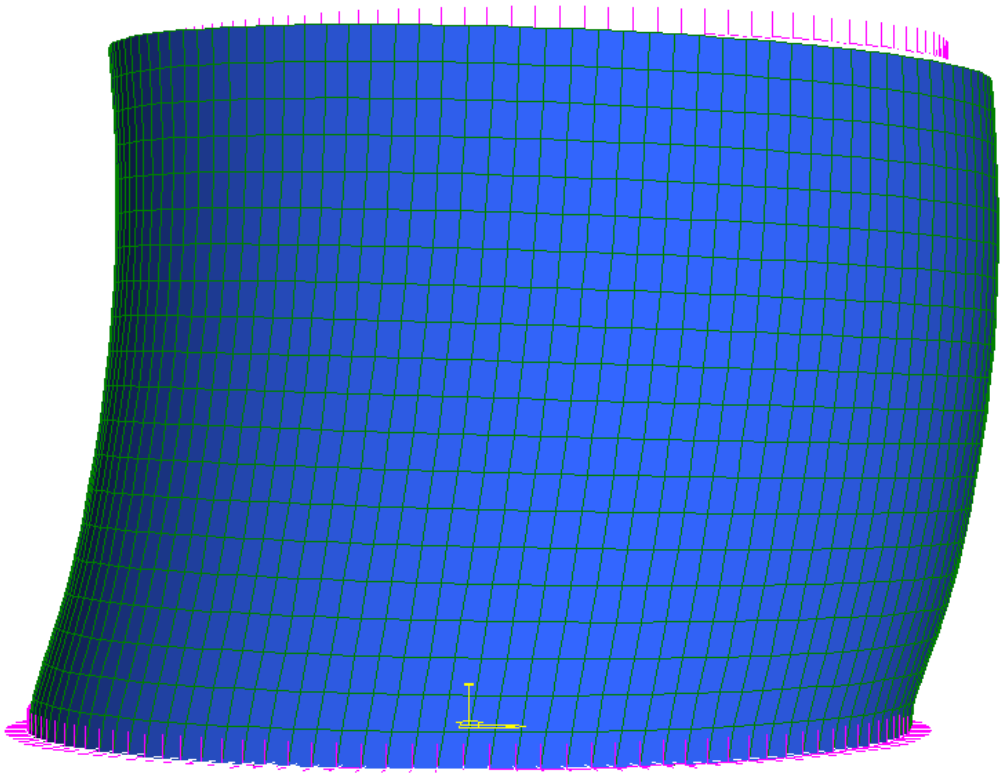

Figure 8.12: Fundamental mode shape for H/R ratio equal to 1.5

The fundamental mode shape of the structures presented in Figures 8.11 and 8.12 correspond with the results presented in Virella (2006). This indicates the fundamental mode shape of a water-retaining structure subjected to seismic excitation may be assumed to be a bending mode with n=1. The fundamental mode shape tends to that of a vertical cantilever beam as the H/R ratio increases as shown in Figures 8.11 and 8.12.

Apart from the high participation factors obtained for the dominant frequency, otherwise referred to as the fundamental frequency, significant participation factors were obtained for other modes of vibration. High participation factors for frequencies other than the dominant frequency were observed in the equally distributed (ED-m_i) and pressure-distributed (PD-m_i) mass models for structures with a H/R ratio of 0.3 and 0.6. These results are presented in Table 8.2.

		Participation factor (%)	
H/R:	**t_w/R:**	**ED-mi:**	**PD-mi:**
0.3	0.006	19.6	34.2
	0.009	34.1	31.0
	0.012	34.8	34.9
	0.015	34.6	34.7
	0.018	35.1	38.1
	0.021	34.5	34.7
	0.024	34.4	34.6
	0.027	34.2	34.4
	0.03	33.9	34.2
0.6	0.006	44.0	0.0
	0.009	33.7	0.0
	0.012	26.9	0.0
	0.015	22.7	0.0

Table 8.2: Participation factor for second mode of vibration

It should be kept in mind the participation factors presented in Table 8.2 were obtained for higher modes of vibration which exclude the dominant frequencies. Figure 8.13 shows the mode shape of a higher mode of vibration obtained with the equally-distributed (ED-m_i) mass model in STRAND7 (2005). The mode shape for the higher mode of vibration of the pressure-distributed (PD-m_i) mass model is similar to that of Figure 8.13.

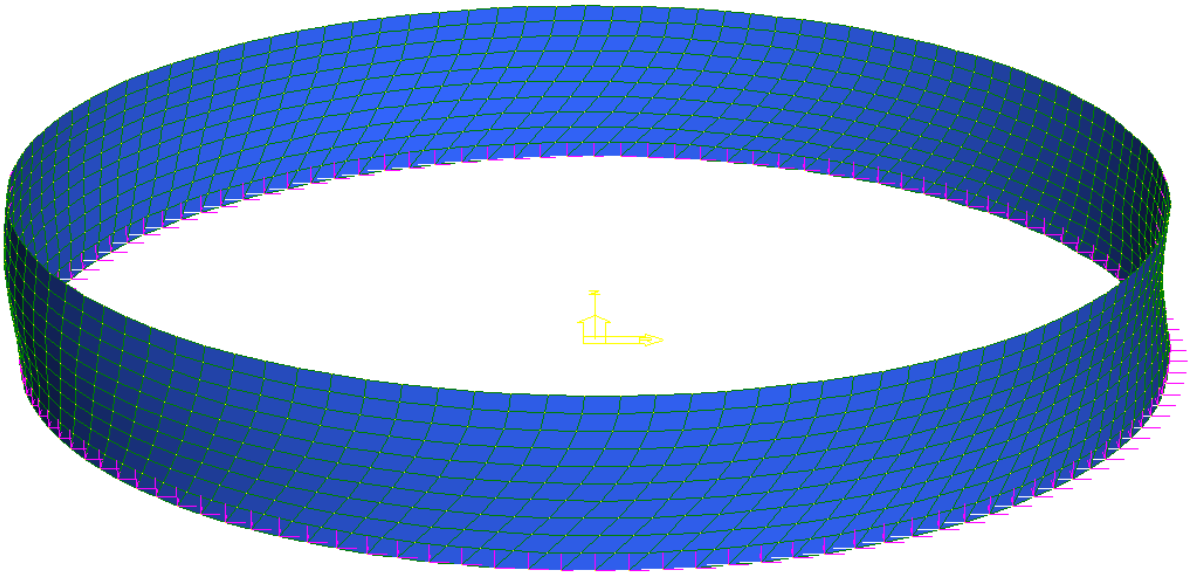

Figure 8.13: Higher mode shape for ED-m_i model

A higher mode of vibration was obtained for broad tanks with the use of the equally and pressure-distributed mass models. The mode shape shown in Figure 8.13 indicates that only in-plane deformation of the tank wall was obtained. The lumped impulsive masses that are situated directly on the tank wall will therefore only undergo tangential movement. Since the impulsive mass is representative of the impulsive pressure, the mass is only permitted to move within the radial direction as discussed in section 2.12. For this reason the mode shape shown in Figure 8.13 is considered to be a "fictitious" mode shape and not considered as a higher mode shape. For clarity purposes the mode shapes as expected for water-retaining structures are presented in Figure 8.14.

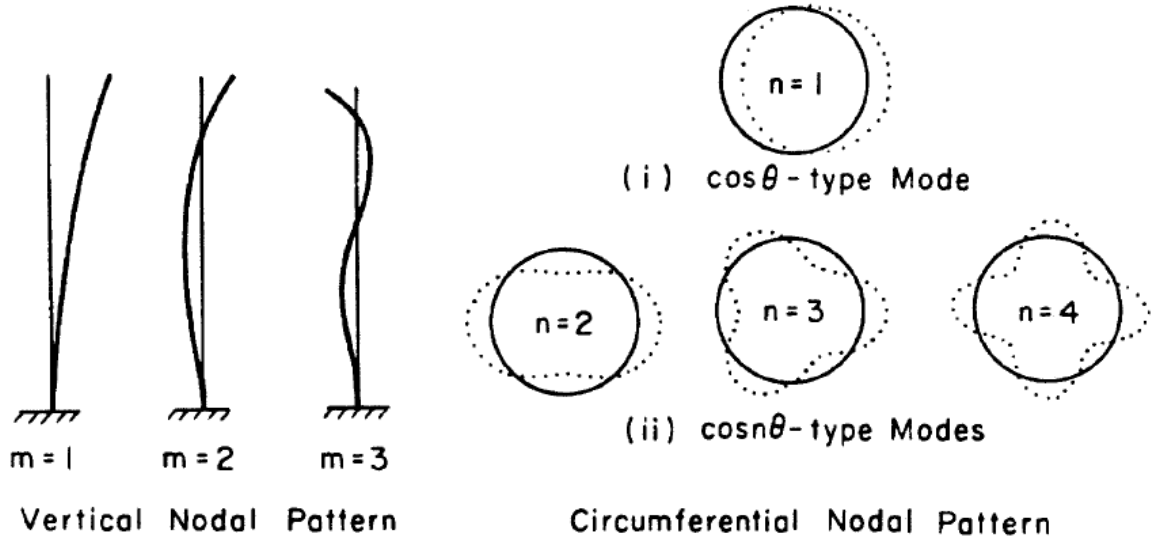

Figure 8.14: Modes of vibration according to Housner (1980)

The higher modes of vibration were not considered in the determination of the reaction and internal forces resulting from the horizontal seismic excitation of a structure. Sufficient results for practical use are obtained with consideration of only the fundamental frequency (Veletsos, 1997 and Eurocode 8: Part 4, 2006).

8.5. BASE SHEAR FORCE

It should be kept in mind that one of the aims of this project was to propose a FE model which is not very complex and that may be used with ease in the design practice for the seismic analysis of a water-retaining structure. For this purpose the three FE models were compared to the numerical method by Veletsos (1997). The three FE models are

respectively the uniformly-distributed (ED-m_i) mass model, the pressure-distributed (PD-m_i) mass model and the model by Virella (2006). A comparison was made to assess the accuracy of each FE model in terms of the prediction of the global behaviour of the structure. The results obtained for the fundamental frequency of a structure, the base shear force and the overturning moment obtained when a structure is subjected to seismic excitation were considered.

During seismic excitation of a water-retaining structure a horizontal acceleration is experienced by both the structure and the contained liquid. This produces a shear force at the base of the structure as well as an overturning moment around an axis perpendicular to the direction of excitation. The results obtained for the base shear force and overturning moment with the numerical methods by Veletsos (1997) and Eurocode 8: Part 4 (2006) as well as the FE models are presented and discussed in this section.

The results obtained with the numerical methods by Veletsos (1997) and Eurocode 8: Part 4 (2006) are presented in Figure 8.15. These results were obtained for structures with a t_w/R ratio equal to 0.024 with consideration of the ultimate limit state.

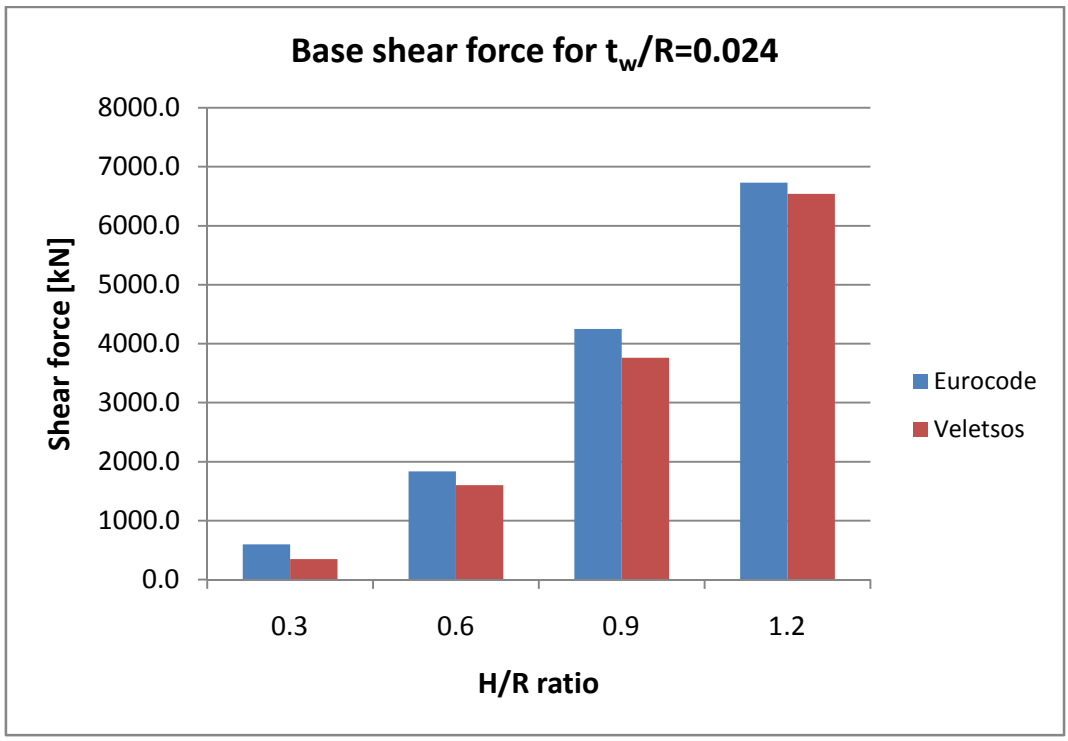

Figure 8.15: Comparison in base shear force between the two numerical methods (PGA=0.15g)

As shown in Figure 8.15 the results obtained with the method by Veletsos (1997) in terms of the base shear force are consistently smaller than the results obtained with Eurocode 8: Part 4 (2006). The difference is attributed to the larger frequencies obtained with the method by Veletsos (1997) which results in a smaller pseudoacceleration and therefore smaller base shear force than obtained with the method by Eurocode 8: Part 4 (2006).

The ultimate limit state values obtained for the base shear force are presented in Figure 8.16. These results were determined with the method by Veletsos (1997) and the FE model by Virella (2006). In order to present the results in a meaningful manner only the results obtained for the t_w/R ratios of 0.024 to 0.03 are presented. These values are applicable to the South African practice. Refer to Appendix D for the comparison between the results obtained with Veletsos (1997) and the FE models of equally-distributed (ED-m_i) and of pressure-distributed (PD-m_i) mass models. In all instances only the impulsive mass of the liquid was considered in both the numerical and FE analyses. The results presented were specifically obtained for the fundamental frequency of vibration, no higher modes of vibration were considered. The results presented in Figure 8.16 were obtained for a peak ground acceleration equal to 0.15g, the results obtained for a peak ground acceleration of 0.25g and 0.35g are presented in Appendix D.

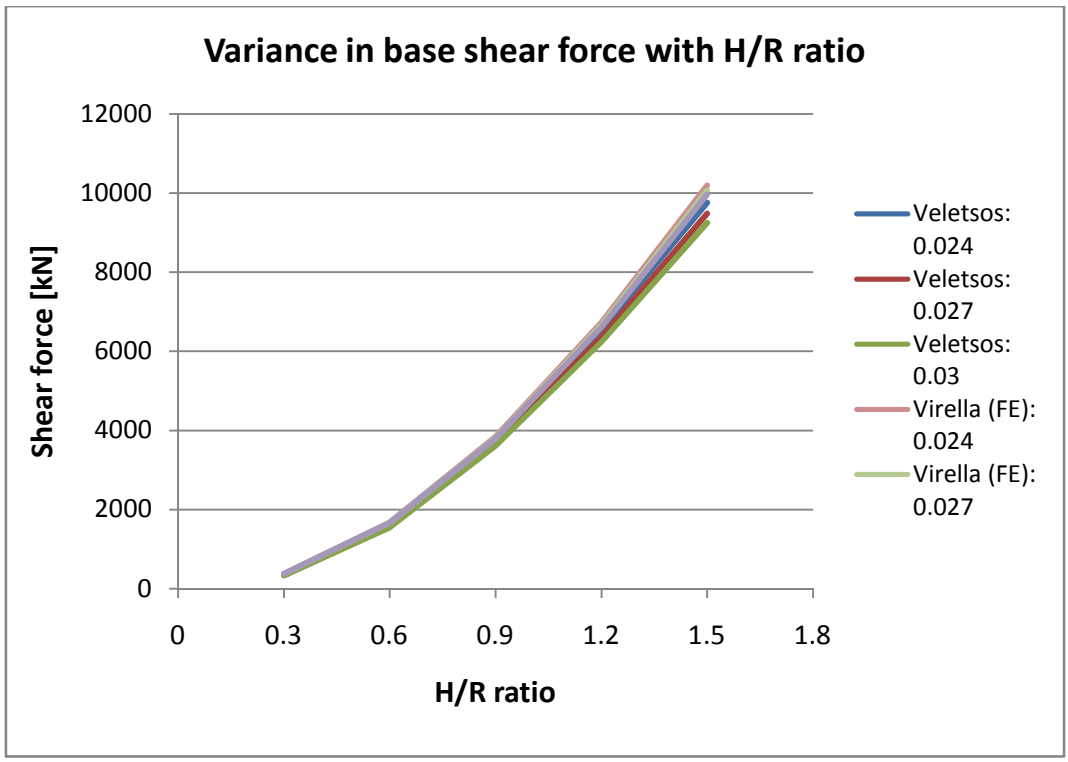

Figure 8.16: Variance of base shear force determined with Veletsos (1997) and Virella (2006)

Figure 8.16 shows that the base shear force results obtained with the Virella (2006) FE model are consistent with the results obtained with the numerical method by Veletsos (1997). Slightly larger values were obtained with the FE model by Virella (2006). This is attributed to the differences obtained in the fundamental period of the structure. The FE model of Virella (2006) predicted higher periods of vibration corresponding to higher pseudoaccelerations as obtained with the response spectrum for elastic analysis. The base shear force is determined with the pseudoacceleration and therefore higher values are obtained with the FE model by Virella (2006) than with the numerical method by Veletsos (1997).

As indicated in Figure 8.16 the base shear force increases with an increase in H/R ratio as expected. This is attributed to the increased influence of the impulsive component as the H/R ratio of the structure increases (Veletsos, 1997). The base shear force graphs obtained for a peak ground acceleration of 0.25g and 0.35g respectively, looks similar to that of Figure 8.16.

The percentage difference between the Virella (2006) FE model and the method by Veletsos (1997) is presented in Figure 8.17 for the ultimate limit state.

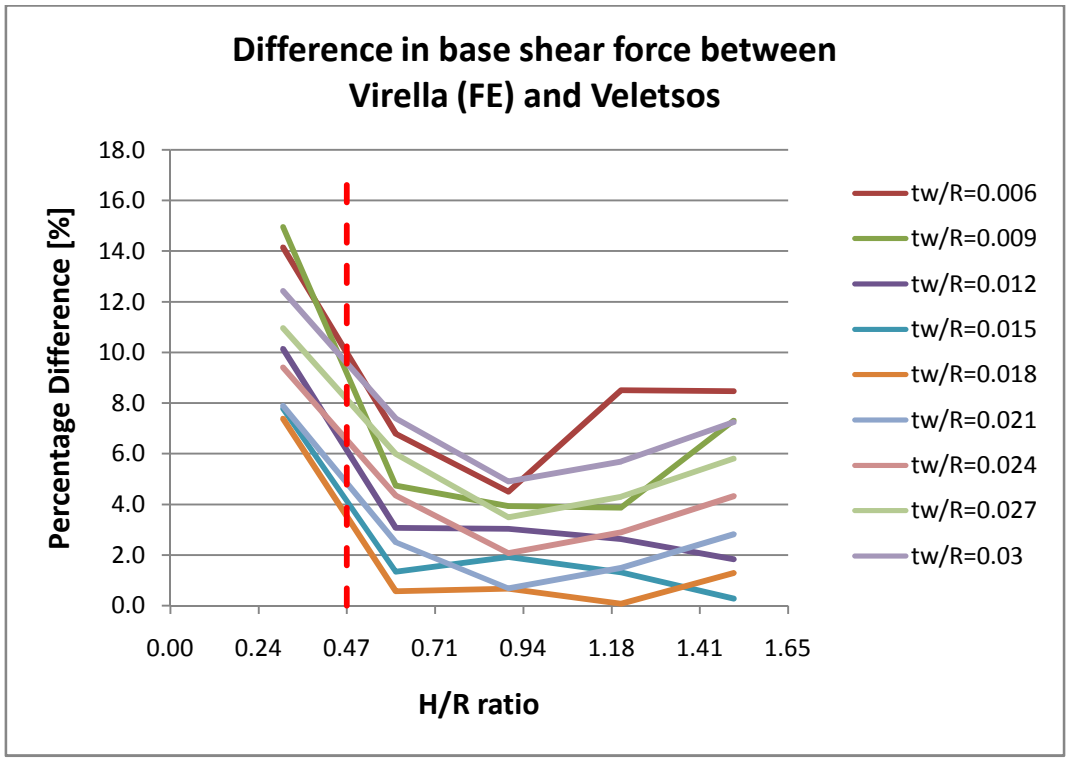

Figure 8.17: Percentage difference in base shear force determined with Virella (2006) and Veletsos (1997)

Figure 8.17 shows a relatively small difference in results obtained with the Virella (2006) model and method by Veletsos (1997). A percentage difference greater than 10% was obtained for H/R ratios smaller than 0.47. This is consistent with the findings for the fundamental frequency with a 10% difference obtained for H/R ratios smaller than 0.6.

The percentage difference graph for the serviceability limit state is similar to the ultimate limit state graph. The values obtained for the ultimate limit state in STRAND7 (2005) were scaled with a factor to obtain the serviceability limit state results. Higher absolute values for the base shear force were obtained for higher values of the peak ground acceleration. However, the percentage difference between the Virella (2006) FE model and the method by Veletsos (1997) remains constant since both of these methods are dependent on the pseudoacceleration of the structure.

The percentage difference obtained between the pressure-distributed (PD-m_i) mass model and the numerical method of Veletsos (1997) is presented in Figure 8.18 for the ultimate limit state.

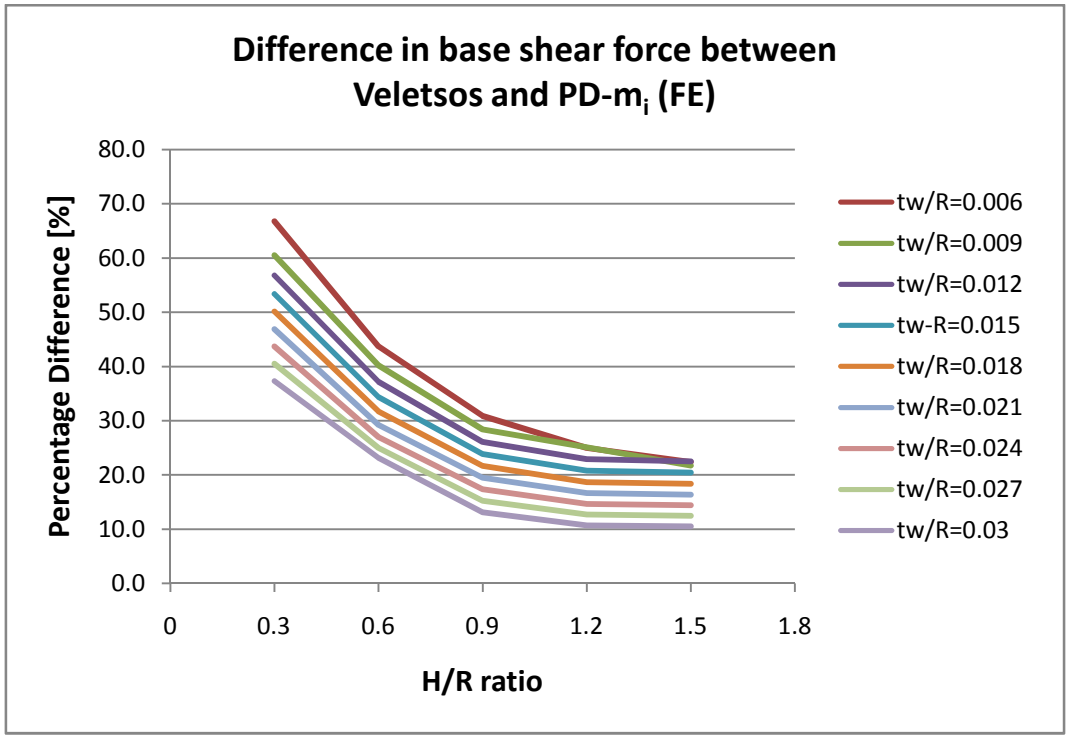

Figure 8.18: Percentage difference in base shear force between Veletsos (1997) and PD-m_i model

As illustrated in Figure 8.18, the base shear force is greatly underestimated by the pressure-distributed (PD-m_i) mass model with regard to the values obtained using the method by Veletsos (1997). This is also the case for the equally-distributed (ED-m_i) mass model, refer to Appendix D. The large difference in base shear force can be attributed to the difference in fundamental frequency obtained between the equally-distributed (ED-m_i), pressure-distributed (PD-m_i) mass models and the method by Veletsos (1997). Both of these FE models consistently underestimated the fundamental frequency of a structure as indicated in section 8.2. The pseudoacceleration experienced by a structure during seismic excitation it therefore underestimated. Due to the underestimation of the pseudoacceleration with the use of the equally-distributed (ED-m_i) and the pressure-distributed (PD-m_i) mass models, a lower base shear force is obtained when compared to the method by Veletsos (1997).

The base shear force results as obtained with the method by Veletsos (1997) and the three FE models are presented in Figure 8.19. These results were obtained for structures a t_w/R ratio of 0.024 with consideration of the ultimate limit state. This graph is representative of the results as obtained with other values of the t_w/R ratio.

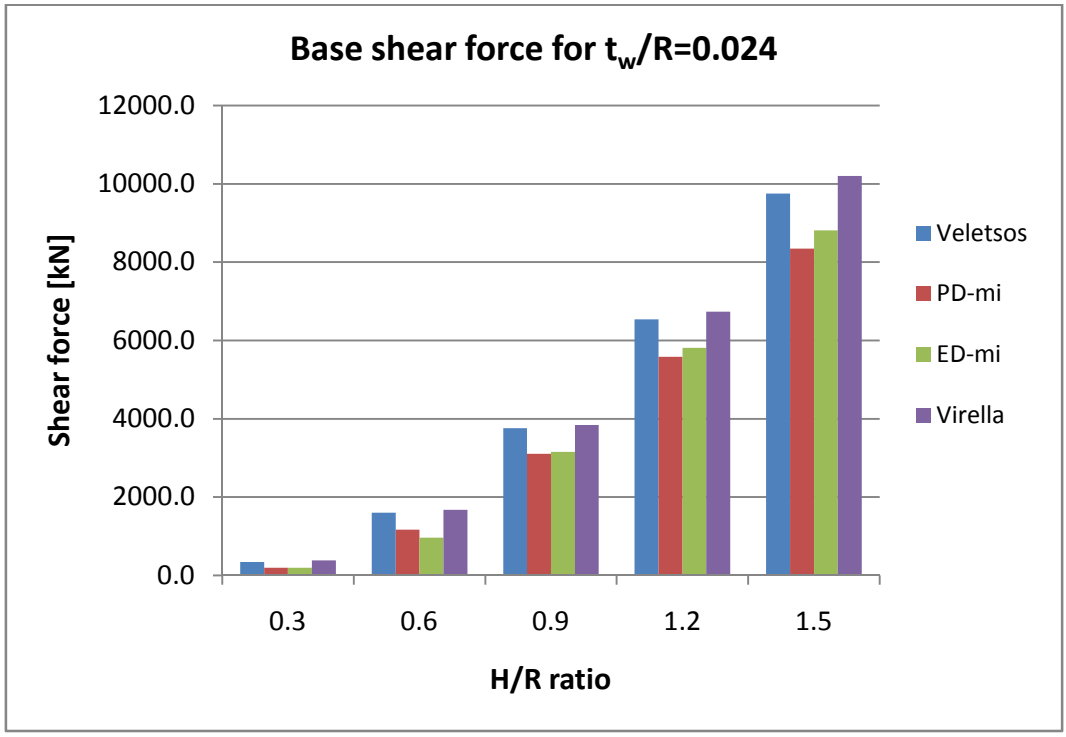

Figure 8.19: Summary of base shear force results (PGA=0.15g)

As shown in Figure 8.19, the base shear force as obtained with the method by Veletsos (1997) is overestimated by the Virella (2006) FE model. This is attributed to the underestimation of the fundamental frequency by the Virella (2006) model which results in a higher pseudoacceleration experienced by the structure. The pressure-distributed (PD-m_i) and equally-distributed (ED-m_i) mass models continuously underestimate the base shear force obtained with the method by Veletsos (1997).

In summary, only the FE model proposed by Virella (2006) compares well with the method by Veletsos (1997) for H/R values greater than 0.47 regardless of the t_w/R ratio. This is indicated with the dashed line in Figure 8.17.

8.6. OVERTURNING MOMENT

In order to determine the accuracy of a FE model with regard to the numerical method by Veletsos (1997) three parameters were compared. These parameters included the fundamental frequency of the structure, the base shear force and the overturning moment. The first two of these comparisons are presented in the preceding sections of this thesis. In this section the results obtained for the overturning moment as computed with the method by Veletsos (1997) and the three FE models are presented. The FE models are the equally-distributed (ED-m_i) mass model, the pressure-distributed (PD-m_i) mass model and the model by Virella (2006).

The numerical method proposed by Veletsos (1997) considers the system to be a single-degree-of-freedom system with the impulsive mass situated at a specified height along the tank wall which produces an overturning moment when subjected to horizontal excitation at the base of the structure. However, the FE models constructed in STRAND7 (2005) were multi-degree-of-freedom systems and the computation of the overturning moment in STRAND7 (2005) is discussed first.

In order to obtain the total overturning moment from the results of the STRAND7 (2005) analysis, two components are considered. These components are the axial force and the bending moment at the base of the wall. The horizontal acceleration of the impulsive mass results in compressive axial forces at one side of the structure and uplifting forces at the other end of the structure. These vertical axial forces produce an overturning moment around an axis perpendicular to the direction of excitation due to the eccentricity between the axial force and the axis of rotation. The second component is the bending moment at the bottom nodes of the tank wall produced by the horizontal pressure applied along the height of the wall. The overturning moment is obtained from the sum of these two components as expressed in equation 8.1.

$$M_y = \sum_{i=1}^{n}(F_i e_i + M_{yi}) \qquad \text{eq 8.1}$$

With F_i = vertical axial force at node number i

e_i = distance of node i from the axis of rotation

M_{yi} = moment about global y-axis at each node i

M_y = overturning moment about global y-axis if excitation is in x-direction

It should be kept in mind the results presented in this section are only the rotation of the tank wall about an axis perpendicular to the direction of excitation that does not include the foundation of the structure. All of the results presented in this section were obtained for a peak ground acceleration of 0.15g. Two other values of the peak ground acceleration, namely 0.25g and 0.35g were also investigated. The results obtained with the use of these two values are provided in Appendix D.

The values obtained for the overturning moment as determined from the FE model by Virella (2006) are presented in Figure 8.20. The values as obtained with the numerical method by Veletsos (1997) are also presented in Figure 8.20. The values obtained with both of these methods are for the ultimate limit state. Corresponding graphs for the equally-distributed (ED-m_i) and the pressure-distributed (PD-m_i) mass models are presented in Appendix D. For clarity purposes only the t_w/R ratios of 0.024, 0.027 and 0.03 are presented in Figure 8.20. These values are generally used in the design of water-retaining structures in South Africa.

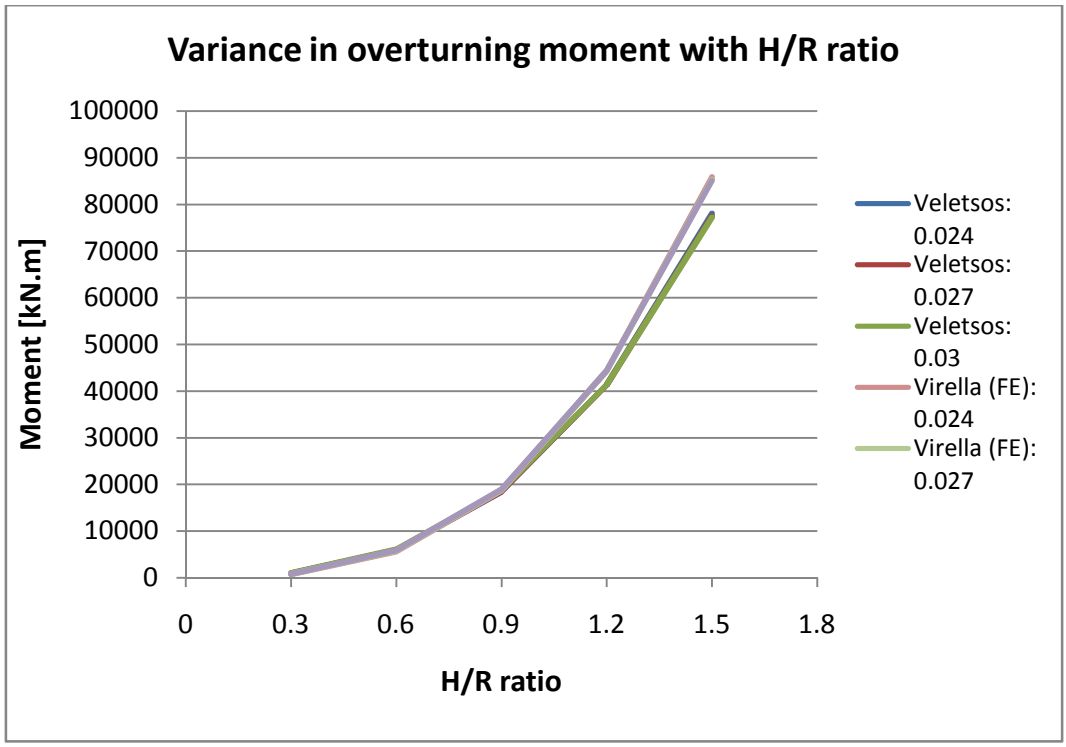

Figure 8.20: Variance of overturning moment determined with Veletsos (1997) and Virella (2006)

The values obtained for the overturning moment with the FE model are consistently higher than those of the numerical model but still relatively similar. The overturning moment increases with an increase in H/R ratio due to the increased influence of impulsive component. The fundamental period determined with the Virella (2006) FE model was also higher than that of the numerical method by Veletsos (1997) resulting in higher overturning moment values.

The percentage difference between the FE model by Virella (2006) and the numerical method by Veletsos (1997) is presented in Figure 8.21 for the ultimate limit state.

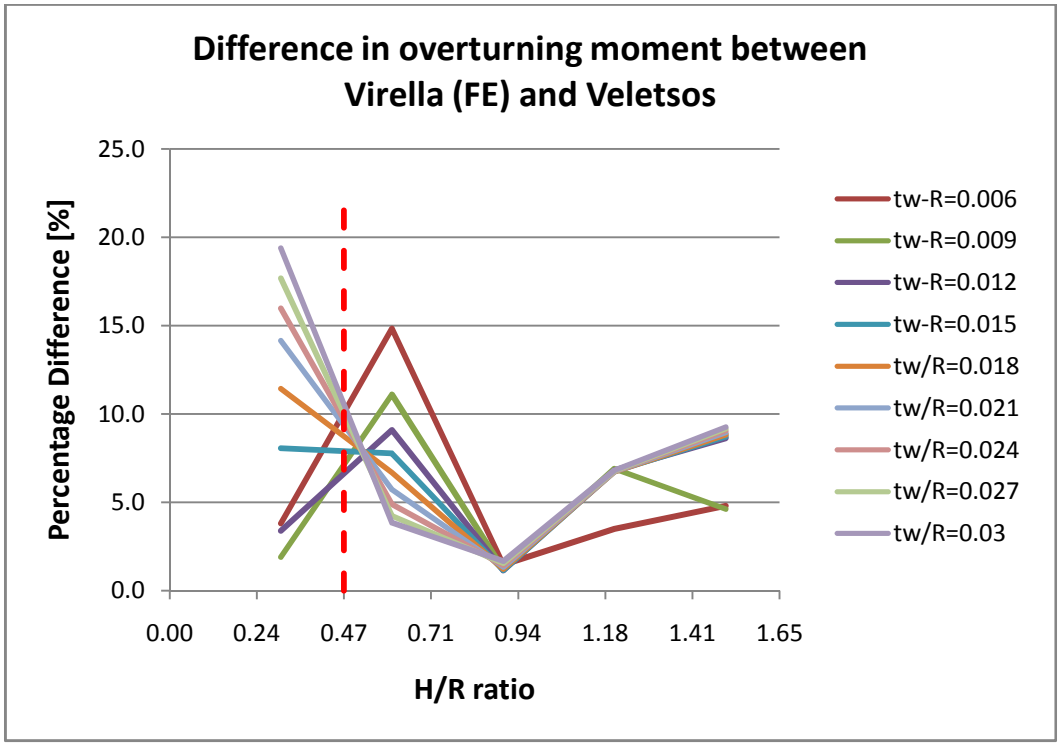

Figure 8.21: Percentage difference in overturning moment for Virella (2006) and Veletsos (1997)

As indicated in Figure 8.21, a percentage difference greater than 10% was obtained for H/R values smaller than 0.47 which is consistent with the results of the base shear force and fundamental frequency.

Figure 8.22 presents the percentage difference obtained between the pressure-distributed (PD-m_i) mass model and numerical method by Veletsos (1997) for the ultimate limit state.

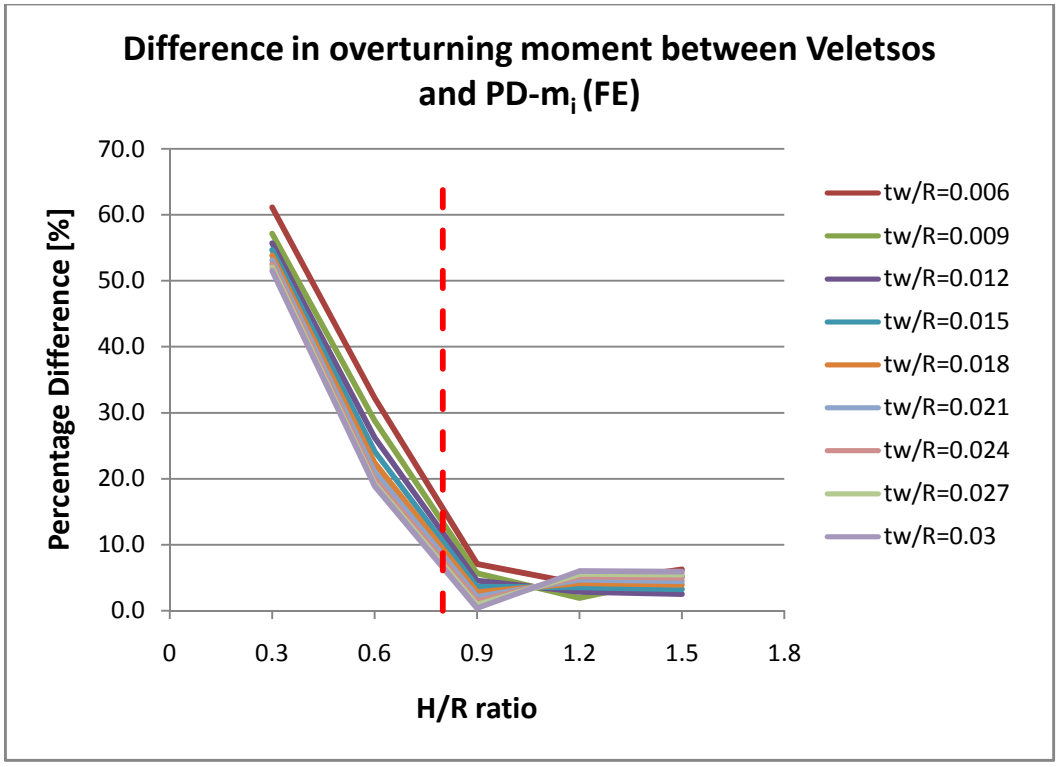

Figure 8.22: Percentage difference in overturning moment between Veletsos and PD-m$_i$

The overturning moment obtained from the pressure distributed (PD-m$_i$) model is consistently smaller than the numerical values and considered to be inaccurate for H/R values smaller than 0.80. The results obtained for the equally-distributed (ED-m$_i$) mass model are presented in Appendix D.

All results pertaining to the global behaviour of the structure have been presented in this chapter. From the presented results only the Virella (2006) FE model is considered to be sufficiently accurate for the computation of the fundamental frequency, base shear force and overturning moment of a structure subjected to horizontal excitation. For this reason only the Virella (2006) model was used for the determination of the local results.

The local results consist of the bending moment and hoop stress in the wall and are presented in the following chapter along with the influence of the peak ground acceleration on the local results. The area of reinforcement was determined for the bending moment and hoop stress in the wall for both the ultimate and serviceability limit states. These results are presented in the following chapter. The influence of using a modified response spectrum instead of the response spectrum as provided in Eurocode 8: Part 1 (2004) is also presented.

9. LOCAL RESULTS

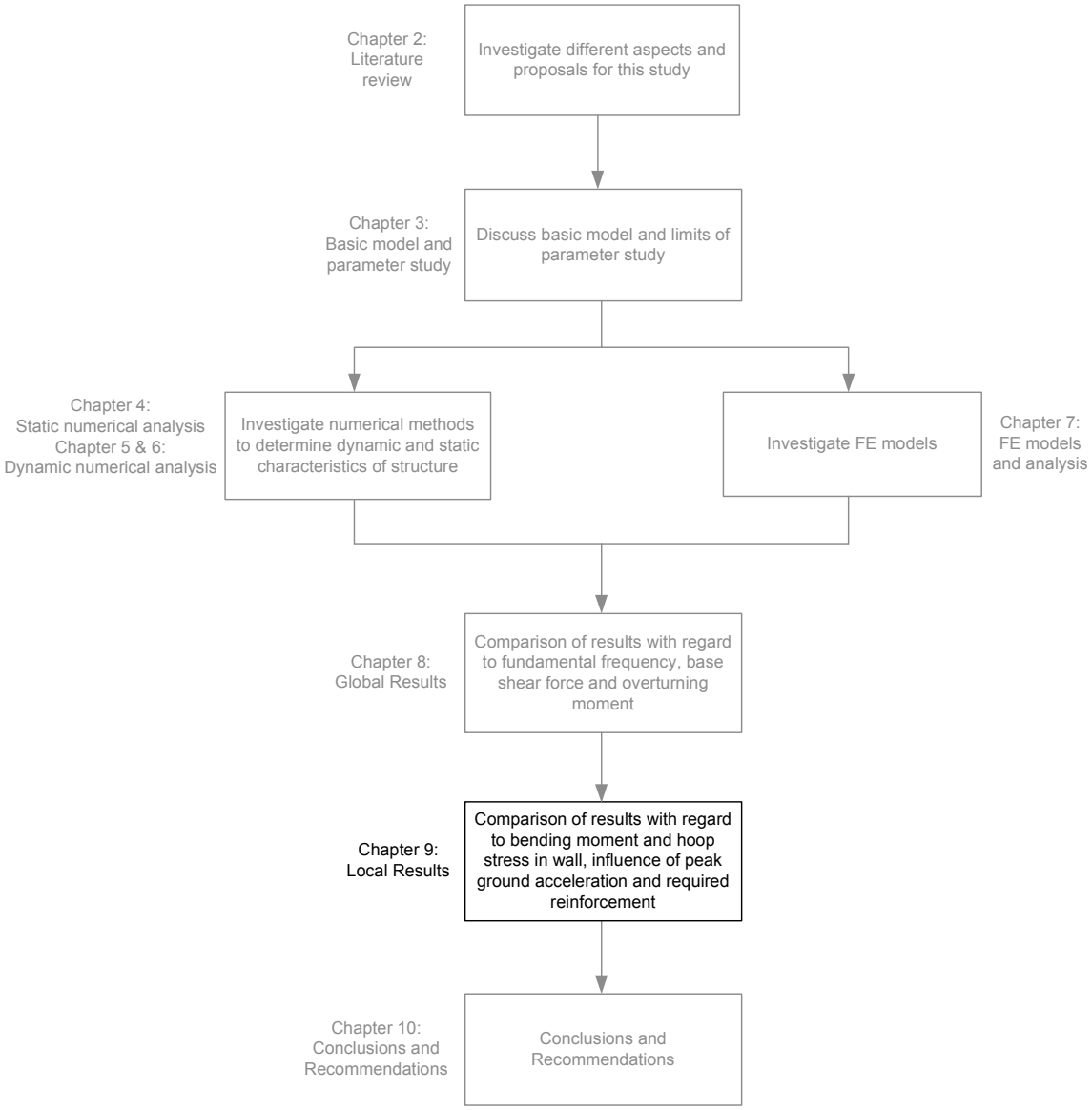

Figure 9.1: Methodology of study

Each structure within the scope of the parametric study was analysed for both static and seismic loads. The global results were presented in Chapter 8 and with reference to Figure 9.1 the local results are presented in this chapter. The local results refer to the bending moment about a horizontal axis and the hoop stress in the wall. The area of reinforcement required for the ultimate and serviceability limit states are presented in this chapter for both the hoop stress and the bending moment. The influence of the peak ground acceleration

and the use of a modified response spectrum on the local forces are also discussed in this chapter.

9.1. METHODS OF ANALYSIS AND PARAMETRIC STUDY

In this section a brief summary is presented of the different methods used for the analysis of a water-retaining structure. The scope of the parametric study and the definition of important terms are also provided in this section.

For the purposes of this study a basic model with a radius of 10 meters was chosen. The height of the tank wall and thickness of the wall was varied within the scope of the parametric study. In all instances reinforced concrete with a cube strength of 40 MPa, density of 2500 kg/m^3 and a Poisson ratio of 0.2 was used. All water-retaining structures in this study were classified as Class IV structures with consideration of only the horizontal component of an earthquake. The parametric study consisted of the following:

- The H/R [Height/Radius] ratio of the tank wall was varied between 0.3 and 1.5 in steps of 0.3.
- The t_w/R [wall thickness/Radius] ratio of the tank wall was varied between 0.006 and 0.03 in steps of 0.003.
- The peak ground acceleration was varied between 0.15g and 0.35g in steps of 0.1g

Two numerical methods were used for the analysis of each structure in the parametric study. These methods are:

- The static numerical method presented by Ghali (1979) for the determination of the hoop stress and the bending moment about a horizontal axis when a structure is subjected to hydrostatic pressure.
- The seismic numerical method presented by Veletsos (1997) for the determination of the hydrodynamic pressure and impulsive liquid mass when a structure is subjected to seismic excitation.

With consideration of the results presented in Chapter 8 for the respective FE models, only the FE model proposed by Virella (2006) was further investigated. All results

presented in this chapter were obtained specifically with the use of the Virella (2006) model. This model can be summarized as follows:

- The impulsive liquid mass was varied along the height of the wall in the same manner as the impulsive pressure.
- The lumped impulsive masses were not varied along the circumference of the tank wall but rather kept constant.
- The lumped masses were not fixed directly to the nodes on the tank wall but rather attached with the use of links.
- Pinned links were used to attach the lumped impulsive masses to their respective nodes on the wall with translation of the impulsive masses only allowed in the radial direction.

Only the influence of the impulsive mass on the behaviour of a water-retaining structure during horizontal seismic excitation was considered. The influence of the convective component was neglected since it becomes negligible for tanks with large radii (Veletsos, 1997).

The terms static results and dynamic results are continuously used in this chapter. The static results were obtained with consideration of the hydrostatic pressure exerted on the tank wall. Hydrodynamic pressure is exerted on the wall during seismic excitation of the structure and the sum of the static and seismic results are considered as the dynamic results. This can be summarized as follows:

- Dynamic = hydrostatic results + hydrodynamic results
- Static = hydrostatic results

Only the results obtained for a peak ground acceleration of 0.15g are presented in this chapter. The results obtained for other values of the peak ground acceleration are presented in Appendix E. All of the presented results were obtained with the use of a response spectrum as presented in Eurocode 8: Part 1 (2004). The influence of a modified response spectrum on the local results is discussed in the last section of this chapter.

9.2. STATIC RESULTS

The hoop force and bending moment about a horizontal axis were calculated using the design tables provided in Ghali (1979). A bending moment develops about a vertical axis due to the poisson effect but was not considered here. Only bending about a horizontal axis resulting from the hydrostatic pressure was considered in this study.

In order to determine the influence of seismic excitation on a water-retaining structure, the dynamic results were compared to the static results. The dynamic results were calculated as the sum of the seismic and the static results. The seismic results were obtained using the FE model by Virella (2006) while the static results were obtained using the method by Ghali (1987). In order to verify the results obtained with the various FE models a static analysis was also completed with the application of the hydrostatic pressure to the model as discussed in section 7.2. The hoop stress and bending moment obtained from the static FE models were verified with the results obtained using Ghali (1987). With the verification of the static results from the FE models the accuracy of the FE models could be assessed and further discrepancies in the computation of the dynamic results could be avoided.

The results obtained with the use of two FE models were verified with the appropriate results using Ghali (1979). Each had a H/R ratio of 0.6 with a t_w/R ratio of 0.006 and 0.024 respectively. The results obtained for a t_w/R ratio of 0.024 are presented in Figure 9.2. Results obtained for a t_w/R ratio of 0.006 presented in Appendix E. It should be noted $M_{y\text{-}y}$ refers to the variation of the bending moment along the y-axis and represents to the moment about the horizontal axis.

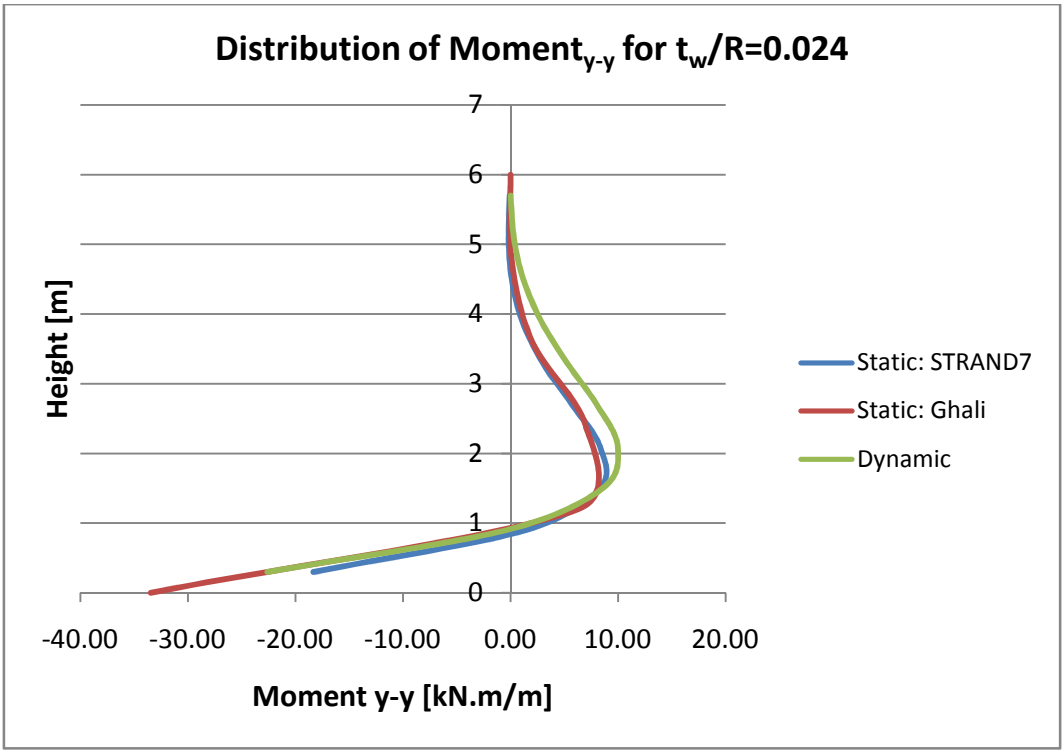

Figure 9.2: Verification of bending moment using Ghali (1979)

Figure 9.2 shows the static results as obtained with the numerical method by Ghali (1979) and the FE model with the hydrostatic pressure applied to the wall. The dynamic results are also presented in Figure 9.2. The dynamic results were computed as the sum of the static FE model and the seismic FE model by Virella (2006), both analysed in STRAND7 (2005). The static results obtained with the method by Ghali (1979) and FE model are similar in terms of the maximum bending moment about a horizontal axis. The comparison of static results obtained for a t_w/R ratio of 0.006 is similar to those presented in Figure 9.2.

The results obtained for the hoop stress for a t_w/R ratio of 0.024 are presented in Figure 9.3. The results obtained with the method by Ghali (1979), the FE model with the hydrostatic pressure applied to the tank wall and the FE model by Virella (2006) for the dynamic results are presented in Figure 9.3.

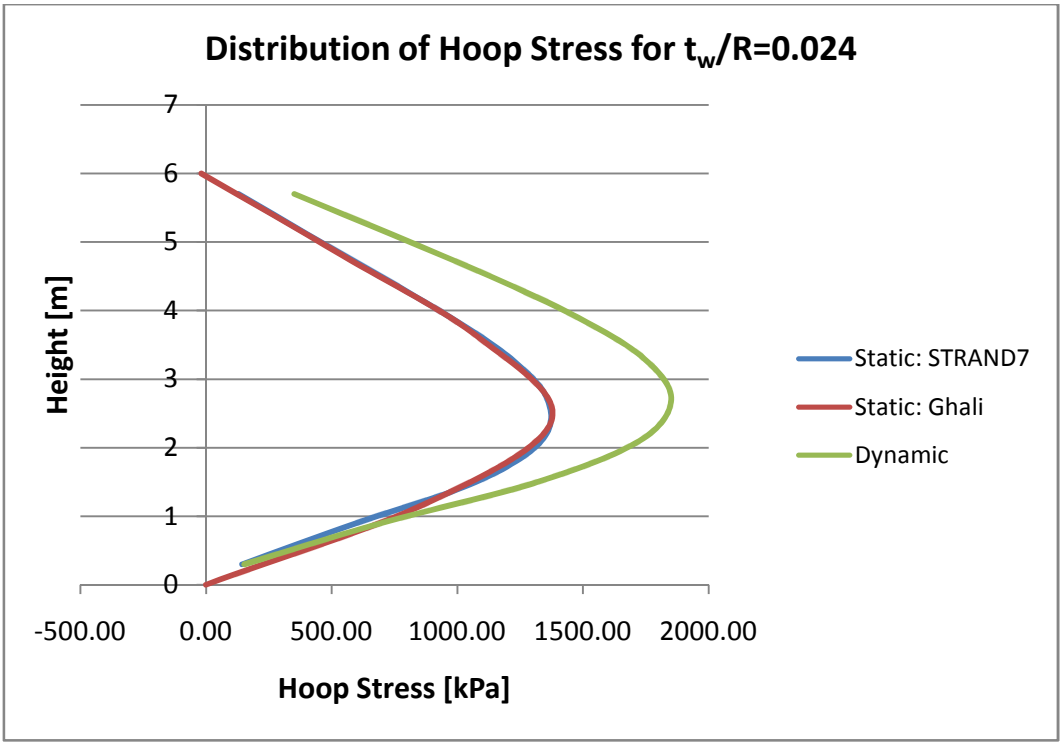

Figure 9.3: Verification of hoop stress obtained with Ghali (1979)

The static hoop stress obtained from the FE model compares well with the results obtained using the numerical method by Ghali (1979). The dynamic hoop stress is also presented on Figure 9.3 which was computed as the sum of the static FE model and the Virella (2006) model in STRAND7 (2005). The static results obtained with a FE model compares well with the numerical method by Ghali (1979) in terms of the hoop stress and the bending moment about a horizontal axis.

The comparison of the static results in Figures 9.2 and 9.3 suggests that the basic FE model as presented in Chapter 7.1 is sufficiently accurate. The use of 4-node plate elements instead of 8-node elements are acceptable for the FE modelling of a water-retaining structure subjected to horizontal seismic excitation. For this reason only 4-node elements were used in the modelling of all structures in the parametric study of this project.

9.3. DYNAMIC BENDING MOMENT

One of the aims of this project was to determine whether seismic loads acting on a water-retaining structure is indeed a critical load case. In order to assess whether the

seismic design of structures is critical, the static results were compared with the seismic results in terms of hoop stress and bending moment in the wall. Results obtained for the bending moment in the wall are presented in this section.

During seismic excitation of a water-retaining structure, bending of the tank wall about a horizontal and vertical axis were obtained. The value of the bending moment about a vertical axis at which cracking will occur was calculated with the use of the minimum area of reinforcement required. The comparison of results as obtained for the cracking moment and the ultimate limit state bending moment obtained with the Virella (2006) FE model is presented in Figure 9.4. The results presented are specifically for structures with a H/R ratio of 0.6. The comparison of results obtained for the other H/R ratio is presented in Appendix E, which is similar to Figure 9.4.

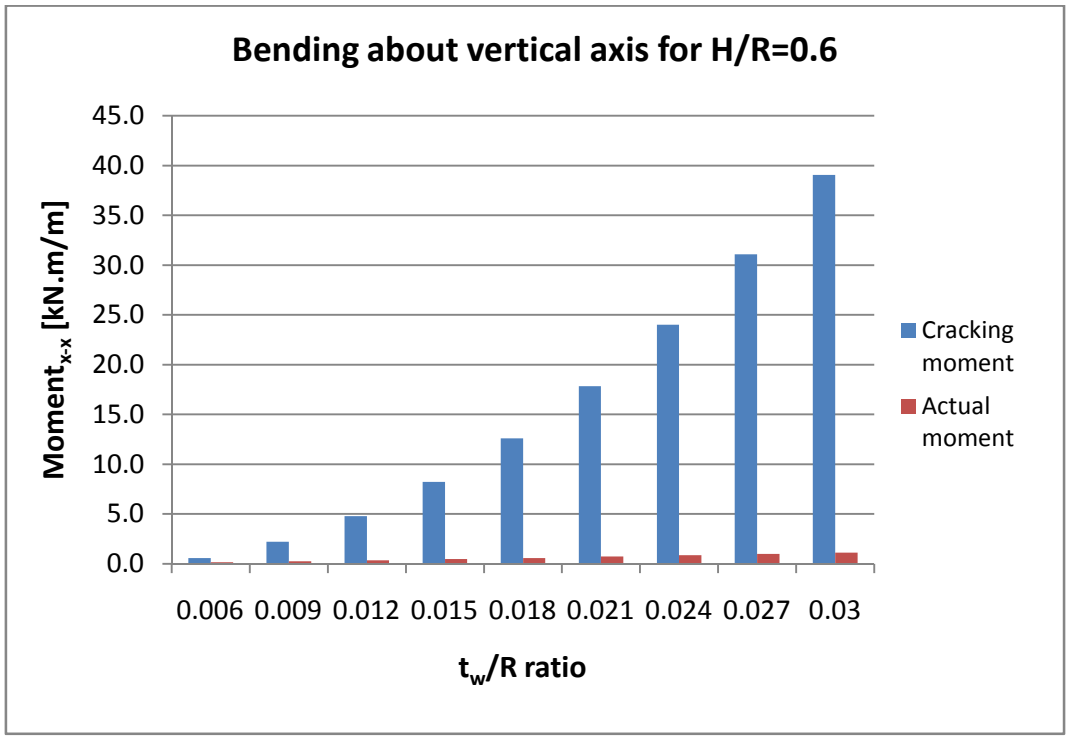

Figure 9.4: Comparison of the cracking moment and the ULS bending moment using Virella (2006) FE model

As shown in Figure 9.4 the bending moment at which cracking will occur is significantly greater than the values obtained for the bending moment about a vertical axis using the Virella (2006) FE model. No cracks will develop due to bending about a vertical axis and therefore the bending moment about a vertical axis is neglected in this study.

The bending moment about the horizontal axis is however not negligible as illustrated in Figure 9.5. The dynamic results presented in Figure 9.5 were obtained for a structure with a H/R ratio of 1.5 with consideration of the ultimate limit state. The sum of the static results using Ghali (1979) and the dynamic results using the Virella (2006) FE model was obtained with consideration of the appropriate partial load factors.

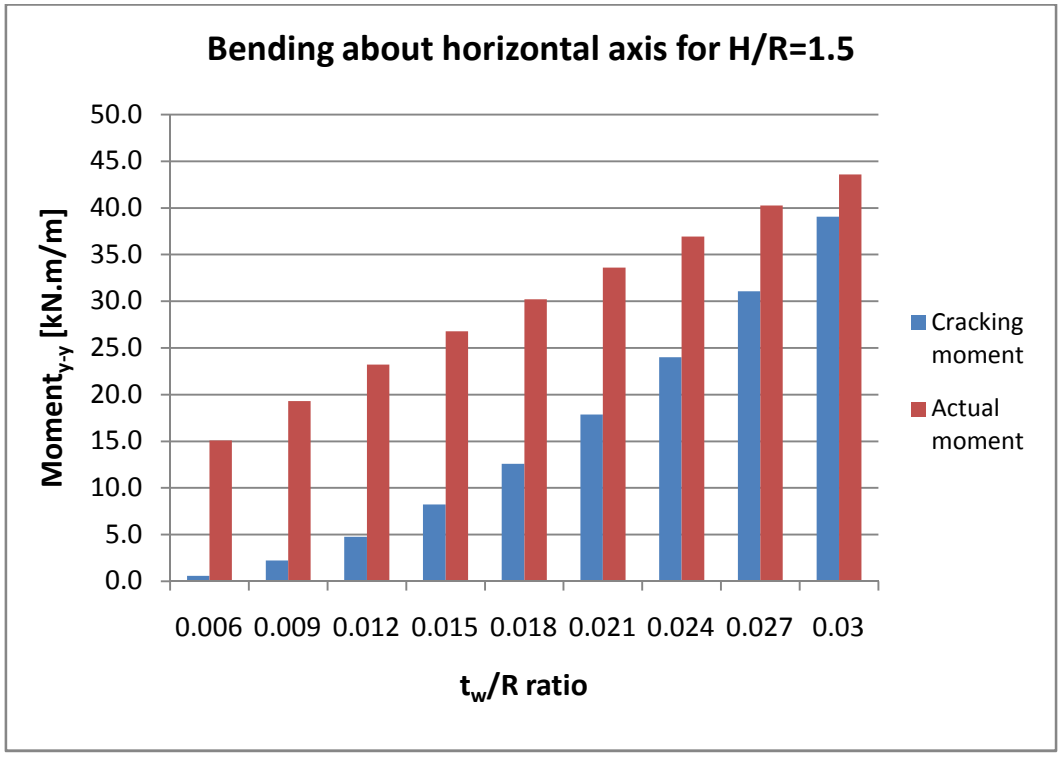

Figure 9.5: Comparison of the cracking moment and the ULS moment using Virella (2006) model

The results obtained using the FE model by Virella (2006) are greater than the bending moment at which cracking will occur. The bending moment about a horizontal axis is not negligible and is therefore further discussed in this section.

The dynamic results obtained for bending about a horizontal axis are presented in Figure 9.6. The results are specifically with consideration of the ultimate limit state and were computed as the sum of the hydrostatic and hydrodynamic results with inclusion of the partial load factors.

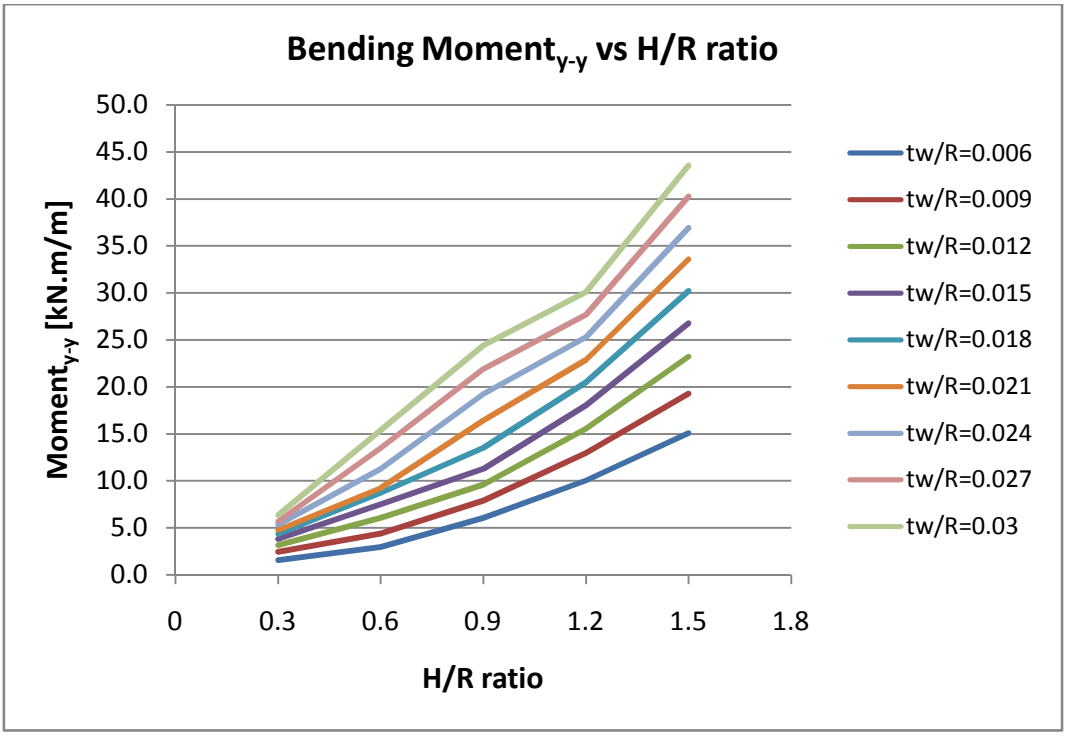

Figure 9.6: Variation in ULS bending moment about a horizontal axis (PGA=0.15g)

It can be seen from Figure 9.6 that the bending moment about a horizontal axis increases with an increase in wall thickness. The bending moment resulting from the hydrostatic pressure is significantly greater than the bending moment obtained for the hydrodynamic pressure as shown in Figure 9.7. The results presented in Figure 9.7 were obtained for the ultimate limit state and for clarity purposes only the t_w/R values between 0.024 and 0.03 are provided. The seismic results shown in Figure 9.7 were obtained with the use of the Virella (2006) FE model in STRAND7 (2005). Since the results obtained for the static analyses are consistently greater than the results obtained for the seismic analyses, the contribution of the hydrostatic pressure to the bending moment is considered to be dominant.

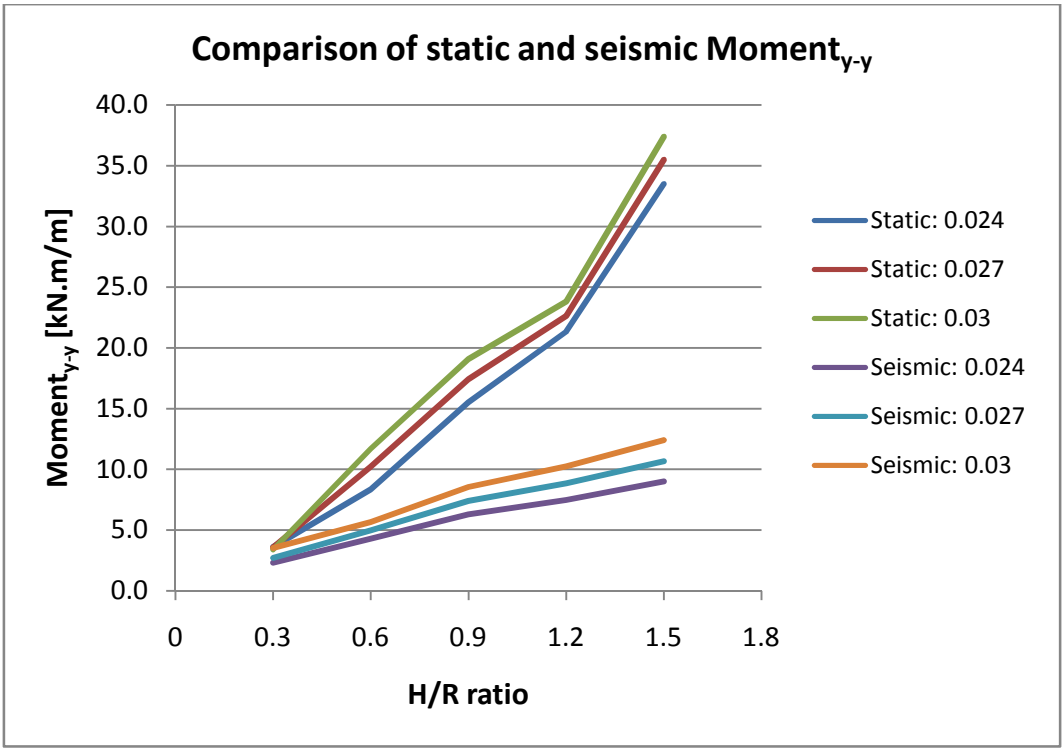

Figure 9.7: Comparison of static and seismic bending moments (PGA=0.15g)

The difference in bending moment between the dynamic response and static design of a structure is provided in Figure 9.8. The values presented in Figure 9.8 were obtained for the ultimate limit state with the use of a peak ground acceleration of 0.15g

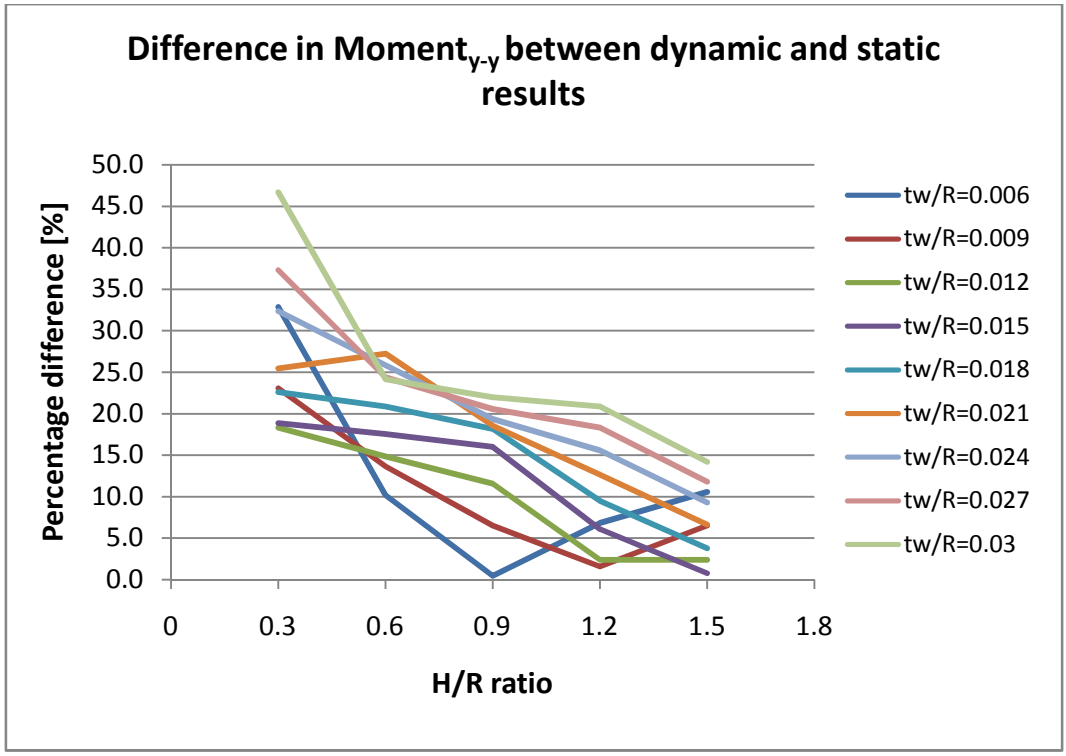

Figure 9.8: Difference in ULS bending moment between dynamic and static response for ULS (PGA=0.15g)

The bending moment about a horizontal axis differs significantly between the dynamic response and the static response of water-retaining structures. However, the difference in results decreases as the H/R ratio of the structure increase. It should be kept in mind the dynamic response was computed as the sum of the static and seismic results. A relatively high percentage difference was obtained in broad tanks with a peak ground acceleration of 0.25g and 0.35g as presented in Appendix E. The same trend was observed with the comparison of results for the serviceability limit state. These results are provided in Appendix E.

The influence of seismic excitation in terms of the bending moments has been presented in this section. Results were provided for the bending moment about a horizontal and a vertical axis. The influence of seismic activity on water-retaining structures, in terms of the bending moment, can be summarized as follows:

- Bending about a vertical axis is negligible.
- The bending moment about a horizontal axis is not negligible and increases with an increase in wall thickness and height of the wall.

- The difference between the dynamic and static bending moments decreases as the wall thickness decreases. The difference in bending moments also decreases as the wall height increases. This is applicable to both the ultimate and the serviceability limit state.

9.4. HOOP STRESS

The hydrostatic and hydrodynamic pressure exerted on a tank wall produces a hoop stress in the wall. One of the aims of this project was to determine whether seismic loads are a dominant load case for the design of water-retaining structures in South Africa. For this purpose both the bending moment and the hoop stress obtained from the dynamic response of a structure were compared to the results obtained from the static response of a structure. The dynamic response refers to the sum of the seismic response and static response of a system.

All graphs provided in this section present the results as obtained for a peak ground acceleration of 0.15g. Values presented here are the maximum values obtained over the height of the wall.

The hoop stress obtained for the dynamic response of a water-retaining structure, with consideration of the ultimate limit state, is presented in Figure 9.9. The dynamic hoop stress was determined as the sum of the static and the seismic loads with inclusion of the partial load factors.

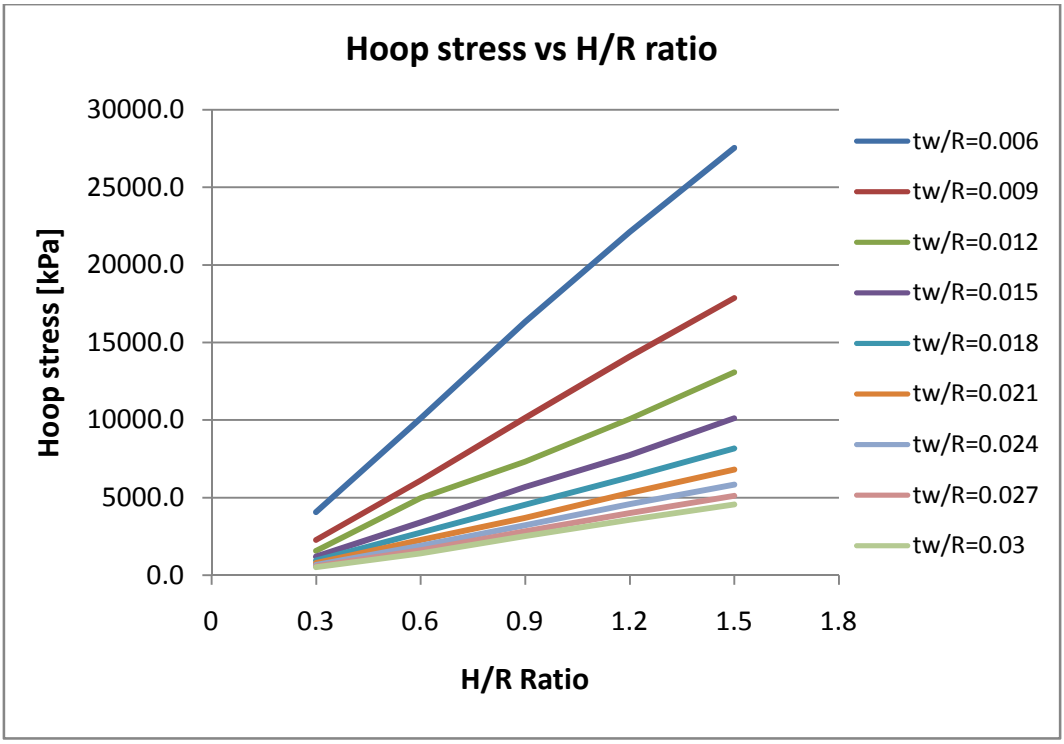

Figure 9.9: Variation of the ULS hoop stress for dynamic analyses (PGA=0.15g)

From Figure 9.9 it is observed that the hoop stress increases with a decrease in wall thickness. The hoop stress in the wall also increases as the wall height increases. The majority of structures considered in this study have a fundamental period smaller than 0.15 seconds and thus fall within the first region of the response spectrum. As the wall height increases or the wall thickness decreases, the fundamental period of the structure becomes longer resulting in a higher pseudoacceleration. The higher pseudoacceleration results in greater hydrodynamic pressure, producing larger hoop stresses in the wall.

It should be kept in mind that the total dynamic response of the structure was computed as the sum of the dynamic analysis in STRAND7 (2005) and the static results obtained using Ghali (1979). The difference in hoop stress obtained from the dynamic response and the static response is presented in Figure 9.10 for the ultimate limit state.

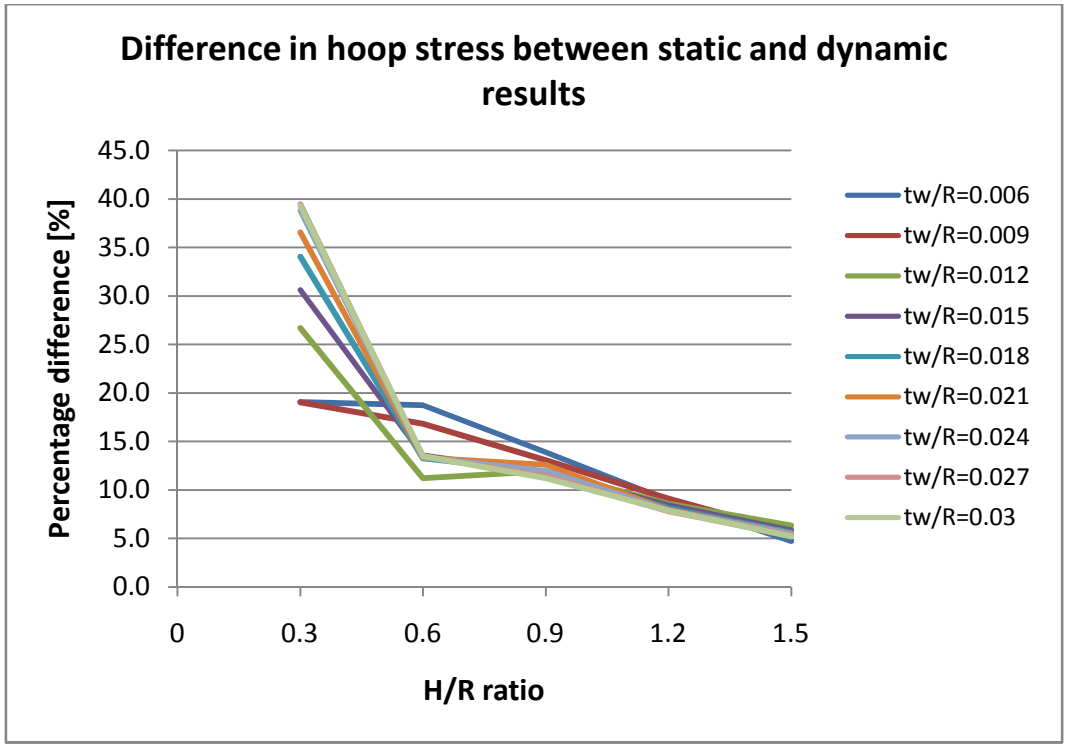

Figure 9.10: Difference in ULS hoop stress between static and dynamic results (PGA=0.15g)

As shown in Figure 9.10, the percentage difference significantly increases as the H/R ratio decreases from a value of 0.6. It should be kept in mind that the results presented in Figure 9.10 is the sum of the seismic and the static results. The steep increase in percentage difference can be attributed to the significant increase of both the static and seismic results in broad tanks with the static results providing the dominant contribution as indicated in Figure 9.7. With greater values obtained for the static analyses than the seismic analyses and with consideration of the difference in partial load factor used for the static results, an increasing percentage difference is obtained as the H/R ratio decreases. The results obtained for the serviceability limit state are similar to that of the ultimate limit state. The serviceability limit state results are presented in Appendix E.

9.5. INFLUENCE OF PEAK GROUND ACCELERATION ON BENDING MOMENT

Both the bending moment about a horizontal axis and the hoop stress in a section have been discussed in the previous section for a peak ground acceleration of 0.15g. In this study three values of the peak ground accelerations were investigated. The peak ground values investigated in this study are 0.15g, 0.25g and 0.35g.

Figure 9.11 illustrates the influence of the peak ground acceleration on the bending moment about a horizontal axis obtained for the ultimate limit state. The percentage difference is computed as the difference between the dynamic and static response of the structure. The dynamic results refer to the sum of the seismic and static results with consideration of the appropriate partial load factors for the ultimate limit state. For clarity purposes only the results obtained for the t_w/R ratios of 0.015 and 0.03 are presented in Figure 9.11.

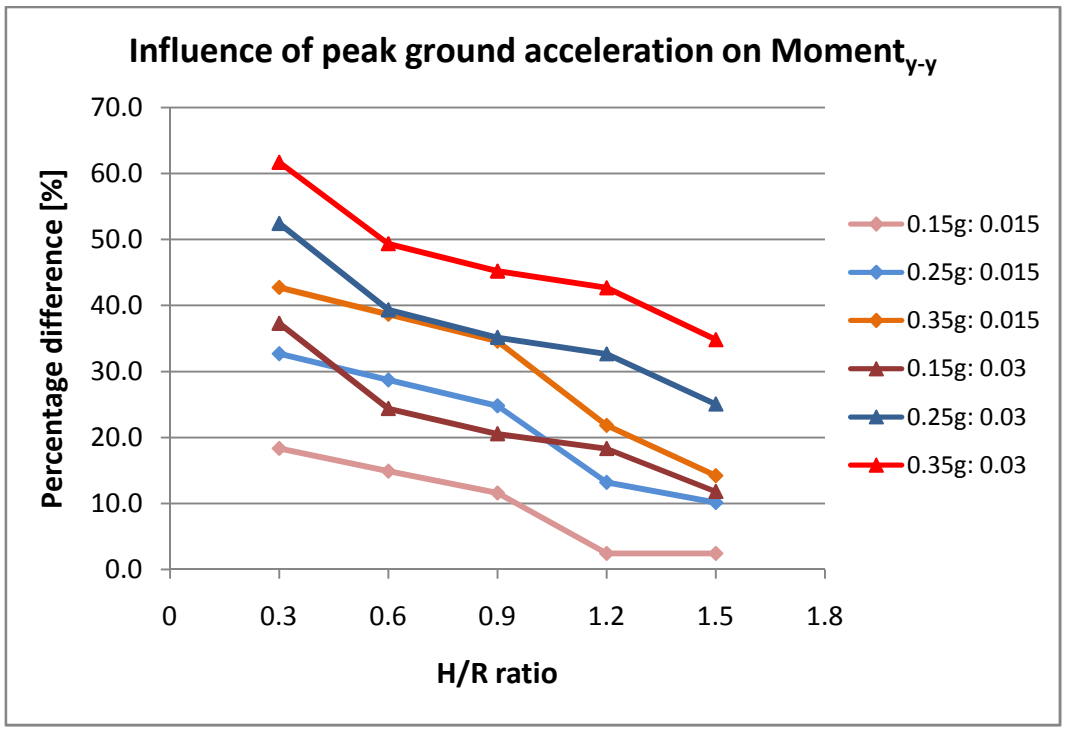

Figure 9.11: Influence of peak ground acceleration on Moment$_{y-y}$ for ULS

Figure 9.11 shows the increase in difference between the dynamic and static bending moment as the peak ground acceleration increases. This indicates that the influence of seismic excitation on a water-retaining structure increases as the peak ground acceleration increases. The influence of seismic excitation decreases as the H/R ratio increases as can be expected.

The ratio between the dynamic results and static results obtained for the bending moment about a horizontal axis is presented in Figure 9.12. The dynamic results refer to the sum of the seismic and static results with the seismic results obtained using the FE model by Virella (2006) and the static results obtained using Ghali (1979). All of the

results presented in Figure 9.12 were obtained for the ultimate limit state. For clarity purposes only the results obtained for the t_w/R ratios of 0.015 and 0.027 are shown in Figure 9.12.

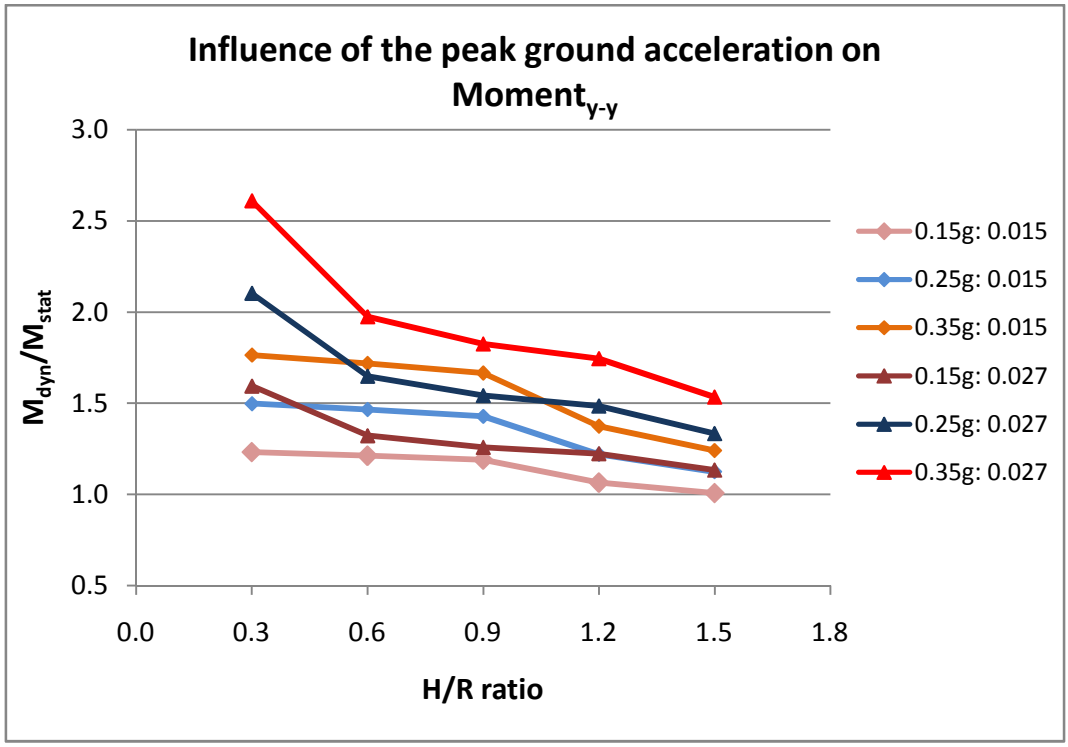

Figure 9.12: Influence of peak ground acceleration on Moment$_{y-y}$ for ULS

The ratio between the dynamic bending moment and static bending moment decrease slightly as the H/R ratio increases. The ratio between the dynamic and static bending moment also increases as the wall thickness ratio [t_w/R] increase as well as with an increase in peak ground acceleration. Significant differences were obtained for very broad tanks with a H/R ratio smaller than 0.6 and a higher t_w/R ratio as shown in Figure 9.12. Water-retaining structures in South Africa are usually designed with a H/R ratio of 0.5 and a t_w/R ratio ranging between 0.025 and 0.03. This falls within the range of structures for which significant differences between the dynamic and static bending moment were obtained.

The influence of a variance in peak ground acceleration on the hoop stress obtained for the ultimate limit state is presented in Figure 9.13. The percentage difference refers to the difference in values obtained for the dynamic analysis and static analysis of the structure respectively. The dynamic response was calculated as the sum of the seismic

and static results with consideration of the partial load factors as prescribed for the ultimate limit state. For clarity purposes only the t_w/R ratios of 0.015 and 0.027 are presented in Figure 9.13.

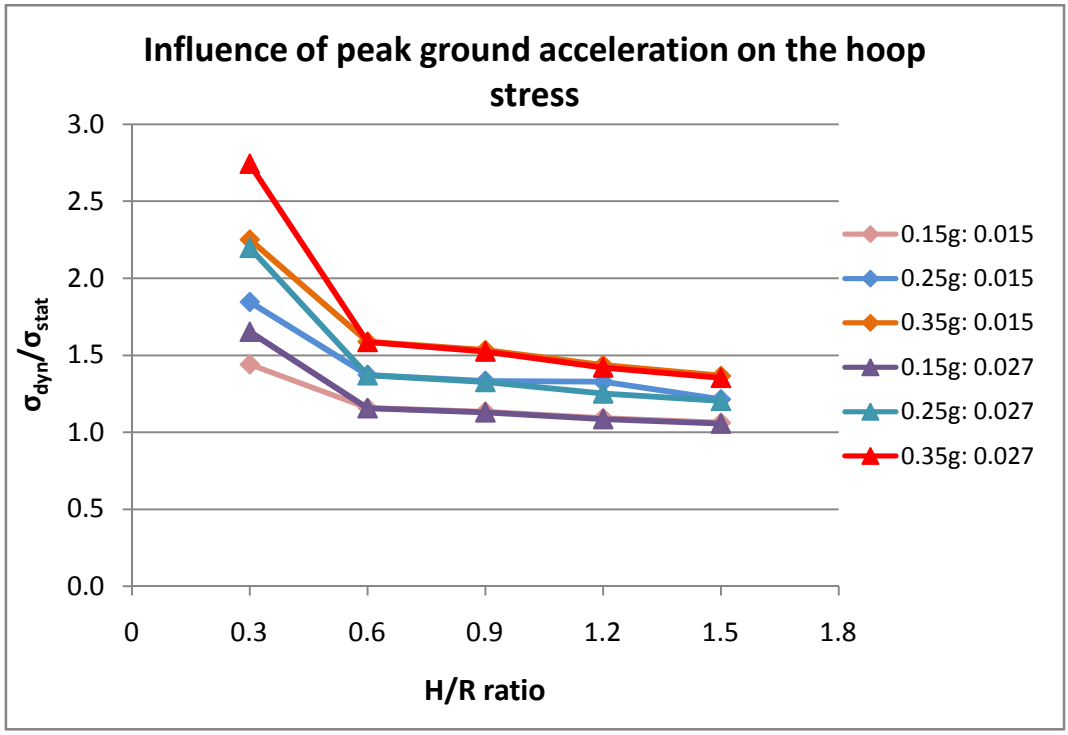

Figure 9.13: Influence of peak ground acceleration on hoop stress for ULS

The influence of the peak ground acceleration on the hoop stress becomes more pronounced with an increase in peak ground acceleration. However, a change in the wall thickness ratio seems to have no significant influence on the hoop stress ratio between the dynamic and static results for the ultimate limit state. The ratio between the dynamic and static hoop stress also remains relatively constant as the H/R ratio increases from 0.6 to 1.5. The ratio of the hoop stress between the dynamic and static results is therefore considered to be independent of the H/R and t_w/R ratios except in the case of very broad tanks with a H/R ratio smaller than 0.6.

9.6. AREA OF REINFORCEMENT REQUIRED

One of the aims of this project was to determine whether seismic loading is a dominant load case in the design of water-retaining structures in South Africa. For this reason the dynamic results were compared to the static results in terms of the hoop stress and

bending moment about a horizontal axis. The results were presented in the previous sections. From the results presented in sections 9.4 and 9.5 it is clear that seismic activity does have a significant influence on a water-retaining structure for both the ultimate and serviceability limit state. The question arises of whether the design of a water-retaining structure with consideration of seismic loads is governed by the ultimate limit state or the serviceability limit state. For this reason the area of reinforcement required for the ultimate limit state was compared to the area of reinforcement required for the serviceability limit state. Comparisons were made for both the hoop stress and the bending moment about a horizontal axis and are discussed in this section.

The hoop stress in the wall has a two-fold effect since it may cause yielding in the reinforcement under ultimate limit state loads. Alternatively the maximum allowable crack width may be exceeded under serviceability limit state loads. The area of reinforcement required for the hoop stress was determined by taking both considerations into account.

Figure 9.14 shows the ratio of reinforcement required in terms of the hoop stress for seismic and static analyses. The reinforcement was calculated with consideration of the hoop stress per meter height of the wall. The results presented in Figure 9.14 are specific to structures with a t_w/R ratio of 0.024. Refer to Appendix E for graphs pertaining to the wall thickness ratios ranging between 0.006 and 0.03.

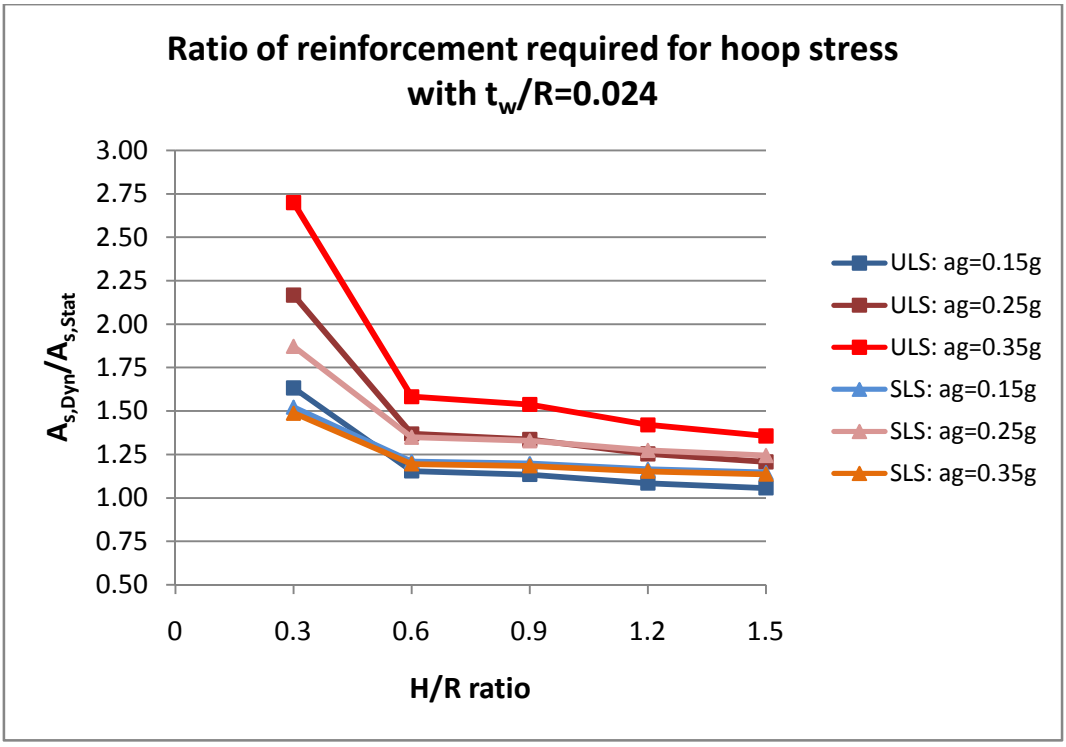

Figure 9.14: Dynamic to static ratio of reinforcement required for the hoop stress

Figure 9.14 shows an increase in reinforcement required as the peak ground acceleration increases from 0.15g to 0.35g. The ratio of reinforcement required for the serviceability limit state remains relatively constant, regardless of the H/R ratio or the peak ground acceleration except when the H/R ratio is smaller than 0.6. However, for the ultimate limit state the ratio of reinforcement required for the dynamic and static analyses of a structure increases with an increase in peak ground acceleration.

It is noted that for the ultimate limit state with a peak ground acceleration of 0.15g a significant increase in the reinforcement ratio is obtained only for structures with a H/R ratio smaller than 0.6. In South Africa a peak ground acceleration of 0.15g is prescribed and a H/R ratio of 0.5 is commonly used. With these values in mind it can be seen from Figure 9.14 that these water-retaining structures are significantly influenced by seismic activity for both the ultimate and serviceability limit states.

The reinforcement required for the serviceability limit state is consistently higher than the reinforcement required for the ultimate limit state with consideration of the seismic loads as shown in Figure 9.15. The results presented in Figure 9.15 were obtained with a peak ground acceleration of 0.15g and a t_w/R ratio of 0.024 which is representative of

parameters used in practice. The serviceability limit state therefore governs the seismic design of water-retaining structures for South African conditions.

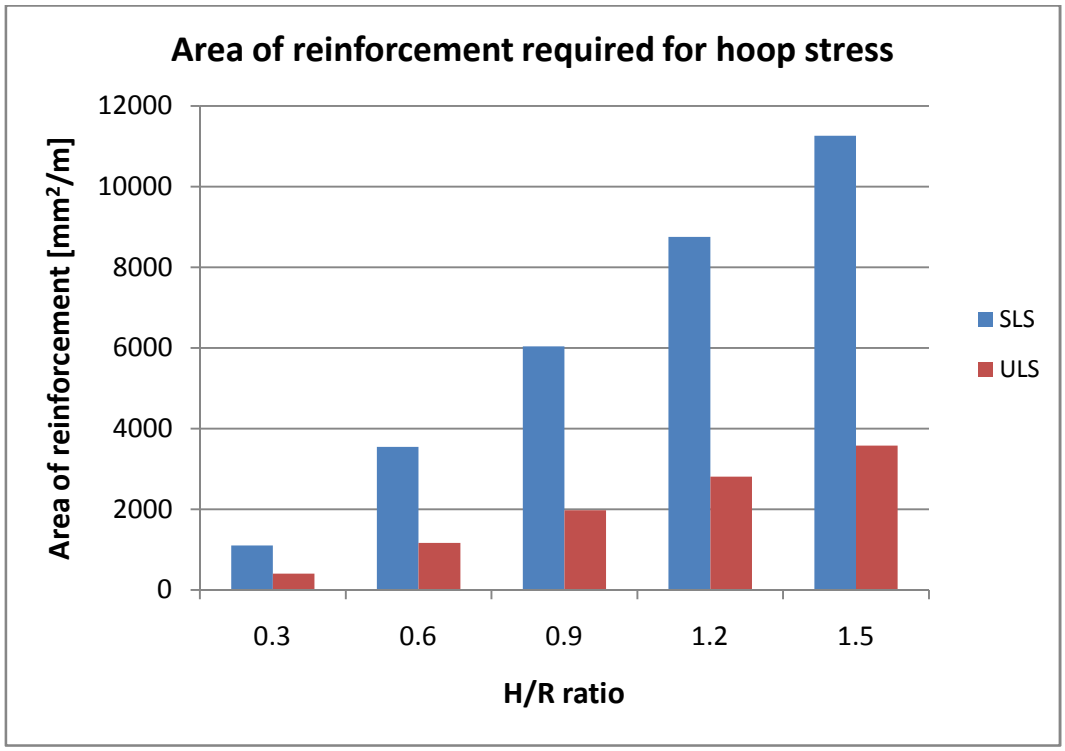

Figure 9.15: Area of reinforcement required for the hoop stress (PGA=0.15g)

The ratio between the reinforcement required for the serviceability limit state and ultimate limit state is presented in Figure 9.16. The results presented in Figure 9.16 were obtained for the hoop stress for both the dynamic and the static analyses of a structure. The dynamic results were calculated as the sum of the seismic response and the static response with consideration of the partial load factors for the serviceability limit state.

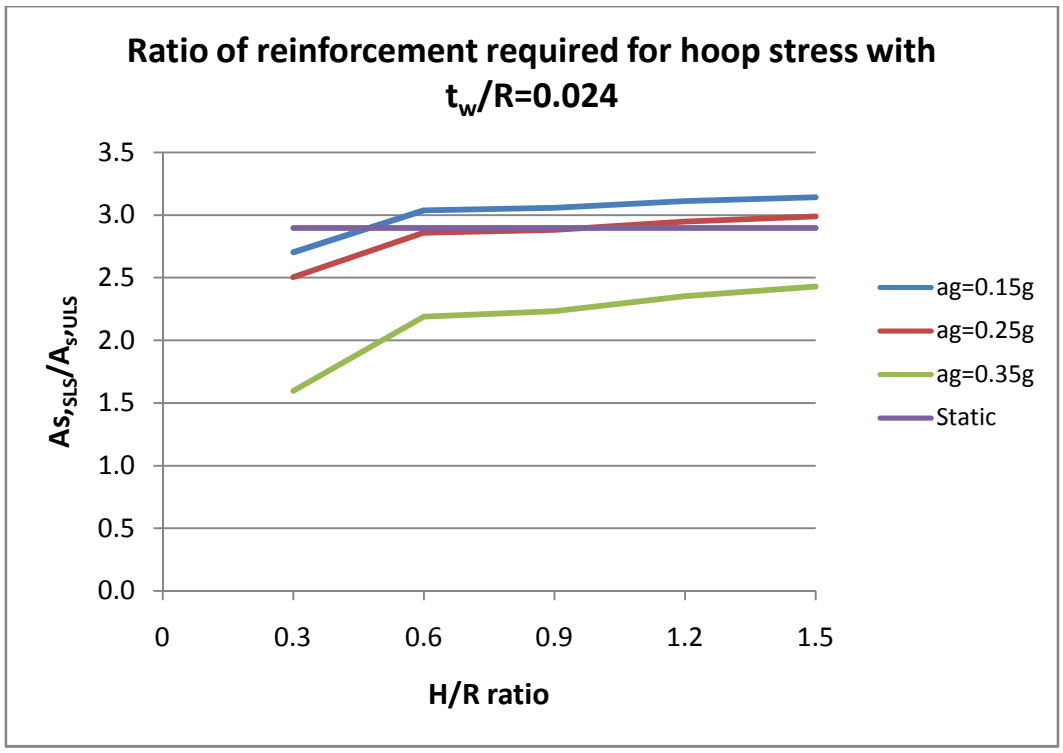

Figure 9.16: Ratio of reinforcement required for dynamic hoop stress between SLS and ULS

It should be noted from Figure 9.16 that the ratio between the reinforcement required for the serviceability and ultimate limit state reduces as the peak ground acceleration increases. This indicates that the influence of seismic excitation in terms of the ultimate limit state increases as the peak ground acceleration increases, corresponding to a smaller difference between the serviceability and ultimate limit state. For values higher than 0.35g the governing factor for design might shift from the serviceability limit state to the ultimate limit state. For a peak ground acceleration of 0.15g the ratio between the serviceability and ultimate limit state is significantly higher for seismic analyses than for static analyses and the seismic design of water-retaining structures for the serviceability limit state therefore cannot be neglected.

The amount of reinforcement required for bending about the horizontal axis was also calculated, with consideration of the minimum reinforcement as prescribed in SABS 0100-1 (2000). For both seismic and static analyses, the amount of reinforcement required for bending decreased with the increase in wall thickness. For broad tanks with H/R ratios ranging between 0.3 and 0.6, the minimum area of reinforcement was used in all instances. The reinforcement required for the taller tanks with H/R ratios ranging between 0.9 and 1.5 required more than the minimum amount of reinforcement as

prescribed. For clarity purposes, only the wall thickness ratios between 0.024 and 0.03 are provided in Table 9.1 as these are applicable to the South African practice. The term "minimum" in Table 9.1 refers to the amount of reinforcement calculated with consideration of the minimum ratio of reinforcement required as prescribed in the design codes. The term "actual" in Table 9.1 refers to the computed area of reinforcement required to resist the bending moment in the wall. The minimum ratio of reinforcement required as prescribed in the design codes, was therefore not considered.

		Minimum			**Actual**		
		a_g=0.15g	a_g=0.25g	a_g=0.35g	a_g=0.15g	a_g=0.25g	a_g=0.35g
H/R:	**t_w/R:**	**A_{Dyn}/A_{Stat}:**	**A_{Dyn}/A_{Stat}:**	**A_{Dyn}/A_{Stat}:**	**A_{Dyn}/A_{Stat}:**	**A_{Dyn}/A_{Stat}:**	**A_{Dyn}/A_{Stat}:**
0.3	0.024	1.00	1.00	1.00	1.00	1.00	1.00
	0.027	1.00	1.00	1.00	1.00	1.00	1.00
	0.03	1.00	1.00	1.00	1.00	1.00	1.00
0.6	0.024	1.00	1.00	1.00	1.00	1.00	1.00
	0.027	1.00	1.00	1.00	1.00	1.00	1.00
	0.03	1.00	1.00	1.00	1.00	1.00	1.00
0.9	0.024	1.26	1.26	1.26	1.56	1.56	1.56
	0.027	1.12	1.12	1.12	1.56	1.56	1.56
	0.03	1.01	1.01	1.01	1.56	1.56	1.56
1.2	0.024	1.00	1.44	1.44	1.00	1.44	1.44
	0.027	1.00	1.44	1.44	1.00	1.44	1.44
	0.03	1.00	1.01	1.45	1.00	1.56	2.25
1.5	0.024	1.00	1.00	1.00	1.00	1.00	1.00
	0.027	1.78	1.78	1.78	1.78	1.78	1.78
	0.03	1.44	2.56	2.56	1.44	2.56	2.56

Table 9.1: Bending reinforcement

The results provided in Table 9.1 for a peak ground acceleration of 0.15g are graphically represented in Figure 9.17. Only the values as obtained for t_w/R ratios of 0.024, 0.027 and 0.03 are presented in Figure 9.17 since these values are commonly used in the South African practice. The values shown in Figure 9.17 are the values obtained without consideration of the minimum ratio of reinforcement as prescribed by the design codes.

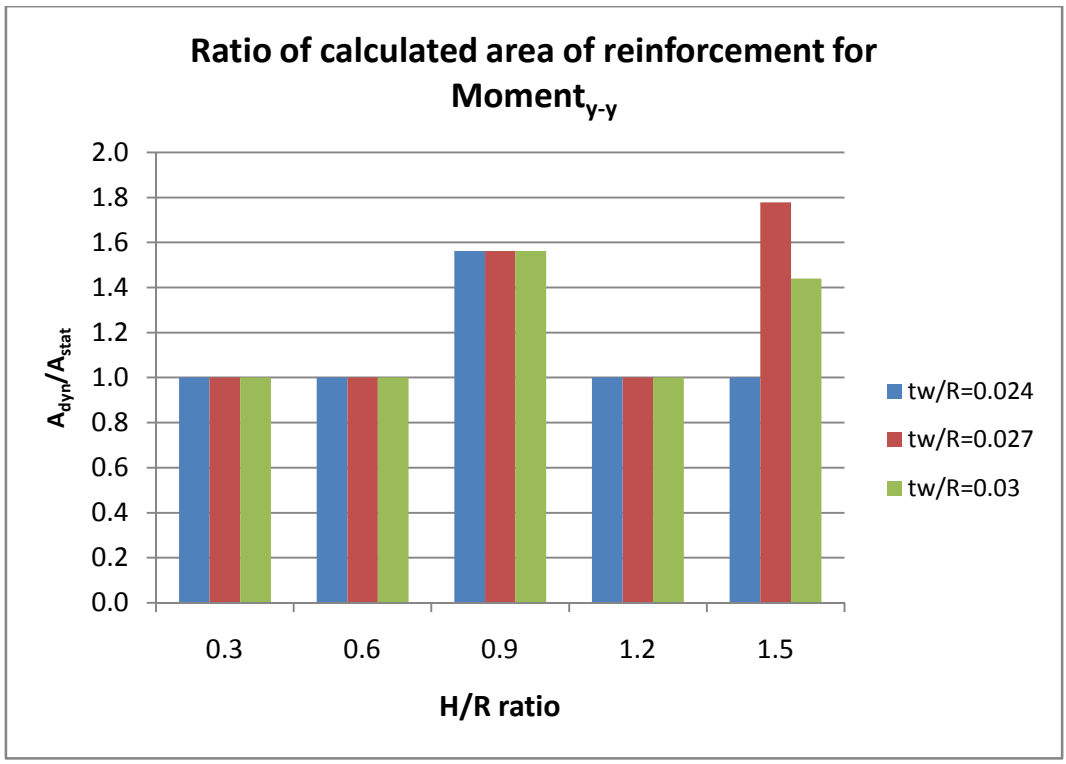

Figure 9.17: Ratio between dynamic and static area of reinforcement (PGA=0.15g)

When considering the actual amount of reinforcement required to resist the bending moment in the wall, it can be seen from Table 9.1 and Figure 9.17 that the ratio between the dynamic and static results remain independent of the wall thickness for H/R ratios smaller than 0.9. However, the ratio between the dynamic and static area of reinforcement required increases from a value of 0.9 for the H/R ratio. This is also the case with consideration of the minimum amount of reinforcement required for bending about a horizontal axis. In terms of bending about a horizontal axis, the influence of seismic excitation on a water-retaining structure only becomes noticeable in taller structures with a H/R ratio between 0.9 and 1.5.

9.7. MODIFICATION OF THE RESPONSE SPECTRUM AS PROVIDED IN EUROCODE 8: PART 1 (2004)

The response spectrum as provided in Eurocode 8: Part 1 (2004) was used throughout this study and is provided in this document in Figure 8.3. However, in practice the first portion of the response spectrum is modified as shown in Figure 9.18. The first portion of the response spectrum is modified since it is assumed that the structure cracks in the

ultimate limit state when subjected to seismic excitation. Correspondingly a longer period of vibration may be observed and it is considered more conservative to use the maximum pseudoacceleration for these structures. Figure 9.18 was obtained for Class IV structures with a damping ratio of 5% that are subjected to a peak ground acceleration of 0.15g. Figure 9.18 is applicable to the ultimate limit state.

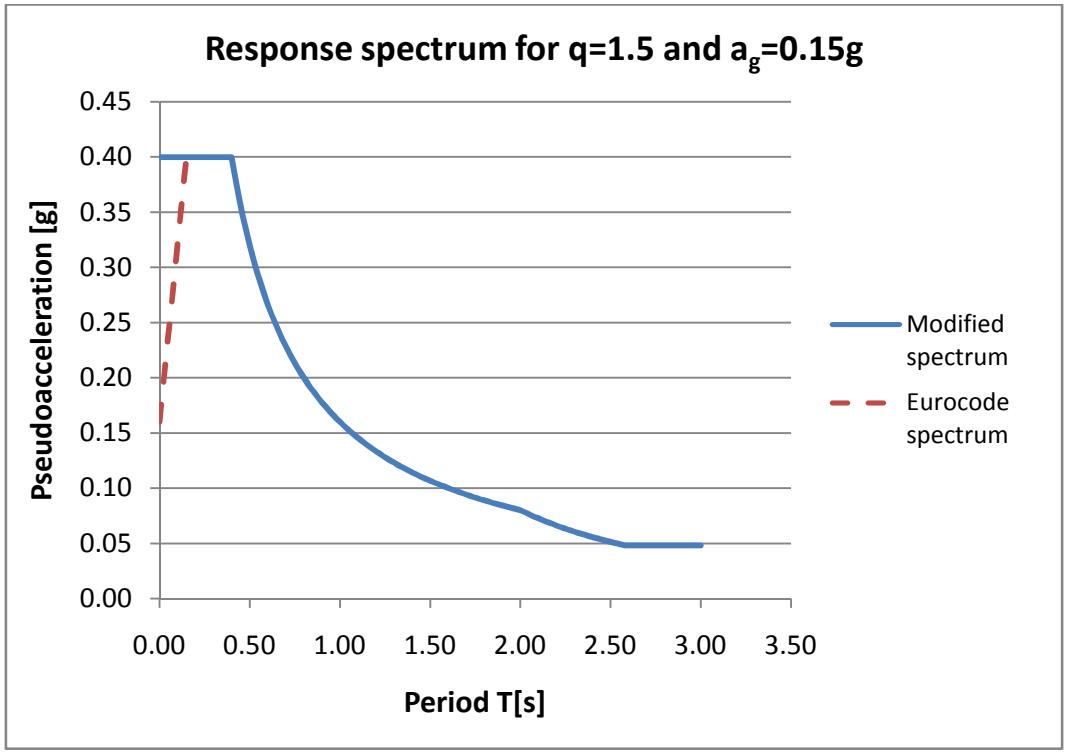

Figure 9.18: Modified response spectrum

This modification of the first portion of the response spectrum has an influence on the base shear force, overturning moment, bending moment and hoop stress in the wall since all of these properties are dependent on the pseudoacceleration. The area of reinforcement required for the internal forces will change subsequently. However, only the influence of the modified response spectrum on the bending moment and hoop stress is discussed in this section. In all instances the dynamic results are presented with the dynamic results computed as the sum of the seismic and static results with consideration of the appropriate partial load factors. The static results refer to the results as computed with the use of Ghali (1979).

The influence of the modified response spectrum on the dynamic bending moment is shown in Figure 9.19 as computed for the serviceability limit state. Only the results obtained for t_w/R ratios of 0.021, 0.024, 0.027 and 0.03 are presented in Figure 9.19 for clarity purposes. The legend in Figure 9.19 refer to the values obtained with the response spectrum provided in Eurocode 8: Part 1 (2004) and the modified response spectrum.

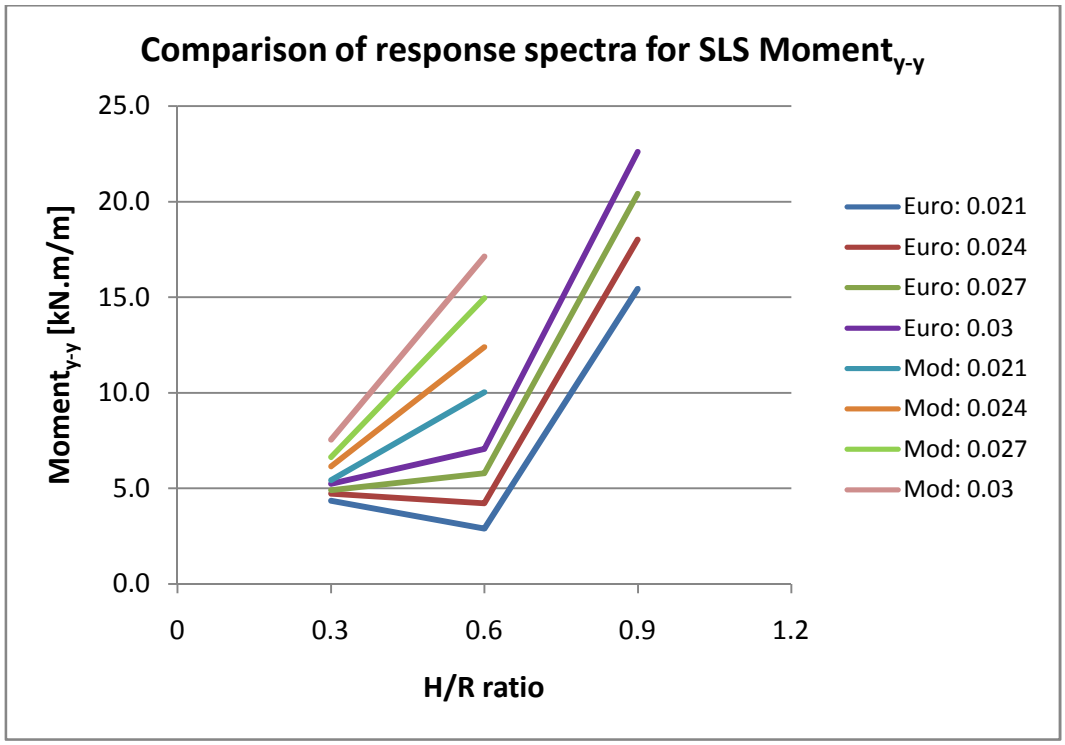

Figure 9.19: Change in SLS bending moment due to the modified response spectrum (PGA=0.15g)

The change in response spectrum results in an increased pseudoacceleration to which the structure is subjected during horizontal seismic excitation. The impulsive pressure increases correspondingly which results in a higher bending moment in the wall. The ratio between the dynamic and static bending moments for the serviceability limit state also changes when the modified response spectrum is used as indicated in Figure 9.20.

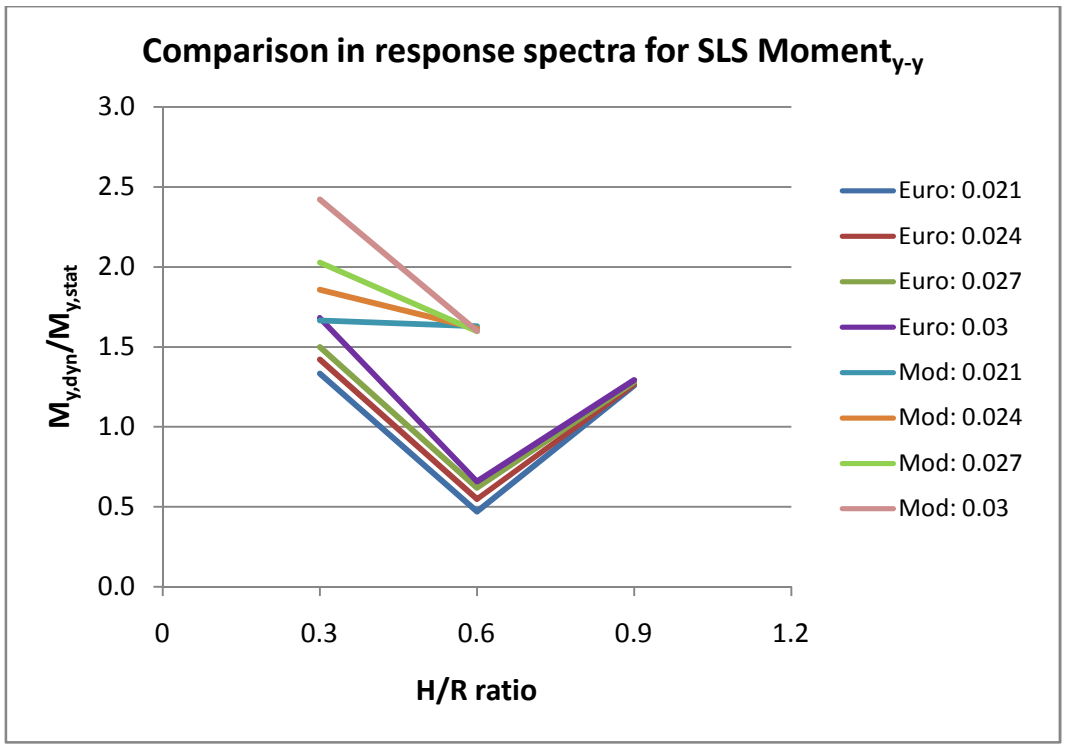

Figure 9.20: Change in dynamic to static bending moment for the SLS (PGA=0.15g)

Figure 9.20 shows that the change in bending moment ratio between the dynamic and static results is significant with the use of the modified response spectrum instead of the response spectrum provided in Eurocode 8: Part 1 (2004). Subsequently the area of reinforcement required to resist the bending moment in the wall will increase with the use of the modified response spectrum instead of the response spectrum in Eurocode 8: Part 1 (2004). However, in most cases the minimum area of reinforcement is required for both the dynamic and static design of water-retaining structures as indicated in section 9.6 of this document. The influence of the modified response spectrum on bending about a horizontal axis may therefore be negligible.

The change in hoop stress with the use of the modified response spectrum is presented in Figure 9.21 for the serviceability limit state. The results presented in Figure 9.21 are the dynamic results which were calculated as the sum of the seismic and static results with consideration of the appropriate partial load factors. Only the t_w/R ratios between 0.021 and 0.03 are presented in Figure 9.21 for clarity purposes.

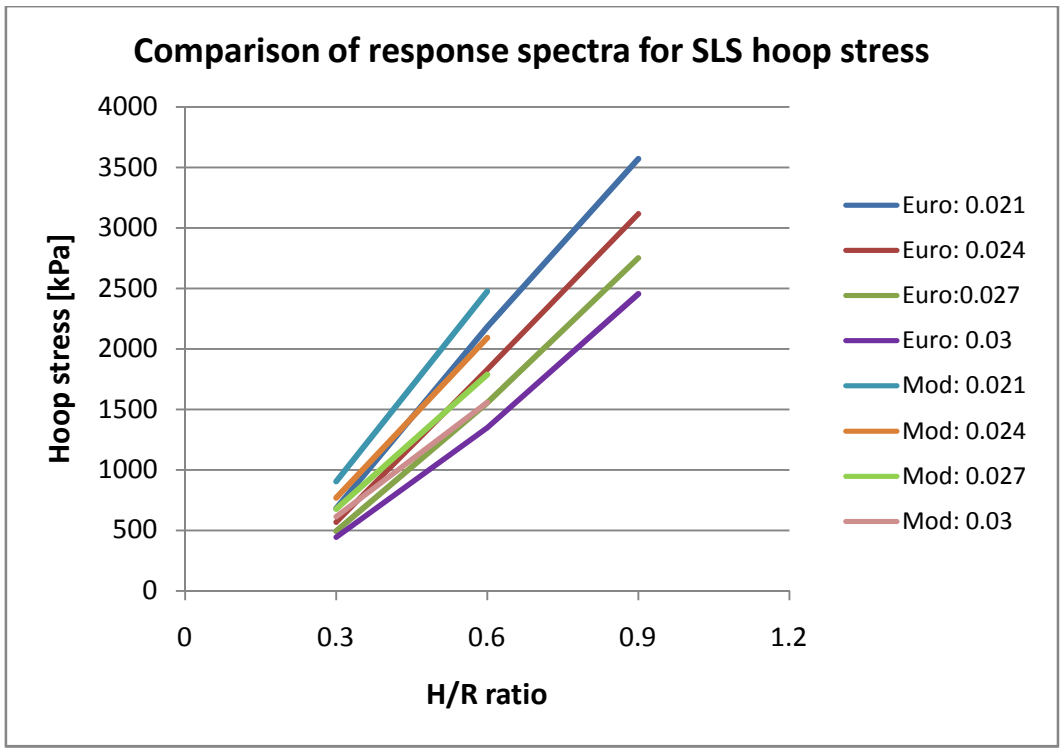

Figure 9.21: Influence of modified response spectrum on the hoop stress for SLS (PGA=0.15g)

As shown in Figure 9.21 the hoop stress increases with the use of the modified response spectrum since the pseudoacceleration experienced by the structure is increased. The change in the hoop stress ratio between dynamic and static results for the serviceability limit state is provided in Figure 9.22. The dynamic results were computed as the sum of the seismic and static response with inclusion of the partial load factors. The static results were obtained with the method by Ghali (1979). For clarity purposes only the t_w/R ratios between 0.021 and 0.03 are presented.

Figure 9.22: Change in SLS hoop stress with the modified response spectrum (PGA=0.15g)

The ratio between the dynamic and static hoop stress significantly increases with the use of the modified response spectrum. As indicated in the previous section, the hoop stress obtained for the serviceability limit state governs the design of water-retaining structures for seismic excitation. Hence, the results obtained with the use of the response spectrum provided in Eurocode 8: Part 1 (2004) may be unconservative since the hoop stress and the hoop stress ratio between dynamic and static results increase significantly with the use of the modified response spectrum.

The accuracy of each of the three FE models with regard to the numerical method by Veletsos (1997) has been discussed in this section. The influence of seismic excitation on a water-retaining structure with regard to the bending moment and hoop stress in the wall and the required reinforcement has also been presented. The consideration of either the serviceability or ultimate limit state for design purposes has been discussed in detail in this chapter.

In the following chapter the most important results are summarized and conclusions drawn with regard to the design of water-retaining structures in South Africa for seismic activity. Recommendations will also be provided in terms of future research work.

10. CONCLUSIONS AND RECOMMENDATIONS

The aims of this project along with an outline of the parametric study are presented in this chapter. A brief summary of the three numerical methods that were used for the analysis of a water-retaining structure, for both static and seismic loads, is presented. Three FE models were investigated in this project and these are summarized in this chapter. The results as obtained in Chapter 8 and Chapter 9 are presented briefly from which conclusion will be drawn. Finally recommendations in terms of this project and future research are presented.

Water-retaining structures in South Africa are often only designed to resist static loading. However, seismic activity does occur within the Western Cape province of South Africa and for this reason the influence of seismic activity on water-retaining structures for South African conditions was investigated. Four different aspects of the seismic design of water-retaining structures were considered in this study. Firstly, the effect of seismic loads on a water-retaining structure for a peak ground acceleration of 0.15g was investigated to determine whether seismic loads are indeed a critical load case for the design of these structures. Secondly, in the event of the seismic loads being a critical load case, the question arose of whether the ultimate limit state or the serviceability limit state would govern the design of water-retaining structures. This was further investigated in this project. The third aim of this project was to assess the accuracy of a simplified numerical method by Veletsos (1997) with regard to the method by Eurocode 8: Part 4 (2006). Finally, the last aim of this project consisted of the assessment of the accuracy of different FE models for the analysis of a water-retaining structure with consideration of seismic activity.

With the various aims of this project in mind, the scope of the parametric study was defined in order to include the parameters generally used in the South African practice and the information provided by the methods of analysis. The parametric study, within which the parameters of all structures in this project were varied, consisted of the following:

- The H/R [Height/Radius] ratio was varied between 0.3 and 1.5 in steps of 0.3.
- The t_w/R [wall thickness/Radius] ratio was between 0.006 and 0.03 in steps of 0.003.
- The peak ground acceleration was varied between 0.15g and 0.35g in steps of 0.1g.

In order to achieve these aims, three numerical methods of analysis were used in this project. These are summarized as follows:

- The method presented by Ghali (1979) was used in all instances for the static analysis of a water-retaining structure.
- The method presented by Veletsos (1997) was primarily used to determine the effect of seismic loading on a water-retaining structure.
- The method presented by Eurocode 8: Part 4 (2006) was only used to verify some of the results obtained with the method by Veletsos (1997).

The method presented by Veletsos (1997) for the seismic analysis of a water-retaining structure was primarily used since it is a simplified method and easier to apply than the method presented in Eurocode 8: Part 4 (2006).

Three different finite element models were investigated in this study for the consideration of seismic loading on water-retaining structures. The models investigated were simplified models since the aim of this project was to propose a FE model which could be used in an engineering design office. The three FE models investigated were:

- The equally-distributed (ED-m_i) model as proposed by Nachtigall (2003). In this model the impulsive liquid mass is uniformly distributed among the nodes on the tank wall and fixed directly to their respective nodes.
- The pressure-distributed (PD-m_i) model as proposed by the supervisor and student of this study. The impulsive liquid mass is distributed along the height of the tank wall in the same manner as the impulsive pressure. However, the lumped masses do not vary along the circumference of the tank wall, but are kept constant. The lumped masses are directly fixed to their respective nodes on the tank wall.
- The Virella model as proposed by Virella (2006). The impulsive mass is distributed along the height of the tank wall in the same manner as the impulsive pressure but is kept constant along the circumference of the tank wall. The lumped impulsive masses are not fixed directly to the nodes on the tank wall but are rather fixed to their respective nodes with pinned links.

Results were obtained with the use of the three numerical methods and the three FE models as discussed in Chapter 8 and Chapter 9. A brief summary of the results are presented in this chapter. It should be kept in mind that these results are specific to Class IV structures with a

radius of 10 meters that were considered to have a flexible wall. The global results obtained were:

- In all instances the impulsive pressure in flexible tanks differs by 20% or more from the impulsive pressure in rigid tanks. It is therefore unconservative to consider concrete water-retaining structures as rigid.
- The numerical methods by Veletsos (1997) and Eurocode 8: Part 4 (2006) differ slightly in the results obtained for the fundamental frequency of the structure as well as the base shear force.
- The fundamental frequency of each flexible structure in the parametric study was determined. The fundamental frequency determined with the Virella (2006) FE model compared well to the method by Veletsos (1997) for structures with an H/R ratio≥0.47. This FE model also provided results consistent with the results obtained using the method by Veletsos (1997) for structures with a H/R ratio≥0.47 in terms of the base shear force and the overturning moment.
- The fundamental frequency determined with the equally-distributed (ED-m_i) mass model compared well to the method by Veletsos (1997) for all structures in the parametric study. The base shear force and overturning moment results obtained with this FE model differed from the method by Veletsos (1997) with more than 10% in all instances.
- The pressure-distributed (PD-m_i) mass model did not provide accurate results for the fundamental frequency in comparison to the method by Veletsos (1997). This model also differed from the method by Veletsos (1997) in terms of the base shear force and the overturning moment.

Only the Virella (2006) FE model was further used for the determination of the local results. The local results can be summarized as follows:

- Bending about a vertical axis during seismic excitation of a water-retaining structure may be neglected since the cracking moment is significantly larger than the results obtained.
- Bending about a horizontal axis may not be neglected since the results obtained using the FE model by Virella (2006) were significantly greater than the cracking moment. The ratio of the dynamic to static bending moment increases as the t_w/R ratio increases. However, the ratio of dynamic to static bending moment decreases

as the H/R ratio increases. Significant differences were obtained for structures with a H/R ratio smaller than 0.6.

- This is also the case with consideration of the hoop stress in the wall resulting from seismic excitation.
- As expected, the influence of seismic activity on a water-retaining structure increases as the peak ground acceleration increases in terms of the bending moment and the hoop stress in the tank wall. Concrete water-retaining structures in South Africa needs to be design for seismic loading and the influence of seismic activity on these structures can not be neglected.

The area of reinforcement was calculated for dynamic and static loading conditions. These results can be summarized as:

- The minimum area of reinforcement as prescribed in SABS 0100-1 (2000) is required in most structures when considering bending about a horizontal axis for both the ultimate and serviceability limit states.
- The ratio of reinforcement required for the dynamic hoop stress to the static hoop stress remains constant with variance of the H/R ratio except for H/R ratios smaller than 0.6. This was observed for both the ultimate and the serviceability limit states.
- The ratio of reinforcement required for the ultimate limit state increases as the peak ground acceleration increases.
- The ratio of reinforcement required for the serviceability limit state to the ultimate limit state decreases as the peak ground acceleration increases. The highest ratio of serviceability to ultimate limit state reinforcement was obtained for a peak ground acceleration of 0.15g.

With these results in mind, the following conclusions may be drawn:

- The numerical method by Veletsos (1997) corresponds well with the method by Eurocode 8: Part 4 (2006) in terms of the fundamental frequency and base shear force. The use of the method by Veletsos (1997) is suggested for practical use since it provides accurate results and is easier to use than the method by Eurocode 8: Part 4 (2006).
- Only the finite element model proposed by Virella (2006) provides results comparable to that of Veletsos (2006). This model is relatively simple and can be used with ease. However, significant differences in results were obtained for

structures with a H/R ratio less than 0.47 which suggests that the cantilever mode shape as assumed by Veletsos (1997) becomes inaccurate for very broad tanks.

- The fundamental mode shape of a water-retaining structure subjected to horizontal seismic excitation is a bending mode which tends to a cantilever beam mode for structures with an H/R ratio greater than 0.6.
- The difference in results obtained for the dynamic and static results suggests that the design of water-retaining structures for seismic loading is a critical load case. In all instances the serviceability limit state governed the design of water-retaining structure subjected to horizontal seismic excitation.

It is recommended that an alternative numerical method be used for the analysis of very broad structures. All literature consulted during the course of this project provided information based on the assumption of a cantilever beam mode shape for the fundamental mode of vibration. However, this assumption becomes inaccurate for structures with a low H/R ratio since the fundamental mode shape is not similar to that of a cantilever beam mode shape.

In this study, only Class IV structures with a radius of 10 meters were investigated. The scope of the parametric study was also limited to structures with a H/R ratio of 1.5 since membrane behaviour is exhibited in structures with H/R ratios greater than 1.5. It is recommended that structures with a H/R ratio greater than 1.5 be investigated.

Only the influence of seismic excitation on circular cylindrical structures was investigated in this study. However, rectangular and square water-retaining structures are also commonly used in South Africa. It is recommended that the influence of seismic excitation on these structures should also be investigated.

REFERENCES

Barton, D.C. & Parker J.V. 1987. Finite element analysis of the seismic response of anchored and unanchored liquid storage tanks. *Earthquake Engineering and Structural Dynamics*, 15(3): 299-322

British Standard BS 8007. 1987. *British Standard Code of practice for design of concrete structures for retaining aqueous liquids*. British Standard Institution (BSI)

British standard BS EN 1998-4. 2006. *Eurocode 8: Design of structures for earthquake resistance – Part 4: Silos, tanks and pipelines*. British Standard Institution (BSI)

Cook, R.D., Malkus, D.S., Plesha, M.E., Witt, R.J. 2002. *Concepts and applications of finite element analysis.* United States: Publication Services, Inc.

Dazio, A. 2009. Short course: Seismic design of building structures. Unpublished class notes. Stellenbosch: University of Stellenbosch

European Standard EN 1998-1. 2004. *Eurocode 8: Design of structures for earthquake resistance – Part 1: General rules, seismic actions and rules for buildings*. European Committee for Standardization (CEN)

European Standard EN 1991-4. 2006. *Eurocode 1: Actions on structures – Part 4: Silos and tanks*. European Committee for Standardization (CEN)

Fardis, M.N., Carvalho, E., Elnashai, A., Faccioli, E., Pinto, P., Plumier, A. 2005. *Designers' Guide to EN 1998-1 and EN 1998-5*. London: Thomas Telford Publishing

Fischer, F.D. & Rammerstorfer, F.G. 1999. A refined analysis of sloshing effects in seismically excited tanks. *International Journal of Pressure Vessels and Piping*, 76: 693-709

Ghali, A. 1979. *Circular storage tanks and silos*. London: E. & F.N. Spon Limited

Haroun, M.A. 1980. Dynamic analyses of liquid storage tanks. *California Institute of Technology: Earthquake Engineering research laboratory.* Pasadena, California

Haroun, M.A. & Housner, G.W. 1981. Earthquake response of deformable liquid storage tanks. *Journal of Applied Mechanics*, 48(2): 411-418

Hibbit, H.D., Karlsson, B.I., Sorensen, P. 2002. ABAQUS manual. Version 6.4. Rhode Island: Hibbit. Karlsson and Sorensen, Inc.

Housner, G.W. 1963. The dynamic behaviour of water tanks. *Bulletin of the Seismological Society of America*, 53(2): 381-389

Malhotra, P. & Veletsos, A.S. 1994. Uplifting response of unanchored liquid storage tanks. *Journal of Structural Engineering*, 120(12): 3525-3547

Nachtigall, I., Gebbeken, N., Urrutia-Galicia, J.L. 2003. On the analysis of vertical circular cylindrical tanks under earthquake excitation at its base. *Engineering Structure*, 25: 201-213

SABS 0100-1. 2000. *The structural use of concrete – Part 1: Design*. The South African Bureau of Standards

SANS 10160. 2009. *Basis of structural design and actions for buildings and industrial structures, Part 2: Self-weight and imposed loads*. The South African Bureau of Standards

STRAND7 software. API release 2.3. Edition 6a. Sydney, Australia. STRAND7 Pty Ltd. 2005

Van Dalsen, H. 2009. Corresponde by Prof J.A Wium. 13 Augustus 2009. Stellenbosch

Veletsos, A.S. & Shivakumar, P. 1997. Chapter 15: Tanks containing liquids or solids, in Dimitri, E.K. & Anagnostopoulos, S.A. (eds.). *Computer Analysis and Design of Earthquake Resistant Structures*. Houston, Texas: WIT Press. 726-774

Veletsos, A.S. & Yang, J.Y. 1977. Earthquake response of liquid storage tanks – advances in civil engineering through mechanics. *Proceedings of the second engineering mechanics specialty conference,* ASCE: 1-24

Virella, J.C., Godoy, L.A., Suarez, L.E. 2006. Fundamental modes of tank-liquid systems under horizontal motions. *Engineering Structures*, 28: 1450-1461

APPENDIX A:

NUMERICAL EXAMPLE ACCORDING TO A.S. VELETSOS (1997)

TANKS CONTAINING LIQUIDS OR SOLIDS: A.S. VELETSOS
RIGIDLY SUPPORTED FLEXIBLE TANKS

SYSTEM CONSIDERED:

Veletsos page 727

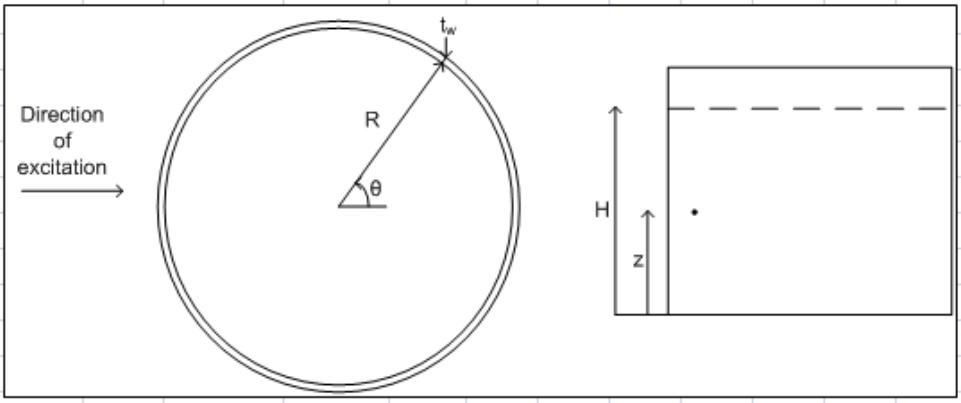

PARAMETERS:

Liquid density:	ρ=	1000	kg/m^3	
Liquid level :	H=	9	m	
Radius of tank:	R=	10	m	
Tank wall thickness:	t_w=	240	mm	
Density of tank material:	ρ_w=	2500	kg/m^3	
Strand7 Young's modulus for tank:	E_w=	34.29	GPa	(40 MPa)
Veletsos Ground acceleration:	a_g=	0.15	g	
page 731 Bessel function:	λ_1=	1.841		
Gravity acceleration:	g=	9.81	m/s^2	
Max pressure angle:	θ=	0	degrees	
Importance class:		IV		

HYDROSTATIC CONDITION:

Pressure distribution: $p(z) = \rho g(H-z)$ [kN/m^2]

with z= variance in liquid height (0→H)

Height z [m]:	9.00	8.10	7.20	6.30	5.40	4.50	3.60	2.70	1.80	0.90	0.00
Pressure p(z):	0.00	8.83	17.66	26.49	35.32	44.15	52.97	61.80	70.63	79.46	88.29

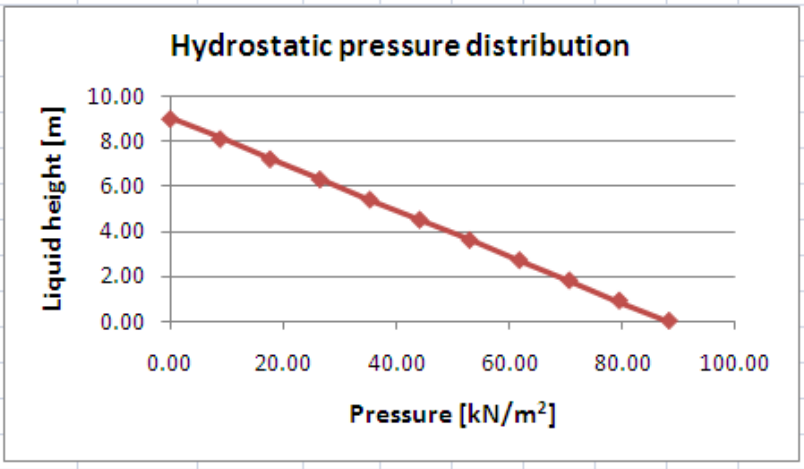

	1. NATURAL FREQUENCY:						
Veletsos	**1.1 IMPULSIVE FREQUENCY AND PERIOD:**						
Table 2	Poisson's ratio:			ν_w=	0.17	(concrete tank)	
	Reference density ratio:			ρ/ρ_w=	0.4	(DensityWater/DensityConcrete)	
	Reference dimensions:			t_w/R=	0.01		
				H/R=	0.90		
	FIRST MODE OF VIBRATION:						
Table 2	Reference C_{i1}:		$(C_{i1})_r$=	0.158			
Page 742	System C_{i1}:		$C_{i1} = (C_{i1})_r \sqrt{\frac{t_w/R}{(t_w/R)_r} \frac{(\rho/\rho_w)_r}{\rho/\rho_w}}$				
			C_{i1}=	0.244			
Page 741	Impulsive frequency:		$f_{i1} = \frac{1}{2\pi} \frac{C_{i1}}{H} \sqrt{\frac{E_w}{\rho_w}}$				f_{i1}=
			f_{i1}=	16.0	Hz		16.01
							Hz
	Impulsive period:		T_{i1}=	$1/f_{i1}$			T_{i1}=
			T_{i1}=	0.062	s		0.062
							s
	Natural frequency:		ω_{n1}=	$2\pi f_{i1}$			ω_{n1}=
			ω_{n1}=	100.6	rad/s		100.60
							rad/s
	1.2 SLOSHING FREQUENCY AND PERIOD:						
page 732	FIRST MODE OF VIBRATION:						
	Sloshing frequency:						
			$f_{c1} = \frac{1}{2\pi} \sqrt{\lambda_1 \frac{g}{R} \tanh[\lambda_1 (\frac{H}{R})]}$				f_{c1}=
			f_{c1}=	0.206	Hz		0.206
							Hz
	Sloshing period:		T_{c1}=	$1/f_{c1}$			T_{c1}=
			T_{c1}=	4.849	s		4.849
							s
	Natural frequency:		ω_{c1}=	$2\pi f_{c1}$			ω_{c1}=
			ω_{c1}=	1.296	rad/s		1.296
							rad/s
	2. DESIGN SPECTRUM FOR IMPULSIVE COMPONENT:						
EN 1998-1:	Ground type:	A					
Table 3.1							
3.2.2.2	Type:	1	elastic response spectra				
Table 3.2	S=	1					
/Table 3.3	T_B(s)=	0.15					
	T_C(s)=	0.4					
	T_D(s)=	2					

EN 1998-4:	**2.1 ULTIMATE LIMIT STATE:**											
4.4	Behaviour factor:			q=	1.5							
2.1.4	Importance factor:			γ_I=	1.6							
EN 1998-1:	Lower bound factor:			β=	0.2							
3.2.2.2	Peak ground acceleration			a_g=	$\gamma_1 a_g$							
				a_g=	0.24	g						
	FIRST MODE OF VIBRATIO											
EN 1998-1:	Design spectrum for elastic analysis:											
3.2.2.5	0≤T≤T_B:	$S_d(T) = a_g S[\frac{2}{3} + \frac{T}{T_B}(\frac{2.5}{q} - \frac{2}{3})]$										
		S_d(T)=	0.260	g								
	Pseudoacceleration:			S_{Ai1}=	S_d(T)							S_{Ai1}=
				S_{Ai1}=	0.260	g						0.260
												g
EN 1998-4:	**2.2 SERVICEABILITY LIMIT STATE:**											
2.3.3.1	Viscous damping ratio:				ξ=	5	%					
	Importance factor:				γ_I=	1.6						
	Peak ground acceleration:				a_g=	0.24	g					
2.2	Reduction factor:				ν=	0.4						
EN 1998-1:												
3.2.2.2	Damping correction factor:				$\eta = \sqrt{10/(5+\varepsilon)}$			≥0.55				
					η=	1.00						
		therefore			η=	1.00						
	FIRST MODE OF VIBRATION:											
	Design spectrum for elastic analysis:											
3.2.2.2	0≤T≤T_B:	$S_e(T) = a_g S[1 + \frac{T}{T_B}(\eta 2.5 - 1)]$										
		S_e(T)=	0.390	g								
	Pseudoacceleration:			S_{Ai1}=	νS_e(T)							S_{Ai1}=
				S_{Ai1}=	0.156	g						0.156
												g
	3. DESIGN SPECTRUM FOR CONVECTIVE COMPONENT:											
	Ground type:	A										
	Type:	1	elastic response spectra									
	S=	1										
	T_B(s)=	0.15										
	T_C(s)=	0.4										
	T_D(s)=	2										

	3.1 ULTIMATE LIMIT STATE:										
	Viscous damping ratio:		ξ= 5	%							
	Importance factor:		Y_I= 1.6								
	Peak ground acceleration:		a_g= 0.24	g							
	Damping correction factor:		$\eta = \sqrt{10/(5+\varepsilon)}$			≥0.55					
			η= 1								
	therefore		η= 1								
EN 1998-1:	Horizontal elastic response spectrum:										
3.2.2.2	Minimum value for $S_e(T)$ if T=4s.										
		$S_e(T) = a_g S \eta 2.5 [\frac{T_C T_D}{T^2}]$									
		S_e(T)= 0.030	g								
	FIRST MODE OF VIBRATION:										
3.2.2.2	T_{c1}>4s:										
	Pseudoacceleration:	S_{Ac1}= S_e(T)									S_{AC1}=
		S_{Ac1}= 0.030	g								0.030
											g
	3.2 SERVICEABILITY LIMIT STATE:										
	Viscous damping ratio:		ξ= 5	%							
	Importance factor:		Y_I= 1.6								
	Peak ground acceleration:		a_g= 0.24	g							
	Reduction factor:		v= 0.4								
	Damping correction factor:		$\eta = \sqrt{10/(5+\varepsilon)}$			≥0.55					
			η= 1.000								
	therefore		η= 1.000								
	Horizontal elastic response spectrum:										
	Minimum value for $S_e(T)$ if T=4s.										
		$S_e(T) = a_g S \eta 2.5 [\frac{T_C T_D}{T^2}]$									
		S_e(T)= 0.030	g								
	FIRST MODE OF VIBRATION:										
	T_{c1}>4s:										
	Pseudoacceleration:	S_{Ac1}= vS_e(T)									S_{AC1}=
		S_{Ac1}= 0.012	g								0.012
											g

4. HYDRODYNAMIC WALL PRESSURES:

Veletsos page 731

4.1 ULTIMATE LIMIT STATE:

Dimensionless functions:

$$c_{c1}(\eta) = \frac{2}{\lambda_1^2 - 1} \frac{\cosh[\lambda_1(\frac{H}{R})\eta]}{\cosh[\lambda_1(\frac{H}{R})]}$$

$c_i(\eta)+c_{c1}(\eta)= 1$

with $\eta = z/H$

Maximum pressure at $\theta=0^\circ$:

Height:	$c_{c1}(\eta)$	$c_{i1}(\eta)$	p_i	p_c	p_{max}
[m]			[kN/m^2]		
9.00	0.84	0.16	4.15	2.46	6.62
8.55	0.78	0.22	5.73	2.28	8.01
8.10	0.72	0.28	7.16	2.12	9.28
7.65	0.67	0.33	8.48	1.96	10.44
7.20	0.62	0.38	9.67	1.83	11.50
6.75	0.58	0.42	10.76	1.70	12.46
6.30	0.54	0.46	11.74	1.59	13.33
5.85	0.50	0.50	12.63	1.49	14.11
5.40	0.47	0.53	13.43	1.39	14.82
4.95	0.45	0.55	14.15	1.31	15.46
4.50	0.42	0.58	14.79	1.24	16.03
4.05	0.40	0.60	15.36	1.17	16.53
3.60	0.38	0.62	15.85	1.11	16.97
3.15	0.36	0.64	16.28	1.06	17.35
2.70	0.35	0.65	16.65	1.02	17.67
2.25	0.33	0.67	16.96	0.99	17.95
1.80	0.33	0.67	17.21	0.96	18.16
1.35	0.32	0.68	17.40	0.93	18.33
0.90	0.31	0.69	17.54	0.92	18.45
0.45	0.31	0.69	17.62	0.91	18.53
0.00	0.31	0.69	17.64	0.91	18.55

Impulsive component:

page 743

$p_i(\eta,\theta,t)= c_{i1}(\eta)S_{Ai1}\rho R\cos\theta$

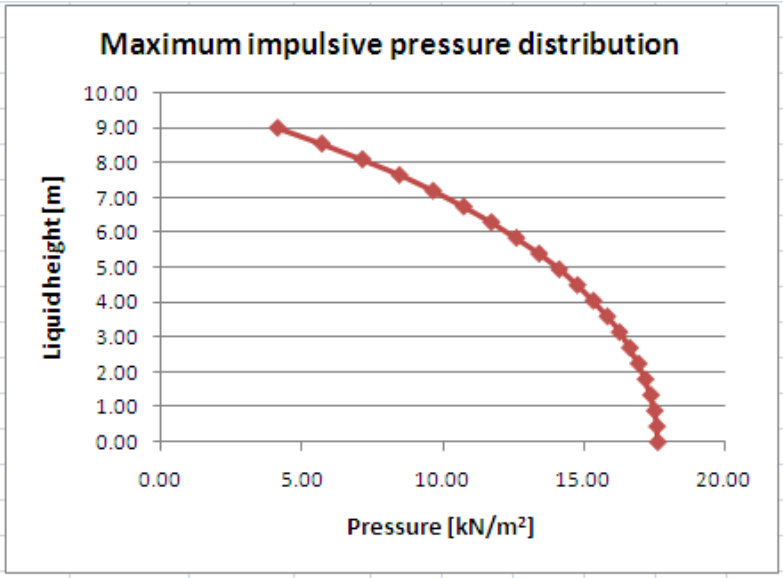

Convective component:

page 730 $p_c(\eta,\theta,t) = c_{c1}(\eta) S_{Ac1} \rho R \cos\theta$

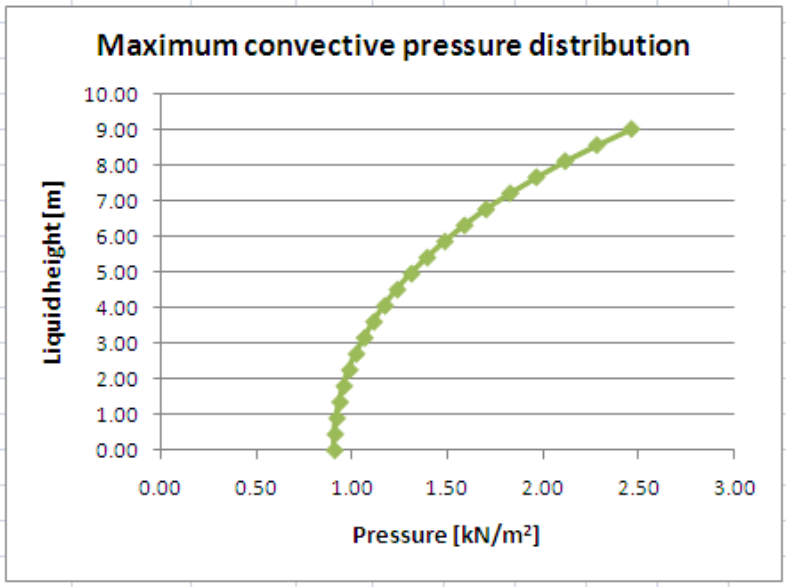

Maximum hydrodynamic wall pressure:

page 730 $p_{max}(\eta,\theta,t) = p_i(\eta,\theta,t) + p_c(\eta,\theta,t)$

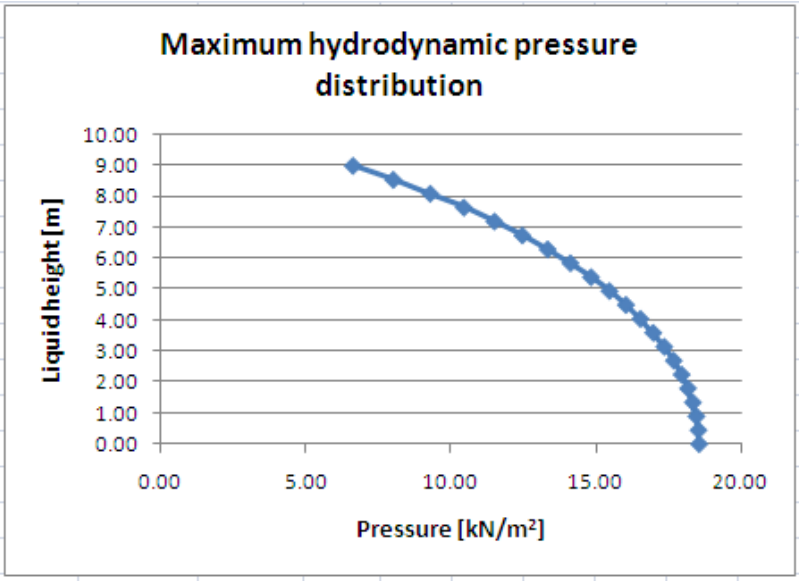

4.2 SERVICEABILITY LIMIT STATE:

Dimensionless functions:

$$c_{c1}(\eta) = \frac{2}{\lambda_1^2 - 1} \frac{\cosh[\lambda_1 (\frac{H}{R}) \eta]}{\cosh[\lambda_1 (\frac{H}{R})]}$$

$c_i(\eta)+c_{c1}(\eta)=$ 1

with $\eta=$ z/H

Maximum pressure at $\theta=0^\circ$:

Height:	$c_{c1}(\eta)$	$c_{i1}(\eta)$	p_i	p_c	p_{max}
[m]			[kN/m²]		
9.00	0.84	0.16	2.49	0.99	3.48
8.55	0.78	0.22	3.44	0.91	4.35
8.10	0.72	0.28	4.30	0.85	5.15
7.65	0.67	0.33	5.09	0.79	5.87
7.20	0.62	0.38	5.80	0.73	6.53
6.75	0.58	0.42	6.45	0.68	7.13
6.30	0.54	0.46	7.04	0.64	7.68
5.85	0.50	0.50	7.58	0.59	8.17
5.40	0.47	0.53	8.06	0.56	8.62
4.95	0.45	0.55	8.49	0.52	9.01
4.50	0.42	0.58	8.87	0.49	9.37
4.05	0.40	0.60	9.21	0.47	9.68
3.60	0.38	0.62	9.51	0.45	9.96
3.15	0.36	0.64	9.77	0.43	10.20
2.70	0.35	0.65	9.99	0.41	10.40
2.25	0.33	0.67	10.18	0.39	10.57
1.80	0.33	0.67	10.32	0.38	10.71
1.35	0.32	0.68	10.44	0.37	10.81
0.90	0.31	0.69	10.52	0.37	10.89
0.45	0.31	0.69	10.57	0.36	10.93
0.00	0.31	0.69	10.59	0.36	10.95

Impulsive component:

$p_i(\eta,\theta,t) = c_{i1}(\eta) S_{Ai1} \rho R \cos\theta$

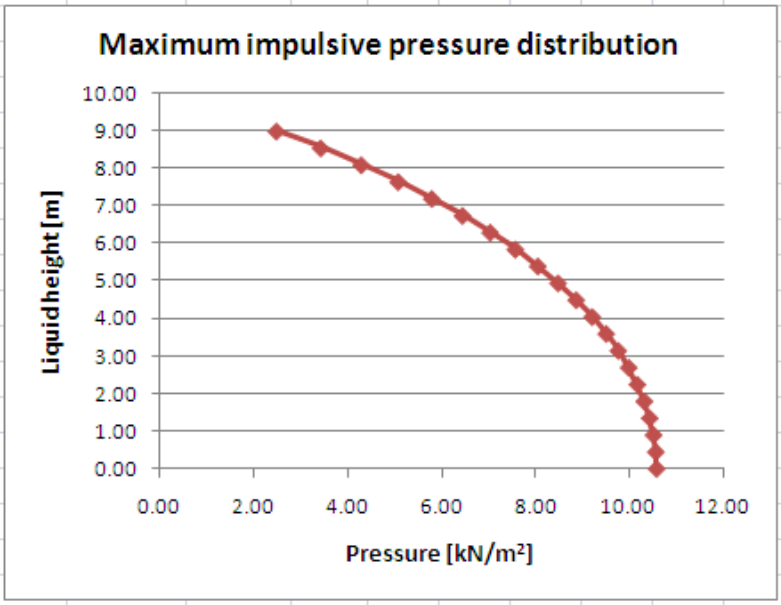

Convective component:

$p_c(\eta,\theta,t) = c_{c1}(\eta) S_{Ac1} \rho R \cos\theta$

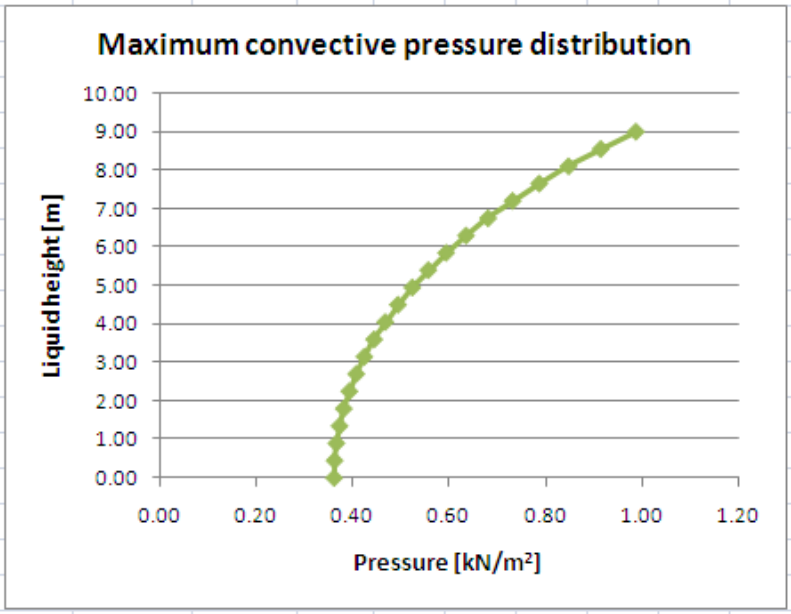

Maximum hydrodynamic wall pressure:

$p_{max}(\eta,\theta,t) = p_i(\eta,\theta,t) + p_c(\eta,\theta,t)$

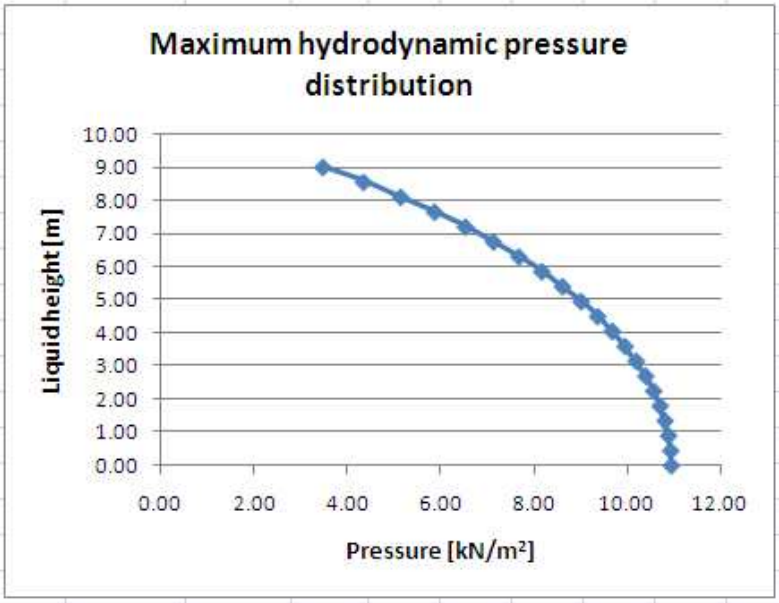

5. TOTAL WALL PRESSURE:

5.1 Ultimate limit state:

Height [m] :	9.00	8.10	7.20	6.30	5.40	4.50	3.60	2.70	1.80	0.90	0.00
p_{max} [kN/m^2]:	6.62	18.11	29.15	39.81	50.14	60.17	69.94	79.48	88.80	97.92	106.84

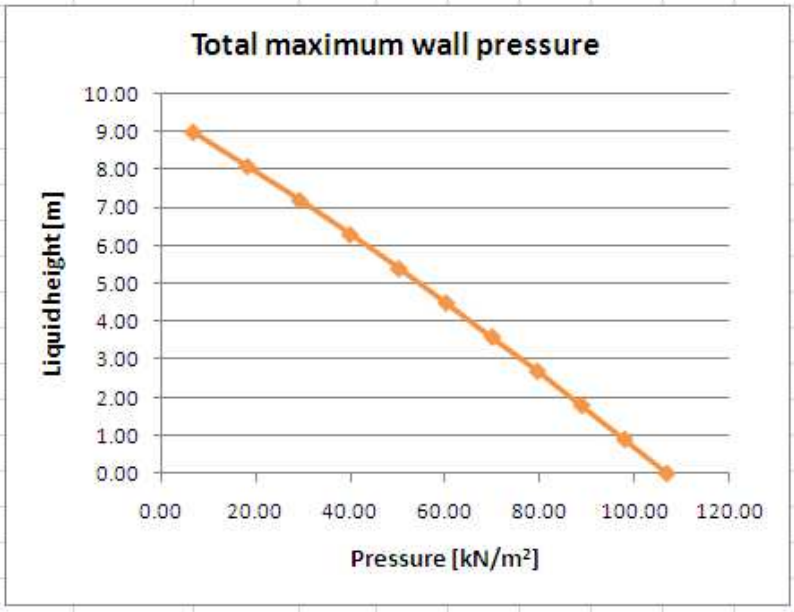

5.2 Serviceability limit sta

Height [m] :	9.00	8.10	7.20	6.30	5.40	4.50	3.60	2.70	1.80	0.90	0.00
p_{max} [kN/m^2]:	3.48	13.97	24.19	34.17	43.93	53.51	62.93	72.20	81.34	90.35	99.24

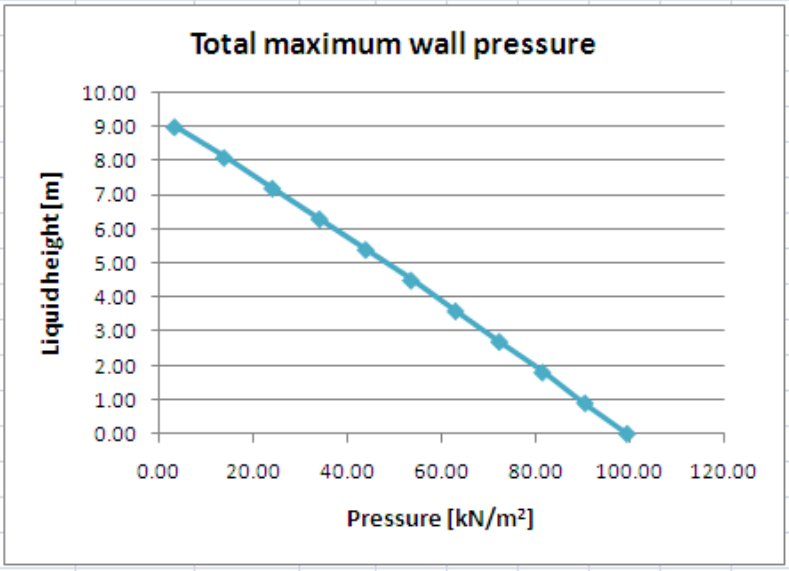

6. TOTAL WALL FORCE OR BASE SHEAR:

Total liquid mass:

$m = \pi R^2 H \rho$

m= 2827433.4 kg

m= 2827433 kg

Veletsos page 737

Convective mass:

$$m_{c1} = \left(\frac{2}{\lambda_1(\lambda_1^2 - 1)\left(\frac{H}{R}\right)} \tanh\left[\lambda_1\left(\frac{H}{R}\right)\right]\right) m$$

m_{c1}= 1328152 kg

Impulsive mass:

page 747

$$\sum_{j=1}^{\infty} m_{ij} = m_i + m_w$$

m_{i1}= 1475072 kg

$m_w = \pi R^2 H \rho_w$

m_w= 343363.5 kg

m_i= 1131708 kg

6.1 ULTIMATE LIMIT STATE:

page 750

Base shear:

$$Q_b(t) = m_{i1} A_{i1}(t) + m_{c1} A_{c1}(t)$$

Maximum total base shear for impulsive component:

$Q_{max} = m_{i1} S_{Ai1}$

Q_{max}= 3761.4 kN

Q_{max}= 3761.37 kN

6.2 SERVICEABILITY LIMIT STATE:

page 750 Base shear:

$$Q_b(t) = m_{i1}A_{i1}(t) + m_{c1}A_{c1}(t)$$

Maximum total base shear for impulsive component:

$$Q_{max} = m_{i1}S_{Ai1}$$

Q_{max}= 2256.8 kN

Q_{max}= 2256.82 kN

7. BASE AND FOUNDATION MOMENT:

page 738 Height at which convective mass is concentrated:

$$h_{c1} = \{1 - \frac{1}{\lambda_1(\frac{H}{R})}\tanh(\frac{\lambda_1 H}{2R})\}H$$

h_{c1}= 5.31 m

Height at which impulsive mass is concentrated:

page 738

$$m_i h_i + m_{c1}h_{c1} = m\frac{H}{2}$$

h_i= 5.01 m

$$\sum_{j=1}^{\infty} m_{ij}h_{ij} = m_i h_i + m_w \frac{H_w}{2}$$

$m_{i1}h_{i1}$= 7218365 kg.m

7.1 ULTIMATE LIMIT STATE:

page 750 Hydrodynamic overturning moment above base:

$$M_b(t) = m_{i1}h_{i1}A_{i1}(t) + m_{c1}h_{c1}A_{c1}(t)$$

Maximum total hydrodynamic overturning moment above base for impulsive component:

$$M_{max} = m_{i1}h_{i1}S_{Ai1}$$

M_{max}= 18406.5 kN.m

M_{max}= 18406.53 kN.m

7.2 SERVICEABILITY LIMIT STATE:

page 750 Hydrodynamic overturning moment above base:

$$M_b(t) = m_{i1}h_{i1}A_{i1}(t) + \sum_{n=1}^{\infty} m_{cn}h_{cn}A_{cn}(t)$$

Maximum total hydrodynamic overturning moment above base for impulsive component:

$$M_{max} = m_{i1}h_{i1}S_{Ai1}$$

M_{max}= 11043.9 kN.m

M_{max}= 11043.92 kN.m

8. SURFACE DISPLACEMENT OF LIQUID:

8.1 ULTIMATE LIMIT STATE:

page 740 Slosh height:

$$d_s = R\sqrt{(0.837\frac{S_{Ac1}}{g})^2}$$

d_s=	0.25	m	d_s=
d_s=	251.1	mm	251.1
			mm

8.2 SERVICEABILITY LIMIT STATE:

$$d_s = R\sqrt{(0.837\frac{S_{Ac1}}{g})^2}$$

			d_s=
d_s=	0.10	m	100.4
d_s=	100.4	mm	mm

APPENDIX B:

NUMERICAL EXAMPLE ACCORDING TO EUROCODE 8: PART 4 (2006)

TANKS CONTAINING LIQUIDS OR SOLIDS: EN 1998-4: 2006

RIGIDLY SUPPORTED FLEXIBLE TANKS

SYSTEM CONSIDERED:

Veletsos page 728

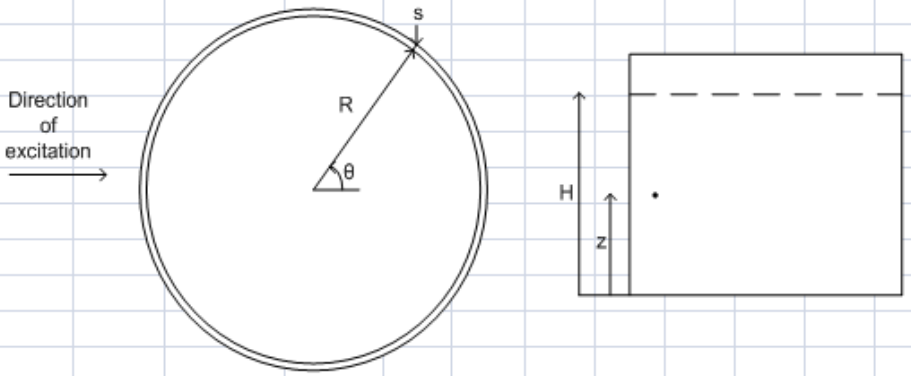

PARAMETERS:

	Height/Radius ratio:	γ=	0.9	
	Wall thickness/Radius ratio:	s/R=	0.024	
	Number of modes:	n=	1	
	Number of iterations:	n=	10	
	Liquid density:	ρ=	1000	kg/m^3
	Wall material density:	ρ_s=	2500	kg/m^3
	Elastic modulus of tank wall:	E=	34.29	GPa
	Poisson ratio of tank wall:	ν=	0.2	
	Radius of tank:	R=	10	m
	Liquid level :	H=	9	m
	Tank wall thickness:	s=	240	mm
EN 1998-4:	Ground acceleration:	a_g=	0.15	g
A.2.1.3	Roots of Bessel function:	λ_1=	1.841	
	Gravity acceleration:	g=	9.81	m/s^2
	Circumferential angle:	θ=	0	degrees
2.1.4	Importance class:		IV	

HYDROSTATIC CONDITION:

Pressure distribution: $p(z) = \rho g(H-z)$ $[kN/m^2]$

with z= variance in liquid height (0→H)

Height z [m]:	9.00	8.10	7.20	6.30	5.40	4.50	3.60	2.70	1.80	0.90	0.00
Pressure p(z):	0.00	8.83	17.66	26.49	35.32	44.15	52.97	61.80	70.63	79.46	88.29

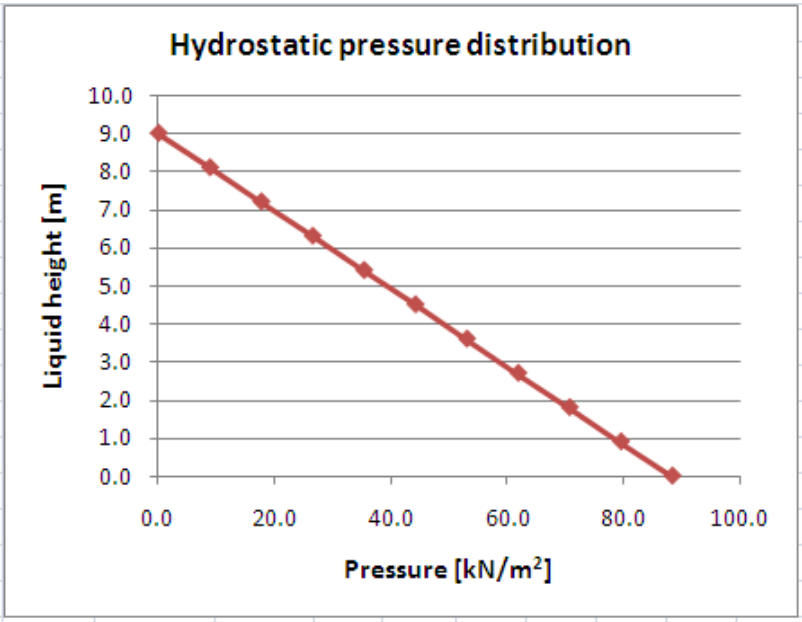

1. NATURAL FREQUENCY:

EN 1998-4: **1.1 NATURAL TANK-FLUID FREQUENCY AND PERIOD:**

A.3.2.2.1 Impulsive frequency:

$$T_{imp} = \frac{C_i\sqrt{\rho H}}{\sqrt{s/R}.\sqrt{E}}$$

T_{imp}= 0.064 s

T_{imp}= 0.064 s

f_{imp}= $1/T_{imp}$

f_{imp}= 15.5 Hz

ω_{imp}= $2\pi f_{imp}$

ω_{imp}= 97.6 rad/s

1.2 NATURAL SLOSHING FREQUENCY AND PERIOD:

FIRST MODE OF VIBRATION:

A.3.2.2.1 Convective frequency: T_{con}= $C_c\sqrt{R}$

T_{con}= 12.5 s

T_{c1}= 12.529 s

f_{con}= $1/T_{con}$

f_{con}= 0.080 Hz

ω_{con}= $2\pi f_{con}$

ω_{con}= 0.501 rad/s

2. DESIGN SPECTRUM FOR TANK-FLUID SYSTEM:

EN 1998-1: Table 3.1 Ground type: A

3.2.2.2 Type: 1 elastic response spectra

Table 3.2		S=	1											
/Table 3.3		T_B(s)=	0.15											
		T_C(s)=	0.4											
		T_D(s)=	2											
	2.1 ULTIMATE LIMIT STATE:													
EN 1998-4:	Behaviour factor:				q=	1.5								
2.3.3.1	Importance factor:				Y_I=	1.6								
2.1.4 (8)	Design ground acceleration:				a_g=	$Y_I a_{gR}$								
					a_g=	0.24	g							
3.2.2.5	0≤T≤T_B:	$S_d(T) = a_g S[\frac{2}{3} + \frac{T}{T_B}(\frac{2.5}{q} - \frac{2}{3})]$												
		S_d(T)=	0.26	g										
	Pseudoacceleration:													
		S_e=	S_d(T)											
		S_e=	0.263	g										
	2.2 SERVICEABILITY LIMIT STATE:													
4.1.3 (1)	Viscous damping ratio:				ξ=	5	%							
	Importance factor:				Y_I=	1.6								
EN 1998-4:	Design ground acceleration:				a_g=	0.24	g							
2.2 (3)	Reduction factor:				ν=	0.4								
EN 1998-1:	Damping correction factor:			$\eta = \sqrt{10/(5+\xi)}$				≥0.55						
3.2.2.2 (3)				η=	1.00									
		therefore		η=	1.00									
3.2.2.2	0≤T≤T_B:	$S_e(T) = a_g S[1 + \frac{T}{T_B}(\eta 2.5 - 1)]$												
		S_e(T)=	0.394	g										
	Pseudoacceleration:													S_e=
		S_e=	νS_e(T)											0.158
		S_e=	0.158	g										g
	3. DESIGN SPECTRUM FOR CONVECTIVE COMPONENT:													
EN 1998-1:	Ground type:	A												
Table 3.1														
3.2.2.2	Type:	1	elastic response spectra											
Table 3.2		S=	1											
/Table 3.3		T_B(s)=	0.15											
		T_C(s)=	0.4											
		T_D(s)=	2											

EN 1998-4	**3.1 ULTIMATE LIMIT STATE:**											
2.3.3.1	Viscous damping ratio:			ξ=	5	%						
2.1.4 (8)	Importance factor:			Y_I=	1.6							
	Design ground acceleration:			a_g=	$Y_1 a_{gR}$							
				a_g=	0.24	g						
EN 1998-1:	Damping correction factor:		$\eta = \sqrt{10/(5+\xi)}$				≥0.55					
3.2.2.2 (3)			η=	1.00								
		therefore	η=	1.00								
3.2.2.2	Horizontal elastic response spectrum:											
	Minimum value for $S_e(T)$ if T=4s.											
		$S_e(T) = a_g S \eta 2.5 [\frac{T_c T_D}{T^2}]$										
		$S_e(T)$=	0.030	g								
	FIRST MODE OF VIBRATION:											
	T_{c1}>4s:											
	Pseudoacceleration:		$S_e(T)$=	$S_e(T)$								S_e=
			$S_e(T)$=	0.030	g							0.030
												g
EN 1998-2:	**3.2 SERVICEABILITY LIMIT STATE:**											
4.1.3 (1)	Viscous damping ratio:			ξ=	5	%						
	Importance factor:			Y_I=	1.6							
EN 1998-4:	Design ground acceleration:			a_g=	0.24	g						
2.2 (3)	Reduction factor:			ν=	0.4							
EN 1998-1:	Damping correction factor:		$\eta = \sqrt{10/(5+\xi)}$				≥0.55					
3.2.2.2 (3)			η=	1.00								
		therefore	η=	1.00								
3.2.2.2	Horizontal elastic response spectrum:											
	Minimum value for $S_e(T)$ if T=4s.											
		$S_e(T) = a_g S \eta 2.5 [\frac{T_c T_D}{T^2}]$										
		$S_e(T)$=	0.030	g								
	FIRST MODE OF VIBRATION											
	T_{c1}>4s:											
	Pseudoacceleration:		$S_e(T)$=	ν$S_e(T)$								S_e=
			$S_e(T)$=	0.012	g							0.012
												g
	4. RIGID IMPULSIVE PRESSURE:											
EN 1998-4:	**4.1 ULTIMATE & SERVICEABILITY LIMIT STATE:**											
A2.1.2	Non-dimensional paramet		ξ=	r/R								
			ξ=	1	(r=1, measure pressure at wall)							

A2.1.2 ς= z/H

A2.1.2 $$\nu_n = \frac{(2n+1)}{2}\pi$$

Impulsive pressure:

A2.1.2 $$C_i(\xi,\varsigma) = 2\sum_{n=0}^{10} \frac{(-1)^n}{I_1'(\nu_n/\gamma)\nu_n^2}\cos(\nu_n\varsigma)I_1(\nu_n\xi/\gamma)$$

$$p_i(\xi,\varsigma,\theta,t) = C_i(\xi,\varsigma)\rho H\cos\theta A_g(t)$$

ς:	Height:	C_i	p_i
	[m]		[kN/m²]
1.0	9.00	0.768	10.172
0.9	8.10	0.768	10.173
0.8	7.20	0.768	10.174
0.7	6.30	0.768	10.174
0.6	5.40	0.768	10.175
0.5	4.50	0.768	10.175
0.4	3.60	0.768	10.176
0.3	2.70	0.768	10.176
0.2	1.80	0.768	10.176
0.1	0.90	0.768	10.176
0.0	0.00	0.768	10.176

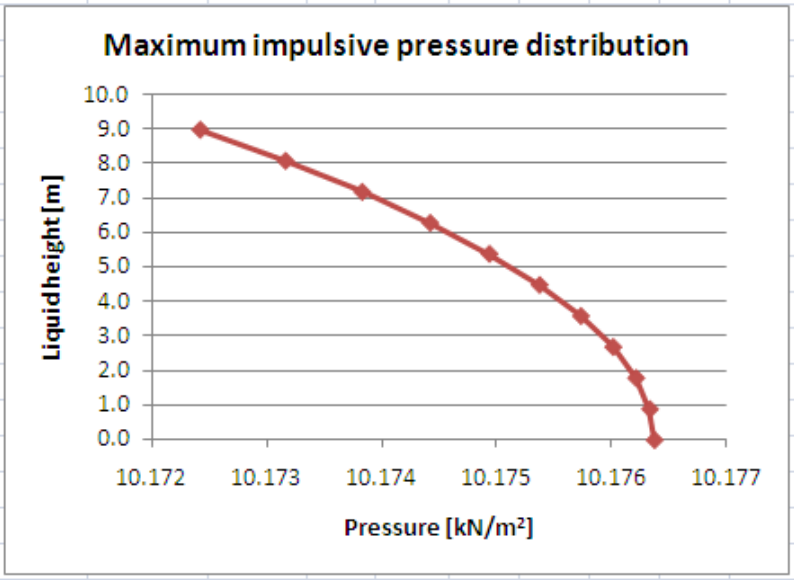

5. FLEXIBLE PRESSURE:

Trial shape:

STRAND7	ç:	Height:	Δ:
-2005	1.0	9.00	0.393
	0.9	8.10	0.382
	0.8	7.20	0.360
	0.7	6.30	0.328
	0.6	5.40	0.285
	0.5	4.50	0.233
	0.4	3.60	0.174
	0.3	2.70	0.114
	0.2	1.80	0.058
	0.1	0.90	0.016
	0.0	0.00	0.000

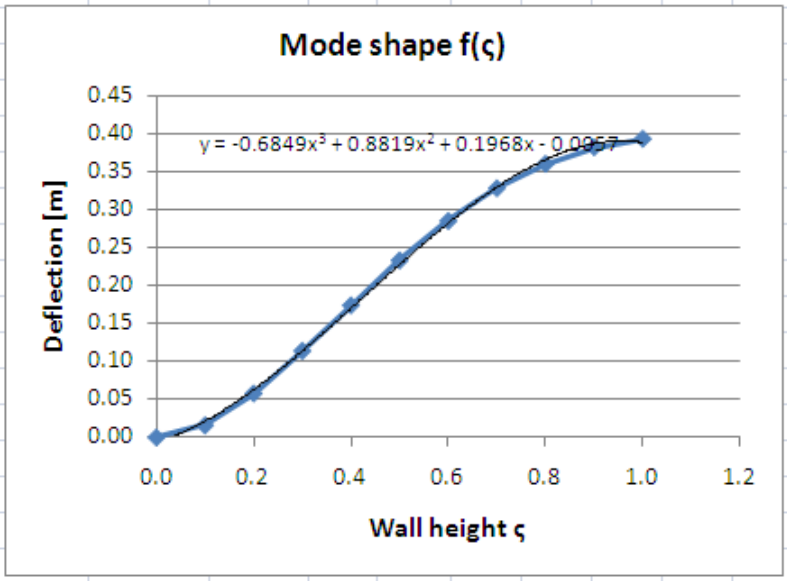

Constants:

a= -0.6849
b= 0.8819
c= 0.1968
d= -0.0057

Dimensionless parameters:

A.3.1

$$b_n' = 2\frac{(-1)^n}{\nu_n^2}\frac{I_1(\nu_n/\gamma)}{I_1'(\nu_n/\gamma)}$$

b_n'= 0.002

$$d_n = 2\frac{\int_0^1 f(\zeta)\cos(\nu_n\zeta)d\zeta}{\nu_n}\frac{I_1(\nu_n/\gamma)}{I_1'(\nu_n/\gamma)}$$

d_n= 0.118

$$\psi = \frac{\int_0^1 f(\varsigma)[\frac{\rho_s S}{\rho H} + \sum b_n' \cos(\nu_n \varsigma)]d\varsigma}{\int_0^1 f(\varsigma)[\frac{\rho_s S}{\rho H} f(\varsigma) + \sum d_n \cos(\nu_n \varsigma)]d\varsigma}$$

ψ= 0.169

5.1 ULTIMATE LIMIT STATE:

A3.1. $$p_f(\varsigma, \theta, t) = \rho H \psi \cos\theta d_n \cos(\nu_n \varsigma) A_{f1}(t)$$

ς:	Height :	p_f
	[m]	[kN/m^2]
1.0	9.00	0.387
0.9	8.10	0.401
0.8	7.20	0.414
0.7	6.30	0.425
0.6	5.40	0.434
0.5	4.50	0.443
0.4	3.60	0.450
0.3	2.70	0.455
0.2	1.80	0.459
0.1	0.90	0.461
0.0	0.00	0.462

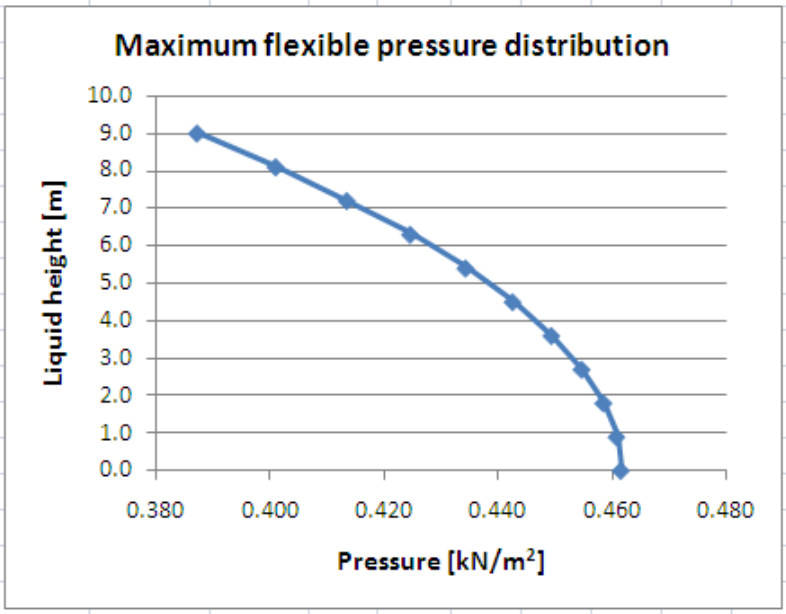

5.2 SERVICEABILITY LIMIT STATE:

A.3.1 $$p_f(\varsigma,\theta,t) = \rho H \psi \cos\theta L_x \cos(\nu_n \varsigma) A_{f1}(t)$$

ς:	Height:	p_f
	[m]	[kN/m^2]
1.0	9.00	0.232
0.9	8.10	0.241
0.8	7.20	0.248
0.7	6.30	0.255
0.6	5.40	0.261
0.5	4.50	0.266
0.4	3.60	0.270
0.3	2.70	0.273
0.2	1.80	0.275
0.1	0.90	0.277
0.0	0.00	0.277

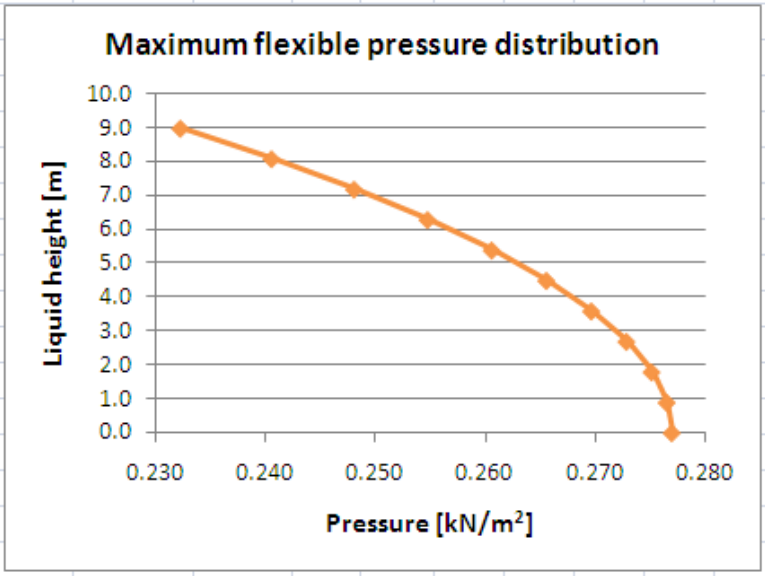

6. INERTIA OF WALL:

A2.1.5 Pressure: $p_w = \rho_s s(\varsigma)\cos\theta A_g(t)$

p_w= 0.88 kN/m^2

p_w= 0.88 kN/m^2

7. MAXIMUM HYDRODYNAMIC PRESSURE:

7.1 ULTIMATE LIMIT STATE:

Height [m] :	9.00	8.10	7.20	6.30	5.40	4.50	3.60	2.70	1.80	0.90	0.00
p_{max} [kN/m^2]:	11.44	11.46	11.47	11.48	11.49	11.50	11.51	11.51	11.52	11.52	11.52

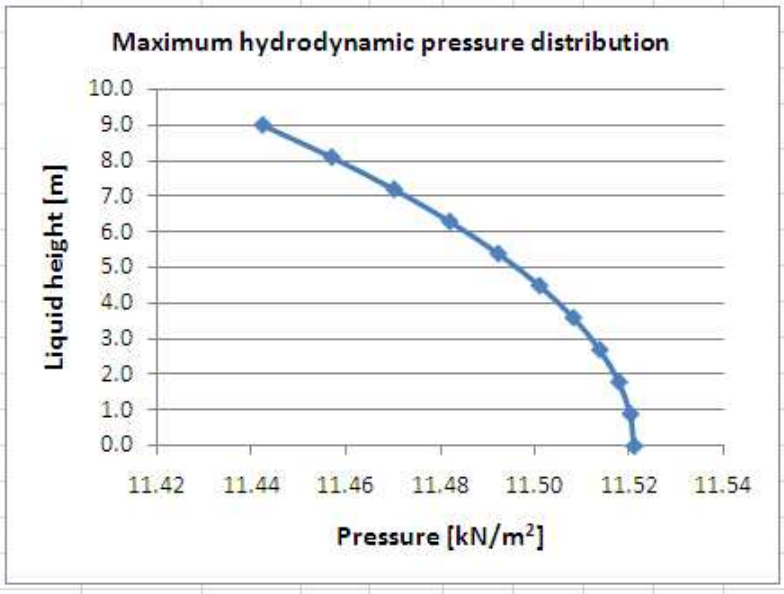

7.2 SERVICEABILITY LIMIT STATE:

Height [m] :	9.00	8.10	7.20	6.30	5.40	4.50	3.60	2.70	1.80	0.90	0.00
p_{max} [kN/m^2]:	11.29	11.30	11.30	11.31	11.32	11.32	11.33	11.33	11.33	11.34	11.34

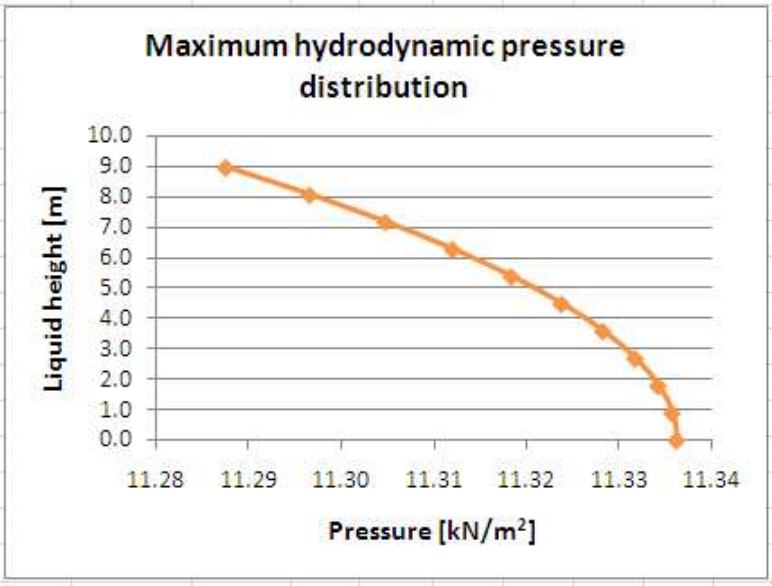

8. TOTAL MAXIMUM PRESSURE:

8.1 ULTIMATE LIMIT STATE:

Height [m] :	9.00	8.10	7.20	6.30	5.40	4.50	3.60	2.70	1.80	0.90	0.00
p_{max} [kN/m^2]:	11.44	20.29	29.13	37.97	46.81	55.65	64.48	73.32	82.15	90.98	99.81

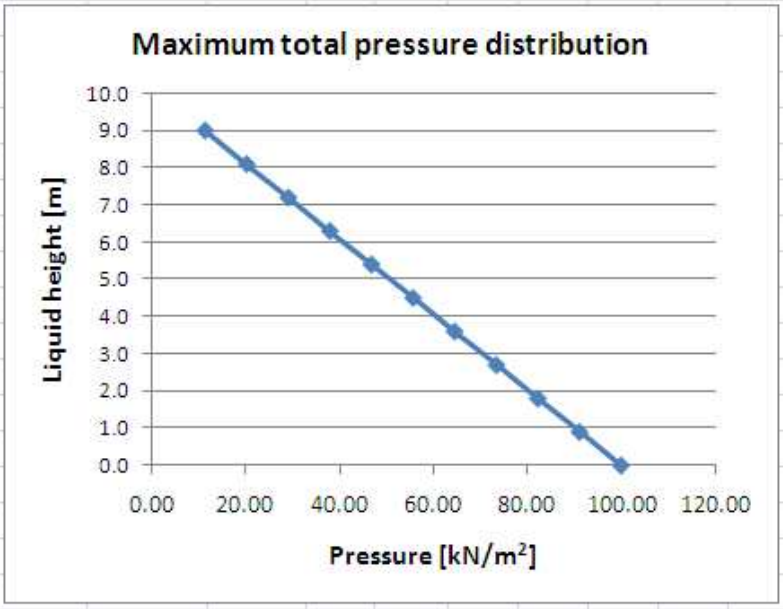

8.2 SERVICEABILITY LIMIT STATE:

Height [m] :	9.00	8.10	7.20	6.30	5.40	4.50	3.60	2.70	1.80	0.90	0.00
p_{max} [kN/m²]:	11.29	20.13	28.96	37.80	46.63	55.47	64.30	73.13	81.97	90.80	99.63

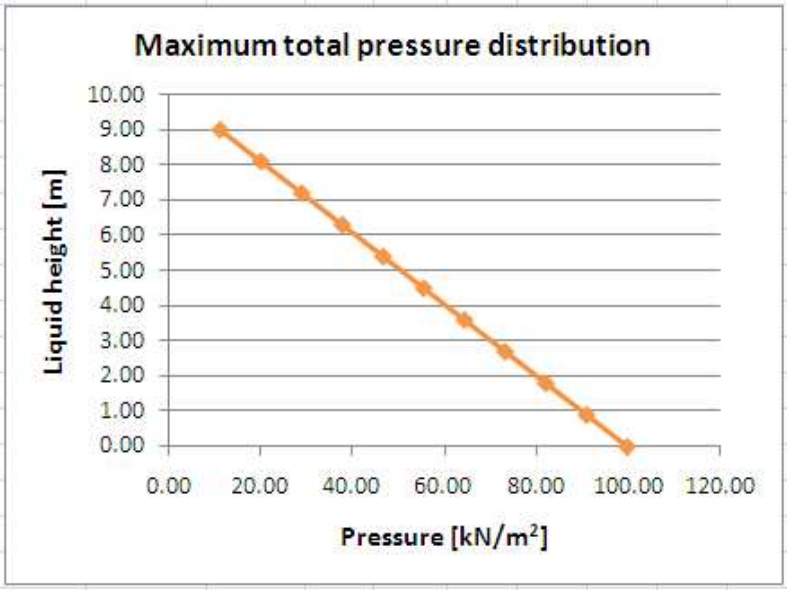

9. TOTAL WALL FORCE OR BASE SHEAR:

Total liquid mass:

$m = \pi R^2 H \rho$ $m =$

$m =$ 2827433 kg 2827433.4 kg

Impulsive mass:

EN 1998-4: A.2.1.2

$$m_i = m\,2\gamma \sum \frac{I_1(\nu_n/\gamma)}{\nu_n^3 I_1'(\nu_n/\gamma)}$$

$m_i =$

$m_i =$ 1436331.2 kg 1436331.2

	Flexible mass:				
A.3.1	$m_f = m\psi\gamma\sum\frac{(-1)^n}{\nu_n}d_n$				m_f=
	m_f=	632766.5	kg		632766.5
					kg
	Inertia mass:				
	m_w=	$\pi\rho_s((R+t_w)^2-R^2)H$			m_w=
	m_w=	343363.5	kg		343363.5
					kg
	9.1 ULTIMATE LIMIT STATE:				
	Base shear force for impulsive component:				
A.3.2.1	Q_b=	$(m_i+m_w)a_g+m_fS_e(T)$			
	Q_b=	4251.15	kN		Q_{max}=
					4251.15
	9.2 SERVICEABILITY LIMIT STATE:				kN
	Base shear force for impulsive component:				
	Q_b=	$(m_i+m_w)a_g+m_fS_e(T)$			
	Q_b=	3598.22	kN		Q_{max}=
					3598.22
	10. SURFACE DISPLACEMENT OF LIQUID:				
EN 1998-4:	**10.1 ULTIMATE LIMIT STATE:**				
A.2.1.4	d_s=	$0.84RS_e(T_{c1})/g$			d_s=
	d_s=	0.25	m		252.0
	d_s=	252.0	mm		mm
	10.2 SERVICEABILITY LIMIT STATE:				
	d_s=	$0.84RS_e(T_{c1})/g$			d_s=
	d_s=	0.10	m		100.8
	d_s=	100.80	mm		mm

APPENDIX C:

VERIFICATION OF STATIC RESULTS USING STRAND7 (2005) WITH THE NUMERICAL METHOD BY GHALI (1979)

ULTIMATE LIMIT STATE GRAPHS:

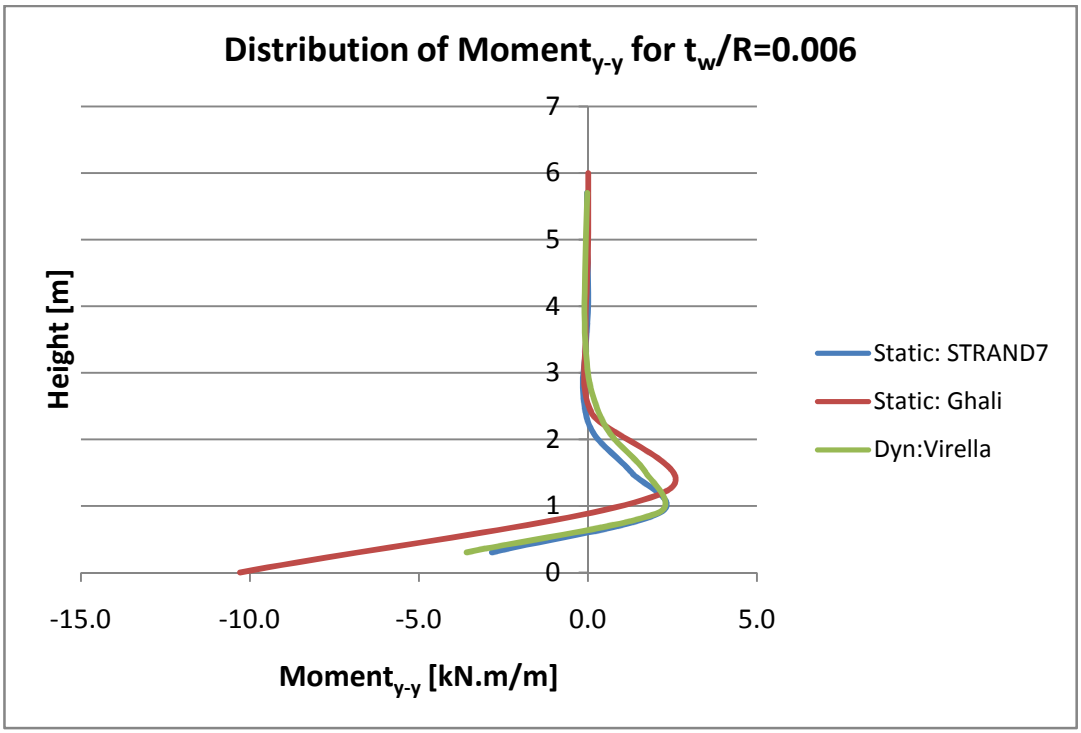

Figure C.1: Distribution of bending moment along wall height for a t_w/R ratio of 0.006

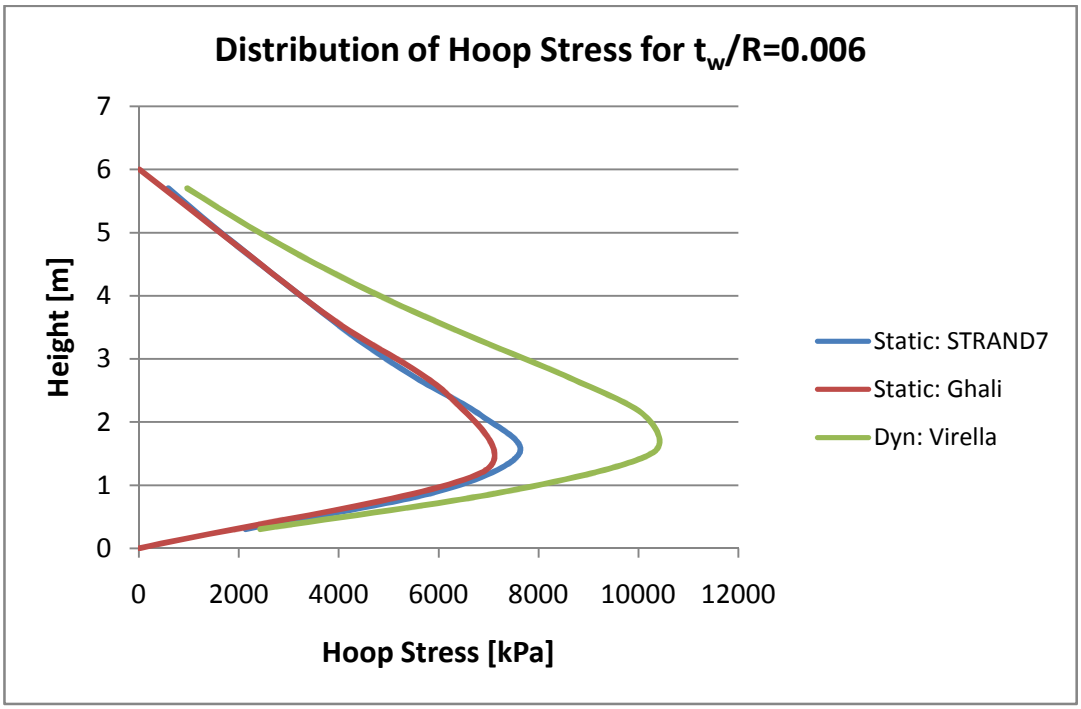

Figure C.2: Distribution of hoop stress along wall height for a t_w/R ratio of 0.006

APPENDIX D:

GLOBAL RESULTS

CLASSIFICATION OF STRUCTURE:

Ultimate limit state:

Impulsive pressure obtained at bottom of the wall for a_g=0.15g

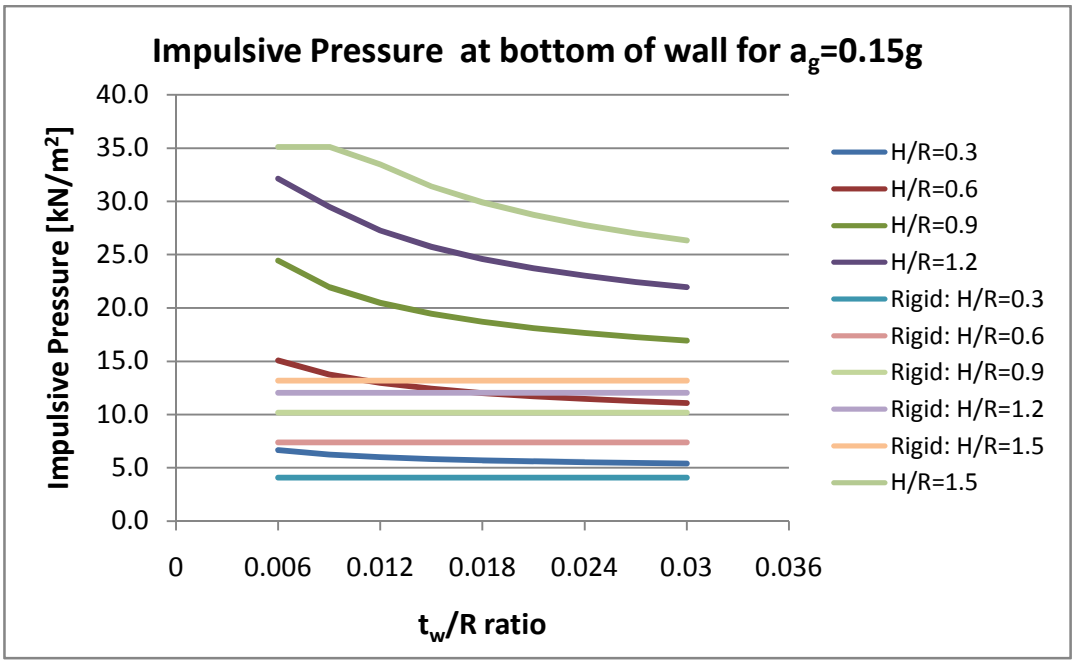

Figure D.1: Impulsive pressure at bottom of wall for ULS (PGA=0.15g)

Serviceability limit state:

Impulsive pressure obtained at free surface of the liquid for a_g=0.15g

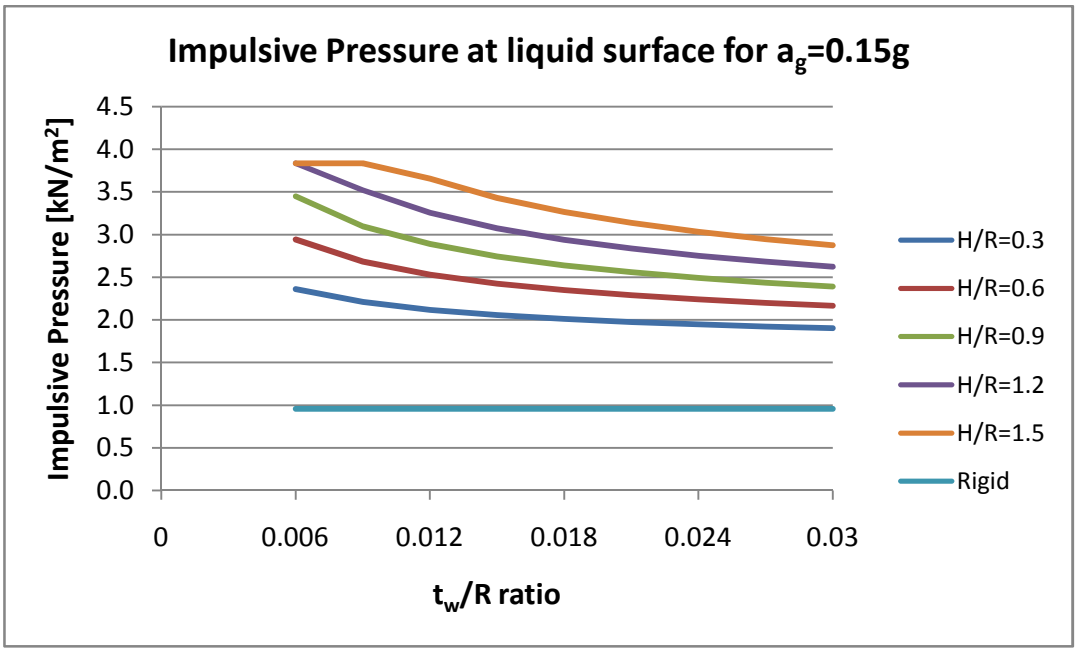

Figure D.2: Impulsive pressure at free surface of liquid for SLS (PGA=0.15g)

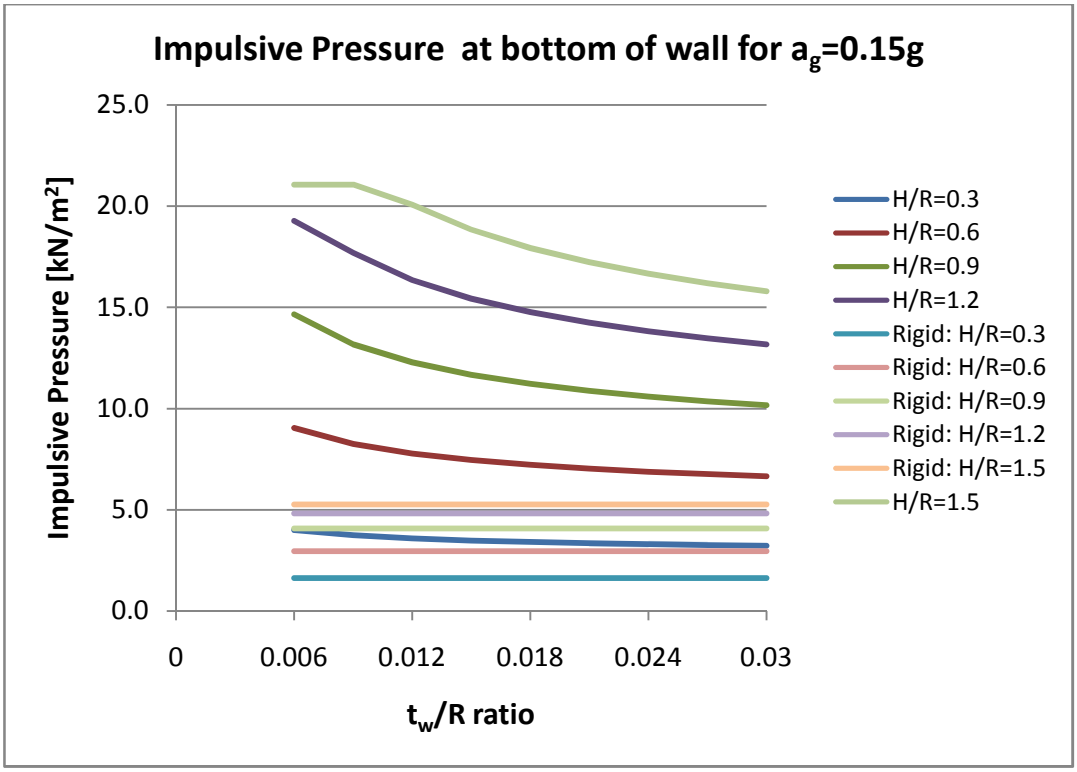

Figure D.3: Impulsive pressure obtained at bottom of wall for SLS (PGA=0.15g)

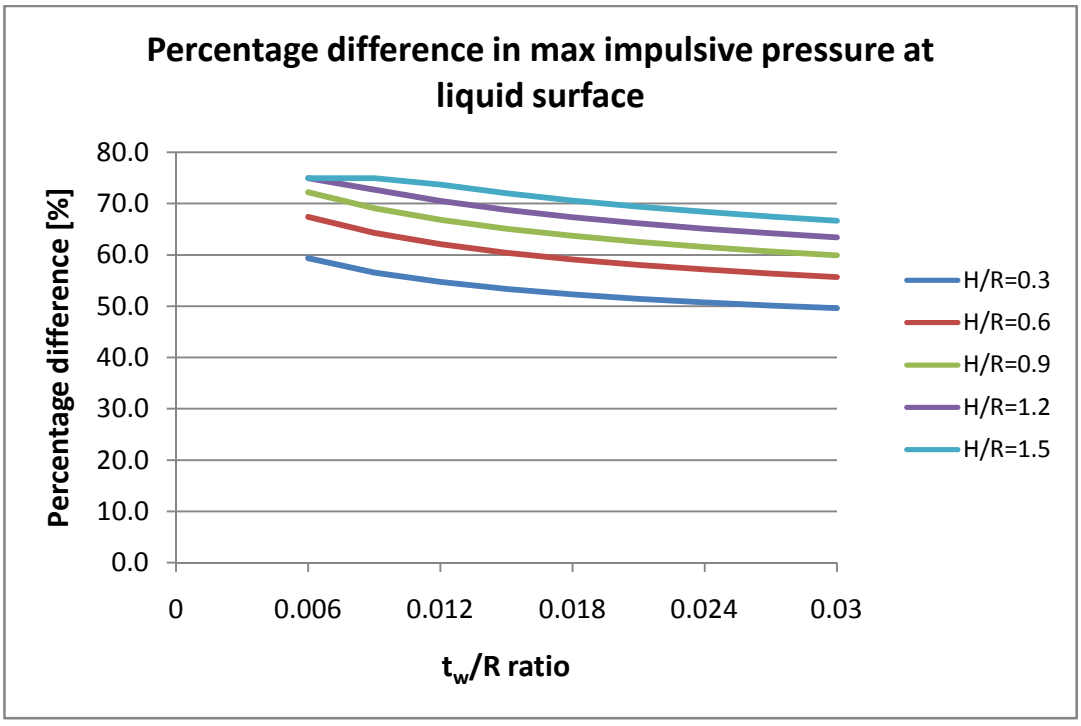

Figure D.4: Percentage difference between flexible and rigid structures for SLS (PGA=0.15g)

BASE SHEAR FORCE:

Results obtained for a peak ground acceleration of 0.25g

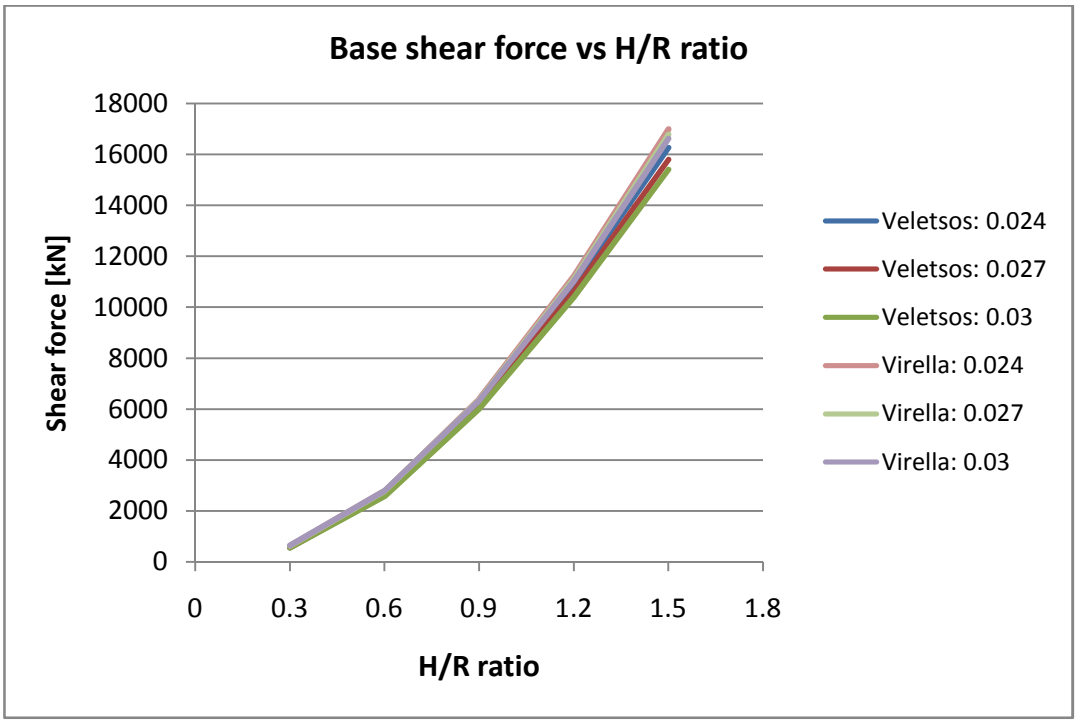

Figure D.5: Variance in base shear force for ULS (PGA=0.25g)

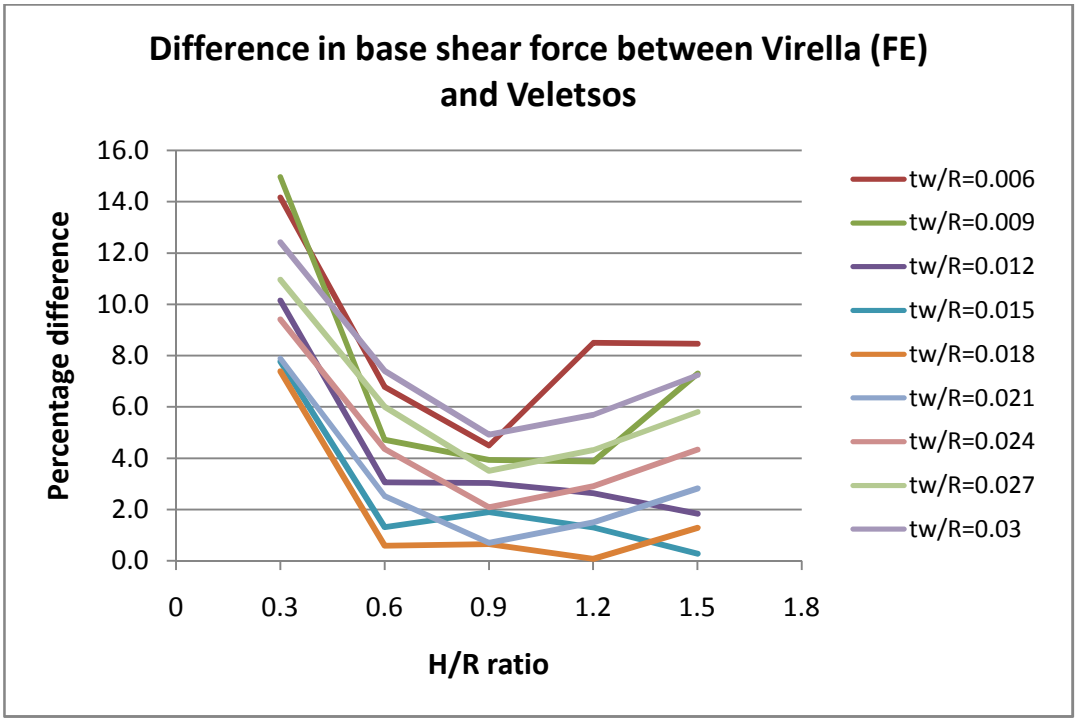

Figure D.6: Percentage difference in base shear force between Virella (2006) and Veletsos (1997) for ULS (PGA=0.25g)

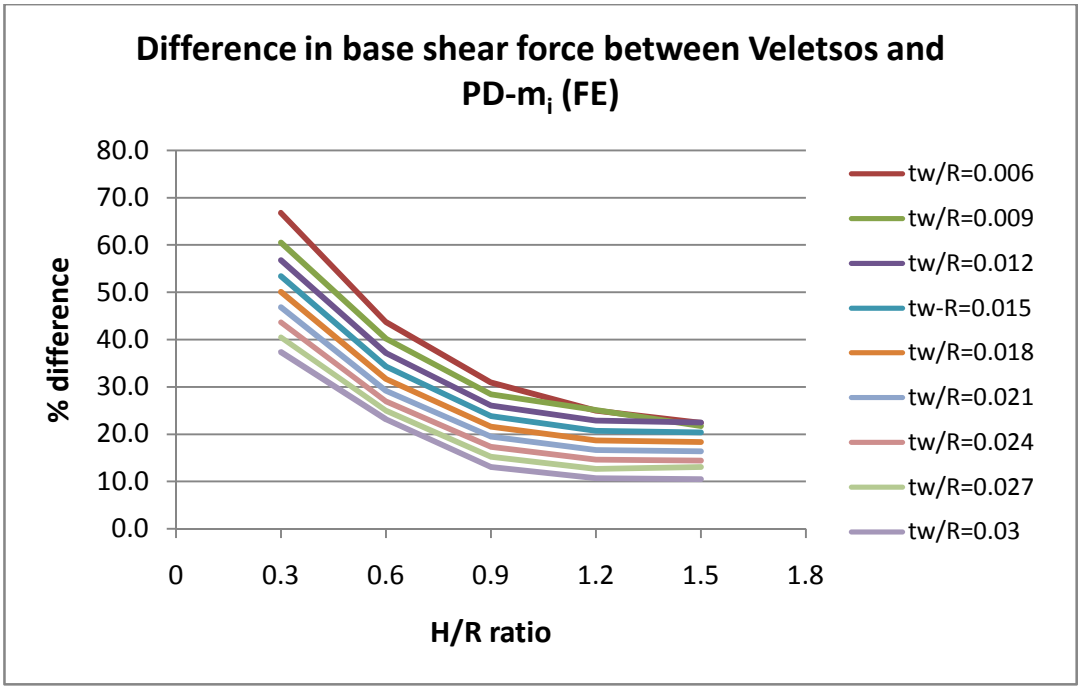

Figure D.7: Percentage difference in base shear force between Veletsos (1997) and PD-m$_i$ model for ULS (PGA=0.25g)

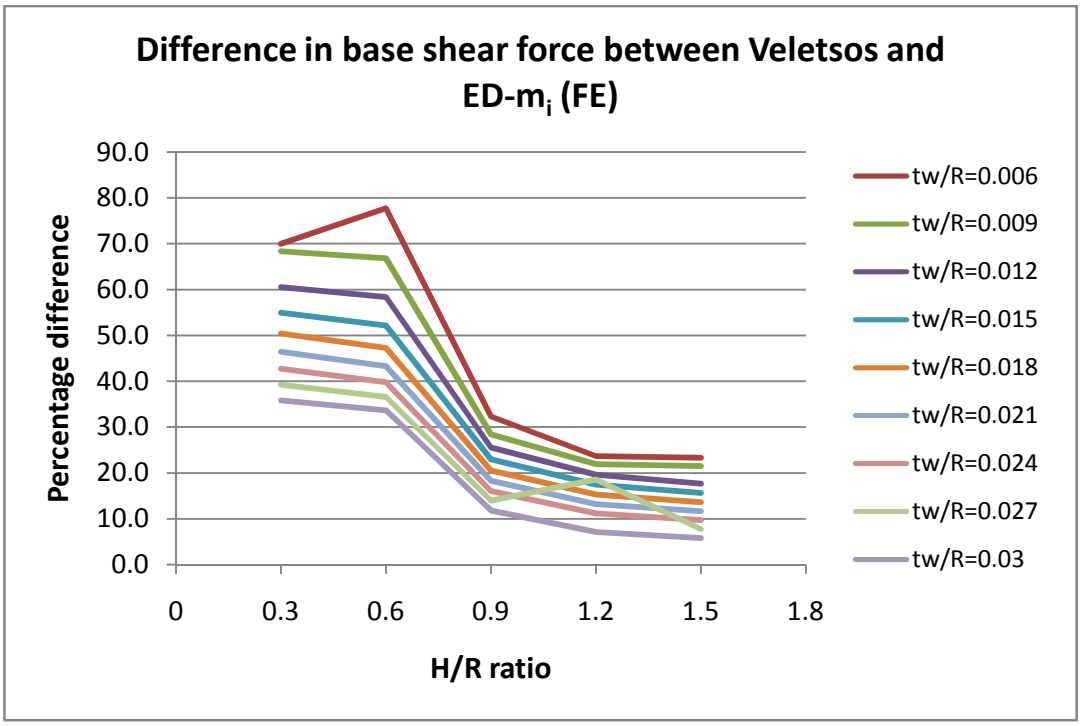

Figure D.8: Percentage difference in base shear force between Veletsos (1997) and ED-m$_i$ model for ULS (PGA=0.25g)

Results obtained for a peak ground acceleration of 0.35g

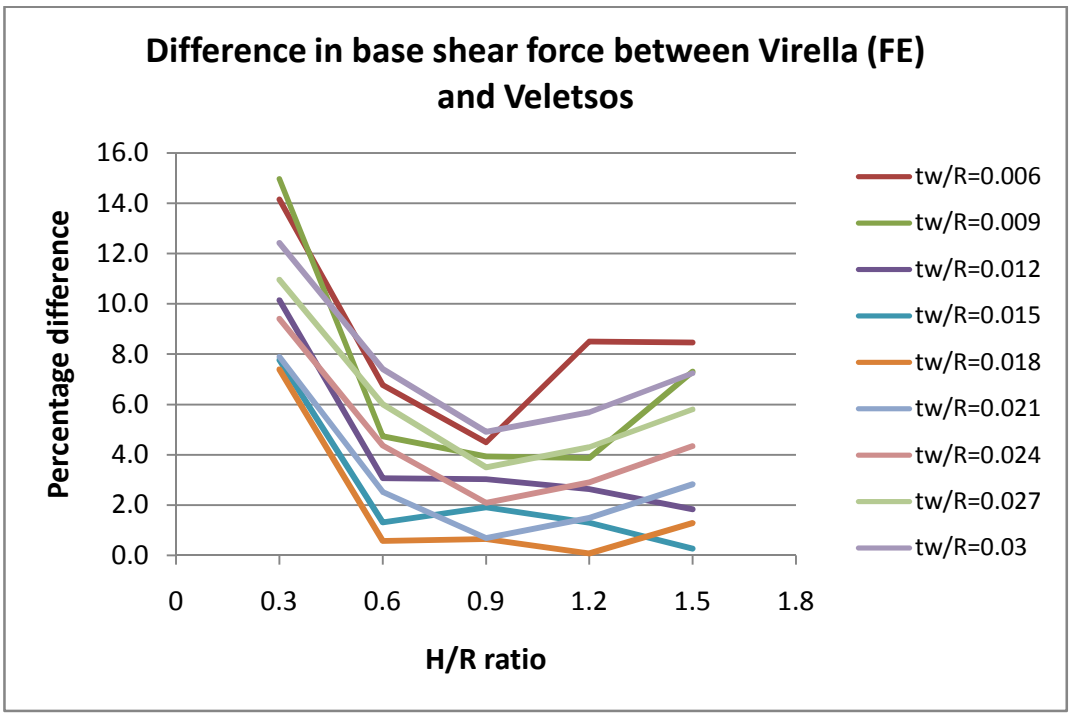

Figure D.8: Percentage difference in base shear force between Virella (2006) and Veletsos (1997) for ULS (PGA=0.35g)

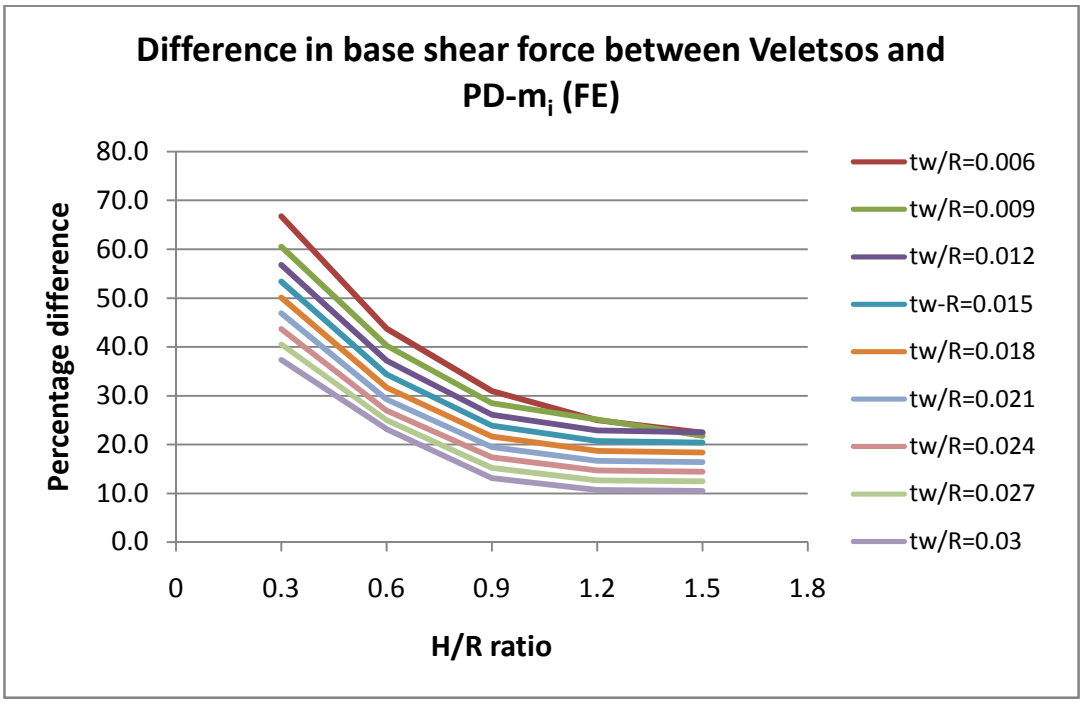

Figure D.9: Percentage difference in base shear force between Veletsos (1997) and PD-m$_i$ model for ULS (PGA=0.35g)

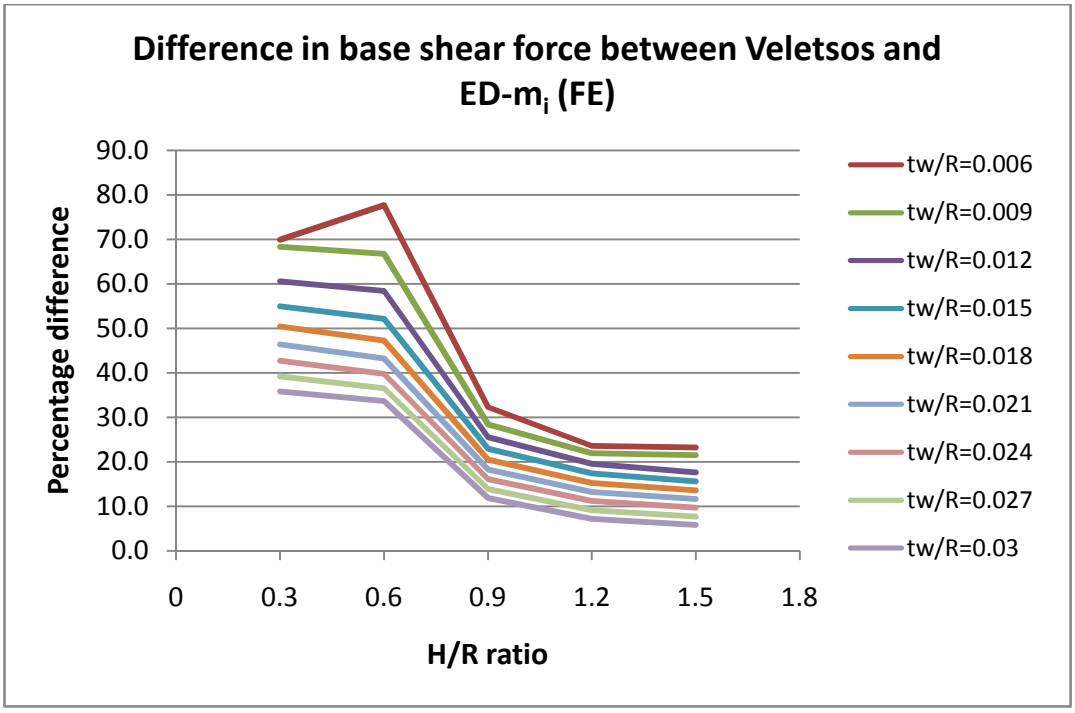

Figure D.10: Percentage difference in base shear force between Veletsos (1997) and ED-m$_i$ model for ULS (PGA=0.35g)

OVERTURNING MOMENT:

Results obtained for a peak ground acceleration of 0.25g

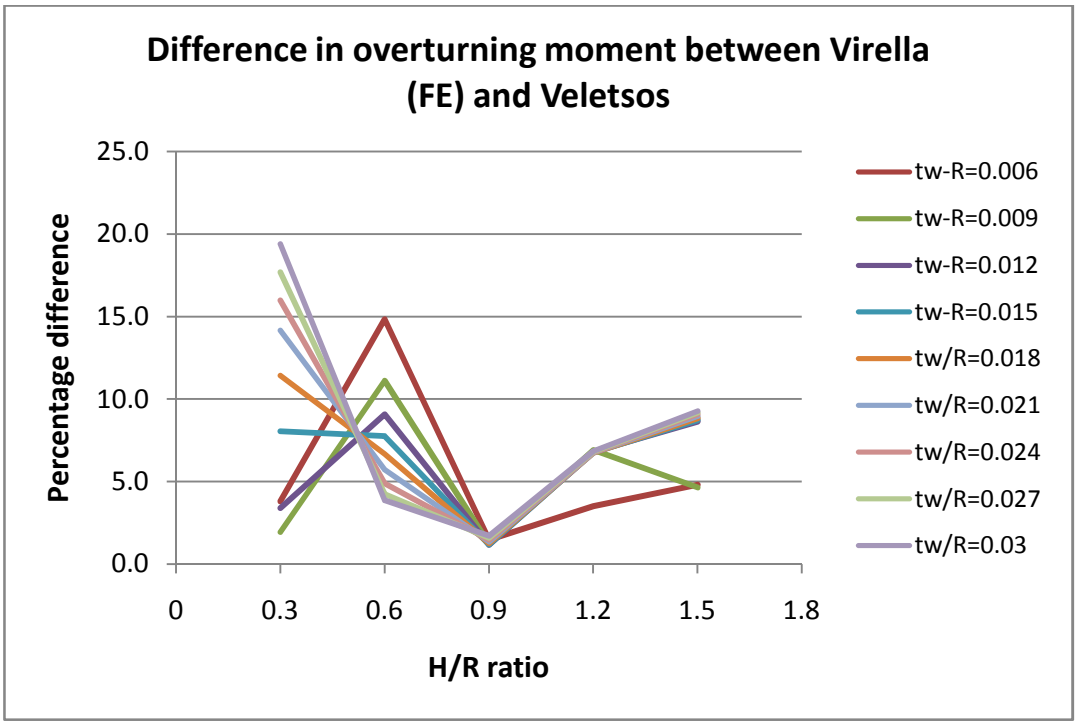

Figure D.11: Percentage difference between Virella (2006) and Veletsos (1997) for ULS (PGA=0.25g)

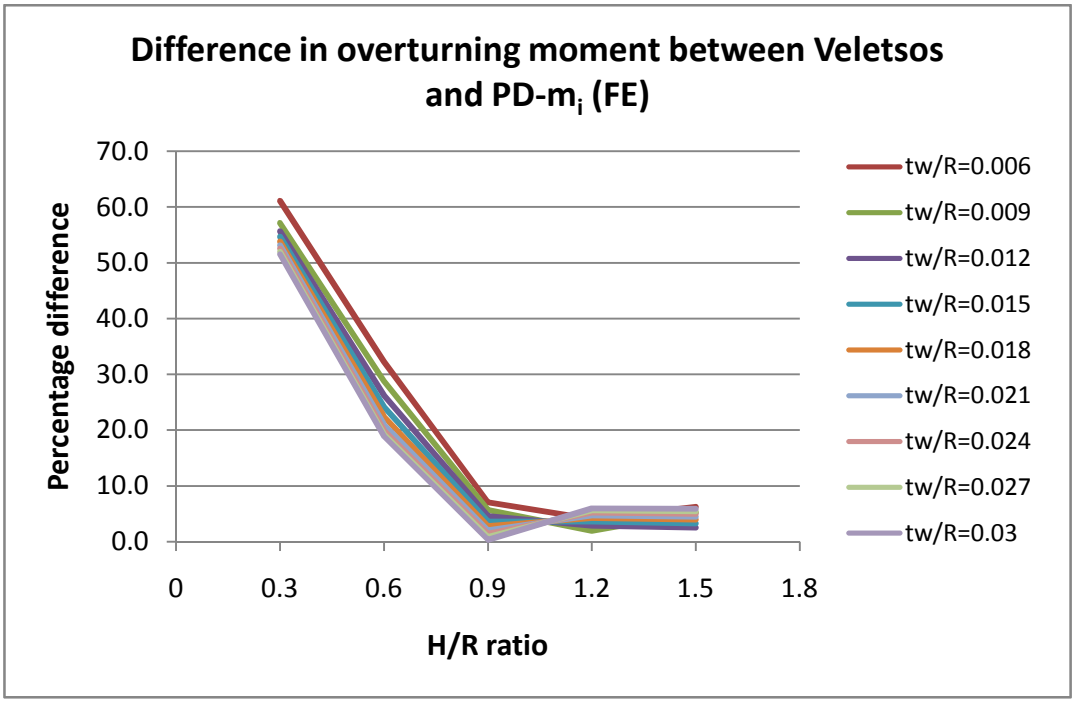

Figure D.12: Percentage difference between Veletsos (1997) and PD-m_i model for ULS (PGA=0.25g)

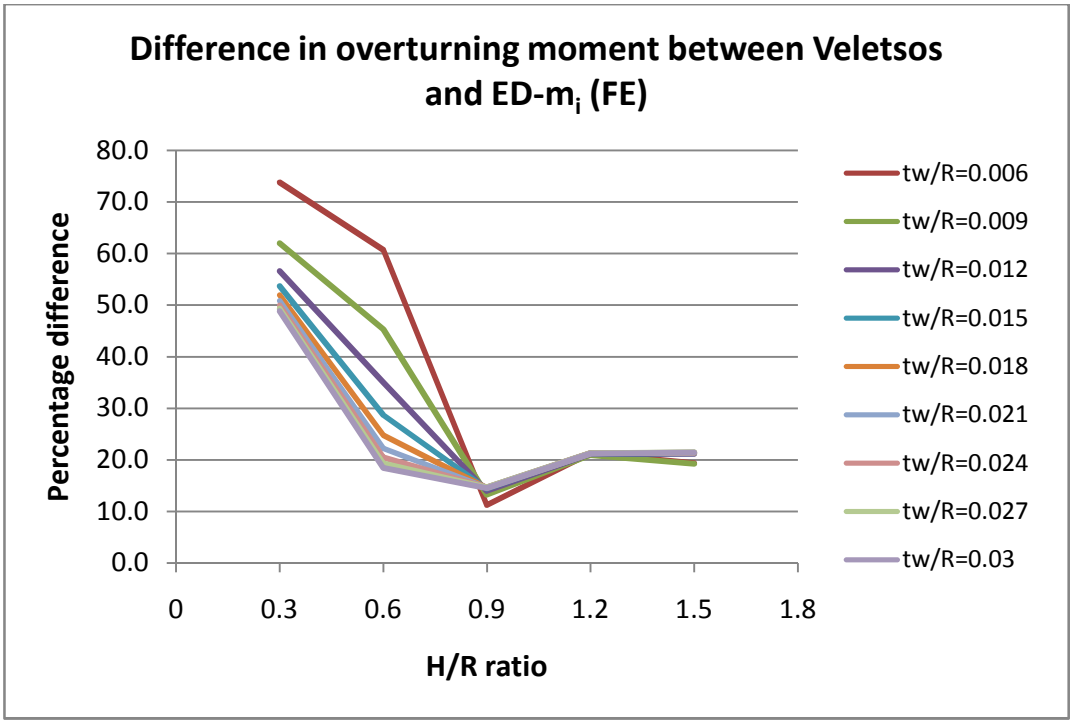

Figure D.13: Percentage difference between Veletsos (1997) and ED-m$_i$ model for ULS (PGA=0.25g)

Results obtained for a peak ground acceleration of 0.35g

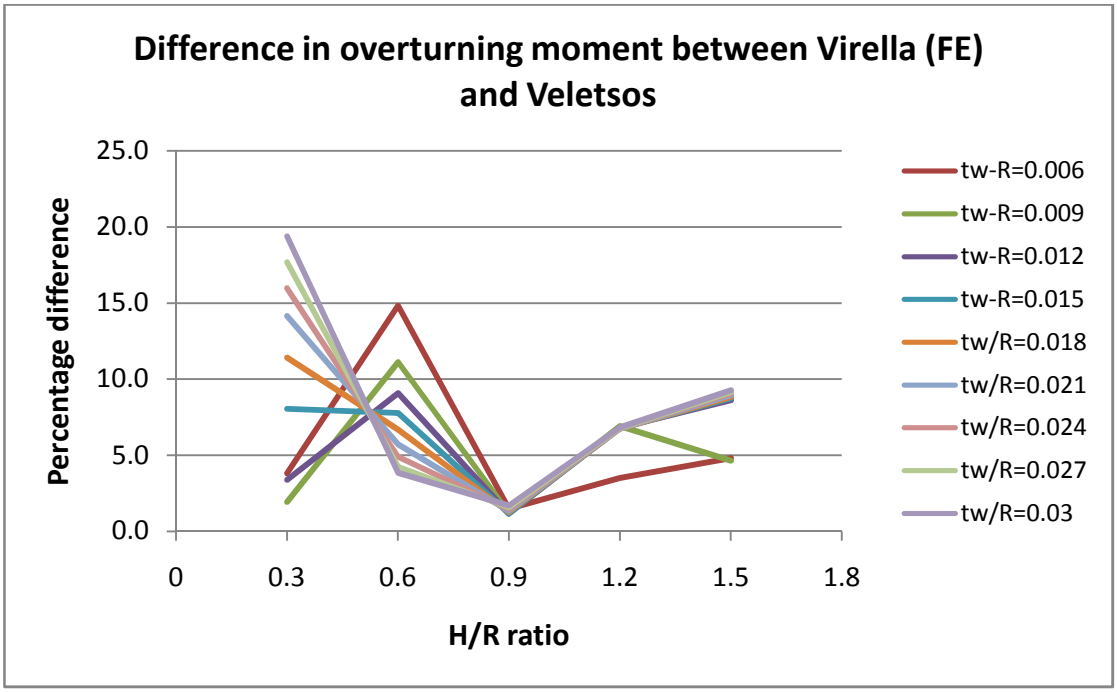

Figure D.14: Percentage difference between Virella (2006) and Veletsos (1997) for ULS (PGA=0.35g)

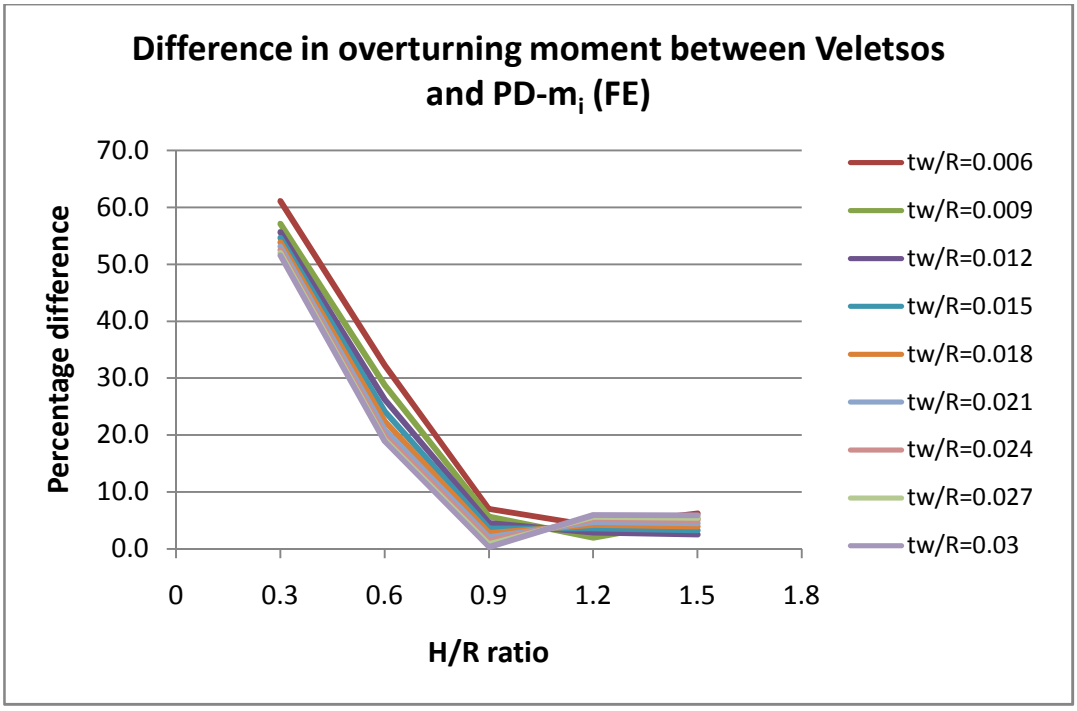

Figure D.15: Percentage difference between Veletsos (1997) and PD-m_i model for ULS (PGA=0.35g)

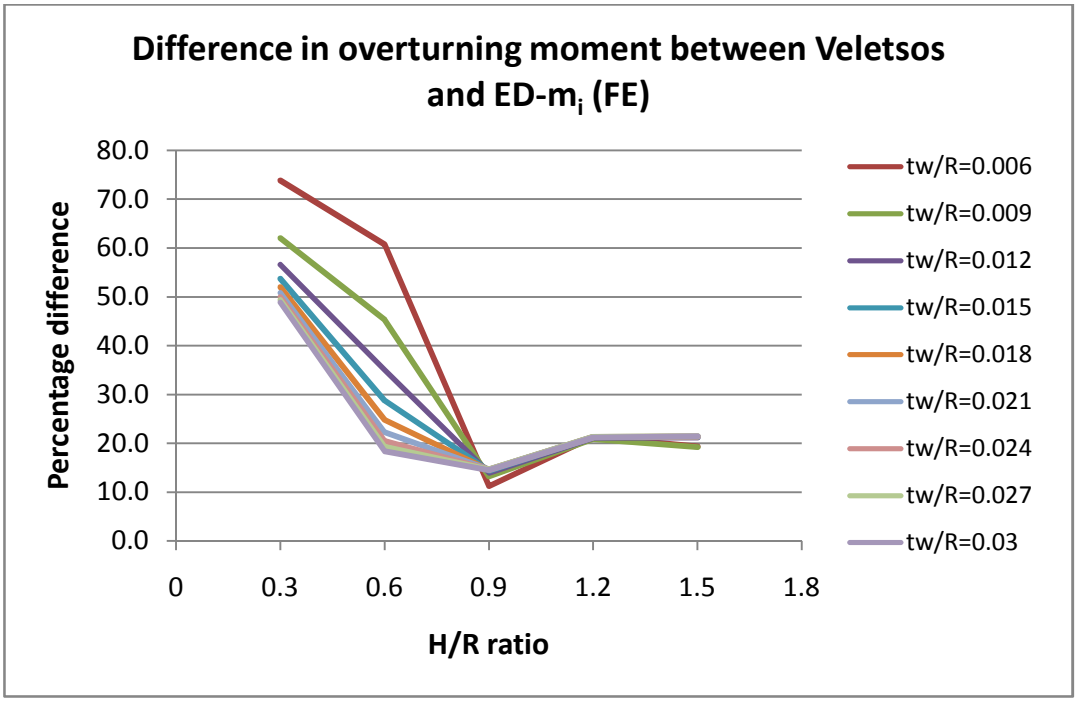

Figure D.16: Percentage difference between Veletsos (1997) and ED-m_i model for ULS (PGA=0.35g)

APPENDIX E:

LOCAL RESULTS

BENDING MOMENT ABOUT A HORIZONTAL AXIS

Results obtained for a peak ground acceleration of 0.25g

Ultimate limit state:

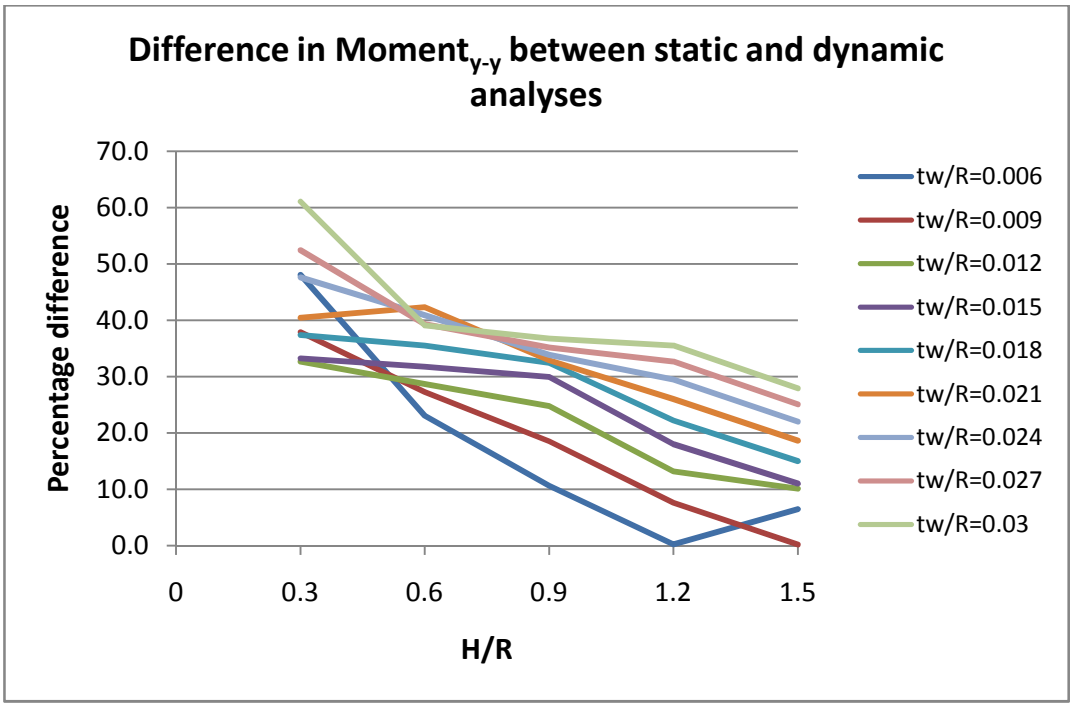

Figure E.1: Difference in momenty-y for ULS (PGA=0.25g)

Serviceability limit state:

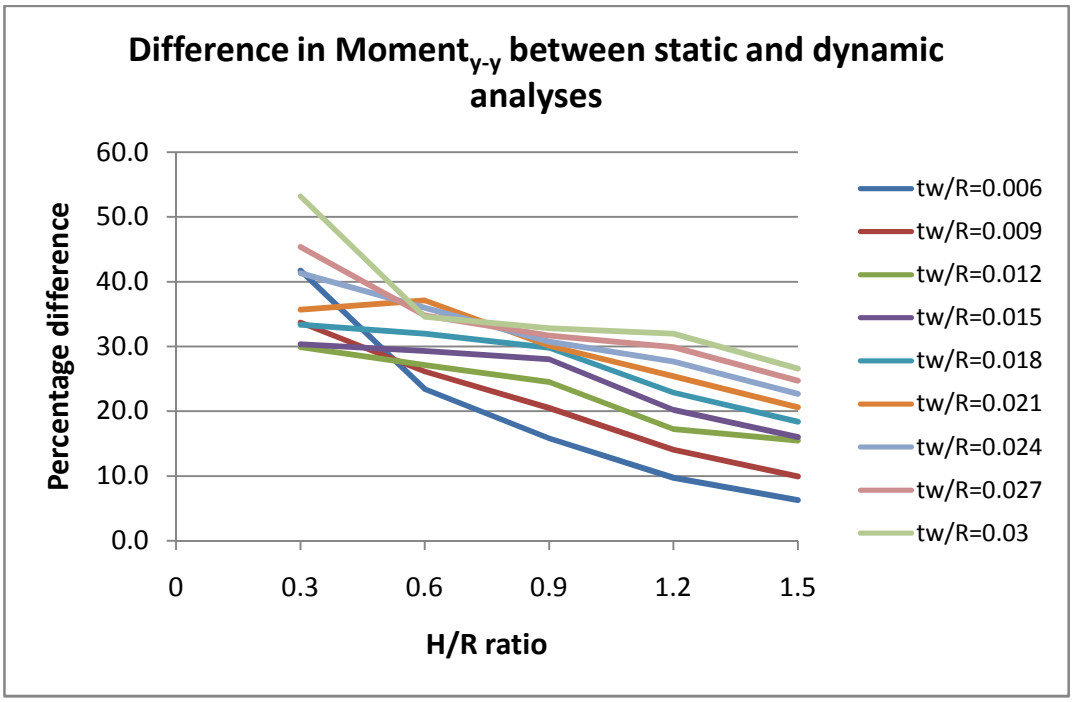

Figure E.2: Difference in momenty-y for SLS (PGA=0.25g)

Results obtained for a peak ground acceleration of 0.35g

Ultimate limit state:

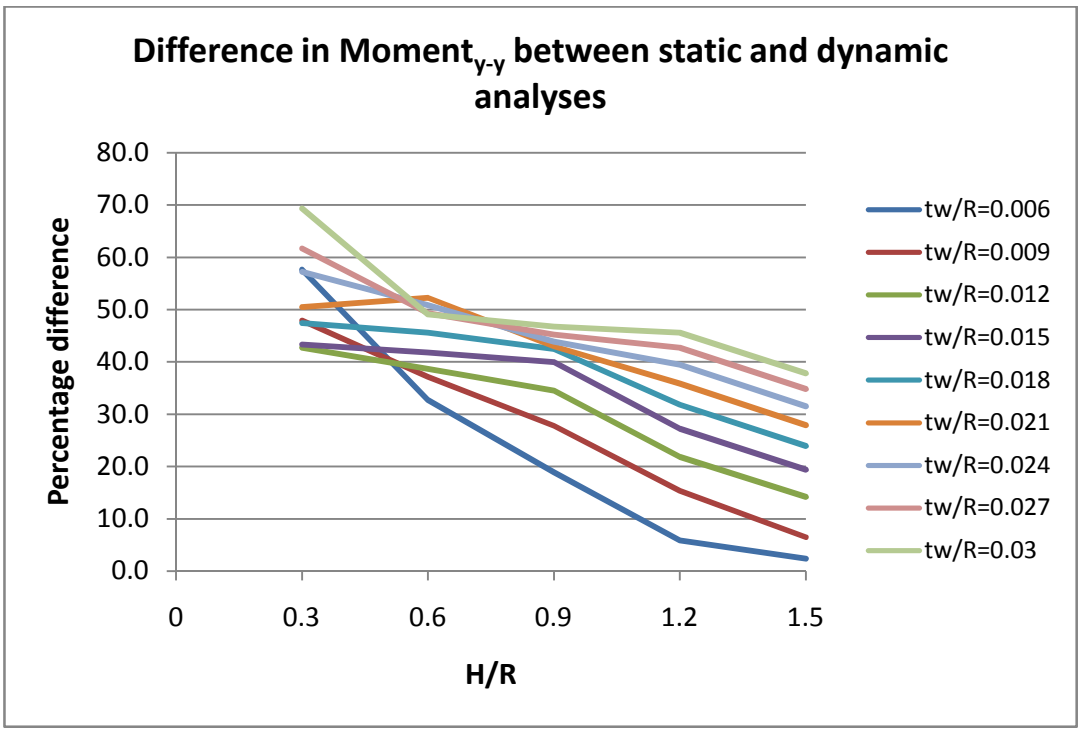

Figure E.3: Difference in momenty-y for ULS (PGA=0.35g)

Serviceability limit state:

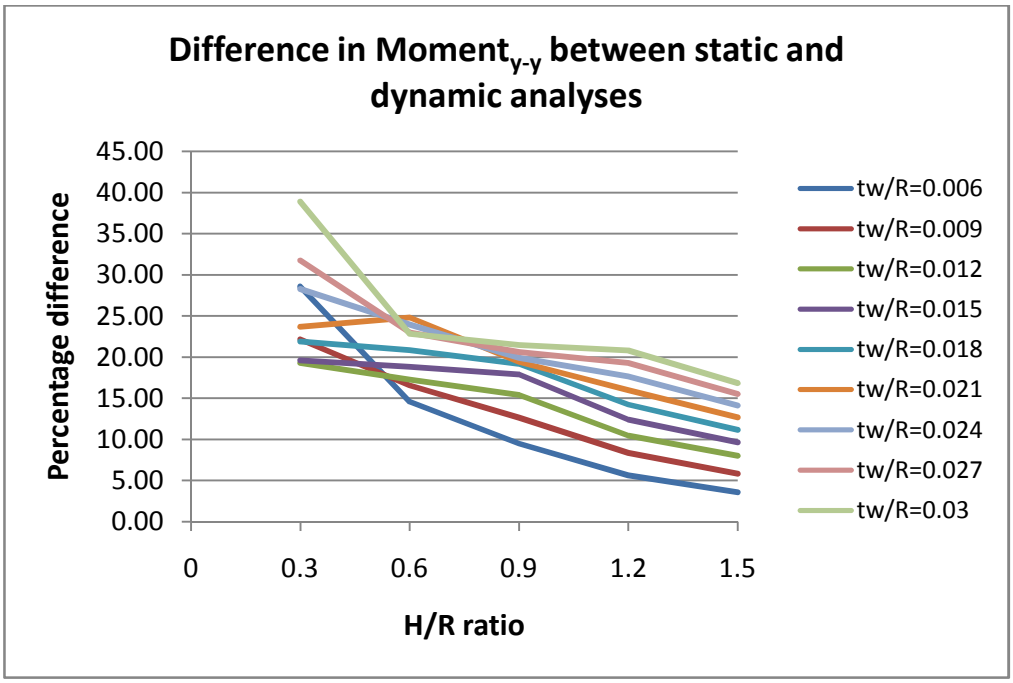

Figure E.4: Difference in momenty-y for SLS (PGA=0.35g)

HOOP STRESS

Results obtained for a peak ground acceleration of 0.25g

Ultimate limit state:

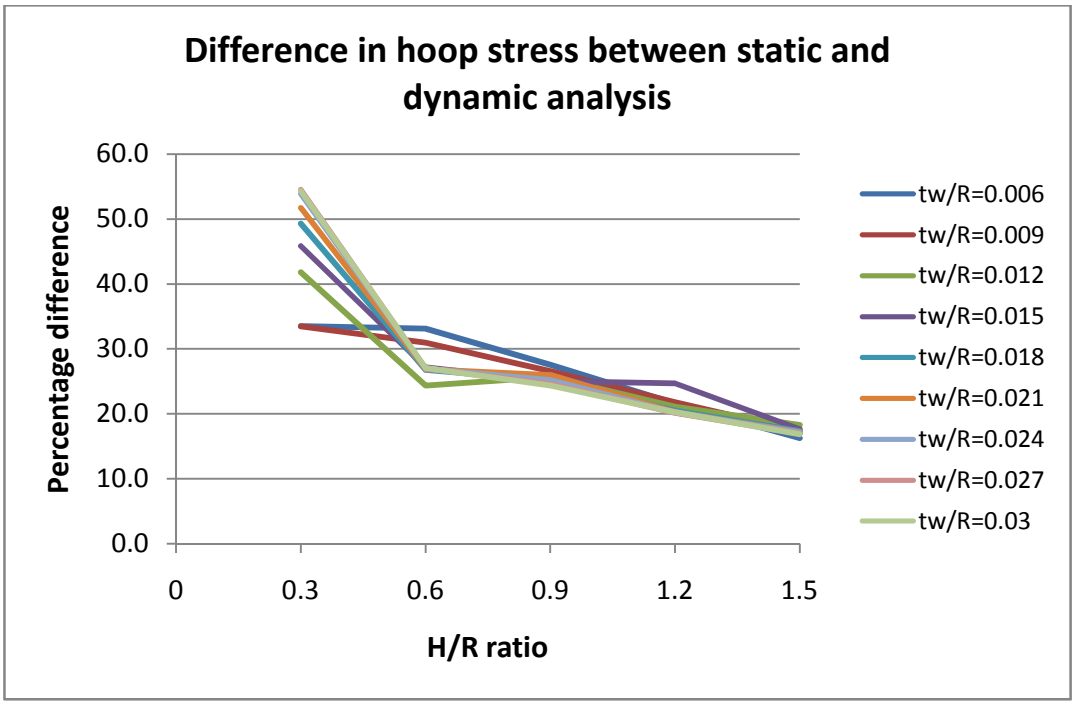

Figure E.5: Difference in hoop stress for ULS (PGA=0.25g)

Serviceability limit state:

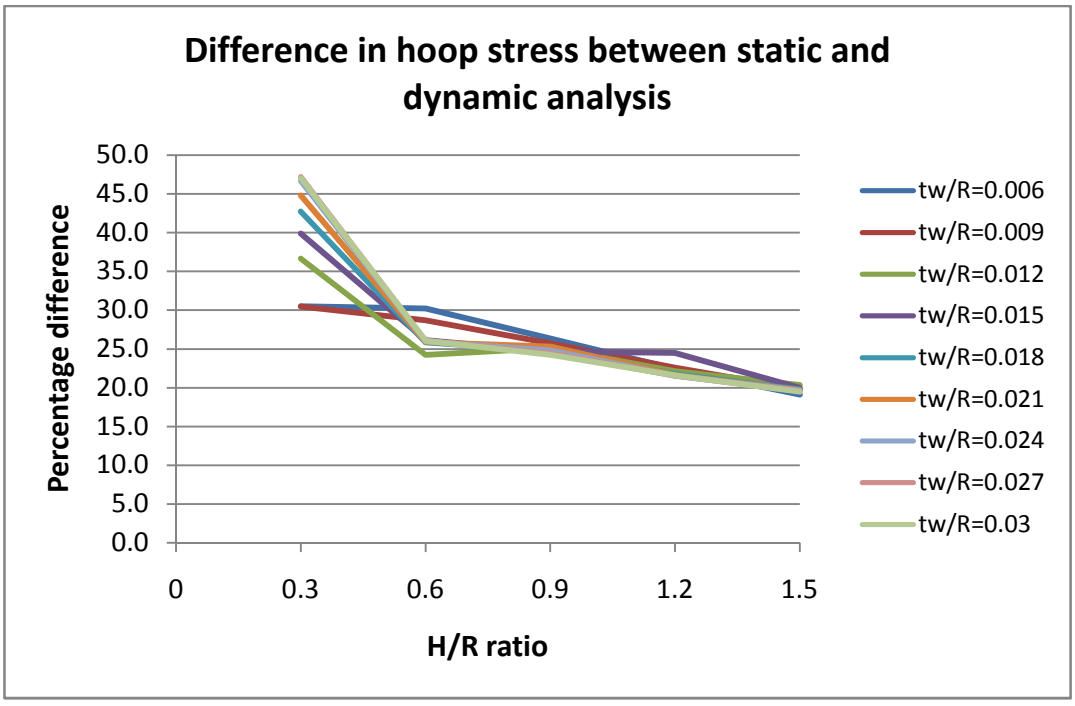

Figure E.6: Difference in hoop stress for SLS (PGA=0.25g)

Results obtained for a peak ground acceleration of 0.35g

Ultimate limit state:

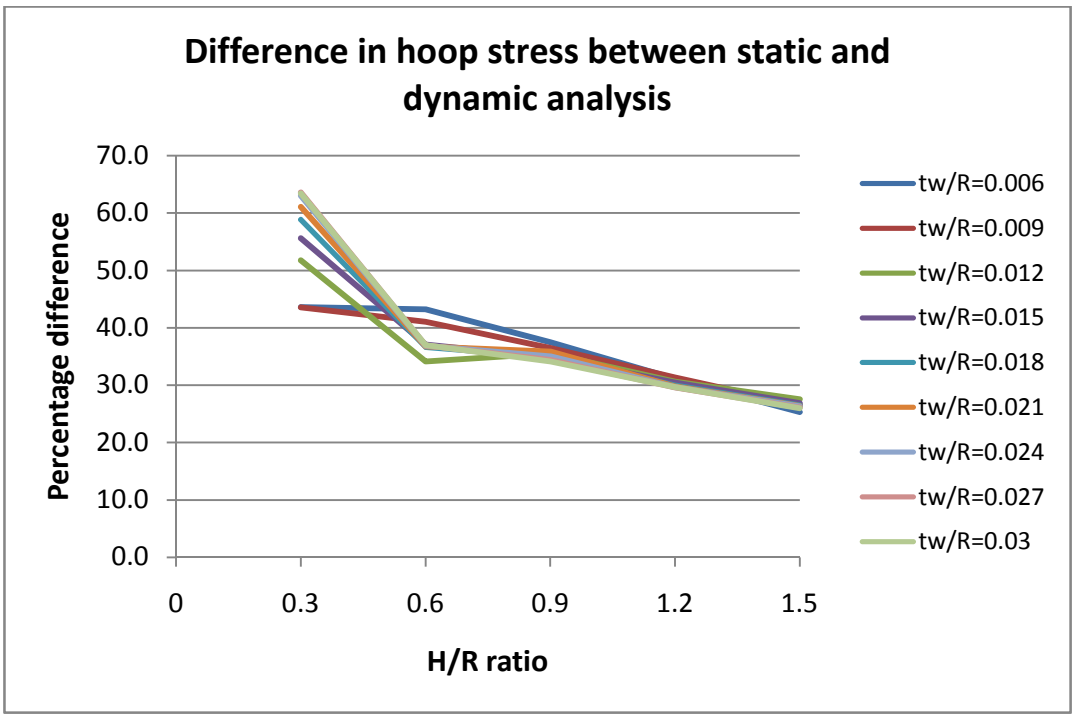

Figure E.7: Difference in hoop stress for ULS (PGA=0.35g)

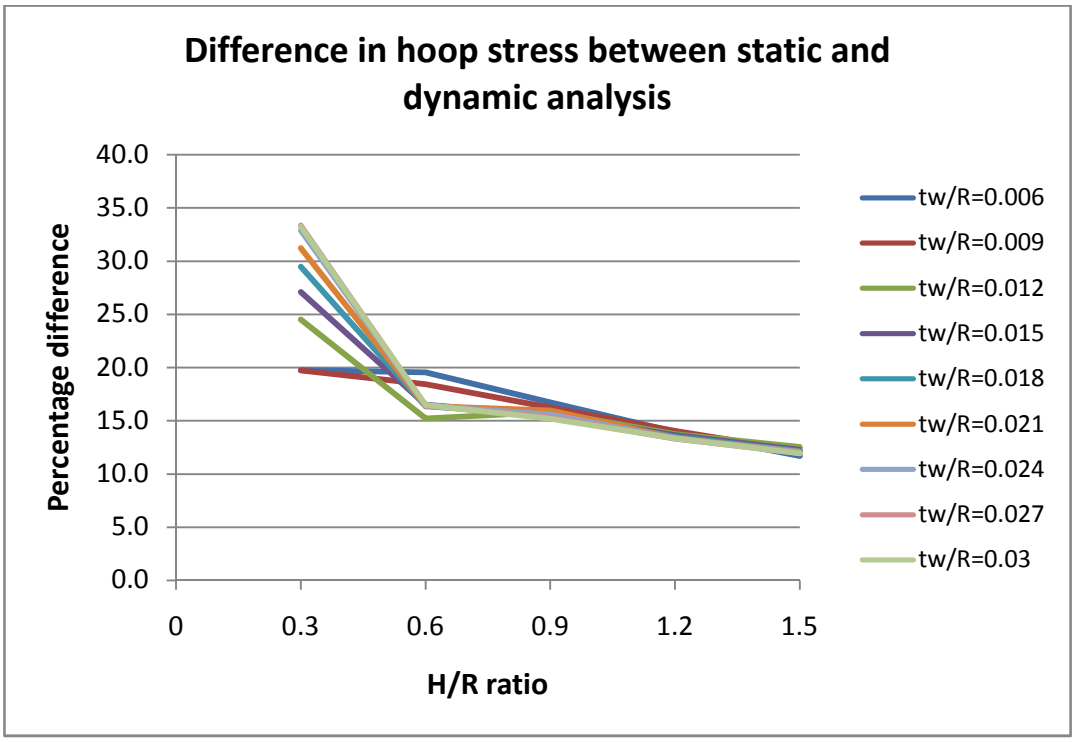

Figure E.8: Difference in hoop stress for SLS (PGA=0.35g)

APPENDIX F:

RESULTS OBTAINED WITH A MODIFIED RESPONSE SPECTRUM

ULTIMATE LIMIT STATE GRAPHS:

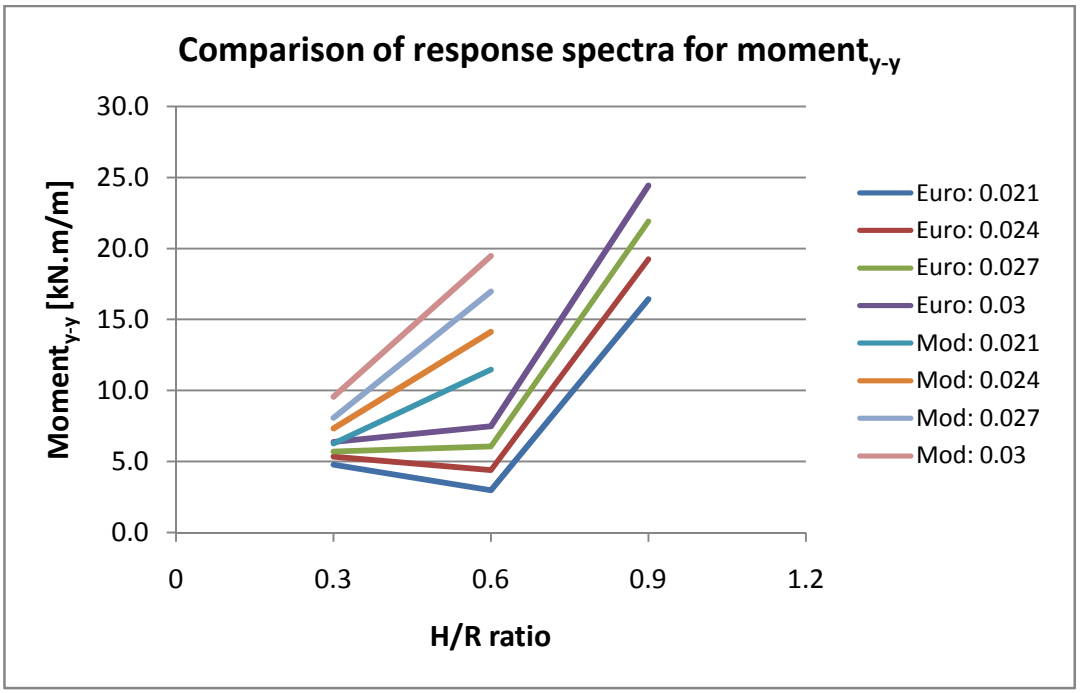

Figure F.1: Comparison of bending moment between Eurocode and Modified response spectrum for ULS (PGA=0.15g)

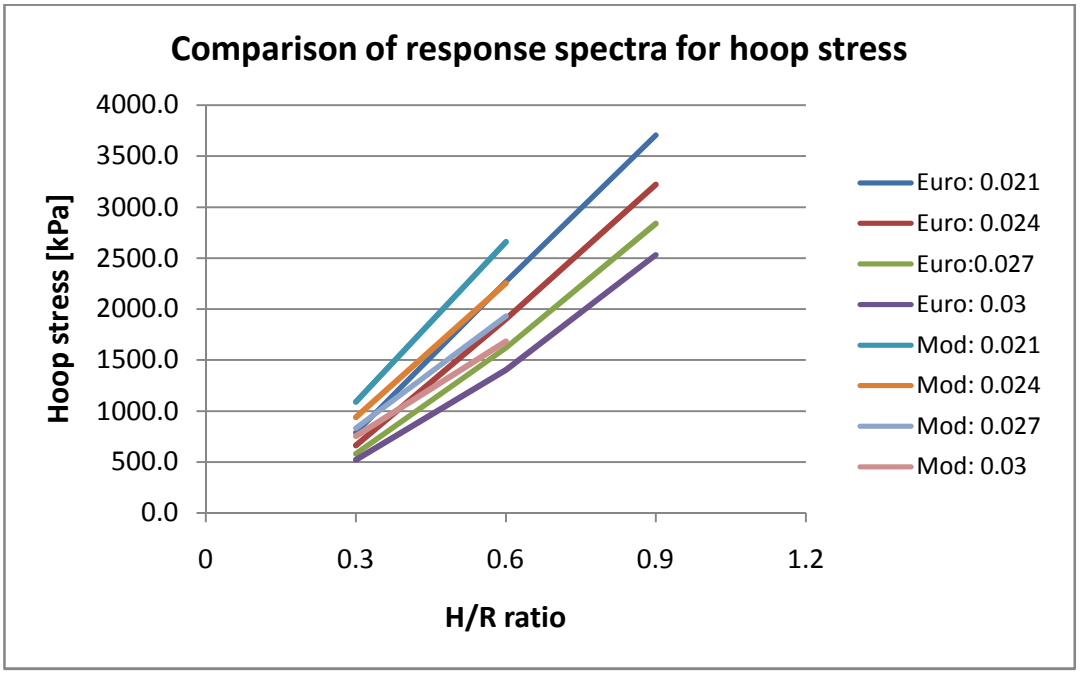

Figure F.2: Comparison of hoop stress between Eurocode and Modified response spectrum for ULS (PGA=0.15g)

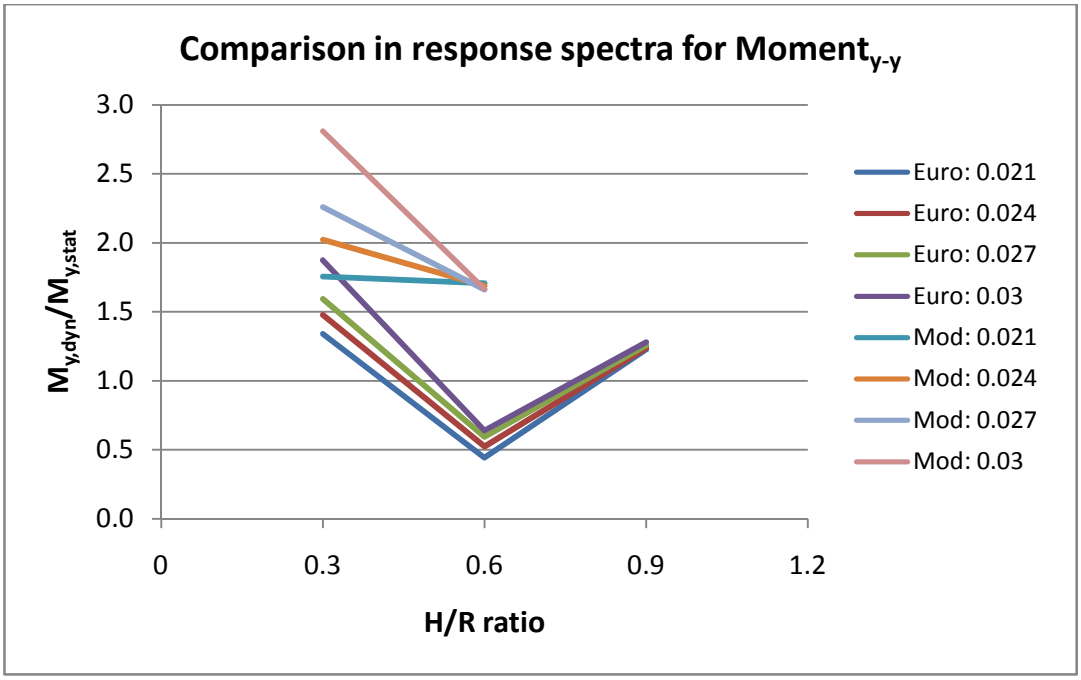

Figure F.3: Ratio between dynamic and static bending moment for ULS (PGA=0.15g)

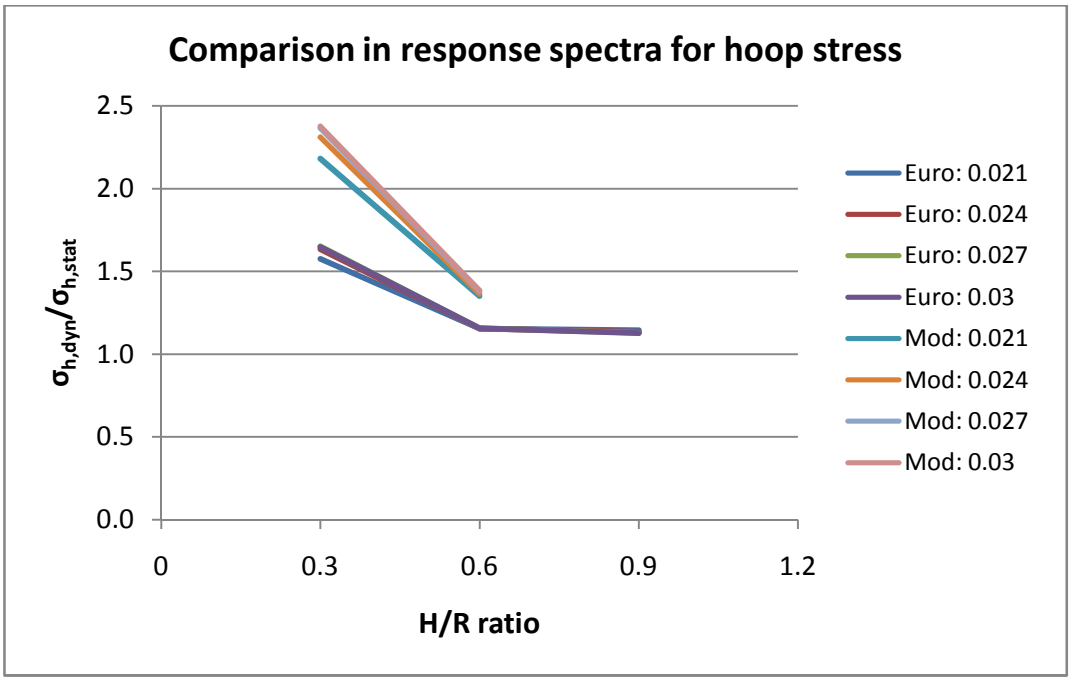

Figure F.4: Ratio between dynamic and static hoop stress for ULS (PGA=0.15g)